The Role of Mesenchymal Stromal Cells in Inflammation and Treatment of Pulmonary Fibrosis

By

Emer Cahill

B.Sc

A thesis submitted to

The National University of Ireland, Maynooth for the degree of

Doctor of Philosophy

NUI MAYNOOTH

Ollscoil na hÉireann Má Nuad

Department of Biology

Institute of Immunology

National University Ireland, Maynooth

October 2013

Research Supervisor: Prof. Bernard Mahon

TABLE OF CONTENTS

Declaration of Authorship

I certify that the work presented herein is, to the best of my knowledge, original, resulting from research performed by me, except where acknowledged otherwise. This work has not been submitted in whole, or in part, at this or any other university

_____ _____

Emer Cahill B.Sc. Date

Summary

The aim of this body of work was to determine the method of action of mesenchymal stromal cell immunomodulation, and their potential benefits in treating pulmonary fibrosis. This was achieved through a series of *in vitro* studies and an *in vivo* model of lung disease, namely, bleomycin induced pulmonary fibrosis.

Firstly MSC expansion of Treg cells was shown to be dependent on Jagged 1 signalling. MSC inhibition of DC maturation and antigen presentation was shown to also involve Jagged 1 however IL-6 signalling is also necessary. MSC inhibition of DC maturation resulted in a semi mature or "tolerogenic" DC, expressing lower levels of co-stimulatory markers. These cells were capable of suppressing antigen specific T cell proliferation and inducing Treg cells from a naive population.

MSC trophic factors were further examined for their ability to promote wound healing. MSC conditioned media cultured with lung epithelial cells encouraged proliferation through the release of the growth factor HGF. MSC CM also reduced the proliferation and activation of primary lung fibroblasts, yet encouraged their migration. These results suggest MSC do not hinder the body's natural wound healing efforts but prevents unsolicited fibroblast activity and encourages epithelial growth and repair. The positive effects of MSC treatment were further examined in vivo, where MSC were shown to improve pathology in a bleomycin driven model of lung fibrosis.

The bleomycin model was examined and refined in order to more accurately represent therapeutic intervention, allowing for investigation of MSC as an anti-fibrotic cell therapy.

Publications

1. Tobin, L.M., **Cahill, E**. F., Mahon B.P and English, K. Notch signalling is required for the expansion of CD4+ CD25+ FoxP3+ regulatory T cells and tolerogenic dendritic cells by murine mesenchymal stem cells. *Submitted for publication.*

2. Griffin MD, Elliman SJ, **Cahill E**, English K, Ceredig R, Ritter T. Adult mesenchymal stromal cell therapy for inflammatory diseases: How well are we joining the dots? Stem Cells, (2013).

3. Heather Kavanagh, Cariosa Noone, **Emer Cahill**, Karen English, Camille Locht, Bernard P. Mahon. Attenuated *Bordetella pertussis* vaccine strain BPZE1 modulates allergen induced immunity and prevents allergic pulmonary pathology in a murine model. (2010). Clinical and experimental Allergy.

Abbreviations

AEC	Alveolar Epithelial Cells
APC	Antigen Presenting Cell
BAL	Bronchiolar Lavage Fluid
BSA	Bovine Serum Albumin
CD	Cluster of Differentiation
CFSE	Carboxyfluorescein Succinimidyl Ester
COPD	Chronic Obstructive Pulmonary Disease
CPI	Composite Physiologic Index
CPM	Counts Per Minute
CTGF	Connective Tissue Growth Factor
DC	Dendritic Cell
D_LCO	Diffusion Of Carbon Monoxide
EAE	Experimental Autoimmune Encephalomyelitis
ELISA	Enzyme Linked Immunosorbant Assay
EMT	Epithelial To Mesenchymal Transition
FACS	Fluorescence activated cell sorting
FGF	Fibroblast Growth Factor
FISH	Fluorescent In Situ Hybridization
FITC	Fluorescein Isothiocyanite
FoxP3	Forkhead Box P3
FVC	Forced Vital Capacity
GvHD	Graft versus Host Disease
HES	Hairy Enhancer Of Split
HEY	Hairy Related
HGF	Hepatocyte Growth Factor

HSC	Hematopoietic Stem Cell
hUTC	Human Umbilical Cord Stem Cells
IDO	Indoleamine 2,3- Dioxygenase
IFNγ	Interferon Gamma
IL	Interleukin
IN	Intranasal
IP	Intraperitonial
IPF	Idiopathic Pulmonary Fibrosis
IV	Intravenous
LPS	Lipopolysaccharide
M1	Classically Activated Macrophage
M2	Alternatively Activated Macrophage
MFI	Mean Fluorescent Intensity
MHC	Major Histocompatibility Complex
MI	Myocardial Infarction
MMP	Matrix Metalloproteinase
MSC	Mesenchymal Stromal Cells
NICD	Notch Intracellular Signalling Domain
NK	Natural Killer
OVA	Ovalbumin
PAMPS	Pathogen Associated Molecular Patterns
PBS	Phosphate Buffered Saline
PDGF	Platelet-Derived Growth Factor
PE	Phycoerytherin

Acknowledgements

I would like to thank my supervisor Bernie for all his help and guidance, and my honorary supervisor Karen who got sucked into the job by my constant, “Hey Karen….?”. Thank you so much for seeing me through to the end. Thank you to the immunology lab, Marc, Helen, Laura C. and Jen, you guys were so supportive and helpful, it was a pleasure to work with you all.

To my girls Laura, Heather, Cariosa Dee, and honorary girl club member, Darren. You guys made the whole experience fun, and kept me coming in every morning with a smile on my face, I genuinely wouldn’t have made it through without you guys, thank you! A big thanks to all the technicians, Nick and Noel, I’m sure you’ll have an easier life with me gone, sorry for breaking pretty much everything at some stage.

To my friends Lynn, Fran, Higgins, Dave, Gav, and Cormac, who I’d be lost without. I’m sure I wasn’t always the easiest person to live with, thank you all for being there for me, always.

I would like to thank my family, my parents, Noel and Angela and my brothers Dave and Eoin. My life as a perpetual student is over now I promise. Thank you for all the support and the laughs when I was struggling and for pretending to be interested when I babble on about my work.

Last but by no means least I would like to thank my boyfriend Ian. Thank you for supporting my decision to go back to school for another 4 years, thank you for actually making me stick at it for the 4 years, and thank you for keeping me sane in the meantime. I wouldn’t have made it this far without you.

Chapter 1

Introduction

1.1 Mesenchymal Stromal Cells

Murine mesenchymal stromal cells (MSC) were first discovered in 1966 as a population of plastic adherent bone marrow cells with the potential to differentiate into bone (Friedenstein *et al.*, 1966). Over 13 years later they were isolated from human bone marrow (Castromalaspina *et al.*, 1980). In 1990 Caplan *et al.* coined the term mesenchymal stem cells, based on the potential of these cells to differentiate into multiple cell types, thus suggesting them as a potential agent for regenerative medicine (Caplan, 1991). In 1999, multilineage differentiation of MSC was demonstrated *in vitro* (Pittenger *et al.*, 1999). Over the next decade scientists become more uncomfortable with the term mesenchymal stem cells, as MSC failed to meet previously established criteria for stemness; "a long-term self-renewing cell that is capable of differentiation into specific, multiple cell types *in vivo*" (Horwitz *et al.*, 2005). As the acronym had become synonymous with the cells, it had to be maintained, however "stem" was substituted for "stromal" to more accurately reflect the cell's phenotype. (Horwitz *et al.*, 2005).

A fundamental role of MSC in the bone marrow is controlling the homeostasis of hematopoietic stem cells (HSC) while maintaining their undifferentiated state. (Omatsu *et al.*, 2010). MSC also contribute to maintaining an immunosuppressive environment in the bone parenchyma, suppressing autoimmune reactions by maturing lymphocytes until naive immune cells are released to the periphery (Dazzi *et al.*, 2006). The interplay between MSC and immune cells coupled with the ease of MSC isolation and culture ex vivo, makes them an attractive candidate for cell therapy. Additionally, MSC demonstrate an immune privileged nature, expressing low levels of MHC class I and no MHC class II, allowing them to evade allogeneic reactions and NK killing (Grinnemo et al., 2004), In 2011 the cell therapy market was valued at $2.7

billion, by 2016 it is estimated to be worth somewhere close to $8.8 billion (Syed and Evans, 2013). To date the positive effects of MSC have been demonstrated in a broad range of experimental animal models including multiple sclerosis (MS) (Zappia *et al.*, 2005), type II diabetes (Lee *et al.*, 2006), myocardial infarction (Lee *et al.*, 2009) and critical limb ischemia (Lian *et al.*, 2010). MSC cell therapy has advanced from a purely academic to a clinical/ industrial setting. Osiris Therapeutics Inc., a USA-based company, are currently assessing their proprietary stem cell product, Prochymal$^{(R)}$ in multiple clinical trials. MSC have also shown promising results in phase II clinical trials for graft versus host disease (GvHD)(Kebriaei et al., 2009). Phase II trials are also being carried out on type 1 diabetes mellitus and chronic obstructive pulmonary disease (COPD)(Mills, 2009). The major focus of the cell therapy field currently is the application of MSC research as evidenced by the 308 clinical trials currently ongoing or in preparation (ClinicalTrials.gov), and FDA approval already granted for MSC in the treatment of multiple sclerosis (MS).

Despite the promising results from clinical trials, there are drawbacks to using MSC. Unlike pluripotent stem cells, the excessive *in vitro* culture of MSC can lead to a reduction in their efficacy and senescence (Katsara et al., 2011). One possible solution to this problem currently being explored in the generation of MSC from inducible pluripotent stem cells (iPSC). iPSC are genetically reprogrammed adult stromal cells that share morphology, proliferation, gene expression and differentiation capacity with embryonic stem cells (Takahashi et al., 2007). iPSC can replicate indefinitely and MSC differentiated from these cells retain this trait while still conforming to the characteristics of normal MSC (Gruenloh et al., 2011). These novel MSC are still undergoing safety testing but may have potential in regenerative medicine, allowing for autologus, patient matched cell replacement therapy.

1.2 Innate and Adaptive immunity

To understand the role of MSC in immune modulation it is important to consider the diversity and nuanced functions of cells that collectively comprise the innate and adaptive immune system. The innate immune system is the body's first line of defence against foreign pathogens. There exists an array of pathogen recognition receptors (PRR), which are expressed by innate immune cells and are responsible for identifying pathogen associated molecular patterns (PAMPS) on foreign material (Akira and Takeda, 2004). Upon activation, the primary objectives of the innate immune system are: the recruitment of immune cells to the site of infection through release of anaphylatoxins, cytokines and chemokines, the activation of the cytotoxic biochemical defences such as the complement cascade, and the removal of foreign material by phagocytic cells (Akira *et al.*, 2006). This is achieved through the actions and interactions of leukocytes. Neutrophils, being the most abundant leukocytes, are commonly the first cells to arrive at the site of infection. Along with basophils and eosinophils they destroy pathogenic cells through respiratory burst, a process by which destructive free radicals are generated and toxic proteins are released from granules in the cell. Mast cells, similarly release granules containing chemokines, cytokines and hormonal mediators, however, they are more commonly found in connective and mucosal tissues. Phagocytic leukocytes, including neutrophils, macrophages, and dendritic cells (DC) are responsible for engulfing and removing pathogens as well as dead cells from the affected site. DC and to a lesser extent macrophages also act as antigen presenting cells, designed to activate the adaptive immune system. DC are generated in the bone marrow and released into the periphery in an inactive form (Steinman and Cohn, 1973), they are constantly

sampling their surrounding environment for foreign material, which once encountered, they will engulf, process into peptides, and present to T cells on major histocompatibility complexes (MHC). Activation of T cells requires a second signal from co-stimulatory molecules such as CD80/CD86 on activated DC, which will interact with CD28 on the T cell surface (Banchereau and Steinman, 1998). Distinct form other immune cells, natural killer cells are responsible for targeting tumor cells and virus infected cells of the host, responding to low levels of "self" antigens known as MHC I. Cells expressing low levels of MHC I are eliminated by NK cells through induction of apoptosis (Noone *et al*., 2013).

The adaptive immune system, comprised of T lymphocytes and B lymphocytes, orchestrates specific responses to infection based on immunological memory, thus adapting the body against reoccurring infection (Gershon *et al.*, 1971). A corner stone of the adaptive immune system is the ability to distinguish self from non-self. T cells and B cells are selected or deleted based on their auto reactivity before they are released from the thymus or bone marrow respectively. T cells that fail to recognise self-MHC or strongly react to self-antigen undergo apoptosis in processes known as positive selection and negative selection respectively (Cantor and Weissman, 1976, Scollay *et al.*, 1980). The remaining T cells are termed naïve T cells, they are permitted to leave the thymus, and will activate and proliferate when they come in contact with antigen cognate to their T cell receptor. In the bone marrow pre and pro B cells are B cells are tested for reaction to self-antigens. If they express low affinity to self the recombination activating genes (RAG) are switched off, otherwise they undergo apoptosis (Buhl et al., 2000). Upon activation T cells either kill pathogen infected cells directly ($CD8^+$ T cells) or through influencing the microenvironment and recruiting other immune cells ($CD4^+$ T cells). B cells function through the

production of antibodies, resulting in the elimination of extracellular microorganisms (Coombs et al., 1969).

1.3 The effect of MSC on immune cells

Initially, *in vitro* work provided insights into MSC interactions with cells of both the innate and the adaptive immune system. More often than not, MSC have an inhibitory effect on immune cells, impeding activation and proliferation, neutrophils are an exception to this observation (Cassatella et al., 2011, Raffaghello et al., 2008). Human MSC interaction with IL-8 activated neutrophils was shown to improve cellular fitness and survival at ratios as low as 1:500. Co-culture also increased neutrophil respiratory burst capacity (Cassatella *et al.*, 2011, Raffaghello *et al.*, 2008). Conversely, MSC cultured *in vitro* with other granular immune cells, namely mast cells, resulted in inhibition of cytokine production and degranulation by both human and mouse MSC (Su *et al.*, 2011, Brown *et al.*, 2011). A key *in vivo* study also demonstrated murine MSC capacity to inhibit infiltration of eosinophils in a mouse model of allergic asthma (Kavanagh and Mahon, 2011). MSC interaction with phagocytic macrophages and DC also resulted in inhibition of activation but more importantly switching from a pro-inflammatory phenotype to regulatory one. *In vitro* co-culture of human MSC with macrophages resulted in a reduction in TNFα and IL-12 production and increased IL-10 and IL-6 secretion. This was accompanied by an increase the expression of a cell surface marker associated with alternatively activated macrophages (Kim and Hematti, 2009). Similar results were seen in macrophages co-cultured with murine MSC, where macrophages were driven from a classically activated pro-inflammatory (M1) phenotype to an alternatively activated pro-repair (M2) phenotype. This process, when utilised in a mouse model of sepsis, helped

prevent the infiltration of neutrophils and thus reduced pathology in the gut (Nemeth et al., 2009). MSC "education" of DC to become regulatory DC has been more intensely studied than MSC and macrophages. Co-culture experiments using human and murine MSC showed a reduction in DC activation, reduced co-stimulatory cell surface markers, and a reduction in IL-12 production (Djouad et al., 2007, English et al., 2008, Jiang et al., 2005). *In vitro* studies with murine MSC have also shown a reduction in DC migration and antigen presentation (English *et al.*, 2008). MSC have further inhibitory effects on natural killer cells (NK), preventing proliferation of freshly isolated human NK cells, while inhibiting the cytotoxic activity of IL-2 or IL-15 activated NK cells (Spaggiari et al., 2006). Low level expression of MHC class I on MSC allows them to avoid resting NK cell mediated apoptosis but not the actions of activated NK cells. However, IFNγ stimulation of human MSC was shown to increase their MHC class I expression, resulting in increased resilience to NK killing (Spaggiari *et al.*, 2006, Noone *et al.*, 2013). MSC effects on immune cells are summarised in figure 1.1.

MSC also interact with and influence cells of the adaptive immune system. Though there are few consistent reports on the influence of MSC on B cells. Human MSC have been reported to increase the *in vitro* proliferation of activated B cells isolated from patients with systemic lupus erythematosus (SLE), compared to healthy donors (Traggiai *et al.*, 2008). On the other hand, several publications show a more inhibitory effect, with MSC suppressing B cell activation and proliferation in both human and mouse cells (Corcione *et al.*, 2006, Glennie *et al.*, 2005, Schena *et al.*, 2010). MSC effect on T cells has been extensively studied. MSC are known to induce T cell anergy, leading T cells to become unresponsive to proliferative stimuli and unable to produce cytokines (Zappia *et al.*, 2005). In addition MSC inhibit the

differentiation of Th-17 cells (Duffy *et al.*, 2011) and promote the expansion of regulatory T cells (Treg) (Del Papa *et al.*, 2013, English *et al.*, 2009, Selmani *et al.*, 2008) (Fig. 1.1).

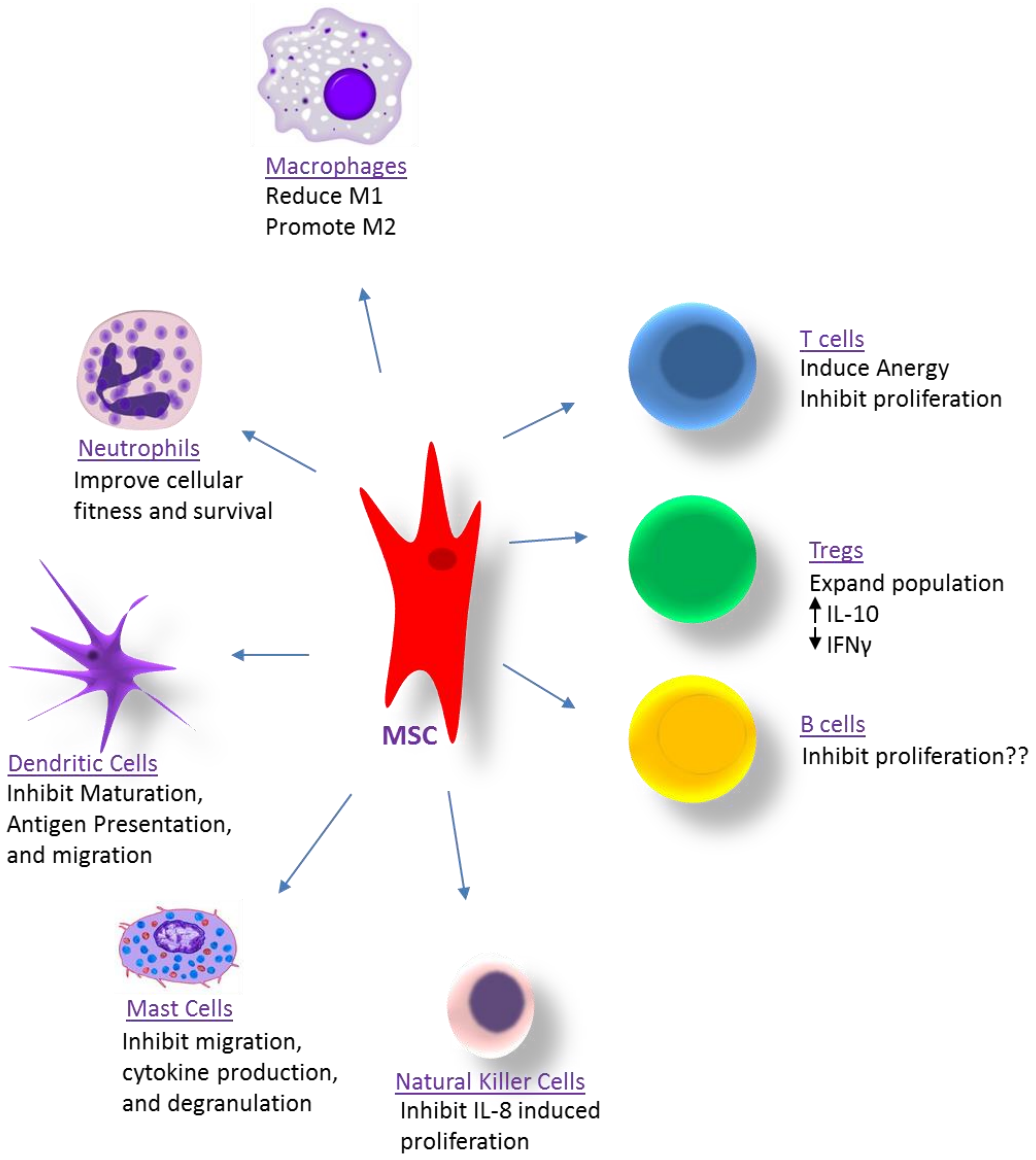

Fig 1.1 Summary of MSC effects on immune cells. MSC inhibit the proliferation of NK cells, T cells, and in some cases B cells. They promote the expansion of Treg cells and drive macrophages towards a regulatory M2 phenotype. They also inhibit the migration and function of DC and mast cells. Although predominately inhibitory towards immune cells, MSC may promote the cellular fitness and survival of neutrophils.

1.4 Soluble factors involved in MSC immunomodulation

MSC communicate with immune cells through the release of soluble mediators, through direct cell-cell contact or through a combination of both. The latter is best demonstrated by MSC production of nitric oxide and the enzyme indoleamine 2,3-dioxygenesae-1 (IDO), both of which require initial IFNγ stimulation of MSC (Krampera et al., 2006, Ren et al., 2008, Ryan et al., 2007). Nitric oxide is a bioactive gas implicated in murine MSC mediated inhibition of T cell proliferation (Ren et al., 2008, Sato et al., 2007). Both murine and human MSC use IDO, an enzyme which catalyses the degradation of tryptophan to N-formyl-kynurenine, to regulate T cell proliferation (English et al., 2007). Murine MSC release of IDO was further implicated in MSC regulation of T cells in an animal model of renal allograft transplantation. Administration of MSC as a cellular therapy resulted in donor specific tolerance through up-regulation of Treg. Decreased Th1 cytokines in favour of Th2, decreased levels of donor-specific IgG, and inhibition of DC maturation were mediated through MSC release of IDO (Ge *et al.*, 2010). The up regulation of various soluble mediators in response to specific stimuli supports the hypothesis that MSC can sense their environment and adapt their responses accordingly. Previous studies in human MSC have also demonstrated that activation of MSC by different TLR signals can result in a pro-inflammatory phenotype or an immunosuppressive one (Waterman et al., 2010). Further, in a murine model of sepsis, Nemeth and colleagues elegantly demonstrate the importance TNFα stimulation of MSC to achieve PGE2 dependent expansion of alternatively activated macrophages. TNFα present in the sepsis model bound to TNFR-1 on the surface of MSC and through NFκB signalling, up-regulated expression of COX-2, a pre-requisite of PGE2 formation (Nemeth *et al.*, 2009).

Several studies have revealed that the lipid mediator PGE2 plays a considerable role in MSC modulation of multiple cell types. Production of PGE2 by murine MSC plays a definitive role in the expansion of Treg cells (English et al., 2009), the inhibition of Th17 cell differentiation (Duffy et al., 2011) and the switching of macrophages to an M2 phenotype (Nemeth *et al.*, 2009). In human MSC, PGE2 signalling was shown to be responsible for MSC inhibition of NK cell activation (Spaggiari et al., 2008) and mast cell infiltration in a model of contact hypersensitivity (Su *et al.*, 2011). Taken together these studies suggest a pivotal role for PGE2 signalling in MSC immunomodulation, however, many of the above studies cite a requirement for cell-cell contact signalling in conjunction with soluble mediator release to illicit immunomodulatory effects (Duffy et al., 2011, English et al., 2009, Spaggiari et al., 2008).

1.5 Cell contact dependent MSC immunomodulation

There is considerable overlap between studies into soluble mediators produced by MSC and cell contact signalling, though, far less is known about cell-cell contact. English *et al.* demonstrated this using a transwell system, where they highlighted a requirement for PGE2 and TGFβ signalling but also a need for cell contact (English et al., 2009). Further evidence of a role for contact dependent signalling came from Akiyama *et al.*, who showed that MSC administration in a mouse model of experimental colitis led to the reduction of a Th-17 phenotype and an increase in Treg. This study elegantly identified FASL signalling as the key contact dependent mechanism utilised by MSC. Binding of FASL to its receptor on T cells resulted in increased apoptosis of activated T cells *in vitro* and *in vivo*, the apoptotic cells stimulated the secretion of TGF- β from macrophages leading to an increase in Treg

(Akiyama *et al.*, 2012). Another potential candidate for MSC contact signalling is the B7 homolog and co-stimulatory programmed cell death receptor (PD) and ligand (PD-L). Both regulatory molecules have been implicated in MSC immunomodulation, with neutralising antibodies against PD-1 resulting in murine MSC suppression of T cell and B cell proliferation *in vitro* (Augello *et al.*, 2005).

1.6 Notch Signalling

The Notch family of receptors (Notch 1-4) and ligands (Jagged 1, 2, Delta-like ligand 1, 2 and 4) are part of a highly conserved signalling pathway, primarily involved in cell growth and development, dictating how cells respond to developmental cues (Artavanis-Tsakonas *et al.*, 1999). Their signalling is involved in diverse cell fate decisions such as the generation of neural glial cells, development of tip-cells in angiogenic sprouting and ventricular myocardial development (Furukawa *et al.*, 2000, Hellstrom *et al.*, 2007, Niessen and Karsan, 2008). Signalling occurs through the binding of Jagged or Delta-like ligands to the extracellular binding subunit of the hetrodimeric Notch receptor complex, followed by cleavage within the transmembrane domain by a metalloprotease enzyme called γ-secretase, this cleavage releases the Notch intracellular signalling domain (NCID) from the cell membrane. The NCID translocates to the nucleus where it heterodimerises with the transcription factor RBP-J to form a nuclear transcription complex and regulates the expression of the effector genes hairy enhancer of split (HES) and hairy related (HEY) (Gordon *et al.*, 2008). The signalling pathway is illustrated in figure 1.2.

The Notch family of receptors and ligands are widely expressed on many cell types including immune cells and MSC. Early studies examining the role of Notch signalling in immune cells involved immature DC and soluble ligand Jagged 1.

Following DC stimulation with soluble Jagged 1, there was an increase in DC maturation markers and proliferation (Weijzen *et al.*, 2002). The following year another study found that DC isolated from Notch-1 deficient mice had significantly lower levels of MHC Class II and the co-stimulatory marker CD86, classic markers of DC maturation. Interestingly this study also demonstrated that fibroblasts overexpressing Jagged 1 cultured with DC, inhibited the maturation of the cells, leading to the accumulation of immature DC precursors (Cheng *et al.*, 2003). This conflicting data was partially explained by Bugeon *et al.* using soluble Jagged 1 to activate immature DC. They observed a similar increase in maturation markers to that seen after lipopolysaccharide (LPS) activation, however only activation with Jagged 1 resulted in an increase in the cytokines IL-10 and IL-2. Further, these novel DC promoted the proliferation of $CD4^+CD25^+$ T cells, which in turn were capable of suppressing $CD4^+CD25^-$ T cells (Bugeon *et al.*, 2008).

In 2004 Fu *et al.* demonstrated that TGFβ signalling can induce $CD4^+CD25^+FoxP3^+$ Treg cells from a $CD4^+$ population (Fu *et al.*, 2004). More recently evidence has emerged for Notch signalling is an essential component of this process. Inhibition of Notch translocation to the nucleus by GSI prevented the expansion of Treg cells, even in the presence of TGFβ (Samon *et al.*, 2008). Overexpression studies with Jagged 1 and T cells also showed a decrease in IL-2 production and an increase in TGFβ. The resulting Treg cells were shown to be functionally suppressive in a lymphocyte proliferation assay (Yvon *et al.*, 2003).

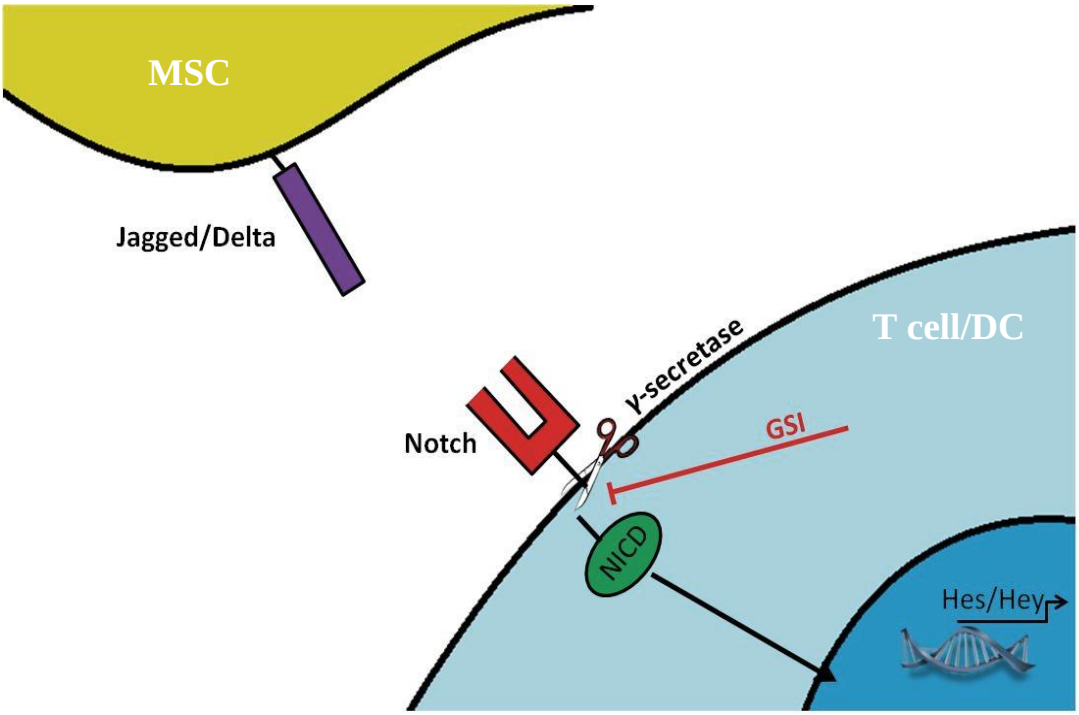

Fig 1.2 The Notch signalling pathway. Signalling occurs through the binding of a Jagged or Delta-like ligands to the extracellular binding subunit of the hetrodimeric Notch receptor complex, followed by cleavage within the transmembrane domain by a metalloprotease enzyme called γ-secretase, this cleavage then releases the Notch intracellular signalling domain (NCID) from the cell membrane. The NCID translocates to the nucleus where it heterodimerises with the transcription factor RBP-J to form a nuclear transcription complex and regulates the expression of the effector genes hairy enhancer of split (HES) and hairy related (HEY)

1.7 MSC and DC

As previously mentioned, the primary objective of DC is to sample the environment for foreign material, engulf and process the material into smaller peptides, migrate to the lymph nodes and present the antigen to antigen specific T cells (Cella et al., 1997). MSC have been reported to interrupt all of these processes, ultimately preventing T cell activation and proliferation. MSC disruption of maturation was discovered through *in vitro* co-culture experiments, they demonstrated MSC reduced the expression of co-stimulatory molecules CD80 and CD86, and reduced cell surface expression of MHC class II (Jiang *et al.*, 2005). Inhibition of maturation was achieved in a dose dependent manner and soluble factors, namely IL-6 played an important role in this effect, however Djouad *et al.* alluded to the requirement for a contact signal (Nauta *et al.*, 2006, Djouad *et al.*, 2007).

MSC disruption of antigen presentation was established by examining the presentation of the antigen ovalbumin (OVA) following co-culture with MSC. OVA pulsed DC which were co-cultured with MSC significantly reduced the amount of proliferation of antigen specific $CD4^+$ T cells (English *et al.*, 2008). Similarly DC presentation of OVA by MHC class I receptors to $CD8^+$ T cells was impaired by MSC co-culture (Chiesa *et al.*, 2011).

In addition to disrupting DC maturation and antigen presentation, MSC had an inhibitory effect on the migration of DC. This was a result of increased expression of the adhesion molecules E-cadherin and reduced expression of the chemokine receptor CCR7, thus impairing migration towards the chemokine CCL19. (English *et al.*, 2008). CCR7 is the chemokine receptor responsible for migration of DC towards to the lymph node, this down regulation of this receptor means DC do not migrate to the

lymph node and thus cannot interact with T cells and leads to impaired T cell priming (Sousa et al., 1997). The impact of MSC on DC migration was best demonstrated by Chiesa and colleagues. DC pulsed with OVA were fluorescently tagged with CFSE and subcutaneously injected into syngeneic mice followed by IV administration of MSC. These mice previously received an injection of DO11.10 naïve T cells. T cells from DO11.10 mice are genetically modified to recognise OVA. Analysis of draining lymph nodes was examined after 3 days. MSC treated mice had significantly fewer DC in the lymph nodes than PBS control mice, indicating impaired migration of activated DC to the lymph node (Chiesa *et al.*, 2011).

1.8 MSC and T cells

MSC modulation of lymphocytes has become one of the defining characteristics of this cell type. As discussed above MSC mechanisms of inhibition can occur through various pathways involving cell contact and soluble factors (Di Nicola *et al.*, 2002, Krampera *et al.*, 2003). MSC are believed to modulate T cells through direct suppression of proliferation, induction of T cell anergy, class switching and expansion of Treg cells. In 2003, Krampera *et al.* showed that MSC inhibited antigen specific memory and effector T cell proliferation in a contact dependent manner, potentially through physically disrupting APC interactions with T cells. This theory has since been modified as our understanding of MSC, APC and T cell interactions has deepened (Krampera *et al.*, 2003). Studies on the proliferation of T cells following MSC co-culture revealed an impaired transition through the stages of cell cycle division. T cells cultured with MSC did not progress past G1 phase, however, when removed from culture and stimulated there was increased expression of IFNγ, but no increase in proliferation, these results suggest MSC induced a state of

split T cell anergy, where not all function is anergised (Glennie *et al.*, 2005). Induction of T cell anergy was further examined in an animal model of experimental autoimmune encephalomyelitis (EAE), an autoimmune disease driven by T cells and macrophages. Following administration of MSC there was a significant reduction in inflammatory infiltrates and a reduction in demyelination, T cells isolated from MSC treated EAE animals were stimulated ex vivo and found to be un-responsive to the encephalitogenic peptide MOG35-55 (Zappia *et al.*, 2005). Given the right environmental cues, MSC are capable of polarising T cells towards Th1 or Th2 phenotypes. *In vitro* analysis of the cytokine profile of T cells following MSC co-culture revealed a down regulation in IFNγ, TNFα, and IL-1α & β, and an up-regulation in Th2 cytokines IL-3, IL-5, IL-10, and IL-13 (Batten *et al.*, 2006). In a TNFα rich animal model of GvHD, administration of MSC reduced levels of $IFN\gamma^+$ T cells and increased $IL\text{-}4^+$ T cells, indicating *in vivo* skewing of T helper cells to a Th2 phenotype (Lu *et al.*, 2009). Conversely when MSC are used in a Th2 driven murine asthma model, they reduce levels of IL-4, IL-5 and IL-13 while increasing levels of IFNγ (Kavanagh et al., 2010). Finally, MSC have been shown to expand the Treg population naturally found in the body, a trait discussed in greater detail in the next section.

1.9 MSC and Regulatory T cells

Immunologcal tolerance is an essential part of immune regulation, and as such has many check points to prevent auto immunity. As previously discussed, positive and negative selection ensures the abolition of self-reactive T cells, however a small sub-population of $CD4^+CD25^+FoxP3^+$ T cells known as regulatory T cells (Treg), play

a crucial role in the suppression of excessive or inappropriate T cell proliferation in the periphery.

Stimulation of MSC with IFNγ can up-regulate the expression of MHC molecules on the cell surface, rendering them susceptible to clearance by the host immune system (Le Blanc et al., 2003). For this reason it is believed that the long term effects seen with MSC therapy are a result of MSC education of immune cells and employment of the body's natural regulatory machinery. This hypothesis is supported by MSC expansion of Treg cells (Del Papa *et al.*, 2013, English *et al.*, 2009, Ge *et al.*, 2010, Kavanagh and Mahon, 2011, Selmani *et al.*, 2008) and education of undifferentiated to tolerogenic DC (Beyth *et al.*, 2005, Li *et al.*, 2008).

MSC co-cultured with a purified population of $CD4^+$ T cells were found to expand a population of $CD4^+CD25^{high}FoxP3^+$ Treg cells, when these cells were re-purified and cultured with MHC mis-matched lymphocytes, they significantly reduced alloantigen driven proliferation. MSC expansion of Treg required a cell contact signal, however there was a non-redundant role for PGE2 and TGFβ signalling (English *et al.*, 2009). In 2011 Kavanagh *et al.* demonstrated the relevance of MSC expansion of Treg in an OVA driven animal model of allergic asthma. Mice were primed by intraperitonial injection of OVA and then challenged by intranasal instillation to produce an allergic response. MSC administration resulted in reduced pathology, inflammation and antigen specific IgE production. In addition, there was a reduction in IL-4 and an increase in IL-10 levels in bronchial alveolar fluid (BAL) and from OVA stimulated splenocytes. Ablation of Treg through administration of cyclophosphamide abrogated the effects of MSC therapy demonstrating a critical role for Treg expansion by MSC (Kavanagh and Mahon, 2011).

While regulatory cells are often associated with the adaptive immune system, the past 10 years has uncovered regulatory cells associated with the innate immune system, namely regulatory macrophages (M2), previously discussed in this chapter, and regulatory or tolerogenic DC. These cells express lower levels of MHC Class II and co-stimulatory markers, reduced IL-12p70 and increased IL-10 production (Morelli and Thomson, 2007). These tolerogenic DC are capable of inducing Treg cells for a naïve T cell population (Beyth *et al.*, 2005, Bugeon *et al.*, 2008, Nauta *et al.*, 2006). The benefits of tolerogenic DC have been observed *in vivo*, in an animal model of organ transplantation. Higher levels of both tolerogenic DC and Treg cells were observed in the spleens of the recipient animals following MSC administration. MSC education of these regulatory cells is believed to be responsible for the tolerance of the allogeneic graft (Ge *et al.*, 2009).

1.10 Fibrosis, wound healing, and repair in the airway

Pulmonary fibrosis is a chronic disease associated with remodelling of the organ architecture and excessive deposition of parenchymal tissue by activated fibroblasts. This leads to formation of scar tissue, which becomes a permanent fixture once formed. Treatment is based upon reducing or preventing further progression, a strategy contingent on identifying and reversing the underlying cause. Fibrosis commonly results from chronic stimuli, i.e. physical, chemical, or biological sources, however many cases are classified as idiopathic. The cause of idiopathic pulmonary fibrosis (IPF), as the name suggests, is unknown, and is associated with a poor survival prognosis of 2-4 years (Raghu et al., 2006). Many researchers believe an underlying genetic predisposition triggers the disease following an initial epithelial injury (Maher et al., 2007, Selman et al., 2006). Unfortunately without a deeper understanding of

the onset of IPF the disease is extremely difficult to treat leaving lung transplantation as the only treatment option in severe cases.

1.11 Epidemiology of Pulmonary Fibrosis

In 2000 the American Thoracic Society (ATS) and the European Respiratory Society (ERS) released guidelines for the diagnosis and treatment of idiopathic pulmonary fibrosis (IPF) (ATS, 2000). While these were useful, it wasn't until the guidelines were updated in 2011 that diagnosis of IPF gained accuracy (Raghu *et al.*, 2011). For this reason studying the epidemiology of IPF has proven very difficult leading to large variability between published studies. In 2012 Nalysnyk *et al.* published a literature review of 15 publications pertaining to epidemiology, incidence and prevalence of IPF between 1990 and August of 2011. They found that when following tight definitions of IPF the prevalence in the USA is between 14 and 27.9 cases per 100,000 with an annual incidence of 6.8–8.8 per 100,000. In Europe the prevalence is 1.25 to 23.4 per 100,000, and the annual incidence is 0.22 to 7.4 per 100,000 population. There a higher prevalence in men than women in both the USA and Europe with the exception of Norway, and incidence increases with age. This means there are approximately 89,000 IPF patients in the USA with 14,000–34,000 new patients per annum. In the UK the figure stands somewhere around 15,000 and approximately 5,000 new patients diagnosed each year (Nalysnyk *et al.*, 2012). According to the Irish Central Statistics Office (CSO) there were 1,334 deaths from chronic lower respiratory diseases in 2010 and 1488 in 2011, accounting for 4.8% and 5.2% respectively of all deaths each year (Central Statistics (Office, 2010).

1.12 Wound Healing and the immune system.

Normal wound healing can be divided into three principle stages; inflammation, proliferation and repair (Fig. 1.2). In the case of pulmonary fibrosis the initial injury can come in the form of a chemical, biological or physical insult, more often than not the stimulus is chronic (Wilson and Wynn, 2009). Irrespective of the source, damage to the lung epithelium results in exposure of endothelium and the basement membrane proteins leading to the recruitment and activation of innate and adaptive immune cells (Wick et al., 2013).

Inflammation commonly occurs within hours of injury. Early inflammation involves the infiltration of neutrophils by diapedesis in response to TGFβ secretion from α granules in the cytoplasm of platelets. They phagocytose and remove any foreign bodies and damaged tissue (Robson *et al.*, 2001). Neutrophils generally do not persist in the wound site, once they have served their purpose they undergo apoptosis and macrophages take over (Wick et al., 2013). The persistence of neutrophils results in chronic inflammation associated with some chronic "non-healing" wounds. Late inflammation is characterised by the arrival of macrophages which are attracted to the site of injury by cytokines such as PDGF and TGFβ, as well as the connective tissue protein elastin, and collagen breakdown products (Ramasastry, 2005). Macrophages are the primary source of TGFβ and FGF which promote fibroblast activation and proliferation (Robson *et al.*, 2001), they are also the primary source of matrix matalloproteinases (MMP), specifically MMP2 and MMP9, both responsible for the breakdown of collagen (Okuma *et al.*, 2004). In an inflammatory Th1 predominant environment macrophages tend towards a classically activated phenotype, as inflammation subsides monocytes can become alternatively activated (M2). M2 macrophages tend to be more anti-inflammatory and produce tissue inhibitors of matrix matalloproteinases (TIMP) (Sica and Mantovani, 2012).

The final cell type recruited is the lymphocyte, these cells are responsible for the increase in IFNγ and TNFα. Apart from the production of cytokines, their role, if any, in wound healing and fibrosis has not been determined, however, there is some evidence that Treg cells have a positive effect on disease state by dampening the inflammatory response (Wilson and Wynn, 2009).

The proliferative phase involves the migration of fibroblasts from the surrounding tissue into the site of damage, they are attracted by TGFβ and PDGF released by platelets and macrophages (Hunt, 1988). The fibroblast will secrete the matrix proteins hyaluronan, fibronectin, proteoglycans as well as type I and II pro-collagen (Hunt, 1988). Myofibroblasts, the activated form of fibroblasts are involved in wound contraction by attaching to collagen and fibronectin in the extracellular matrix and retracting their pseudopodia. Collagen deposited by the fibroblasts acts as structural support to the intracellular matrix (Eckes *et al.*, 2000).

The final phase of wound healing, repair, is a delicate balance between the degradation of scar tissue and the generation of new epithelium, and depending on the type of wound can take years (Robson et al., 2001). MMPs are produced by fibroblasts, macrophages and neutrophils and their activity is closely regulated by inhibitors called tissue inhibitors of matrix metalloproteinases (TIMPs). As remodelling continues the presence of inflammatory cells and fibroblasts is no longer required and they undergo apoptosis, this is critical for resolution of wound healing and the aberrant signalling at this juncture is believed to play a critical role in fibrosis. Fibroblasts isolated from patients with IPF have been shown to be more resistant to apoptosis then those from a healthy lung (Moodley *et al.*, 2003) (Fig. 1.2).

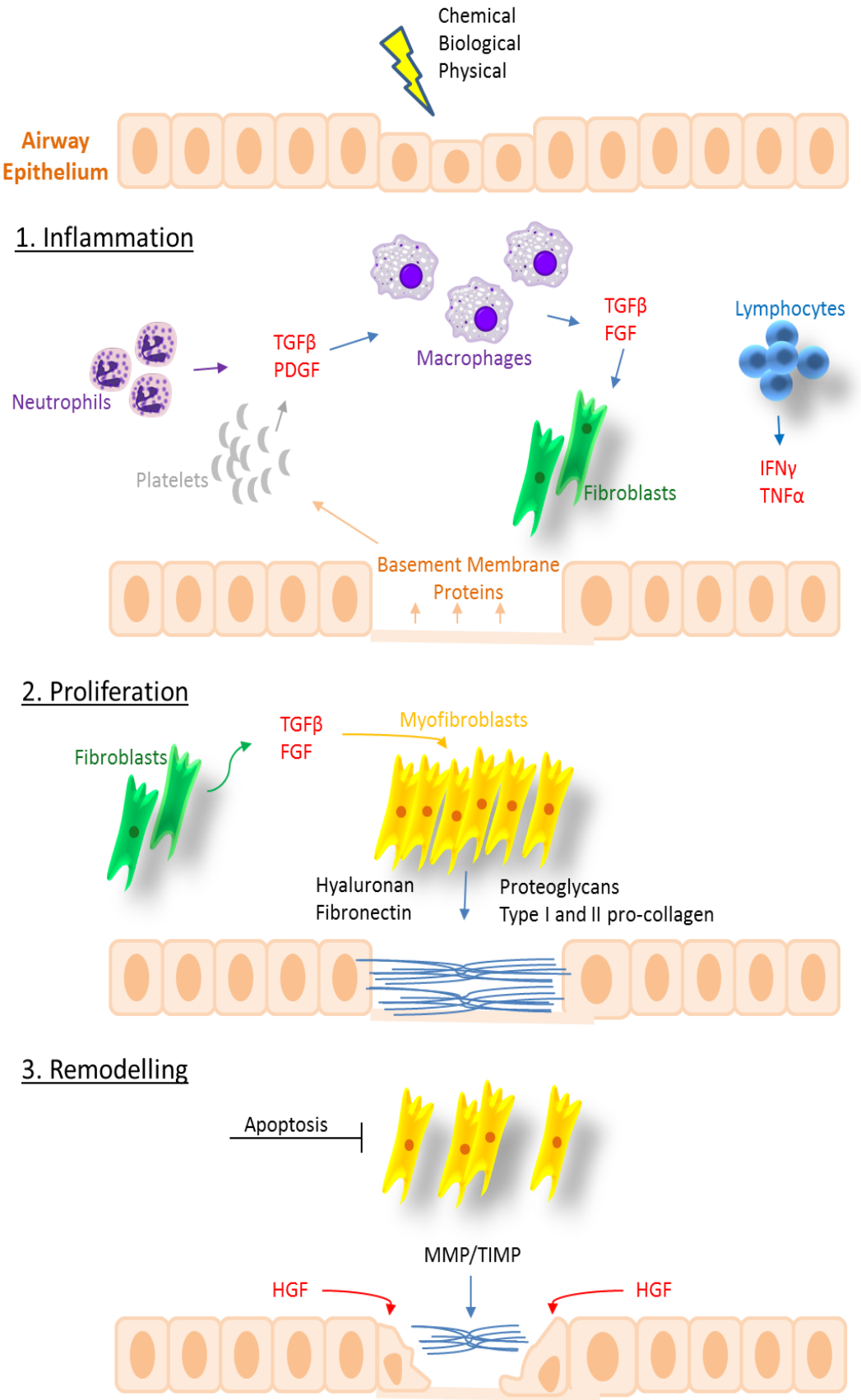
Chemical
Biological
Physical
Airway
Epithelium
1. Inflammation
Neutrophils
TGFβ
PDGF
Macrophages
TGFβ
FGF
Lymphocytes
Platelets
Fibroblasts
IFNγ
TNFα
Basement Membrane
Proteins
2. Proliferation
Fibroblasts
TGFβ
FGF
Myofibroblasts
Hyaluronan
Fibronectin
Proteoglycans
Type I and II pro-collagen
3. Remodelling
Apoptosis
MMP/TIMP
HGF
HGF

Fig 1.2 Stages of Normal Wound Healing. Damage to airway epithelium leads to exposure of basement membrane proteins which attract platelets to the site of damage. Platelets, through the release of TGFβ and PDGF recruit neutrophils and ultimately macrophages, thus initiating the first phase of wound healing, the inflammatory phase. The release of TGFβ and FGF by macrophages activates fibroblasts to myofibroblasts. The inflammatory environment created leads to neutrophil infiltration. The second phase of wound healing involves the proliferation of fibroblasts and myofibroblasts, these cells create a backbone across the wound area and myofibroblasts contraction leads to closure of the wound edges. They also produce ECM proteins and collagen. The final phase of wound healing is remodelling. This phase is maintained for weeks to months and involves the gradual replacement of collagenous and fibrosis scar tissue with functional epithelial cells. Activated fibroblasts undergo apoptosis and MMPs breakdown the scar tissue. HGF is a key growth factor in encouraging the proliferation of alveolar epithelial cells into the wound site.

1.13 Fibroblasts, Myofibroblasts, and Fibrosis

Fibrosis is a well characterised disease state and has been studied extensively in the last number of years, however it is still unclear precisely what causes normal wound healing to become dysregulated, leading to the excessive deposition of collagen and destruction of functional tissue. Fibroblasts are known to be a major cause of disease pathology, more specifically, the activated form, myofibroblasts, however it is important to note that their initial presence in the site of injury is essential to the healing process (Eckes et al., 2000). As mentioned above myofibroblasts play an important role in wound contraction and along with fibroblasts their production of ECM products protects the basement membrane from further exposure to the external environment. Fibrosis occurs with excessive proliferation of myofibroblasts potentially through resistance to programmed cell death (Moodley *et al.*, 2003). This leads to disparity between the deposition and breakdown of collagen and an imbalance between MMPs and TIMPs (Gillard et al., 2004). Patients with IPF also have higher numbers of myofibroblasts and higher levels of TGFβ in their lungs (King *et al.*, 2011). Myofibroblasts are characterised by the expression of α-smooth muscle actin (αSMA) and increased production of collagen, and are thought to arise from TGFβ activation of fibroblasts (Hu *et al.*, 2003). Another potential source of myofibroblasts is alveolar epithelial cells (AEC) through a process of epithelial to mesenchymal transition (EMT). EMT is a process by which epithelial cells loose cell-cell contact, re-organise their actin cytoskeleton, and acquire a fibroblast like morphology (Hay, 1995). In fibrotic lungs, AEC are believed to undergo this process under the influence of TGFβ, resulting in increased myofibroblasts marker expression and collagen deposition (Willis *et al.*, 2005).

1.14 Therapeutic Approaches to Pulmonary Fibrosis

The majority of drugs used in clinical trials for lung fibrosis were previously tested in animal models, unfortunately there has been a poor correlation between animal model success and results achieved in clinical trials, the potential reasoning behind this, is discussed in section 1.4.1.

1.15 Murine models

Several animal models of pulmonary lung fibrosis have been established, some of these include the use of organic particles such as silica, irradiation, gene transfer of cytokines, namely TGFβ, TNFα or IL-1β, adoptive transfer of fibroblasts, and the most common model, bleomycin. There are advantages and disadvantages to each model, and while their use has helped characterise the milieu associated with the pulmonary fibrosis, none of the models fully recapitulate the human disease (Moore and Hogaboam, 2008).

Bleomycin was originally used in the treatment of various cancers, however generation of pulmonary fibrosis in up to 5% of patients receiving the drug limited its use. The damaged to lung architecture was caused by bleomycin induced reactive oxygen species and cleavage of DNA strands (Lown and Sim, 1977). Many cytokine and chemokines have also been implicated in bleomycin induced pulmonary fibrosis including TNFα (Piguet et al., 1989), TGFβ (Nakao et al., 1999), IL-1β (Scheule et al., 1992), macrophage-inflammatory protein-1α (MIP 1α) (Smith et al., 1994), and monocyte chemoattractant protein-1 (MCP-1) (Zhang et al., 1994), though the exact mechanism of action is still unclear. Intranasal instillation of the drug results initially in damage to the alveolar epithelial cells followed by infiltration of inflammatory cells, proliferation of fibroblasts and deposition of extracellular matrix. Histological

changes are generally observed by day 14 and collagen deposition peaks anywhere between days 21 to 28 (Moore and Hogaboam, 2008). This model of fibrosis is self-limiting and after 28 days begins to resolve, this is one of the major differences from the human disease, and in the absence of the continuous stimulus suspected to be involved in the human disease, the benefits seen in the animal model can fail to translate in clinical trials. There are also differences between mouse strains, C57BL/6 mice are high responders to bleomycin treatment, resulting in reproducible fibrosis, however, they also recover faster. DBA/2 mice are medium responders and BALB/c mice are low responders. Importantly both of these strains are Th2 biased, while C57BL/6 mice are Th1 biased. Given the capacity for IFNγ to inhibit TGFβ and reduce collagen production, this bias have been suggested as a reason for the inconsistency in bleomycin induced fibrosis between strains (Chung et al., 2003).

One of the major issues arising from recent *in vivo* publications is the time point at which treatment is administered. In 2006 Chaudhary *et al.* described a switch in the cytokine profile associated with bleomycin treated rats, describing an initial increase in inflammatory cytokines, with an increase in fibrotic cytokines following later. This "Switch" was hypothesised to occur between day 7 and 9 (Chaudhary *et al.*, 2006). Following on from this work Moeller et al published a review examining all publications involving anti-fibrotic therapy in the bleomycin model between 1980 and 2006. 232 publications were identified and of those boasting successful anti-fibrotic effects only 13 documented administration of the therapeutic after the switch from inflammatory environment to fibrotic one. The authors believe that many of the beneficial effects witnessed in these studies were associated with reduced inflammation in the early stages of the disease. Unfortunately when these results are

translated to a clinical setting where fibrosis has already occurred they cannot recreate the same efficacy (Moeller *et al.,* 2008).

1.16 Drug Intervention

To date the main focus in the treatment of fibrosis has been on controlling and reducing the associated inflammation, either through inhibition of the activation and proliferation of immune cells or by killing them. This approach has demonstrated limited success as it does not address the underlying fibrotic condition. Examples of such therapies include cytokine antibodies such as anti- TGFβ (Arribillaga *et al.,* 2011, Kolb *et al.,* 2001), anti-PDGF (Chaudhary *et al.,* 2007), TNFα inhibitors (Piguet and Vesin, 1994), and angiotension receptor blockers (Marshall *et al.*, 2004, Molina-Molina *et al.,* 2006). Despite the number of papers published about anti-fibrotic compounds, and trails testing new drug candidates, lung transplant is still the most common treatment for idiopathic pulmonary fibrosis. The future of therapeutic discovery will more than likely lie in targeting excessive fibrosis and not associated inflammation.

There have been many studies on blocking TGFβ signalling as potential treatments for lung fibrosis. Recently Arribillaga *et al.* described the TGFβ inhibitor peptide P17 as a potential drug candidate. Studies *in vitro* on human lung fibroblasts showed a decrease in the production of connective tissue growth factor (CTGF), a mediator of TGFβ1 signalling. *In vivo* studies using bleomycin treated mice receiving P17 two days after bleomycin IN, showed a reduction in αSMA expressing myofibroblasts in lung tissue sections, a decrease in lymphocyte infiltration and lower mRNA expression levels of collagen and fibronectinin lung tissue (Arribillaga *et al.,* 2011).

The angiotensin II (ANG II) receptor antagonist Losartan was originally approved for the treatment of systemic hypertension and diabetic nephropathy, however several labs have tested the drug in animal models of pulmonary fibrosis and demonstrated inhibition of fibrotic progression (Fang *et al.*, 2002, Marshall *et al.*, 2004, Molina-Molina *et al.*, 2006, Yao *et al.*, 2006). Angiotensin II became a target in lung fibrosis when it was discovered to be a pro-apoptotic factor for lung epithelial cells and high levels have been recorded in BAL samples from patients with IPF (Wang *et al.*, 1999). In 2006 Marshall et al showed increased levels of ANG II 3 days after bleomycin treatment in wistar rats, ANG II levels increased periodically until death at day 21. Treatment with Losartan decreased ANG II levels while also reducing levels of pro-collagen production (Marshall *et al.*, 2004). The positive effects of Losatran potentially arise from increased production of PGE2 in bleomycin animals treated with the compound (Molina-Molina *et al.*, 2006). Typically after bleomycin administration there is a fall in PGE2 levels, given the capacity of PGE2 to inhibit fibroblast proliferation (Lama *et al.*, 2002), the restoration of PGE-2 by Losartan would explain the positive effects demonstrated following administration.

1.17 Clinical Trials

To date there have been few successful clinical trials on patients with IPF, it should be noted however that the endpoints of a successful phase III trial are not consistent between trials as they have not been officially standardised (Table 1.1). The principle endpoints commonly used are based on how a patient feels, functions, and survives. Mortality is the most robust endpoint but can be measured in 3 different ways, namely, “all cause” mortality, respiratory-related mortality, or IPF-related mortality. “All Cause” mortality encompasses all outcomes resulting in death of the

patient and is a more useful endpoint as it accounts for any secondary reactions to the drug being tested.

Some of the most common methods for recording function are, forced vital capacity (FVC), the diffusion of carbon monoxide (D_LCO), and the "6 minute walk test" which measures the distance the patient can walk in 6 minutes. The results from these and other pulmonary tests are compiled into a composite physiologic index (CPI), an overall score of pulmonary function. While this information is useful it does not give an accurate indication as to how the patients manage day to day tasks. A set of more robust and standardised endpoints would greatly improve quality of the clinical trials being conducted (Raghu *et al.*, 2012b).

N-Acetylcysteine (NAC) is a precursor to the anti-oxidant glutathione, it has been studied as a protective agent in bleomycin models of fibrosis, abrogating the destructive effect of oxidant/antioxidant imbalance in lung alveolar epithelial cells (Kinnula *et al.*, 2005). The IFIGENIA study was a placebo controlled double blind study involving NAC as part of a combined therapy with azathioprine and prednisone. The study followed 155 patients for 1 year with primary endpoints being, FVC, D_LCO and CPI. The results significantly favoured the combination therapy that included NAC over the azathioprine and prednisone alone, although the difference was moderate and there was a large drop-out rate (Demedts *et al.*, 2005). A follow on study PANTHER-IPF explored the combination therapy against NAC treatment alone, however after recommendation from the safety committee the combination therapy was abandoned as there was a higher mortality rate when compared to the placebo. The NAC alone groups are still being followed however to date not enough data exists to determine its efficacy as a standalone treatment (Raghu *et al.*, 2012a).

One of the more recent trials to take place was the CAPACITY trial of the anti-fibrotic drug Pirfenidone. Studies of the drug demonstrated an ability to inhibit the transcription of TGFβ by up to 33% in a bleomycin model of fibrosis, it also inhibits the translation of TNFα resulting in reduced fibroblast proliferation and collagen deposition *in vivo* (Iyer *et al.*, 1999, Nakazato *et al.*, 2002). The phase III double blind clinical trial was separated into 2 groups 004 and 006, the difference being the dose of Pirfenidone received. Group 004 contained 435 patients who received a daily dose of either a placebo or Pirfenidone in a 2:1:2 ratio for 72 weeks, group 006 received a 1:1 dose of Pirfenidone. The primary endpoint of the study was a change in FVC. After 72 weeks patients in group 004 showed a statistically significant change in predicted FVC levels, however group 006 failed to meet the primary endpoint. Pirfenidone was well tolerated with few reported adverse events and those reported were mild to moderate in severity (Noble *et al.*, 2011). These results suggest Pirfenidone could be a potential candidate for IPF treatment, further study is being carried out in the US in the ASCEND trial to determine a clinically meaningful effect on FVC (Rafii *et al.*, 2013).

Table 1.1 List of clinical trials in fibrosis.

Name	Drug Target	Details	Outcome
Imatinib	Tyrosine kinase inhibitor PDGFR A&B	119p 96w	Good time to onset, Bad DlCO, absolute change in FVC, and the distance walked using a 6-minute walk test
IFNγ1β (INSPIRE)	IFNγ1β	826p 48w	Trial halted at 64 weeks, as failed to meet min benefit to mortality ratio compared to placebo
Pirfenidone (CAPACITY)	Regulate TGFβ and TNFα	Study 004: 435p 72w Study 006: 344p 72w	004: Significant reduction in FVC decline. 006: Failed to meet primary endpoint
Bosentan (Build 1-3)	Endothelin A&B Receptor Antagonist	Build 1: 158 1y Build 3: 616p 1y	Build 1: No significant positive result for survival, but there was a trend towards prolonged survival Build 3: Failed to meet primary endpoint, a measure of time to worsening of IPF or death.
Ambrisentan (ARTEMIS-IPF)	Endothelin A Receptor Antagonist	492p 34w	Terminated due to low likelihood of demonstrating efficacy, along with increased risk of pulmonary hospitalisation
N-Acetylcysteine (IFIGENIA)	Reduces free radicals	182p 1y	No improvement in survival but significantly delayed onset of FVC deterioration.
Etanercept	TNFα Receptor antagonist	88p 48w	No difference in endpoints vs placebo (FVC, D_{LCOHb}, P(a–a)O2)
Sildenafil (STEP-IPF)	Pulmonary vasodilation	180p 12w	Failed to meet primary outcome of 20% increase in 6 minute walk test.

1.18 Cell therapy

The use of MSC in cell therapy has become increasingly popular in the last number of years, and is gaining momentum. In 2010 there were 63 ongoing clinical trials involving MSC and 23 completed (Ankrum and Karp, 2010), in 2013 a search of clinicaltrails.gov returned 338 trials involving MSC, 202 of which were still open. A range of diseases are currently being examined including myocardial infarction (MI), graft versus host disease (GvHD) and chronic obstructive pulmonary disease (COPD) to name but a few (Hare *et al.*, 2009, LeBlanc *et al.*, 2008, Mills, 2009). There have been varying levels of success but one of the most promising aspects of MSC as a cell therapy is how well received they are by the recipient. Procyhmal, A proprietary MSC based cell therapy product developed by Osiris Therapeutics tested in patients with MI, reported very few adverse reactions following human MSC administration (Hare *et al.*, 2009).

.

1.19 MSC in fibrosis

MSC have previously been examined for their potential benefit in treating fibrosis, a wide variety of *in vitro* and *in vivo* publications have demonstrated their efficacy however the reason behind the pathological and immunological improvements observed are still unclear.

MSC have been used to demonstrate the importance of chemotaxis, engraftment (Ortiz *et al.*, 2003, Rojas *et al.*, 2005) and cytokine production (Ortiz *et al.*, 2007, Maher *et al.*, 2010, Mizuno *et al.*, 2005) in preventing bleomycin induced pathology, however there is still much unknown about how they function. In 2003 Ortiz and Gamelli *et al.* pursued the theory that intravenous administered MSC travel to the lung and can engraft at the site of damage. Using the bleomycin model in female

C57BL/6 mice he administered male BALB/c MSC and after 14 days the lungs were examined by PCR and fluorescent in situ hybridization (FISH) for presence of the Y chromosome. They discovered that there was an increase in male DNA at the site of bleomycin induced injury, they also detected male DNA in type II alveolar epithelial cells suggesting the MSC were engrafting and differentiating into epithelial cells. Reduced collagen deposition and MMP 2 and 9 expression indicated that MSC are involved in preventing excess extracellular matrix build-up (Ortiz *et al.*, 2003). Though it is possible some MSC may engraft or simply become stuck in the lung architecture, it is now widely believed that MSC function through paracrine means and are cleared from the body after they become activated. Experiments using whole bone marrow fractions were not as effective at reconstituting the lung epithelium indicating high numbers of purified MSC are required for cell therapy (Kotton *et al.*, 2005). In the case of epithelial damage, MSC are known to interact with macrophages in the mound bed, MSC attract pro-inflammatory M1 macrophages to deal with the initial insult (Chen *et al.*, 2008). Further MSC can repolarise the M1 cells to anti-inflammatory M2 macrophages (Maggini *et al.*, 2010), which promote wound healing, thus combining immunomodulatory properties with repair.

1.20 MSC Cytokine Influence on Pathogenesis

MSC release of certain cytokines may play an important role in the benefits observed from MSC therapy. As previously discussed there are many ongoing trials involving cytokine treatment for IPF, two such cytokines, produced by MSC are hepatocyte growth factor (HGF) and PGE2.

HGF is paracrine growth factor involved in growth proliferation and migration of epithelial and endothelial cells, its primary function being tissue repair (Matsumoto

and Nakamura, 1993). As early as 1997, Yaekashiwa and colleagues demonstrated the positive effect that administration of HGF exerted on bleomycin induced fibrosis. This study showed a reduction in pathology and collagen deposition following immediate and delayed administration (Yaekashiwa *et al.*, 1997). HGF treatment also encouraged the proliferation of epithelial cells both *in vitro* and *in vivo* (Dohi *et al.*, 2000). HGF interaction with its receptor, c-met, on the surface of myofibroblasts resulted in increased production of MMP2 and MMP9, which in turn reduced collagen levels and encouraged myofibroblasts apoptosis (Mizuno *et al.*, 2005). Further evidence of the importance of HGF in IPF was demonstrated by Phin *et al.* when examining the difference in pro-HGF and HGF levels in bleomycin treated mice. Activation of HGF from pro-HGF is achieved through the actions of the serine protease HGF activator (HGFA), following bleomycin administration the ability of lung BAL fluid to activate pro-HGF diminished, along with mRNA expression of HGFA (Phin *et al.*, 2010).

PGE2 is a lipid mediator of growth and repair in the lung, acting as an anti-inflammatory agent. *In vitro* studies have shown PGE2 produced by lung alveolar epithelial cells had an inhibitory effect on the proliferation of fibroblasts (Moore *et al.*, 2003). PGE2 was also shown to inhibit the TGFβ driven differentiation of fibroblasts to myofibroblasts, an effect mediated through the E prostanoid receptor 2 (Kolodsick *et al.*, 2003). Bronchial epithelial cells taken from the lungs of IPF patients express significantly lower levels of PGE2 further supporting the beneficial effects of PGE2 signalling in lung fibrosis. *In vivo* studies using PGE2 in bleomycin treated mice demonstrated a positive effect on lung pathogenesis and cellular infiltration when administered 7 days prior to bleomycin treatment, PGE2 administered 14 days after bleomycin had no therapeutic effect. These results suggested a role for PGE2 in

dampening down early inflammation, and preventing activation of fibroblasts, however when given retrospectively PGE2 has no effect on reversing the existing damage (Dackor *et al.*, 2011). The limitations of the bleomycin model become apparent when comparing results from animal and human studies of PGE2 treatment. Fibroblasts from patients with IPF display resistance to Fas mediated apoptosis, contributing to higher fibroblast presence associated with the disease. Administration of PGE2 increases susceptibility to FasL killing and conversely protects ACE cells from apoptosis, essentially opposing the effects of TGFβ signalling (Maher *et al.*, 2010).

1.21 Aims and Objectives

This chapter has briefly introduced the potential of cellular therapy in the future treatment of an array of diseases. At the forefront of this is the capacity of MSC to serve as a therapeutic in the treatment, not only of inflammatory disease but also in regenerative medicine. Modulation of immune cells and trophic manipulation of the microenvironment are key characteristics of MSC that can be exploited for therapeutic intervention. The goal of this work is to further our understanding, not just of what MSC can accomplish but how they achieve it. The hypothesis put forward in this study is that MSC, through cell education and trophic manipulation can serve as a viable candidate for cellular therapy, with particular focus on pulmonary fibrosis. This hypothesis was tested under the following aims:

1. To discover the contact dependent signal through which murine MSC modulate immune cells, namely T cells and DC.
2. To determine the effects of MSC paracrine signalling on pulmonary cells, with an aim to examine MSC mechanisms of action *in vivo*.
3. To refine the bleomycin murine model of fibrosis to more accurately represent therapeutic intervention, consequently using this model to determine MSC efficacy as a cellular therapy in fibrosis.
4. To utilise platform technologies such as neutralising antibodies, siRNA, and shRNA to investigate potential key mechanisms of action in MSC inhibition of inflammation and fibrosis.

Overall this study will advance the understanding of MSC function *in vitro* and *in vivo.* It will also offer greater understanding of therapeutic *in vivo* screening, with particular emphasis on bleomycin induced fibrosis.

Chapter 2

Materials & Methods

2.1 METHODS

2.2 ETHICAL APPROVAL

All procedures involving animals were carried out by licensed personnel. Ethical approval for all work was received from the ethics committee of NUI Maynooth. Licence number B100/2562.

2.3 COMPLIANCE WITH GMO AND SAFETY GUIDELINES

All GMO/GMM work was performed according to approved standard operation procedures and recording protocols approved by the Environmental Protection Agency (Ireland). Safe working practices were employed throughout this study as documented in the Biology Department of Safety manual NUI Maynooth.

2.4 ANIMAL STRAINS

The following mouse strains were used: BALB/c, C57BL/6 (Harlan, Bichester, Oxon, UK), BALB/c-Tg(DO11.10)10Loh/J (Gift from Trinity College Dublin) and eGFP FoxP3 Knock-in (Jackson Labs, Bar Harbour, Maine, USA). All mice were housed according to the Dept. of Health (Ireland) guidelines and used with ethical approval. Sample sizes for animal experiments were determined by statistical power calculations.

2.5 ISOLATION AND CULTURE OF CELLS

2.5.1 ISOLATION AND CULTURE OF ADULT MURINE MESENCHYMAL STEM CELLS (MMSC)

6-8 week old female BALB/c or C57BL/6 mice were sacrificed by cervical dislocation. Femurs and tibias were dissected and the surrounding muscle removed. The ends of each bone were removed and the bone marrow was flushed into a sterile Petri dish using a 27 gauge needle and either Complete Isolation Media (CIM) (Table 2.1), or Mesenchymstem (PAA, GE Healthcare, NJ, USA) media supplemented with 100 U/ml penicillin. Cell aggregates were disrupted using a 19 gauge needle and 5 ml syringe. Cells were then centrifuged at 400 g for 5 min and re-suspended in 5 ml CIM. Bone marrow cells were counted by ethidium bromide/acridine orange (EB/AO) viable staining (section 2.6) and seeded at a concentration of 6.0-6.5 $\times 10^7$ cells in T75 flasks in 15ml of CIM or complete mesenchymstem or 2.0-2.5 $\times 10^7$ cells in T25 flasks in 8 ml of CIM or complete mesenchymstem.

Non-adherent cells were removed after 3 hours, the flasks were washed with sterile PBS after 24 and 48 hours. Cells were maintained in either hypoxic (5% O_2) or normoxic (21% O_2) conditions in 5% CO_2 at 37°C for 2-3 weeks until colonies of fibroblast like cells developed. Cells were passaged by trypsinisation with 0.25 % (v/v) trypsin / 1 mM EDTA (Invitrogen-Gibco) for 2 minutes at 37°C. Trypsin was neutralised by addition of CIM and cells were centrifuged at 400 g for 5 min. Cells (passage 1) were counted and re-seeded at 5-6 $\times 10^6$ cells in T75 flasks or 1-2 $\times 10^6$ cells in T25 flasks in fresh CIM or mesenchymstem media. Media were replaced every 3-4 days. At passage 2 cells were changed to complete αMEM (CEM) (Table 2.1).

CEM was replaced every 3-4 days. At passage 3 cells were characterised before use *in vitro* or *in vivo*.

2.5.2 GENERATION OF STABLE KNOCKDOWN MSC CELL LINES

2.5.2.1 LIQUID CULTURE OF PLASMID

Five Jagged-1 and HGF short hairpin RNA (shRNA) plasmids were designed and purchased from Open Biosystems (Thermo), they were expressed in the lentiviral vector pGIPZ. 10µl of the glycerol stocks were thawed and added to 5 ml of 2X LB Broth (low salt) supplemented with peptone and yeast extract (Table 2.3) in a 15ml polypropylene tube. The tubes were incubated at 45° angle at 37 °C for 16 h with vigorous shaking (300 rpm). The antibiotic carbenicillin (Merck Millipore, Darmstadt, Germany) was added to the liquid culture to select for *E. coli* containing the pGIPZ vector which infers antibody resistance.

2.5.2.2 MINIPREP EXTRACTION OF PLASMID DNA

Vector DNA was extracted from bacteria using a Qiagen HiSpeed Plasmid Midi and Maxi Kit (Qiagen) according to the manufacturer's instructions. 5 ml of overnight bacterial culture were harvested by centrifugation at 4500 x g for 20 min at 4^{o}C. The supernatant was removed and the pellet was re-suspended in 0.3 ml Buffer P1 (Qiagen). 0.3 ml Buffer P2 (Qiagen) was added and mixed vigorously. The samples were incubated at RT for 5 min and 0.3 ml of chilled Buffer P3 (Qiagen) was added. The solution was mixed vigorously and incubated on ice for 5 min. The lysate was then transferred into a 1.5ml eppendorf and centrifuged at 14000 g for 10 min.

The supernatant was removed and transferred to a Qiagen-tip 20 that was equilibrated with 1ml of buffer QBT. The supernatant was allowed to empty by gravity flow and the tip was washed twice with 2 ml of buffer QC. The DNA was eluted from the tip using 0.8 ml buffer QF. The DNA was precipitated by adding 0.56 ml of isopropanol and centriguged at 12000 g for 30 min. The supernatant was removed and the remaining DNA pellet was washed with 70% ethanol and centriguged at 12000 g for 10 min. The supernatant was removed and the pellet allowed to air dry for 5 min. The pellet was re-suspended in 50µl of TE buffer, the DNA yield was determined using a Nanodrop 2000 spectrophotometer (ThermoScientific, Wilmington, DE, USA) at 260 nm.

2.5.2.3 PRODUCTION OF LENTIVIRAL PARTICLES IN HEK CELLS

HEK293T (HEK) (cells were a gift from Prof. Paul Moynagh) cells were used as a packaging cell line and were split 1:2 each day for 3 days prior to transfection in order to ensure active division during transfection. HEK cells ($1.5x10^{6)}$ were plated in a T-75 flask in complete DMEM (Table 2.1) and left to settle overnight. Next 1.8µg of the Jagged-1 or HGF plasmid DNA was added to 6µl of the packaging plasmid Trans-Lentiviral packaging mix (Open Biosystems) and brought up to a final volume of 480µl with serum free DMEM (High glucose, Sigma) then incubated at room temperature (RT) for 20 min. The transfection reagents, Gene Juice (Merck, Millipore), TransIT-LT1 or TransIT-293 (Mirus Bio LLC, Wisconsin, USA) were brought up to RT, 21µl of transfection reagent was added to the plasmid mix and incubated at RT for a further 10 min. Following incubation the transfection reagent:DNA complex mixture was added drop wise to 7mls of serum free DMEM in the HEK flask. After 24h transfection the HEK cells were switched to 30% FBS, 48h

after transfection the supernatant containing the Jagged-1 or HGF lentivirus was collected. BALB/c MSC were seeded at $1x10^6$ cells in a T-75 flask and allowed to settle overnight. The cells were then transduced with 6 ml of viral medium and 6 ml of CEM for 72h. At this point 4µg/ml puromycin was added to the MSC media to positively select the cells that had been successfully transfected.

2.5.3 DENDRITIC CELL ISOLATION AND CULTURE

6-8 week old female BALB/c or C57BL/6 mice were sacrificed by cervical dislocation. Femurs and tibias were removed intact under aseptic conditions as described in section 2.3.1. Bone marrow cells were counted and seeded at a concentration of 6×10^6 cells per 10cm non-tissue culture grade Petri dish (Falcon BD) in 10 ml cRPMI supplemented with 20 ng/ml Granulocyte Macrophage-Colony Stimulating Factor (GM-CSF) (PeproTech, Rocky Hill, NJ). On day 3, non-adherent cells were removed and 10 mls of fresh cRPMI supplemented with 20 ng/ml GM-CSF was added to each dish. On day 6, 10 ml of fresh cRPMI supplemented with 20 ng/ml GM-CSF was added. After 8 days, cells were harvested by gentle aspiration and centrifuged at 300 g for 5 min. Cells were re-suspended in cRPMI (Table 2.1) and counted. Cells were seeded at appropriate concentrations relevant to experimental assays.

2.5.4 MURINE SPLENOCYTE ISOLATION

Murine spleens were aseptically dissected into cRPMI (Table 2.1). Spleens were homogenised through a 70 µm filter and the homogenate was centrifuged at 300

g for 5 min and re-suspended in 2 ml of red blood cell lysis buffer solution (BioLegend, San Diego, CA,) for 2 min on ice. 30 ml of cold PBS was added to the suspension to neutralise the lysis solution which was then centrifuged at 300 g for 5 min. Supernatant was removed and the cells were then re-suspended in fresh cRPMI and counted.

2.5.5 T CELL ISOLATION

$CD3^+$ T cells were isolated using MagCellect $CD3^+$ T cell isolation kit according to manufacturer's instructions (R & D Systems, Minneapolis, MN). Briefly, splenocytes were re-suspended in 1X MagCellect buffer to a cell density of 1.0×10^8 cells/ml. For every 1×10^7 cells processed, 10 µl of $CD4^+$ T cell biotinylated antibody cocktail was added and cells incubated for 15 min at 4 ˚C. Following incubation, 12.5 µl of streptavidin ferrofluid per 1×10^7 cells was added and further incubated for 15 min at 4 ˚C. Following the incubations, the cell suspension was brought up to 3 ml with MagCellect buffer. The tubes were placed into a magnetic stand twice for 6 min at RT. The magnetically labelled cells migrated towards the magnet, leaving the desired $CD3^+$ T cells behind in suspension. The $CD3^+$ T cell suspension was centrifuged at 300 g for 5 min then re-suspended in cRPMI and counted. $CD4^+$ T cells were isolated using MACS bead technology (Miltenyi Biotec, Surrey, United Kingdom). Splenocytes were re-suspended in MACS buffer (Table 2.2) at a concentration of $1x10^7$ cells/90µl. Next 10µl of $CD4^+$ MACS beads were added to the cell suspension and incubated at 4 degrees for 15 min. Following incubation cells were centrifuged at 300 x G for 10 min then re-suspended in 1ml of MACS buffer and passed through an LS column by gravity flow. The beads are removed from the

column by adding 5 ml of MACS buffer and forcefully inserting a plunger and collecting the resulting flow through. Cells are centrifuged at 300 x G for 5 min and re-suspended in cRPMI and counted.

2.6 ISOLATION OF PRIMARY LUNG FIBROBLASTS

Primary lung fibroblast were isolated from female C57BL/6 mice which were sacrificed by intraperitoneal injection of pentabarbitone. The lungs were washed by perfusion with PBS and sterilely excised. The lungs were filled intratracheally with pre-warmed trypsin solution (40mg trypsin in 10ml Ca/Mg^{+} solution) and incubated for 15min at 37°C. The lungs were then diced and the trypsin neutralised with FBS (1ml/lung). The tissue was transferred to a 50ml tube and a DNase I solution (6.25mg DNase in 25ml in 10ml Ca/Mg^{-} solution) was added and shook firmly by hand for 4 min after which it was passed through a 100µm filter and then a 40µm filter. The cell suspension was centrifuged at 60xG for 6 min in a bench top centrifuge and the pellet re-suspended in DNase II solution (2.5mg DNase in 50ml in 10ml Ca/Mg^{-} solution), then spun again and re-suspended in differential attachment medium (Table 2.1). The cell suspension was plated into a 10cm non-tissue grade petri dish and incubated for 1hr at 37°C during which time, fibroblasts and macrophages adhere to the surface of the petri dish. Non-adherent cells are removed and the adherent cells allowed to reach confluence in fibroblast media. Fibroblasts were isolated from macrophages through selective passaging with 2min trypsin washes. At passage 2 the cells were characterised and stocks frozen in liquid nitrogen. Primary fibroblast were used in experiments up to passage 5.

2.6 MEASUREMENT OF CELL VIABILITY (FLUORESCENT MICROSCOPY)

Cells were re-suspended in their specific growth media and diluted 1/10 in 2 % (w/v) ethidium bromide/acridine orange (EB/AO) (Sigma-Aldrich, Arklow, Ireland). 10 µl was pipetted onto a haemocytometer and live cells (green) were counted using a fluorescent light microscope.

2.7 CHARACTERISATION OF MSC

2.7.1 CHARACTERISATION OF MSC AND GENERAL FLOW CYTOMETRY

For analyses by flow cytometry, cells (MSC, DC or $CD4^+$ T cells) were harvested, washed in sterile PBS and re-suspended in PBS supplemented with 10 % BSA (heat inactivated bovine serum albumin) to yield approximately 1 x 10^5 cells/FACS tube (4 ml polypropylene tubes) (Falcon, BD Biosciences). Fluorochrome conjugated antibodies (Tables 2.4 & 2.5) or isotype controls were incubated with cells for 15 min at 4 °C. After 15 min, cells were washed in 2 ml of PBS supplemented with 10 % BSA, vortexed and centrifuged at 300 g for 5 min. The supernatant was removed and cells re-suspended in 200 µl PBS supplemented with 10 % BSA or 300 µl of cell fixative (PBS supplemented with 1 % (v/v) paraformaldehyde (PFA) (Sigma-Aldrich)). Cells were then analysed by flow cytometry (FACS Calibur, FACS Accuri, California, USA) using CellQuest or CFlowPlus software respectively (BD Biosciences, Oxford, UK).

2.7.2 MIXED LYMPHOCYTE REACTION

Freshly isolated murine splenocytes from two MHC mismatched strains were co-cultured in a two-way MLR at a density of 2 x 10^5 cells/well in a 96-well tissue

culture plate in 225 µl final volume. MSC effect on lymphocyte proliferation was assessed by adding MSC to the MLR at a density of 1.5 x 10^4 cells/well. The mitogen Concanavalin A (Con A) was used at a concentration of 5 µg/ml as a positive control. The 96 well plate was incubated at 37 °C for 72 h after which 0.5 µCi/ml of [^{3}H]-Thymidine (Perkin Elmer, MA, USA) was added for the final 6 h of culture. Cells were harvested using a Micro96 Harvester (Skatron Flow Laboratories, Oslo, Norway) onto 96 well glass fibre filter mat. The mats were then dried and placed in a plastic sample bag, 4ml of β-scintillation fluid (Beta-Plate Scint, Perkin Elmer, MA, USA) was added and the dispersed evenly throughout the filter mat, the bag was sealed and placed in a cassette. [^{3}H]-Thymidine uptake was measured using a β-scintillation counter (1450 MICROBETA Liquid Scintillation Conter, Wallac-Perkin Elmer). Results were expressed in counts per minute (CPM).

2.7.3 DIFFERENTIATION OF MSC

MSC were seeded at a density of 5 x 10^4 cells/well in a 6-well tissue culture plate in 2 ml CEM for osteogenic and adipogenic differentiation, or 2x10^5 cells are centrifuged in a 15ml falcon tube at 200 g for 8 min to form a cell pellet for chondrogenic differentiation. Once 70 % confluence was reached (typically 2-3 days), cells were incubated in osteogenic, adipogenic or chondrogenic differentiation medium (Table 2.1), CEM media was added to control wells. Fresh medium was added every 3-4 days for 21 days. At day 21, the medium was removed from the bone and fat cultures and the cells were washed in PBS and then fixed in 10 % (v/v) neutral buffered formalin for 20 min at room temperature. Formalin was removed and cells were washed in 2 ml of PBS. 1 ml of 1 % Alizarin Red, or 0.5 % Oil Red O (Table

2.2) was added to the fixed bone or fat cells and allowed to stain for 20 min at RT. Excess stain was removed and the cells were washed with dH_2O. Finally, 1 ml of dH_2O was added to each well and cells were examined under the microscope. The chondrocyte cell pellets were harvested by aspirating off all the media and washing pellets twice with PBS. Pellets were placed in 1 ml of trizol and stored at -20°C. Chondrocyte pellets were analysed for the expression of collagen II and aggrecan by RT-PCR (Table 2.7 & 2.8). Briefly, RNA was isolated from the pellets (section 2.9.1), reversed transcribed into cDNA (section 2.9.3) and the expression of chondrocyte markers were analysed by RT-PCR (section 2.15).

2.8 CELL SORTING

$CD3^+$ T cells were isolated as described in section 2.5.4. Fluorescently labelled antibodies for CD3, CD4, and CD25 (Table 2.3) were added to the cells and incubated for 15 min at 4 °C. Following incubation the cells were washed with PBS supplemented with 1% FBS and centrifuged at 300 g for 5 min, the cells were re-suspended in PBS supplemented with 1% FBS at a concentration of $1x10^7$ cells/ml and sorted into $CD4^+CD25^+$FoxP3-GFP^+ and $CD4^+CD25^-$FoxP3-GFP^- populations using the ARIA cell sorter (BD Biosciences). The cell sorter was set up for aseptic sort according to manufactures guidelines and calibrated for sorting using Accudrop beads (BD Biosciences). The sorted populations were aseptically collected in 15 ml falcons containing 500µl of FBS and centrifuged at 500 g for 5 min. The cells were counted, prior to use a small sample of both populations were analysed for purity by running them through the flow cytometer.

2.9 MSC CO-CULTURE WITH $CD4^+$ T CELLS

$CD4^+$ T cells were isolated as described in section 2.5.4 and cultured in the presence or absence of MSC for 24 or 72 h. The seeding densities used were, 1 x 10^5 MSC: 3 x 10^5 $CD4^+$ T cells in 24 well plate or 3 x 10^5 MSC: 1 x 10^6 $CD4^+$ T cells in 6 well plate. The expression of notch receptors (Notch 1 & 2), and Notch ligands (Jagged 1, 2 & Delta like ligand 1) (Table 2.3) were analysed by RT-PCR after 24 h (Table 2.4). Expression of CD25 and the transcription factor FoxP3 were examined after 72 h by flow cytometry, $CD4^+$ T cells isolated from FoxP3-GFP mice were genetically manipulated to express the GFP protein at the promoter region of the FoxP3 gene. When the gene is transcribed the nucleus of the cell fluoresces green and can be detected by flow cytometry. For the neutralisation study, mouse anti-Jagged 1 (5 µg/ml), mouse anti-notch-1 (10µg/ml) or corresponding control antibody was added to the co-cultures and the expression of CD25 and FoxP3-GFP were analysed by flow cytometry (Table 2.4). The Notch inhibitor, γ-secretase inhibitor (GSI) (Calbiochem, Merck, Germany) reconstituted in DMSO (Sigma-Aldrich), was added to $CD4^+$ T cells: MSC at a concentration of 1 µM co-cultures for 72 h and the expression of CD25 and FoxP3-GFP were analysed by flow cytometry.

2.10 MSC CO-CULTURE WITH DC

Immature DC were harvested on day 8 (section 2.5.3) and matured in the presence of lipopolysaccharide (LPS) (Sigma-Aldrich) at 100 ng/ml for 24 or 48 h in the presence or absence of MSC. The seeding densities used were, 1 x 10^5 MSC: 3 x 10^5 DC in 24 well plate for 24 h YAe analysis or 3 x 10^5 MSC: 1 x 10^6 DC in 6 well plate for 48 h flow cytometry analysis. After 48 h, the maturation markers MHCII and CD86 (Table

2.4), and corresponding isotype controls were analysed by flow cytometry on DC. For the YAe study 10 µg/ml I-Eα peptide 52-68 (ASFEAQGALANIAVDKA) (Anaspec, San Jose, CA) was added to the DC for 24 h in the presence or absence of MSC, as a control, DC were cultured with MSC alone. Peptide binding was detected by flow cytometry using an anti-I-A^b: Eα complex specific antibody, Y-Ae (eBioscience). In some experiments, the Notch inhibitor, γ-secretase inhibitor (GSI) (Calbiochem, Merck, Germany) reconstituted in DMSO (Sigma-Aldrich), at 1 µM was added to DC: MSC co-cultures for 48 h and the expression of maturation markers were analysed by flow cytometry.

2.11 TOLEROGENIC DC FUNCTIONAL ASSAY

Immature DC were harvested on day 8 (section 2.5.3) and matured in the presence of ovalbumin (OVA) (Sigma-Aldrich) at 20µg/ml for 48 h in the presence or absence of MSC at a density of 3 x 10^5 MSC: 1 x 10^6 DC in 6 well plate. After 48 h, a fraction of the cells were analysed for the maturation markers MHCII and CD86 (Table 2.4), and corresponding isotype controls by flow cytometry. The remaining DC were washed with PBS and co-cultured with $CD4^+$ T cells and plated in a 96 well plate at a density of 2 x 10^5 DC: 8 x 10^5 $CD4^+$ T cells. The cells were cultured for 72 h after which 0.5 µCi/ml of [^{3}H]-Thymidine (Perkin Elmer, MA, USA) for the final 6 h. The cells were harvested as described in section 2.7.2 and proliferation was measured by [^{3}H]-Thymidine uptake using a β-scintillation counter (1450 MICROBETA Liquid Scintillation Conter, Wallac-Perkin Elmer). Results were expressed in counts per minute (CPM).

2.12 RNA ISOLATION

Total RNA was extracted using trizol® reagent (Invitrogen) according to the manufacturer's instructions. Briefly, 1 x 10^6 cells were lysed in 1ml trizol at room temperature for 5 min. 100 µl of RNA-grade 1-Bromo-3-chloropropane (Sigma-Aldrich) was added to the cells, vortexed for 10 sec and incubated at room temperature for 5 min. Samples were centrifuged at 12,000 g for 15 min at 4 °C. Two distinct layers resulted with RNA remaining in the clear, aqueous upper layer. 350-400 µl of RNA was carefully removed, ensuring the lower white DNA layer was not disturbed, and precipitated with 500 µl isopropanol (Riedel-deHaen). The samples were incubated at room temperature for 10 min followed by centrifugation for 10 min at 4 °C. The resulting RNA pellet was washed with 1 ml 75 % (v/v) ethanol and centrifuged at 7,500 g for 5 min at 4 °C. The ethanol was aspirated and the RNA pellet was allowed to briefly air dry prior to resuspension in 30 µl RNase-free water (Promega, Southhampton, UK). The purity and concentration of RNA was determined using a spectrophotometer (Nanodrop 2000, ThermoScientific, Wilmington, DE, USA) which calculated the ratio of absorbance at 260 nm to 280 nm. A ratio between 1.8 and 2.0 indicated sufficient purity of the RNA. Samples outside this range were discarded.

2.13 DNASE TREATMENT OF RNA

Genomic DNA was removed from RNA samples by treatment with DNase I (Invitrogen, Paisley, UK). 1 µl of DNase (Amplification grade) was added to 1 µg of RNA and incubated for 15 min at room temperature. 1 µl of 25mM EDTA (Promega) was added to the mixture and incubated at 65°C for 10 min to inactive the enzyme.

2.14 cDNA Synthesis

Following DNase treatment, total RNA was reverse transcribed using 25 Units Superscript II (Invitrogen). Each reaction contained a 1 x GoTaq reaction buffer (Promega), 2.5 mM $MgCl_2$ (Promega) , 10 mM dNTP mix (Promega), 50 U/ml of ribonuclease inhibitor (Invitrogen) and 20 µg/ml Oligo (dT) $_{12\text{-}18}$ primer (Invitrogen) diluted in nuclease-free water (Promega). The conditions for cDNA synthesis were as follows:, 42 ^{o}C for 50 min, 72 ^{o}C for 10 min and 4 ^{o}C for 10 min. Quantification of cDNA was performed by measuring the absorbance value of the sample 260 nm. Samples were stored -20 ^{o}C until required.

2.15 Reverse Transcription-Polymerase Chain Reaction (RT-PCR)

PCR was used to determine the presence of specific DNA sequences (or mRNA following reverse transcription) using primers summarised in Table 2.6 and 2.7. Expression of the housekeeping gene, Glyceraldehyde 3-phosphate dehydrogenase (GAPDH) was used as a positive control. PCR reactions contained 2.5 mM $MgCl_2$ (Promega), 25 mM dNTP (Promega), 1 x GoTaq reaction buffer (Promega), 40 U/ml Taq polymerase (Promega) and 0.4 pM of the appropriate primer pairs (Sigma). The reaction mastermix was adjusted to a final volume of 24 µl with nuclease-free water. The PCR conditions were as follows: denaturation at 95 °C for 45 sec (2 min for first cycle), annealing for 45 sec (optimal annealing temperatures are summarised in Table 2.4 and extension for 45 sec at 72°C. DNA products were

resolved on a 1.3 % w/v agarose gel and detected by binding of gel red (Biotium, Hayward, CA).

2.16 REAL TIME-POLYMERASE CHAIN REACTION (QRT-PCR)

cDNA was analysed for the quantification of mRNA expression. Briefly, cDNA (1µg) was amplified in the presence of SYBR® Green JumpStart™ Taq ReadyMix (Sigma). Accumulation of gene-specific products was measured continuously by means of fluorescence detection over 40 cycles. Each cycle consisted of: denaturation at 95 °C for 15 sec, annealing at optimum temperature (Table 2.4) for 30 sec, and extension at 72 °C for 45 sec followed by a melt curve cycle of 95 °C for 15 sec, 55 °C for 15 sec and 95 °C for a final 15 sec. Expression was quantified in relation to the housekeeper GAPDH. Quantification of target gene expression was obtained using an Eco Real-Time PCR System (Illumina, Inc. San Diego, CA USA).

2.17 SILENCING OF RNA (SIRNA)

MSC were seeded at 4 × 10^4/well in 24 well plates in duplicate until approximately 60% confluent. siRNA for murine Jagged-1 was pre-designed (Silencer® Select siRNA, Applied Biosystems, Warrington, UK) and diluted in RNase free water (supplied with kit) to different concentrations, as per manufacturer's instructions. Lipofectamine (Invitrogen, Paisley, UK) was used as a transfection reagent for all siRNA experiments, as per manufacturer's instructions. MSC with or without siRNA were cultured in Opti-Mem®I media (Gibco-Invitrogen, Paisley, UK).

After 24 h, MSC RNA was isolated (Section 2.12) and transcribed into cDNA (Section 2.14). Murine Jagged-1 expression on MSC was examined by RT-PCR (Section 2.15).

2.18 IMMUNOFLUORESCENCE

Cells were plated at appropriate seeding density on a poly-L-lysine (Sigma) coated well of a glass chamber slide (Labtec, Fisher). Once cells reached the desired density the culture medium was removed and the wells washed with PBS. Ice cold methanol was added to the wells and the cells placed at -20°C for 5 min. Methanol was removed and the cells allowed to air dry for 20 min after which they were stored at -20°C or used immediately. Following methanol fixation, the cells were equilibrated in 1X Tris buffered saline (TBS; Table 2.2). Wells were blocked in TBS supplemented with 1% w/v BSA for 30 min at room temperature, and washed with 0.1% TBST (Table 2.2). Primary antibody was diluted to working concentrations (Table 2.3) in 1% BSA/TBS, cells were incubated overnight with primary antibody at 4°C on a piece of moist tissue. Wells were washed 3 times with 0.1% TBST for a total of 10 min. Secondary antibody (Table 2.3) was diluted in 1%BSA/TBS and incubated for 30 min at room temperature. Wells were washed a final time in TBST and counterstained using 4′,6-Diamidino-2-phenyindole (DAPI) (Table 2.3) for 1 min and washed 3 times with water. A cover slide was mounted onto Faramount aqueous mounting medium (Dako, Glostrup, Denmark) and fluorescence was examined using a Nikon Eclipse E600 flourescent microscope.

2.19 SCRATCH ASSAY

The underside of a 6 well plate was scored with 3 parallel lines using a safety blade. Fibroblast or LA4 (lung alveolar epithelial cells) cells were plated a concentration of $1x10^5$ cells/well and allowed to form a confluent monolayer overnight. Using a P200 pipette tip (Sarstedt) a line was scratched down the centre of the well perpendicular to the 3 lines on the underneath of the plate. The wells were washed with warm PBS to remove floating cells, fresh medium was added to all the wells and recombinant FGF or HGF to positive control wells at a concentration of 10µg/ml. Conditioned media (CM) collected from MSC plated in the appropriate media was concentrated using Amicon Ultra Centrifugal Filters (Merck-Millipore, Darmstadt, Germany), the resulting protein was added to designated wells. The width of the scratch was measured using Photoshop (Adobe, San Jose, CA, USA) from images taken using an inverted light microscope, the lines scored on the bottom of the wells were used as an alignment guide. The wells were observed daily, once the first well fully closed the cells were fixed with ice cold methanol for 5 min and stained with crystal violet for 10min. The width of the scratch was measured from the same position and the resulted were graphed as a percentage of closure.

2.20 PROLIFERATION ASSAY

Fibroblasts or LA4 cells were seeded in a 24 well tissue culture plate (1×10^5 cells/well) and allowed to form a confluent monolayer. The cells were scratched with a P1000 pipette tip and washed with PBS to remove detached cells. Fresh media was added to all the wells and FGF or HGF was added to fibroblast (10ng/ml) and LA4 (10ng/ml) cultures respectively as a positive control. MSC (1×10^5 cells/well) were plated in normal CEM and once settled they were washed and switched to LA4 or

fibroblast media. The conditioned media (CM) was collected after 24 hours and concentrated using Amicon Ultra Centrifugal Filters before being added to the designated wells. [^{3}H]-Thymidine (Amersham Biosciences, Buckinghamshire, England) at 0.5 µCi/ml was added to each well and incubated at 37 °C 5 % CO_2. Cultures were harvested after 3 days by removing the media and washing each well 3 times with PBS. The cells were lysed using 500µl of 1% sodium dodecyl sulphate (SDS, Sigma) and the lysate transferred to 3ml plastic counting tubes. 2 ml of β-scintillation fluid (UltmaGold, Wallac-PerkinElmer) was added to each tube, vortexed, and placed in a 24 well cassette for reading. [^{3}H]-Thymidine incorporation was quantified by a β-scintillation counter (1450 Microbeta Liquid Scintillation Counter; Wallac-Perkin Elmer) and results were expressed in counts per minute (cpm).

2.21 ELISA

All ELISAs were carried out according to manufacturer's instructions. Specific capture antibodies (murine IFNγ, TNFα, IL-1β, TGFβ, IL-6 & HGF) in PBS were added to 96 well microtitre plates (NUNC) and incubated overnight at room temperature. Plates were then washed 3 times in wash buffer (Table 2.2) and then incubated in blocking solution (Table 2.2) for a minimum of 1 h. Plates were then washed and incubated with 100 µl/well of sample supernatant or corresponding cytokine standard for 2 h at room temperature. After washing, plates were incubated with specific detection antibodies for a further 2 h at room temperature. Plates were washed again and incubated with 100 µl/well of streptavidin horseradish peroxidase (HRP) (R & D Systems) conjugate diluted 1/200 in specific reagent diluent for 20 min. After washing, plates were incubated with 100 µl/well of tetramethylbenzidine (TMB)

substrate (Sigma-Aldrich) for 20 min at room temperature out of direct light. The reaction was stopped after 20 min by adding 50 µl/well of 1 M H_2SO_4. The absorbance (optical density (O.D)) of the samples and standards were measured at 450 nm for all ELISA using a plate reader (Labsystems, Helsinki, Finland). The cytokine concentration of each sample was determined by comparison to the standard curve of known cytokine concentrations.

2.22 PGE-2 SPECIFIC ELISA (ACE™ COMPETITIVE ENZYME IMMUNOASSAY)

The amount of PGE-2 produced by MSC in unstimulated or stimulated conditions was measured using a commercially available ELISA Kit from Cayman Chemical (Ann Arbour, MI, USA). The PGE-2 assay is based on the competition between PGE-2 and PGE-2 acetylcholinesterase (AChE) conjugate (PGE-2 tracer) for a limited amount of PGE-2 monoclonal antibody. The concentration of the PGE-2 tracer is held constant, while the concentration of the PGE-2 varies. Therefore the amount of PGE-2 tracer that can bind to the PGE-2 monoclonal antibody will be inversely proportional to the concentration of PGE-2 in the well. ELISA were carried out according to manufacturer's instructions. The microplate (96 well polystyrene microplate) was pre-coated with goat anti-mouse polyclonal antibody. Controls consisted of blank (Blk), nonspecific binding (NSB), maximum binding (B0), and total activity (TA which is analogous to the specific activity of a radioactive tracer) wells. 100 µl and 50 µl of EIA buffer was added to Non-Specific Binding (NSB) wells and Miximum Binding (B0) wells respectively. The standards and samples in triplicate and controls in duplicate (50 µl) were added to the plate. The PGE-2 AChE Tracer (50 µl) was then added to all wells except the total activity (TA) wells. 50 µl of PGE-

2 monoclonal antibody was added to the appropriate wells (i.e. all wells except TA, NSB and the Blk wells) and incubated at 4°C for 18h with the plate covered. Ellmann's Reagent was prepared fresh by reconstituting one vial of Ellman's reagent with 20ml of ultrapure water. After washing in wash buffer provided, 200 µl of Ellman's Reagent was added to each well and 5 µl of tracer was added to the TA wells. The plate was covered with plastic film and allowed to develop protected from light while on an orbital shaker for 60-90 min. The plate was checked periodically, until the B0 wells had reached a minimum absorbance (OD) of 0.3 with the blank subtracted, and read at an absorbance of 405 nm using a multiscan plate reader (LabSystems). Calculations required that the average OD from the blank wells were subtracted from all OD. The corrected maximum binding was then calculated by subtracting the NSB average from the B0 average. Subsequently the % B/B0 (% sample or standard bound/maximum bound) was calculated for all remaining wells. A standard curve was then plotted of %B/B0 for standards versus PGE-2 concentration (pg/ml) on a semi-log scale. The concentration of each sample was determined using a standard curve of known concentration and results were stated as mean concentration ± SE.

2.23 *IN VITRO* APOPTOSIS ASSAY

Murine LA4 cells at 1 x 10^5/well of a 24 well plate were allowed to settle overnight. The media was changed and replaced with 500µl of fresh cDMEM F:12 and cultured in the presence or absence of 50ng/ml of TNFα (Peprotech, USA) with or without the addition of concentrated MSC CM proteins. Briefly 500µl of CM from MSC, HGF knockdown MSC or non-silencing control MSC were transferred to a

Amicon Ultra centrifugal filter unit (Merck-Millipore, Darmstadt, Germany), and centrifuged at 14000 g for 20 min, the unit was then inverted into a fresh eppendorf and centrifuged again at 1000 g for 2 min. The concentrated CM protein was collected and added to the designated wells. The analysis of MSC induced apoptosis was analysed by flow cytometry. As a positive control, a chemotherapy drug, cisplatin (Sigma-Aldrich) at 250 µg/ml was added to selected wells. After 24 h, all LA4 cells were recovered from culture by trypsinisation with 0.25 % (v/v) trypsin / 1 mM EDTA and apoptosis was detected by the binding of Annexin V/Propidium iodide (PI) staining (eBioscience,). Cells were washed in PBS and centrifuged at 300 g for 5 min, then re-suspended in 1 X binding buffer at a concentration of 1 x 10^6 cells/ml. 1 x 10^5 cells (100 µl) were transferred to a 5 ml tube. 5 µl of Annexin V-FITC (0.5 mg/ml) and 5 µl of propidium iodide (PI) (20 µg/ml) (eBioscience) were added to each tube. Cells were gently vortexed and incubated for 15 min at room temperature in the dark. After 15 min, 400 µl of assay buffer (eBioscience) was added to each tube and analysed by flow cytometry within 1 h.

2.24 BLEOMYCIN INDUCED MOUSE MODEL OF LUNG FIBROSIS

A Bleomycin model of pulmonary fibrosis was developed and optimised from a protocol described by Ortiz *et al.* (Ortiz, 1999). C57BL/6 mice were administered 4U/kg of Bleomycin by intranasal instillation. The mice were lightly anaesthetised with gaseous isoflourine and 20µl of Bleomycin diluted in PBS was administered to the nostrils (i.n.) allowing the solution to be inhaled into the lungs. Control groups were given 20µl of PBS. MSC or NIH3T3 fibroblasts (4.4x10^4/g) were administered by intravenous injection to the tail vein using a 27 gauge needle and a 1 ml syringe either between 6 h and 8 h after i.n. or 7 days later, PBS was injected as a negative

control. Animals were returned to their cages where they were monitored closely for the first hour and at regular intervals thereafter for any signs of distress or ill health.

2.25 ISOLATION OF LUNG TISSUE FROM BLEOMYCIN MOUSE MODEL

Lungs were removed aseptically and using a sterile forceps, and transferred to a petri dish and sectioned using a sterile scalpel. The right lobes were divided between two 1.5 ml eppendorfs containing either 500µl of RNA Later (Qiagen) or Complete Protease Inhibitor Cocktail (Roche) and frozen. The left lobe was fixed in 10% (v/v) formalin (Sigma-Aldrich) for histological analysis. The tissue in RNA later was transferred to 1 ml of trizol and homogenised using a handheld homogeniser (IKA) and processed for PCR as described previously. Similarly the lobe in protease inhibitor was homogenised and diluted into a total volume of 3 mls, the homogenate was centrifuged and the supernatant collected and used for analysis by ELISA.

2.26 HISTOLOGY

2.26.1 TISSUE PREPARATION

Lungs were removed from experimental mice and processed for histology using an automated processor (Shandon Pathcentre, Runcorn, UK), which immerses the tissues in fixatives and sequential dehydration solutions, including ethanol (70%, 80%, 95% x 2, 100% x 3) and xylene (x 2) (BDH AnalaR® Laboratory Supplies Poole, UK). Tissues samples were then embedded in paraffin wax using the Shandon Histocenter 2 (Shandon) and left to set overnight at 4 °C. 5µm sections were cut using a microtome (Shandon Finesse 325, Thermo-Shandon, Waltham, MA, USA).

Sections were placed in cold water containing ethanol followed by transfer to a hot water bath (42 °C) to smooth out any folding in the sections. Sections were placed on microscope slides (Thermo Scientific), air-dried overnight at RT before staining with Trichrome stain.

2.26.2 TRICHROME STAINING

Prior to staining, 5 µm tissues section slides were incubated at 56 °C for a minimum of 1 h to set the tissue on the slide and aid the removal of the wax. Slide sections were immersed in two changes of xylene for 10 min each, following by re-hydration in three decreasing concentrations of ethanol (100% x 2, 95% and 80% v/v) for 5 min each, then placed in two changes of water to rinse off excess xylene. Bouin's solution (Sigma-Aldrich) was used to mordant the tissue, slides were left in the solution overnight at room temperature or for 15 min at 56°C, then rinsed under running tap water to remove the yellow colour. Next the slides were immersed in working Weigert's Iron Hematoxylin Solution (Sigma-Aldrich) for 5 minutes, washed in running tap water for 5 min, and finally washed in deionised water. Slides were counterstained in Scarlet-Acid Fucshin for 5 min and washed again in deionized water. Slides were immersed in working Phosphotungstic/Phosphomolybdic Acid Solution (Table 2.2) for 5 min prior to staining with Aniline Blue solution for 5 min, this step aids the binding of the Aniline blue dye to connective tissue. The slides were then rinsed in Acetic Acid, 1%, for 2 minutes. Finally, slides were put through a series of dehydration steps in ethanol (80%, 95% and 100%) for 5 min each. Slides were then mounted with DPX mountant (BDH) and examined under a light microscope.

2.26.3 HISTOLOGICAL SCORING

Following trichrome staining, slides were coded without reference to prior treatment and examined in a blind fashion. A semi-quantitative scoring system was used to assess collagen deposition and changes in lung architechure in the lung, (Ashcroft, 2008). The scoring was carried out as follows:

	Alveolar Septa	Lung Structure
0	Normal	Normal
1	Isolated gentle fibrotic changes (septum ≤3× thicker than normal)	Alveoli partly enlarged and rarefied, but no fibrotic masses present
2	Clearly fibrotic changes (septum >3× thicker than normal) with knot-like formation but not connected to each other	Alveoli partly enlarged and rarefied, but no fibrotic masses
3	Contiguous fibrotic walls (septum >3× thicker than normal) predominantly in whole microscopic field	Alveoli partly enlarged and rarefied, but no fibrotic masses
4	Variable	Single fibrotic masses (≤10% of microscopic field)
5	Variable	Confluent fibrotic masses (>10% and ≤50% of microscopic field). Lung structure severely damaged but still preserved
6	Variable, mostly not existent	Large contiguous fibrotic masses (>50% of microscopic field). Lung architecture mostly not preserved
7	Non-existent	Alveoli nearly obliterated with fibrous masses but still up to five air bubbles
8	Non-existent	Microscopic field with complete obliteration with fibrotic masses

2.27 CRYOPRESERVATION AND RECOVERY OF CELLS FROM LIQUID NITROGEN

Cells were suspended at 1 x 10^6/ml of freezing medium and temperature reduced 1 °C per minute overnight and stored in liquid Nitrogen within 24 h. Freezing medium consisted of basic media containing 10%-20% (v/v) FCS supplemented with 10 % (v/v) Dimethyl Sulfoxide (DMSO) (Sigma-Aldrich). To recover cells, vials were quickly thawed at 37 °C. Just as the vial contents thawed, 8 ml of warmed medium was added and cells were centrifuged at 400 g for 5 min. Supernatant was discarded and the cells washed once more. The final pellet was re-suspended in 2 ml of desired media and placed in T175 flask for culturing in cell specific media.

2.28 STATISTICAL METHODS

The students paired t test was used when statistical analysis was required between two experimental groups. One way ANOVA was used to test for statistical significance of differences when multiple experimental groups were compared. Kaplan Meier curves (log rank test) were used to compare survival between treatment groups. Power analysis was carried out to determine the number of animals that would yield a significant difference in the in vivo studies. Statistical methods (Power analysis (SISA)) were used to determine the minimum number of animals per treatment group to obtain a power in the study. SISA software is online at http://home.clara.net/sisa/power.htm.

Table 2.1 Media for cultured cells

Media	Componants	Supplier
Complete Isolation Media	RPMI 1640	Invitrogen-Gibco
	100 U/ml penicillin	Invitrogen-Gibco
	100 µg/ml streptomycin	Invitrogen-Gibco
	2 mM L-glutamine	Invitrogen-Gibco
	10 % (v/v) horse serum	Hyclone
	10 % (v/v) heat inactivated, low-endotoxin foetal calf serum (FCS)	Biosera
Complete Expansion Media	Minimum Essential Medium alpha (MEM)	Invitrogen-Gibco
	100 U/ml penicillin	Invitrogen-Gibco
	100 µg/ml streptomycin	Invitrogen-Gibco
	2 mM L-glutamine	Invitrogen-Gibco
	10 % (v/v) horse serum	Hyclone
	10 % (v/v) heat inactivated, low-endotoxin foetal calf serum (FCS)	Biosera
Osteoblast Media	Minimum Essential Medium alpha (MEM)	Invitrogen-Gibco
	1 mM dexamethasone,	Sigma-Aldrich
	20 mM β-glycerolphosphate,	Sigma-Aldrich
	50 µM L-ascorbic acid-2-phosphate,	Sigma-Aldrich
	50 ng/ml L-thyroxine sodium pentahydrate	Sigma-Aldrich
Adipocyte Media	Minimum Essential Medium alpha (MEM)	Invitrogen-Gibco
	5.0 µg/ml insulin in 0.1N acetic acid	Sigma-Aldrich
	50 µM indomethacin	Sigma-Aldrich
	1 µM dexamethasone	Sigma-Aldrich
	0.5 µM IBM x in MeOH	Sigma-Aldrich
Chondrocyte Media	Minimum Essential Medium alpha (MEM)	Invitrogen-Gibco-
	100 nM dexamethasone	Sigma-Aldrich
	50 µg/ml ascorbic-acid-2-phosphate	Sigma-Aldrich
	40 µg/ml proline	Sigma-Aldrich

Table 2.1 Media for cultured cells continued

Media	Componants	Supplier
	1 mM sodium pyruvate	Sigma-Aldrich
	1 % v/v ITS + supplement	BD Biosciences
	10 ng/ml TGF-β3	TS:beta
Murine Dendritic Cell Medium	RPMI 1640	Invitrogen-Gibco
	100 U/ml penicillin	Invitrogen-Gibco
	100 µg/ml streptomycin	Invitrogen-Gibco
	2mM L-glutamine	Invitrogen-Gibco
	10% (v/v) heat inactivated low-endotoxin FCS	Biosera
	20 ng/ml recombinant murine GM-CSF	Peprotech
CD4+ T Cell or Murine Splenocyte Medium (cRPMI)	RPMI 1640	Invitrogen-Gibco
	100 U/ml penicillin	Invitrogen-Gibco
	100 µg/ml streptomycin	Invitrogen-Gibco
	2mM L-glutamine	Invitrogen-Gibco
	10% (v/v) heat inactivated low-endotoxin FCS	Biosera
	0.01% (v/v) beta mercaptoethanol	Invitrogen-Gibco
HEK Cell Media	Dulbecco's Modified Eagle's Media (DMEM) containing 4000 mg/ml glucose	Invitrogen-Gibco
	100 U/ml penicillin	Invitrogen-Gibco
	100 µg/ml streptomycin	Invitrogen-Gibco
	2mM L-glutamine	Invitrogen-Gibco
	10% (v/v) heat inactivated low-endotoxin FCS	Biosera
LB Broth	20 g/l LB Broth (low salt)	Lennox
	10 g/l Peptone	Merck
	5 g/l Yeast Extract	BD Bioscience
	100 µg/ml Carbenicillin	Novagen

Table 2.1 Media for cultured cells continued

Media	Componants	Supplier
Fibroblast/NIH 3T3 Media	Dulbecco's Modified Eagle's Media (DMEM) containing 4000 mg/ml glucose	Invitrogen-Gibco
	100 U/ml penicillin	Invitrogen-Gibco
	100 µg/ml streptomycin	Invitrogen-Gibco
	2mM L-glutamine	Invitrogen-Gibco
	10% (v/v) heat inactivated low-endotoxin FCS	Biosera
LA4 media	Dulbecco's Modified Eagle's Media (DMEM)F:12	Invitrogen-Gibco
	100 U/ml penicillin	Invitrogen-Gibco
	100 µg/ml streptomycin	Invitrogen-Gibco
	2mM L-glutamine	Invitrogen-Gibco
	10% (v/v) heat inactivated low-endotoxin FCS	Biosera
Ca/Mg^{+} Solution	0.9%w/v Sodium chloride	Sigma- Aldrich
	0.15M Potasium chloride	Sigma- Aldrich
	0.11M Calcium chloride	Sigma- Aldrich
	0.15M Magnesium sulfate	Sigma- Aldrich
	0.10M Phosphate buffer pH 7.4	Sigma- Aldrich
	0.2M HEPES	Sigma- Aldrich
Ca/Mg^{-} Solution	0.9%w/v Sodium chloride	Sigma- Aldrich
	0.15M Potasium chloride	Sigma- Aldrich
	0.10M Phosphate buffer pH 7.4	Sigma- Aldrich
	0.2M HEPES	Sigma- Aldrich
Differential Attachment Medium	1:1 M199:Hams/F12	Invitrogen-Gibco
	2mM L-Glutamine	Invitrogen-Gibco
	100U/ml Penicillin/Streptomycin	Invitrogen-Gibco

Table 2.2 Buffers

Application	Buffer	Componants	Concentration	Supplier
PBS	Cell Culture	Sodium chloride	8 g/l	BDH
	ELISA	Di-sodium phosphate	1.16 g/l	Sigma
		Posatium chloride	0.2 g/l	Merck
		Ethylenediaminetetraacetic acid	10mM	Qiagen
Buffer P1	Plasmid Miniprep	Tris-Cl pH 8.0	50mM	Qiagen
		Potassium phosphate monobasic	0.2 g/l	Qiagen
		Rnase A	100 µg/ml	Qiagen
Buffer P2	Plasmid Miniprep	Sodium hydroxide	200 mM	Qiagen
		Sodium dodecyl sulfate	1% w/v	Qiagen
Buffer P3	Plasmid Miniprep	Potassium acetate pH 5.0	3 M	Qiagen
Buffer QBT	Plasmid Miniprep	Sodium Chloride	750 mM	Qiagen
		3-(N-morpholino)propanesulfonic acid pH 7	50 mM	Qiagen
		isopropanol	15% v/v	Qiagen
		Triton X-100	0.15% v/v	Qiagen
Buffer QC	Plasmid Miniprep	Sodium Chloride	1 M	Qiagen
		3-(N-morpholino)propanesulfonic acid pH 7	50 mM	Qiagen
		isopropanol	15% v/v	Qiagen
Buffer QF	Plasmid Miniprep	Sodium chloride	1.25 M	Qiagen
		Tris-Cl Ph 8.5	50 mM	Qiagen
		isopropanol	15% v/v	Qiagen

Table 2.2 Buffers continued

Time	Buffer	Componants	Concentration	Supplier
TE buffer	Plasmid Miniprep	Tris-Cl Ph 8	10 mM	Qiagen
		Ethylenediaminetetraacetic acid	1 mM	Qiagen
MACS Buffer	MACS Bead Seperation	30% Bovine Serum Albumin	16.67 ml/l	Sigma
		Ethylenediaminetetraacetic acid	0.74 g/l	Sigma
		PBS		
TBS	Immunoflourescence	Tris-HCl	0.01M	Sigma
		Sodium chloride	0.15M	Sigma
		pH adjusted to 7.5		
TBST	Immunoflourescence	Tris-HCl	0.01M	Sigma
		Sodium chloride	0.15M	Sigma
		Tween 20	0.1% v/v	Sigma
		pH adjusted to 7.5		
Block Buffer	ELISA	PBS		
		Bovine Serum Albumin	1%	Sigma
Wash Buffer	ELISA	PBS		
		Tween 20	0.10%	Sigma
Reagent Diluent	ELISA	PBS		
		Bovine Serum Albumin	1%	Sigma
Stop Solution	ELISA	Sulphuric Acid	1M	Sigma
Phosphotungstic/Phosphomolybdic Acid Solution	Trichrome Staining	Phosphotungstic Acid Solution	25% v/v	Sigma
		Phosphomolybdic Acid Solution	25% v/v	Sigma
		In Deionised Water		

Table 2.3 Antibodies

Application	Antibody	Flourochrome	Isotype	Supplier
Flow Cytometry	CD3e	PerCP		eBioscience
	CD4	APC		eBioscience
	CD11b	FITC	Rat IgG2b	eBioscience
	CD11c	FITC	Armenian hamster IgG1	eBioscience
	CD25	PeCy5	Rat IgG1	eBioscience
	CD 34	FITC	Rat IgG2a	eBioscience
	CD44	PE	Rat IgG2b	eBioscience
	CD45	PE	Rat IgG2b	eBioscience
	CD73	PE	Rat IgG1	eBioscience
	CD86	PE	Rat IgG2a	eBioscience
	CD90.2	FITC	Rat IgG2b	eBioscience
	CD 105	PE	Rat IgG2a	eBioscience
	CD106	FITC	Rat IgG2a	eBioscience
	CD117	FITC	Rat IgG2b	eBioscience
	MHC Class I	FITC	Mouse IgG2a	eBioscience
	MHC Class II	PE	Rat IgG2b	eBioscience
	Sca-1	PE	Rat IgG2b	eBioscience
	Notch 1	PE	Mouse IgG1	eBioscience
	Notch 2	PE	Armenian hamster IgG1	eBioscience
	Jagged 1	PE	Armenian hamster IgG1	eBioscience
	Jagged 2	PE	Armenian hamster IgG1	eBioscience
	Delta like ligand 1	PE	Armenian hamster IgG1	eBioscience
	Annexin V	FITC	NA	eBioscience
	Propidium Iodide	PE	NA	eBioscience
Immunoflourscence	Alpha Smooth Mucle Actin	Anti-Mouse 488 1/3000	Rabbit anti-mouse	Sigma
	Vimentin	Anti-Mouse 488 1/2000	Rabbit anti-mouse	Sigma
	PCNA	Anti-Mouse 488 1/3000	Rabbit anti-mouse	Sigma

Table 2.4 Primers

Primer	Forward 5'-3'	Reverse 3'-5'	Prod size (bp)	Anneal temp (°C)
GAPDH	GCACAGTCAAGGCCGAGAAT	GCCTTCTCCATGGTGGTGAA	151	58
Collagen 2a	GCGATGACATTATCTGTGAAG	TATCTCTGATATCTCCAGGTTC	150	58
Aggrecan	CTACCTTGGAGATCCAGAAC	TGGAACACAATACCTTTCAC	121	58
Notch-1	GTCGCTGGATACAAGTGCAA	TGTGGGACAGACACAGGAAA	150	55
Notch-2	CGTGTGAGAATGCTGCTGTT	TTGTGGCAGACACCATTGTT	148	60
Jagged-1	GCAAGACTTGTCAGTTAGATG	CTGGCAATCAGATTCTTACAG	82	58
Jagged-2	AGGCACCTACTGCCATGAAA	CGTTGGGATTGATGTCACAG	143	55
Delta like ligand-1	CAACAAGAAGGCGGACTTTC	CACTTGGTGTCACGTTTGCT	150	57
TNFα	GGATGAGAAGTTCCCAAAT	TGAGAAGATGATCTGAGTG	75	58
IFNγ	TGAGTATTGCCAAGTTTGAG	CTTATTGGGACAATCTCTTCC	159	58
IL-1β	GGATGATGATGATAACCTGC	CATGGAGAATATCACTTGTTGG	163	58
IL-6	TCCTTCAGAGAGATACAGAAC	TTCTGTGACTCCAGCTTATC	124	58
HGF	CAAATGCAAGGACCTTAGA	CTTCTTTTGGATAAGTTGCC	189	58
TGFβ	GGATACCAACTATTGCTTCAG	TGTCCAGGCTCCAAATATAG	161	58
Procollagen	CGTATCACCAAACTCAGAAG	GAAGCAAAGTTTCCTCCAAG	183	58
Fibronectin	CGAACAGCTATTTACCAACC	TTGAATTGCCACCATAAGTC	199	58
E-cadherin	CATGTTCACTGTCAATAGGG	GTGTATGTAGGGTAACTCTCTC	81	58
α Smooth Muscle Actin	CATCTTTCATTGGGATGGAG	TTAGCATAGAGATCCTTCCTG	97	58

Chapter 3

Notch signalling is required for the induction of a functional, tolerogenic, dendritic cell population and the expansion of Treg cells by MSC

3.1 Introduction

The immunomodulatory potential of MSC can be divided into two categories; direct and indirect. When considered in relation to inflammation and infection, MSC predominately respond through indirect cell education, altering the phenotype of immune cells so they in turn can temper the local inflammatory environment (Chapter 1). Over the past decade, this phenomenon has been examined in the Mahon laboratory focusing on DC and Treg. English *et al.* demonstrated that murine MSC suppress DC migration, maturation and antigen presentation (English et al., 2008) and promoted Treg cell expansion (English et al., 2009). The importance of Treg for the therapeutic effect of MSC *in vivo* was elegantly shown using an animal model of allergic asthma (Kavanagh and Mahon, 2011). Work by Tobin et al further investigated the effect of MSC on DC function and concluded that cell contact was a key requirement for MSC modulation of DC maturation and antigen presentation, (Tobin, Cahill et al., in Submission). Similar findings have been published on DC, detailing MSC inhibition of maturation and a reduction of $CCR7^+$ DC *in vivo*. MSC were shown to rapidly inhibit DC migration following subcutaneous injection into a primed mouse. The DC were pulsed with OVA and activated with LPS prior to injection. The mice were primed to OVA through adoptive transfer of DO11.10 T cells, the T cells from DO11.10 mice are genetically modified to respond to OVA antigen (Chiesa et al., 2011).

A common thread that runs through MSC research is that more is known about what MSC can do, and less about how they do it. This chapter aims to delve into precisely how MSC mediate their effects and to determine the pathways being utilised by these cells that cause such dramatic changes to their environment. Murine MSC were examined for interactions with T cells to determine their role in expansion of

Treg, MSC inhibition of DC maturation and induction of tolerogenic DC were also studied. A great deal has been published about the role of soluble factors released by MSC and immune modulation. Despite the proven need for a contact signal, less is known about direct MSC-immune cell interactions. Using *in vitro* methods involving receptor inhibitors, neutralising antibodies, siRNA and ultimately lentiviral shRNA to create stably knocked down cells, the importance of the Notch family signalling pathway in MSC was examined, with particular emphasis on the ligand Jagged 1. These experiments aimed to demonstrate the influence of murine MSC on the immune system through induction, expansion and education of immune cells and to identify the contact dependent signal through which murine MSC modulate the immune function of T cells and DC.

3.2 Characterisation of Murine MSC

Characterisation of murine MSC has been the subject of much scrutiny over the last 10 years as different labs have differing culture methods. There are no absolute markers for specifically distinguishing these cells, and so consistency of methodology and outcome have proven elusive. To that end, efforts have been made to standardise the characterisation of MSC (Tropel et al., 2004). As mentioned in the introduction the three principle stipulations for characterisation became: adherence to plastic, specific cell surface marker expression and tri-lineage differentiation. This study began by characterising the murine MSC to be used subsequently, an issue that would need to be returned to following each major MSC manipulation.

Murine BALB/c or C57BL/6 MSC can be isolated from bone marrow by immunodepletion in selective media and by using their capacity to adhere to plastic.

Following this, cells must express particular cell surface markers, namely, CD105, CD44, CD73 and Sca-1 while lacking haematopoietic and endothelial markers such as CD45, CD34, and CD11b. Typically MSC lack allogeneic reactivity associated with reduced expression of MHC class I and Class II and a lack of the co-stimulatory markers CD80 and CD86. Though these guidelines to define MSC are generally consistent, different methods of isolation, the strain of mice used and the age of the cells can alter levels of expression (K English, unpublished data). Using the methodology described in section 2.7, murine MSC were isolated and characterised.

Flow cytometric analysis of the isolated cells demonstrated expression of CD44, Sca-1, CD106, CD73, CD90 and no MHC Class I expression. This pattern of expression coupled with the absence of the haematopoietic marker CD45, the lymphocyte maker CD34, the co-stimulatory marker CD86 or MHC Class II indicated that the cells isolated were non-hematopoietic, stromal cells (Fig. 3.1). This method of characterisation was routinely used through successive passages and manipulations, with a similar outcome to assure the purity of the cells used experimentally.

MSC must by definition demonstrate multi lineage differentiation capabilities, specifically to osteoblasts, adipocytes, and chondrocytes. Isolated candidate MSC were grown as described in section 2.7.3 using selective media for 21 days. Differentiation to bone and fat cells was detected by staining using alazarin red and Oil Red O respectively, while chondrocyte differentiation was detected by measuring mRNA expression of Collagen IIa, collagen III and Aggrecans. The control cultures were treated with the same conditions in the absence of differentiation components, but failed to develop the same distinctive patterns of expression (Fig. 3.2). While differentiation into both bone and fat was observed in both C57BL/6 MSC and BALB/C MSC, the environment in which they were cultured affected the extent of the

differentiation. Cells grown under normoxic conditions tended towards a more adipogenic phenotype, while cells grown under hypoxic conditions favoured osteogenic differentiation. It was also observed that cells cultured in hypoxia more readily maintained the ability to differentiation at later passages, I feature sometimes lost by cells cultured in normoxia.

Finally, candidate MSC were examined for their capacity to suppress both autologous and allogeneic proliferation of lymphocytes. Though not a defining characteristic of MSC, suppression of lymphocyte proliferation has become synonymous with the cell type. MHC mis-matched splenocytes were cultured with MSC in the presence or absence of the mitogen Concovalin A (ConA) and analysed by tritiated thymidine uptake for incorporation into replicating DNA. Fig. 3.3 illustrates the significant immunosuppressive capacity of MSC for mitogen driven proliferation. In an MHC mis-matched environment the MSC significantly reduced the proliferation of lymphocytes in a two way mixed lymphocyte reaction (***, $P<0.001$).

Taken together these data indicate that the candidate BALB/c or C57BL/6 MSC used here and in further experiments conformed to the accepted definition of MSC isolated from murine bone marrow.

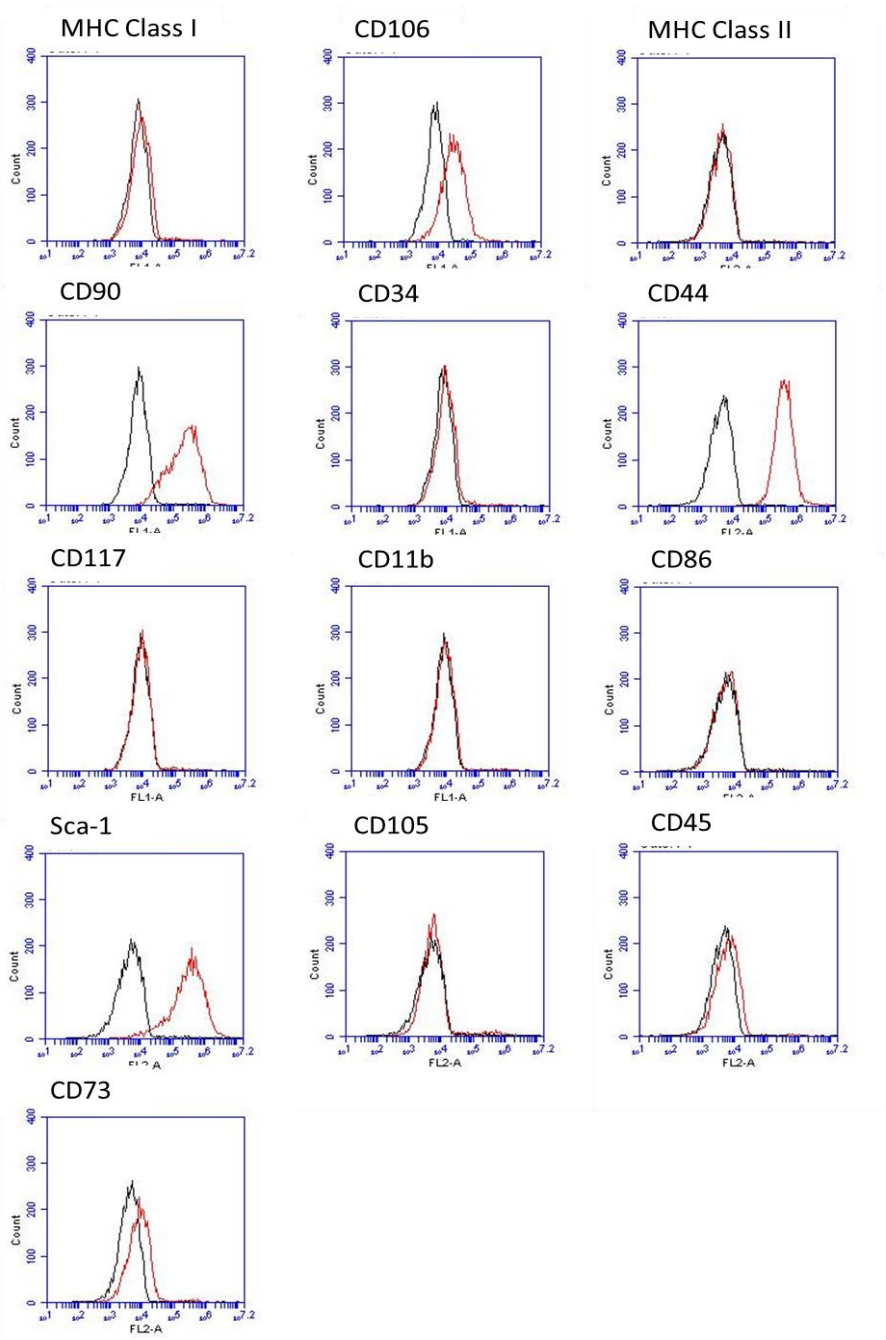

Fig. 3.1 MSC characterisation for cell surface markers. Murine BALB/c or C57BL/6 MSC (in this instance from C57BL/6 at passage 7) were characterised by staining the cells for variety of cell surface markers (red line) against their corresponding isotypes (black line). The cells were analysed using flow cytometry with 10,000 events were recorded for each marker. These results are representative of multiple experiments, with cells analysed at various passages from 3 to 12.

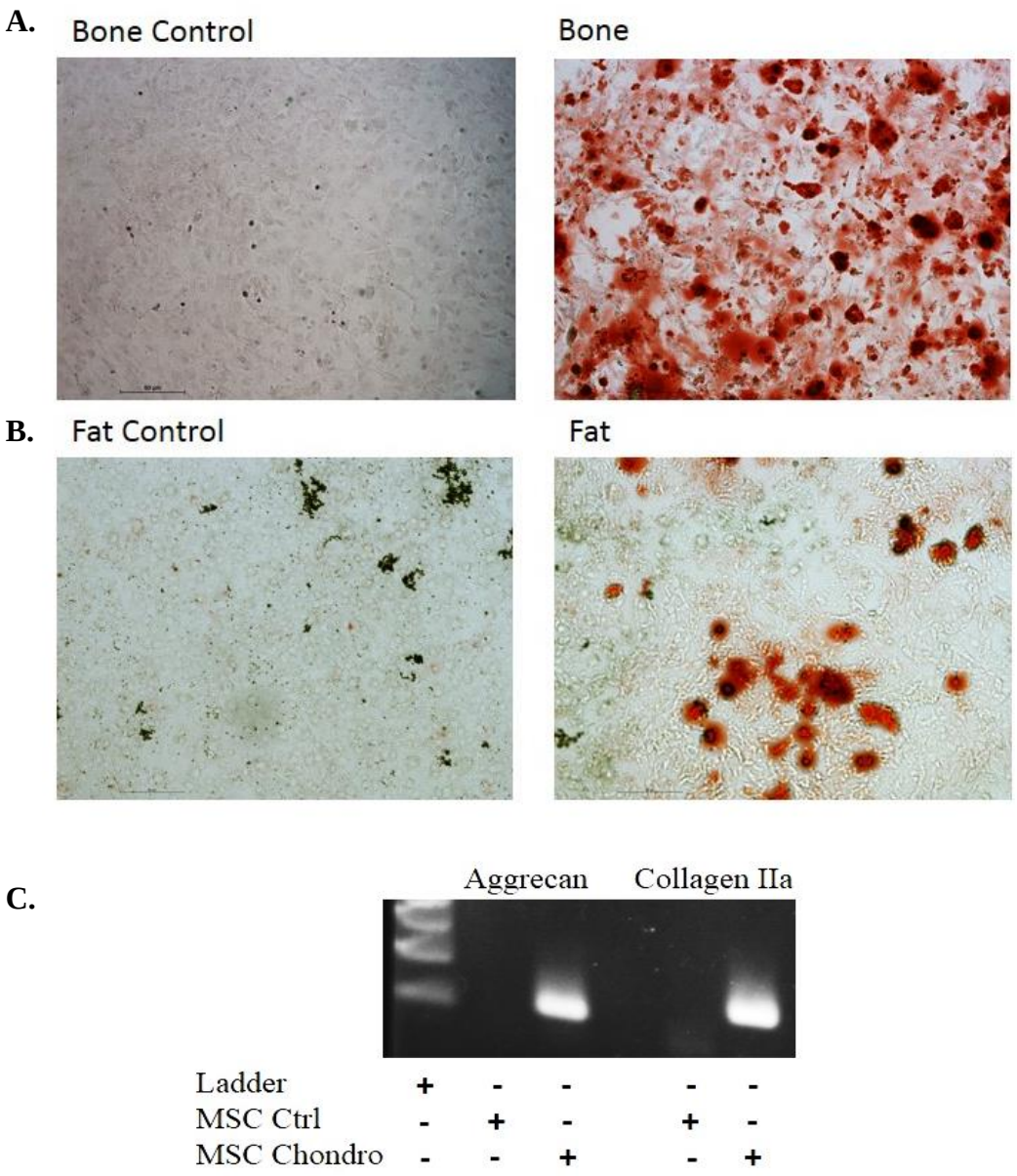

Fig. 3.2 Trilineage differentiation of MSC. C57BL/6 MSC ($5x10^4$) were cultured for 21 days in control medium or with osteogenic or adipogenic medium. Cultures were stained with Alazarin Red (A) and Oil Red O (B). In Chondrocyte differentiation studies, $2x10^5$ MSC were centrifuged at 200xG for 8 min to form a cell pellet, control medium or chondrocyte medium was added to the tube and the cells were cultured for 21 as a 3D cell mass. After 21 days trizol was added to the cell pellet, following RNA extraction and cDNA synthesis, the mRNA was tested for the chondrocyte markers aggrecan and collagen IIa (C). These results are representative of multiple experiments using both BALB/c and C57BL/6 MSC, with cells analysed at various passages from 3 to 12. (Magnification x100).

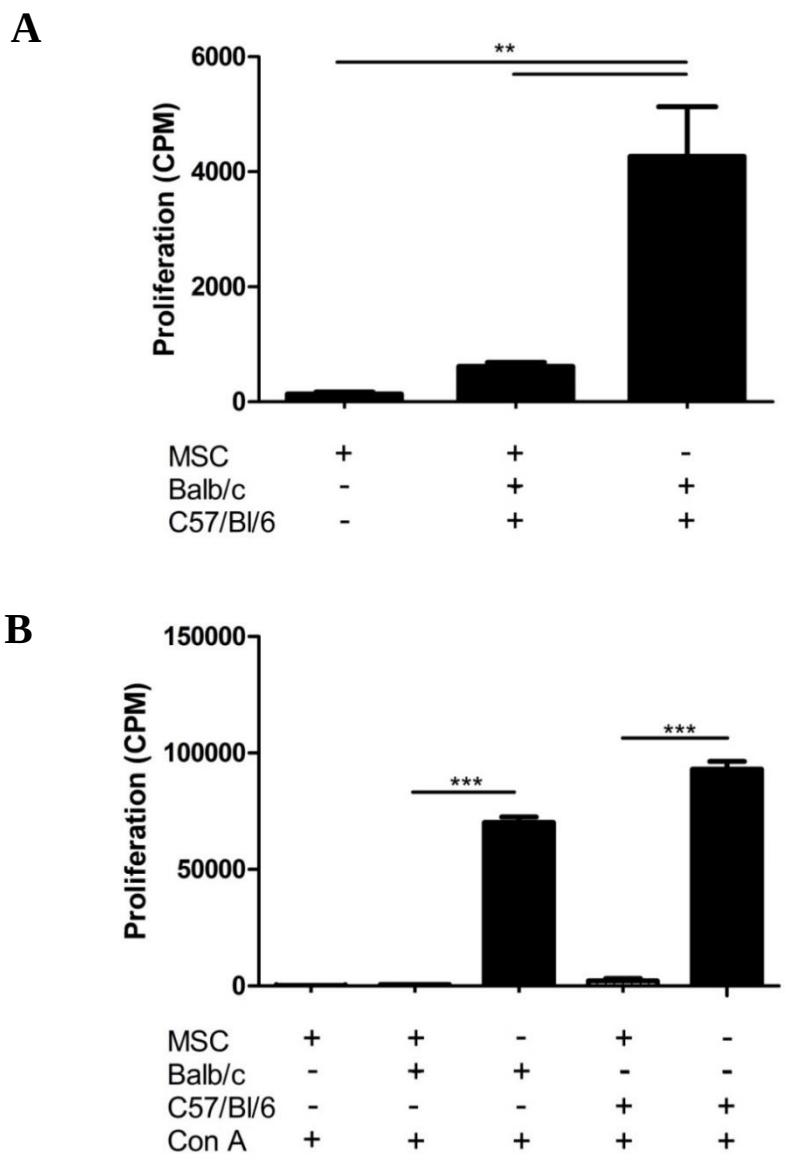

Fig. 3.3 MSC inhibit A) alloantigen and B) mitogen driven spleen cell proliferation. BALB/c MSC were co-cultured with splenocytes from BALB/c and C57BL/6 mice for 72h. Proliferation was measured by [^{3}H] thymidine uptake over a 6h period. Mitogen driven proliferation was examined using Con A (5ug/ml) added at day 0. Results are represented in counts per minute. The results are representative of several experiments over multiple passages using both BALB/c and C57BL/6 MSC, and statistical significance determined by ANOVA analysis (p**<0.01), (p***<0.001).

3.3 MSC expand Regulatory T cells

English *et al* previously demonstrated that human MSC induce functional Treg cells expressing the transcription factor FoxP3 through the release of soluble factors PGE2 and TGFβ1, while also requiring a cell contact signal (English et al., 2009). That study did not establish whether MSC were inducing Treg from naive cells or expanding a pre-existing Treg population. In order to determine the origin of murine Treg following MSC co-culture, *in vitro* experiments were carried out using $CD4^+$ cells isolated from FoxP3-eGFP knock-in mice. These mice are genetically engineered to co-express eGFP and the Treg transcription factor FoxP3 following activation of the promoter region. They accurately determine FoxP3 expression with 97% of $FoxP3^+$ cells displaying eGFP fluorescence (Lin et al., 2007). MSC co-cultured with $CD4^+$ cells isolated from FoxP3-eGFP reporter mouse splenocytes caused an increase in CD25 and FoxP3 expression when compared to $CD4^+$ cells cultured alone (Fig. 3.4). In order to determine if this increase was a result of MSC induction or expansion of a regulatory population, $CD4^+CD25^-FoxP3GFP^-$ cells were sorted from Foxp3-GFP reporter mouse spleens and subsequently cultured with allogeneic MSC for 72h. In this system, MSC were incapable of inducing $CD25^+FoxP3^+$ cells (Fig. 3.5). These data show that MSC do not directly activate Treg from a naive population but suggest that they support the expansion of pre-existing $Foxp3^+$ regulatory T cells.

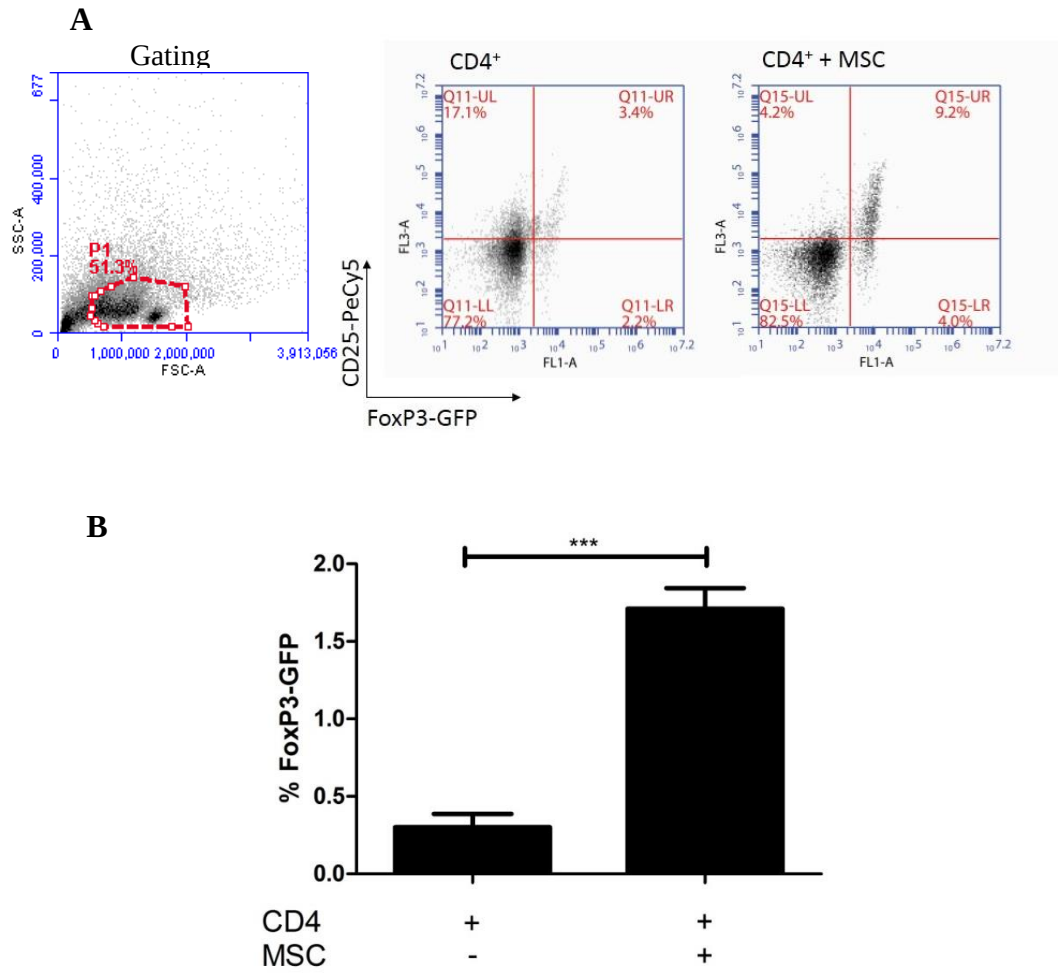

Fig. 3.4 MSC increase the number of cells expressing CD25 and FoxP3. Allogeneic murine MSC were co-cultured with $CD4^+$ FoxP3-eGFP spleen cells for 72h at a ratio of 1:3. Following this, the $CD4^+$ cells were recovered from co-culture by aspirating off the suspension cells from the adherent MSC and examined for expression of FoxP3-GFP and CD25. (A); representative example of T cell expression of FoxP3-eGFP and CD25-PeCy5 (B); mean of 7 experiments showing an increase in FoxP3 expression in T cells co-cultured with MSC. Statistical analysis by student t test (p***<0.001).

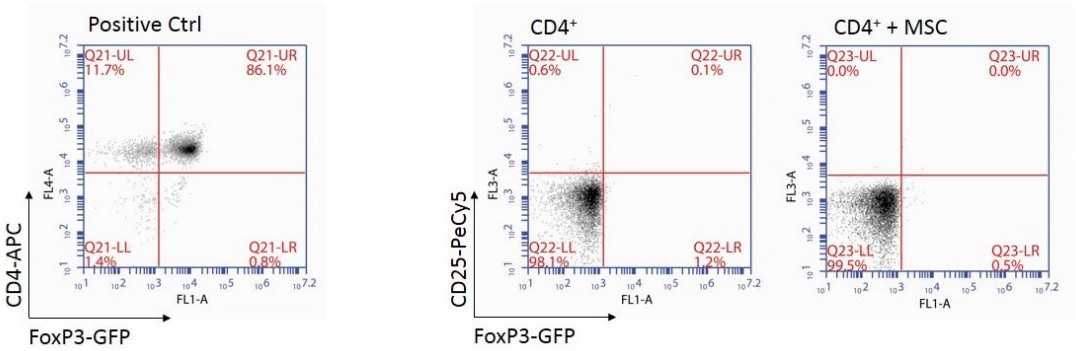

Fig. 3.5 MSC promote the expansion but not induction of regulatory T cells in vitro. T cells from FoxP3-eGFP mice were purified either by bead isolation (CD4) or cell sorting ($CD4^+CD25^-FoxP3^-$), the cells were subsequently cultured with or without MSC for 72h and examined for CD25 and FoxP3-eGFP expression by flow cytometry. CD25+FoxP3-eGFP+ cells isolated during cell sorting were used as a positive control for staining after 72h culture with IL-2 (300U/ml). The sorted $CD4^+CD25^-FoxP3^-$ cells alone and those co-cultured with MSC for 72h were unable to induce Treg cells. Data representative of 3 experiments.

3.4 MSC inhibit DC maturation and induce a tolerogenic DC phenotype

Typically, DC encounter with antigen leads to maturation, which involves increased co-stimulatory marker, and MHC Class II expression. A further mechanism of MSC immunomodulation is their ability to inhibit the maturation of DC. MSC reduced the DC expression of co-stimulatory markers MHC Class II, and CD86 (Fig.3.6), and were previously shown to increase DC production of IL-10 while reducing Il-12p70 (Tobin, unpublished data). These semi-mature DC were further studied to determine any potential function in immunomodulation.

To determine the functionality of these semi-mature or candidate "tolerogenic" cells, DC derived from BALB/c mice were cultured with or without allogeneic MSC in the presence or absence of the protein ovalbumin (OVA) for 48h. These MSC "educated" DC were recovered from the adherent MSC by aspirating the cells suspended in the medium, the cells were washed and subsequently co-cultured with $CD4^+$ T cells isolated from DO11.10 mice (Fig. 3.7). DO11.10 mice have been genetically modified so that MHC Class II restricted rearranged T cell receptor transgene expressing T cells will react to the peptide antigen derived from OVA (Murphy et al., 1990). Mature DC pulsed with OVA, supported the proliferation of the $CD4^+$ T cells as expected, however, the "tolerogenic" DC were able to reduce this proliferation even in the presence of OVA. Paraformaldehyde fixed MSC were used as a control to demonstrate that live viable MSC were required to confer DC with the capability of inhibiting or not supporting T cell proliferation (Fig. 3.7).

Induction of regulatory T cells was postulated to account for the inhibition seen in the proliferation assay (Fig. 3.3). To test this theory, DC were isolated from C57BL/6 mice and co-cultured with BALB/c MSC for 48h in the presence (mDC and tDC) or absence (iDC) of LPS. The DC were separated from the adherent MSC by

aspirating the cells suspended in appropriate medium and further co-cultured with $CD4^+CD25^+FoxP3^-$ T cells isolated from a FoxP3-eGFP knockin mouse. $CD3^+$ cells were isolated from murine spleen using bead separation, and subsequently stained for CD4 and CD25. The $CD4^+CD25^+FoxP3^-$ cells were separated from the $CD4^+CD25^+FoxP3^+$ population by cell sorting and then co-cultured with the DC for 72h. Induction of $CD4^+CD25^+FoxP3^+$ cells from the null population by immature, mature (iDC) and tolerogenic DC (tDC) was determined by FACS (Fig. 3.8). After 72h immature and mature DC induced a small population of Treg, 4.6% and 10.0% of the total population respectively. DC that had encountered MSC (candidate tolerogenic DC) on the other hand induced a substantially larger population at 35.3%. These results support the hypothesis that MSC induce tolerogenic DC and consequently Treg cells, which may contribute to the reduction in antigen driven T cell proliferation.

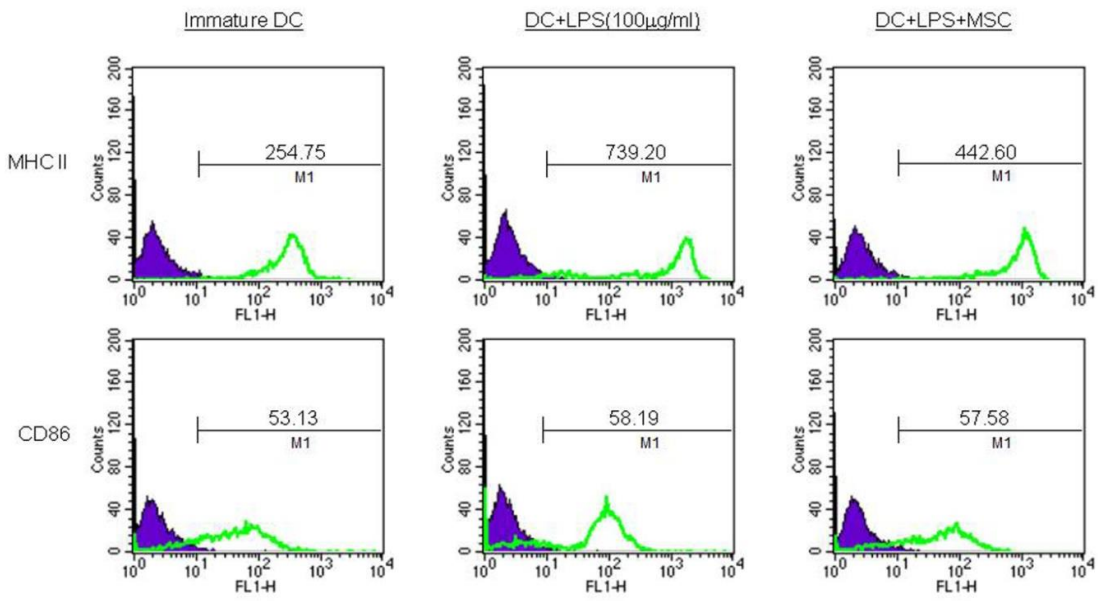

Fig. 3.6 MSC prevent the LPS induced maturation of DC. Naive BALB/c derived DC were stimulated with 100ng/ml LPS to promote maturation. Expression of maturation markers MHC Class II and CD86 were examined by flow cytometry. Histograms depicting isotype controls (purple) and specific markers (green) are analysed for mean fluorescence intensity (MFI). DC which were co-cultured with MSC demonstrated reduced maturation marker expression. Data are representative of three experiments.

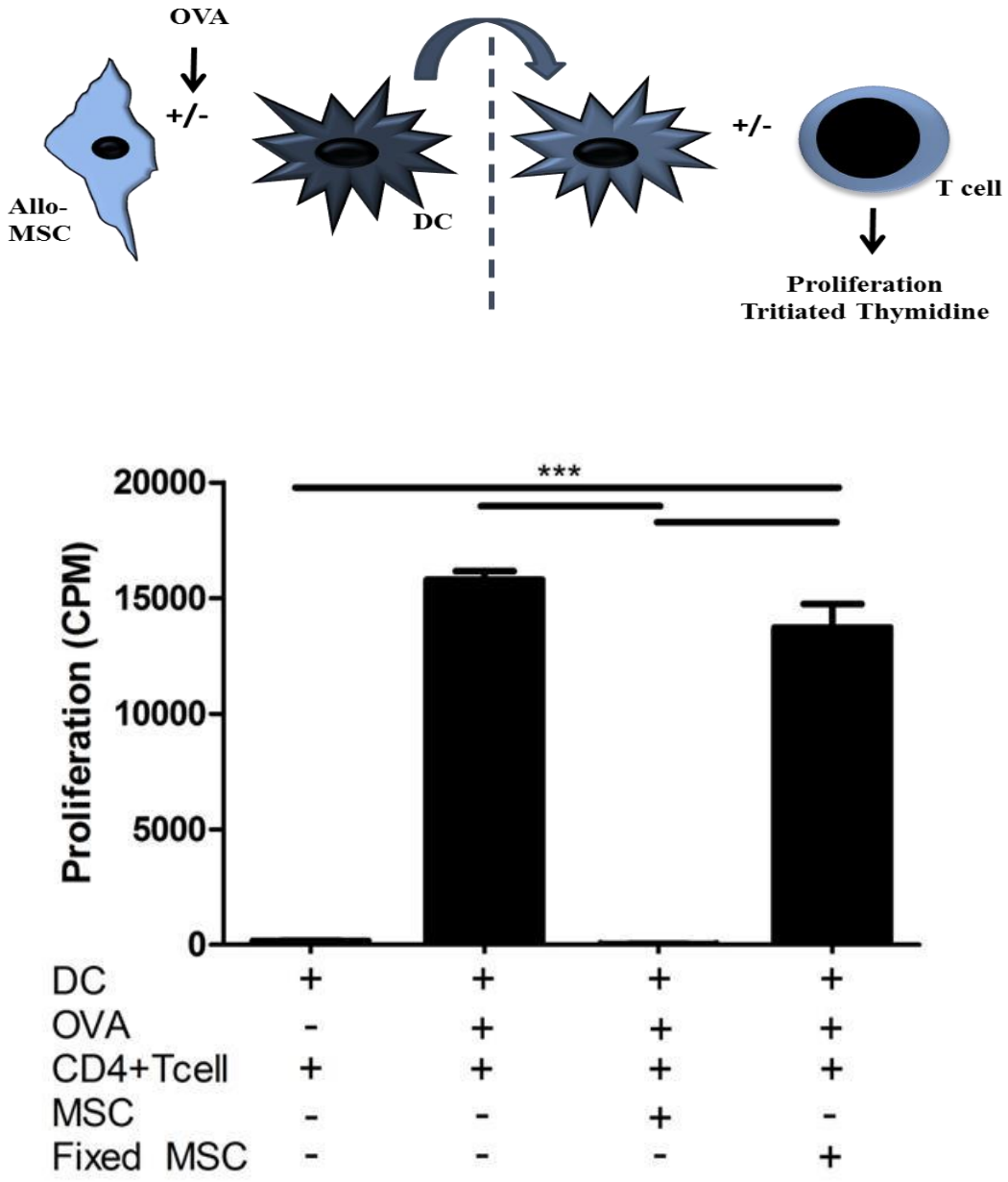

Fig. 3.7 Allogeneic MSC educate DC to inhibit antigen driven T cell proliferation. Immature BALB/c derived DC were co-cultured with or without allogeneic MSC in the presence or absence of OVA. Paraformaldehyde fixed MSC were used as a control. The DC were recovered by aspiration after 48h and washed before co-culturing with DO11.10 $CD4^+$ T cells. After 72h, proliferation was examined over a 6h period by measuring tritiated thymidine uptake. Proliferation was measured in counts per minute (CPM). MSC, but not fixed MSC educated DC were capable of significantly suppressing OVA driven T cell proliferation ($p^{***}<0.001$). Statistical analysis performed by ANOVA with an n=3.

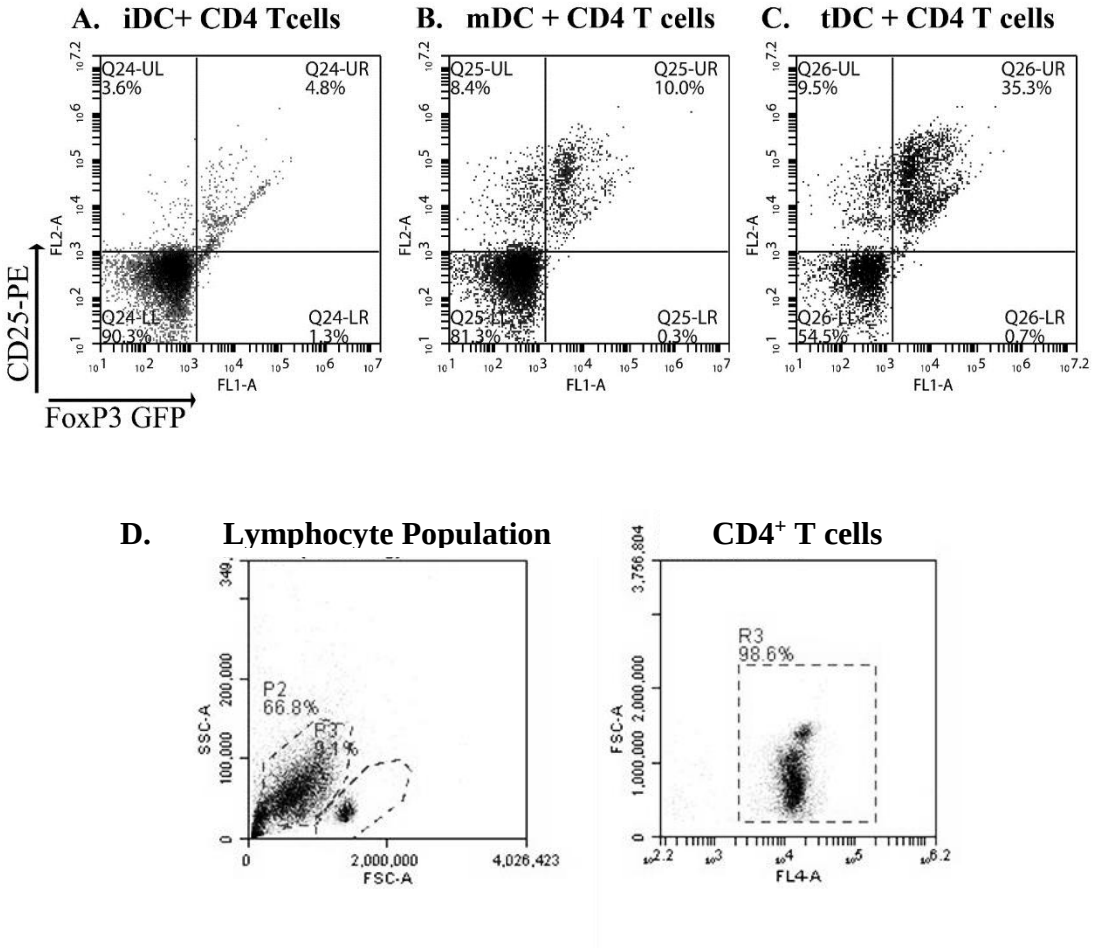

Fig. 3.8 Tolerogenic DC induce regulatory T cells. BALB/c DC cultured with or without allogeneic MSC in the presence or absence of LPS, were re-purified after 48h. iDC received no LPS, mDC were cultured in the presence of LPS, and tDC were cultured with LPS and MSC but separated from the MSC before co-culture with T cells. The cells were washed and further cultured with $CD4^{+}CD25^{-}FoxP3^{-}$ T cells from an eGFP knock in mouse, at a ratio of 1:4, for 72h. T cells were labelled for CD3 to discriminate them from the DC and expression of CD25 and FoxP3-eGFP was examined by flow cytometry. Tolerogenic DC had a greater capacity to induce regulatory T cells. Data are representative of two experiments. Gating strategy (D).

3.5 Notch Receptor and Ligand Expression on Murine MSC

Soluble factors play an important role in the immunological effects of MSC, however there is a non-redundant role for cell-cell contact. This was previously described by English *et al.* in human MSC (English et al., 2009), and Tobin *et al.* in mouse MSC (unpublished data). Many potential contact signals have been investigated by the Mahon laboratory, Siglecs, LICOS, Nestin, SDF1, and PDL, however, to date the most compelling results have come from studying the Notch signalling pathway. Further work by Tobin *et al.* demonstrated an important role for Notch in MSC modulation of DC (Tobin, Cahill et al, in submission)

Notch-Notch ligand expression on MSC and T cells was determined by PCR (Fig. 3.9). MSC express high levels of Notch 2, Jagged 1 and Delta-like ligand 1, while T cells express high levels of the receptor Notch 1 and 2 and low levels of Jagged 2 and Delta like ligand 1 (Fig. 3.9).

Given the high level of Notch receptor expression and the low level of ligand expression on T cells, it was hypothesised that MSC signal to CD4 T cells and DC. This theory was further supported by examining the manner in which Notch signals. The intracellular domain is cleaved and translocates to the nucleus of the cells, signalling downstream changes through the target genes HES and HEY (Gordon et al., 2008). Notch 1 signalling has been shown to be involved in Smad-3 binding to the promotor region of the FoxP3 gene and plays a key role in induction of Treg cells by TGFβ (Samon et al., 2008). While MSC ligand signalling to T cells and DC is the most likely scenario, the presence of Notch ligands on the T cells means signalling may be occurring in reverse.

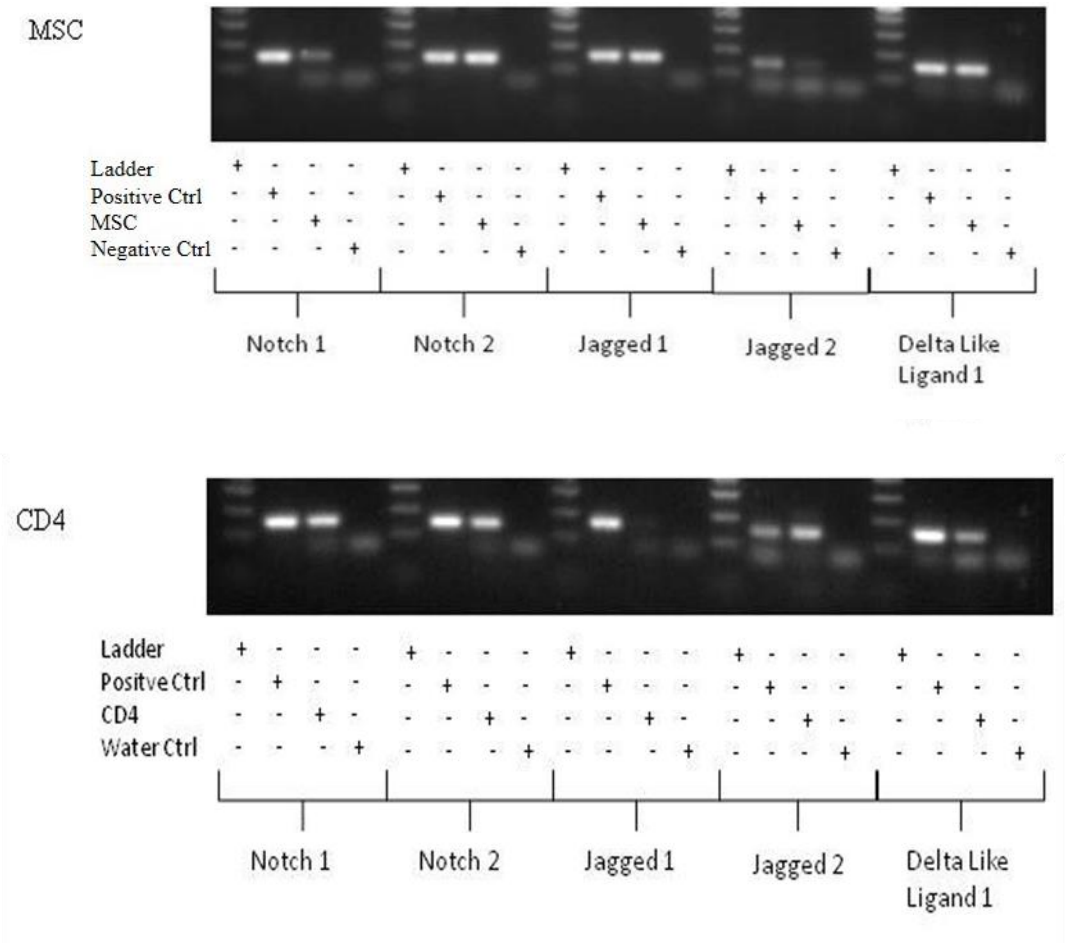

Cells	Notch 1	Notch 2	Jagged 1	Jagged 2	Delta-like ligand 1
MSC	+	+	+	-	+
$CD4^+$ T ells	+	+	-	+	Low

Fig. 3.9 Notch/Jagged family expression profile on murine MSC and $CD4^+$ T cells. Murine MSC and $CD4^+$ T cells were examined for expression of the Notch/Jagged family mRNA by RT-PCR. Cells were cultured separately for 24h, mRNA was then isolated and cDNA produced according to the method outlined in sections 2.13 and 2.14. Known positive control cells were used for each set of primers, Notch 1, Delta Like ligand 1 (spleen), Notch 2 (bone marrow), Jagged 1 and Jagged 2 (J774). Results are representative of BALB/c and C57Bl/6 strains.

3.6 Is the Notch family involved in Regulatory T cell Induction?

Gamma secretase is a cell membrane integrated protease complex involved in the cleavage of the Notch intracellular domain (NICD), thus facilitating NCID translocation to the nucleus and subsequent gene transcription. The function of these secretases is inhibited by gamma secretase inhibitors (GSI) (LaVoie and Selkoe, 2003). By exploiting this pathway all Notch receptors can be simultaneously blocked and receptor participation in MSC signalling can therefore be studied.

The use of FoxP3-eGFP $CD4^+$ T cells in flow cytometry allowed for the rapid and accurate observation of $CD4^+FoxP3^+$ regulatory T cells. As previously shown MSC readily expand Treg (Fig. 3.4), in order to determine whether a role existed for Notch in this expansion a global inhibitor of Notch receptor signalling, GSI, was used. FoxP3-eGFP spleen cells were isolated and $CD4^+$ cells separated by bead extraction. These cells were cultured with allogeneic MSC for 72h in the presence or absence of GSI (1μM) or DMSO (vehicle control). Cells were examined by flow cytometry, where by $CD4^+$ cells were gated and expression of FoxP3 was determined. While MSC enhanced Treg expansion, the presence of GSI ablated this effect. (Fig. 3.10). These results clearly indicate MSC expansion of Treg cells involves Notch receptor signalling

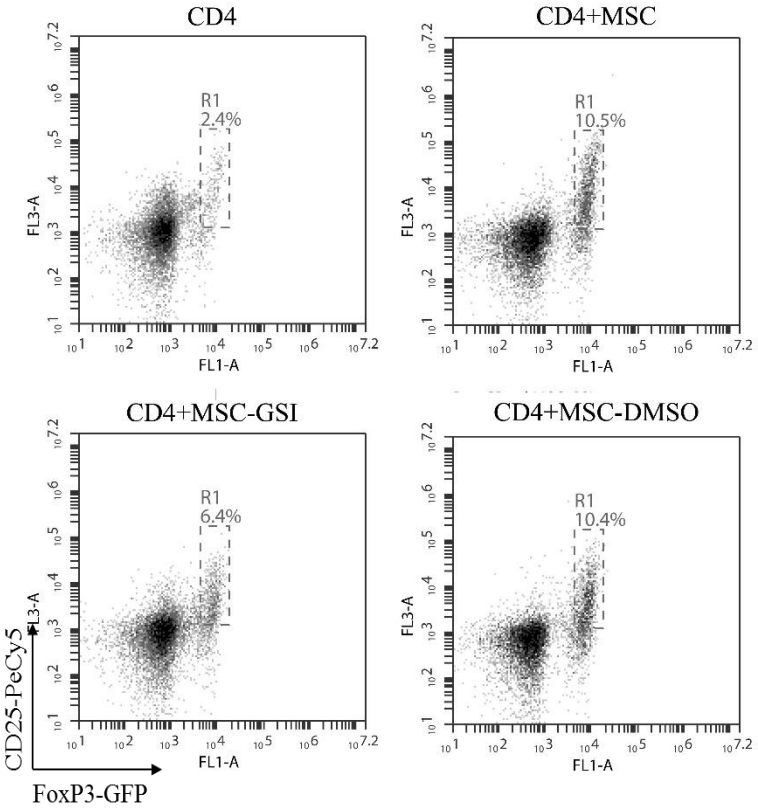

Fig. 3.10 Murine MSC expand a regulatory T cell population in a Notch dependent manner. FoxP3eGFP $CD4^+$ T cells were co-cultured for 72h with allogeneic MSC in the presence or absence of GSI (1μM) or its diluent DMSO. MSC expansion of the Treg population is reduced by the addition of GSI but not the diluent alone. Treg expansion was examined by flow cytometry for FoxP3-eGFP expression. Data representative of at least three experiments.

3.7 Notch signalling is required for Murine MSC induction of Tolerogenic DC

In order to examine the possible role of Notch signalling in the induction of a tolerogenic DC by murine MSC, a co-culture system was employed. BALB/c DC were pulsed with OVA in the presence or absence of C57BL/6 MSC. DC were then harvested by gentle aspiration from adherent allogeneic MSC and placed in a proliferation assay with OVA specific DO11.10 $CD4^+$ T cells. As seen previously, DC pulsed with OVA were capable of supporting DO11.10 $CD4^+$ T cell proliferation. However, DC pulsed with OVA in the presence of allogeneic MSC were unable to support $CD4^+$ T cell proliferation. Interestingly, by blocking Notch signalling through the addition of GSI, MSC were no longer able to induce functional tolerogenic DC, as indicated by a significant increase in $CD4^+$ T cell proliferation ($p<0.0001$) (Fig. 3.11). The increase in T cell proliferation with GSI treated tDC beyond that of mDC can be accounted for by considering GSI treated MSC no longer inhibit the maturation of DC, conceivably the DC could therefore react to the mis-matched MHC in the allogeneic MSC co-culture. Vehicle control had no effect. These data confirmed that Notch signalling was required for the induction of a functional, tolerogenic DC population by MSC *in vitro*.

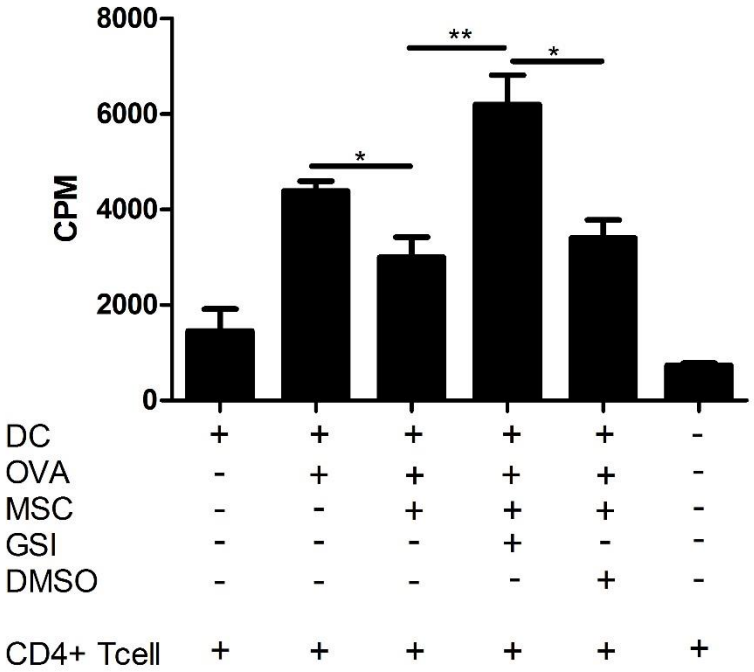

Fig. 3.11 GSI prevents MSC generated tolerogenic DC ability to inhibit T cell proliferation. Immature DC, isolated from BALB/c bone marrow, were co-cultured with or without allogeneic MSC in the presence or absence of OVA. GSI or DMSO was added at a concentration of 1µM. The DC were pulled back after 48h and washed before co-culturing with DO11.10 $CD4^+$ T cells. After 72h, proliferation was examined over a 6h period by measuring tritiated thymidine uptake. Proliferation levels were measured in counts per minute (CPM). GSI treated tolerogenic DC restored OVA driven T cell proliferation when compared to untreated tolerogenic DC (p**, 0.01). Statistics generated by ANOVA with three repeats..

3.8 Attempted strategies for determining which Notch receptor and ligand pairing is involved in MSC immunomodulation.

After determining that the Notch/Jagged pathway is involved in MSC immunomodulatory functions, the next step was to find out which ligand or receptor was specifically involved in signalling. Notch 1 and Jagged 1 have previously been identified to play key roles in DC/Treg modulation, using inhibitors to show increases in Treg cells and inhibition of DC maturation (Liotta et al., 2008, Bugeon et al., 2008). Furthermore, MSC express high levels of Notch 1 and Jagged 1 and thus were chosen as potential candidates. Three approaches were used to determine the precise signalling pathway, they included; a Notch 1 neutralising antibody, a Jagged 1 neutralising antibody and Jagged 1 siRNA.

$CD4^+$ cells were co-cultured with allogeneic MSC for 72h in the presence or absence of Notch 1 neutralising antibody (10µg/ml) or isotype control (mouse IgG2b). Cells were examined by flow cytometry, $CD4^+$ cells were gated and expression of FoxP3 was determined. Cells co-cultured with MSC have increased levels of FoxP3 however this is only marginally reduced with the addition of the anti-Notch 1 antibody and the result was neither reproducible nor statistically significant (Fig. 3.12).

The role for Jagged 1 was examined using a neutralising antibody in MSC-T cell co-culture. Anti-Jagged 1 was used at 5µg/ml (concentration determined by L. Tobin, unpublished) and the isotype control was mouse IgG1. As seen in Fig. 3.13 the neutralising antibody did not reduce the levels of FoxP3 in the $CD4^+$ cells, there was however a mild effect from the isotype control. These experiments demonstrated

that neutralising antibodies can be insufficient in reductionist studies and were not a reliable approach here.

In order to obtain full, quantifiable, knockdown of Jagged 1, small interfering RNA (siRNA) constructs were designed as described in section 2.17. Jagged 1 KD was examined using RT-PCR. Analyses were performed on all samples, after 24h there was clear knockdown of Jagged 1 mRNA at 15nM siRNA concentration (Fig. 3.14), unfortunately after 48h, mRNA levels began to increase again. As with the neutralising antibodies, the time frame of the MSC and T cell co-culture (72 h) exceeded the maximum length of knockdown achievable with siRNA. In order to pursue Jagged 1 as a potential target in MSC signalling a stably knocked down cell line was required.

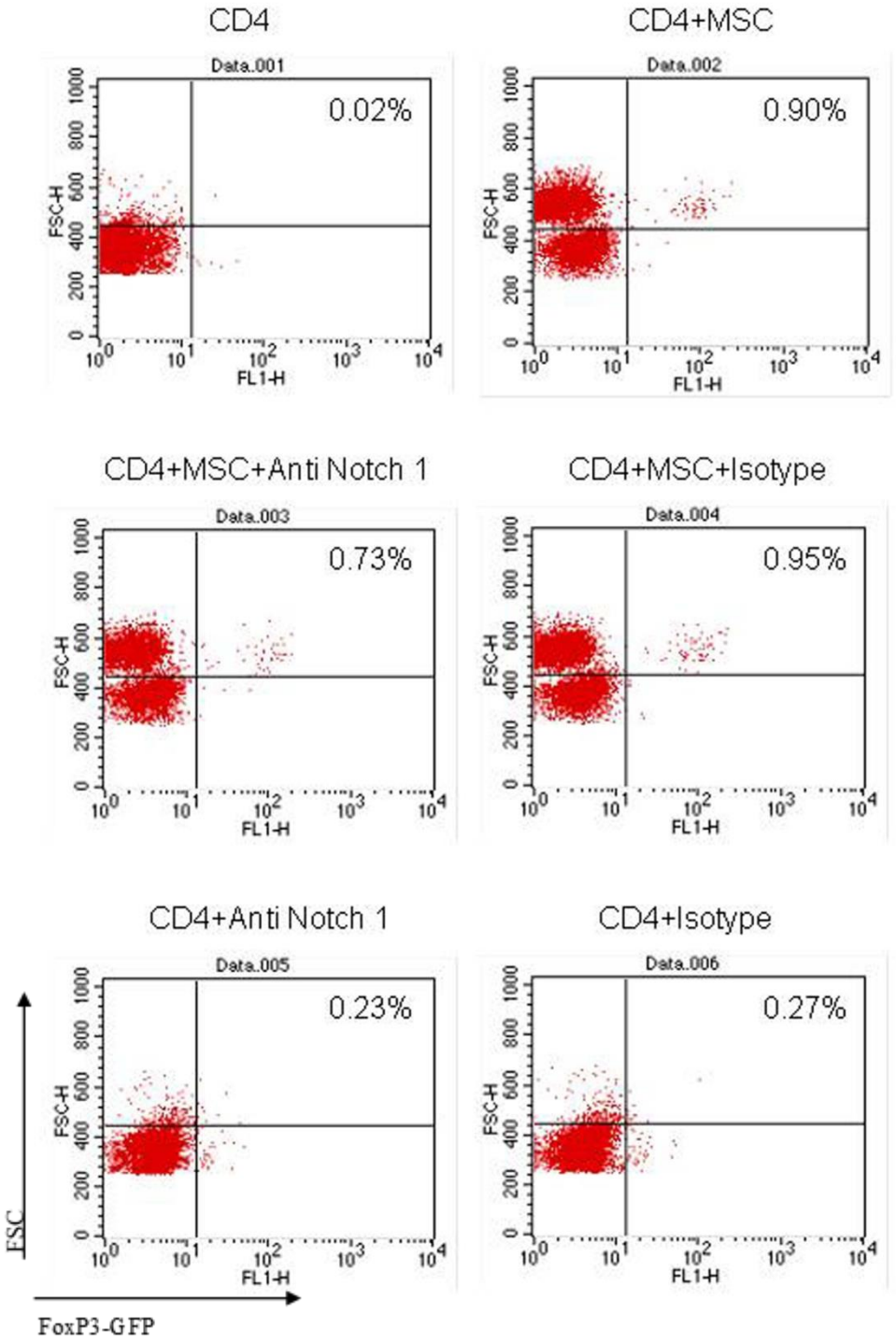

Fig. 3.12 Neutralisation of Notch 1 has little effect on MSC expansion of Treg. $CD4^+$ T cells were co-cultured for 72h with MSC in the presence or absence of Anti Notch 1 (10µg/ml) or its control isotype mouse IgG2b. MSC expansion of the Treg population is marginally reduced by the addition of anti Notch 1 but not the isotype. Anti-Notch 1 cultured with the $CD4^+$ cells alone do not expand a Treg population. Treg expansion was examined by flow cytometry for FoxP3-eGFP expression. Data representative of three experiments.

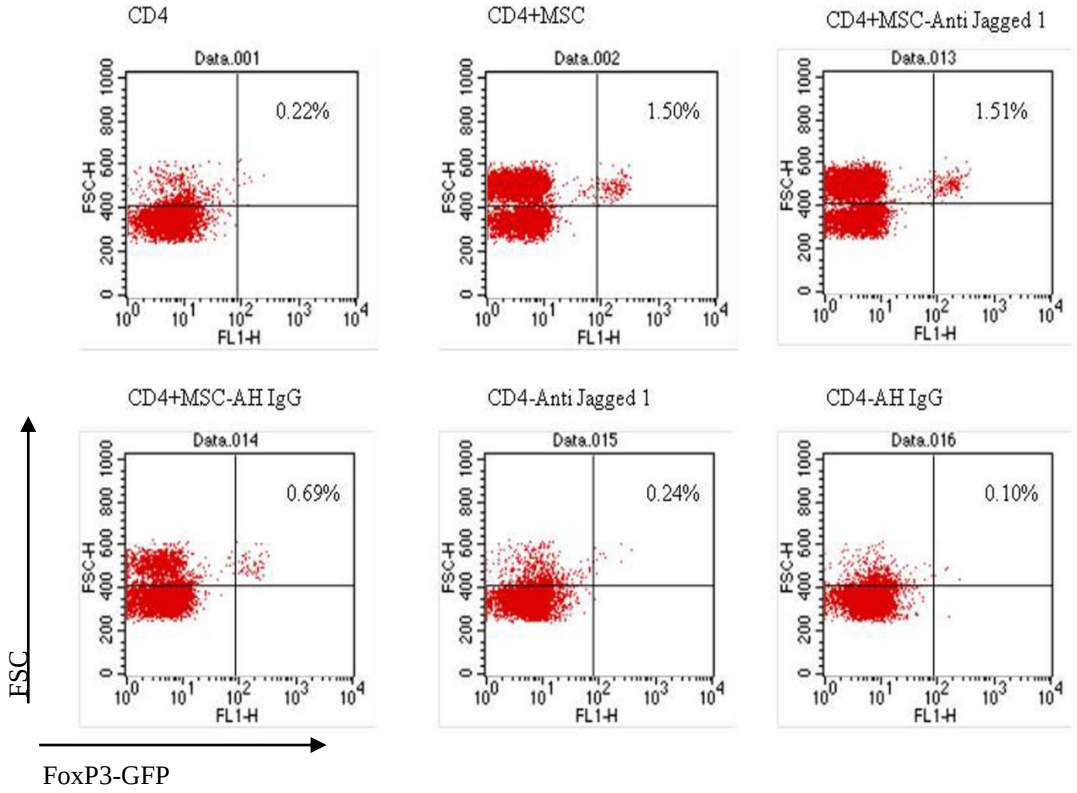

Fig. 3.13 Jagged 1 neutralising antibody was ineffective at reducing MSC expansion of Treg. $CD4^+$ T cells were co-cultured for 72h with MSC in the presence or absence of anti Jagged1 neutralising antibody (5µg/ml) or its isotype mouse IgG1. MSC expansion of a Treg population was not affected by the addition of anti Jagged 1. Ant-Notch 1 cultured with the CD4+ cells alone did not expand a Treg population. Treg expansion was examined by flow cytometry for FoxP3-eGFP expression. Data representative of three experiments.

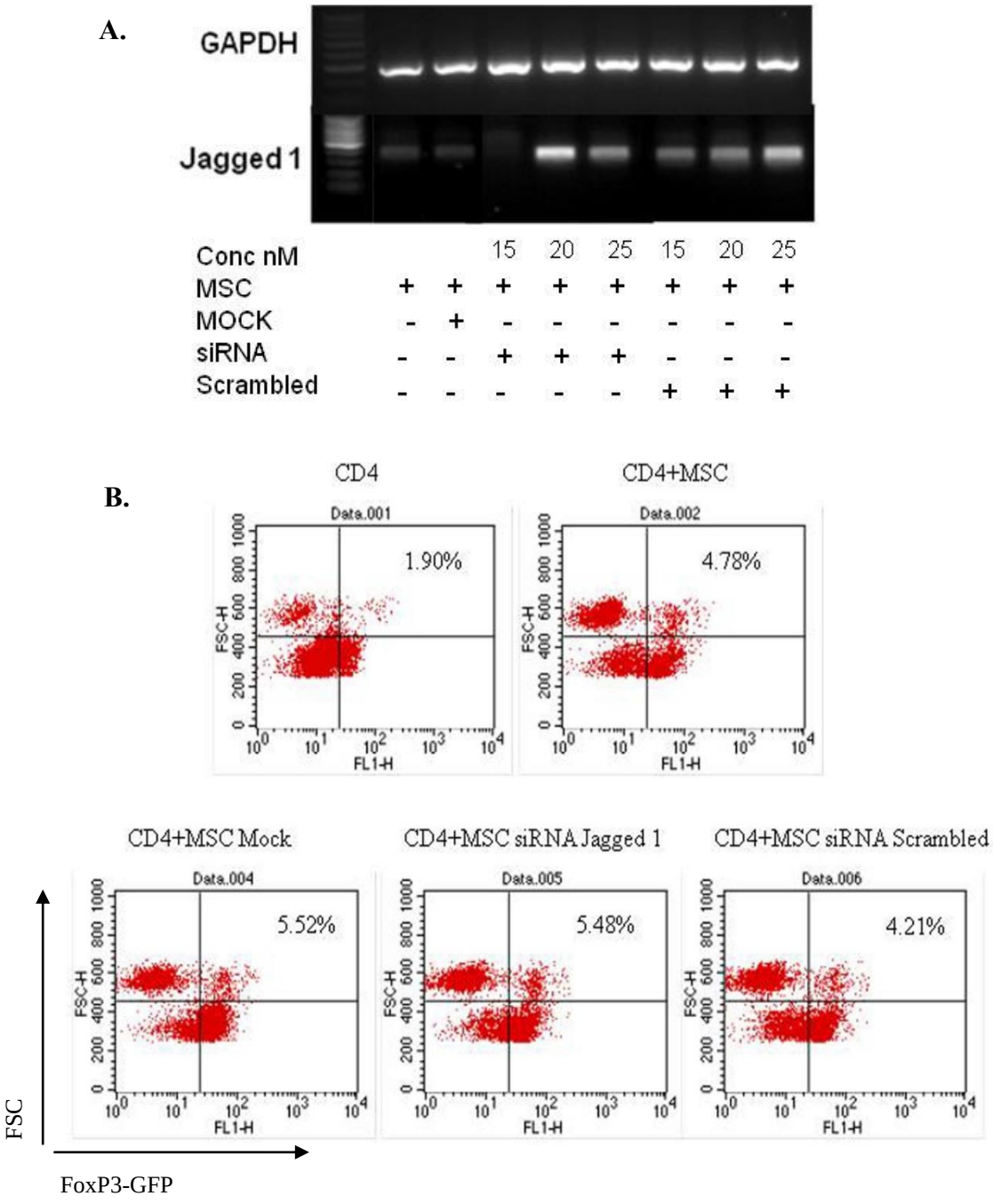

Fig. 3.14 Jagged 1 silencing using siRNA was ineffective at reducing MSC expansion of Treg. A concentration gradient for siRNA ranging from 15nM to 25nM revealed 15nM to be an effective dose for Jagged 1 silencing as determined by PCR after 24h (A). This dose was used in a co-culture experiment involving CD4+ T cells and MSC. There was no reduction in the expansion of Treg cells over a 72h period as determined by flow cytometry for FoxP3-eGFP (B). Data representative of two experiments.

3.9 Establishment of a stably transduced Jagged 1 knock out cell line

In order to create a stably knocked down Jagged 1 MSC line, lentiviral particles containing short hairpin RNA (shRNA) were employed. shRNA uses the cell's internal processing to turn shRNA into siRNA which activates RISC (RNA induced silencing complex). This in turn cleaves the RNA of interest, preventing it from being transcribed (Paddison et al., 2002). Five different Jagged 1 shRNA plasmids were designed and pooled to achieve maximum knockdown. The plasmids were transfected into HK293T cells along with lentiviral packaging plasmids. The HEK cells packaged the Jagged 1 plasmid into functional virus which was released into the medium and collected for transduction of the MSC (Fig. 3.15).

Initial transfections into HEK293T cells using lipofectamine resulted in a substantial amount of cell death, leading to a very low viral titre. Optimisation of three different transfection reagents was carried out, each designed to protect the cell during transfection. Fig. 3.16 shows how each of the three constructs were capable of producing high levels of virus; however, Gene Juice was chosen based on microscopic examination of the cells. Cells cultured with Gene Juice displayed greater levels of proliferation and looked healthier. For the remainder of the project GeneJuice was used at the transfection reagent in all shRNA work.

The viral titre of media obtained from HEK cells was determined by the number of transducing units (TU) per ml of media. $2x10^5$ HEK were transduced with a serial dilution of viral media and left to culture for 48h. The plasmids used in this experiment were all GFP tagged and the number of GFP positive cells was counted after 48h. Using the following formula the titre was determined (Fig. 3.16).

GFP colonies counted x dilution factor x 40 = #TU/mL

Multiplicity of infection (MOI) is the number of TU required to achieve knockdown in any given cell line. The accuracy of the MOI with regard to the MSC was not vital in this case as the non-transduced MSC would be purified out by Puromycin selection. Resistance to the antibiotic is only conferred to cells that have been positively transduced.

A

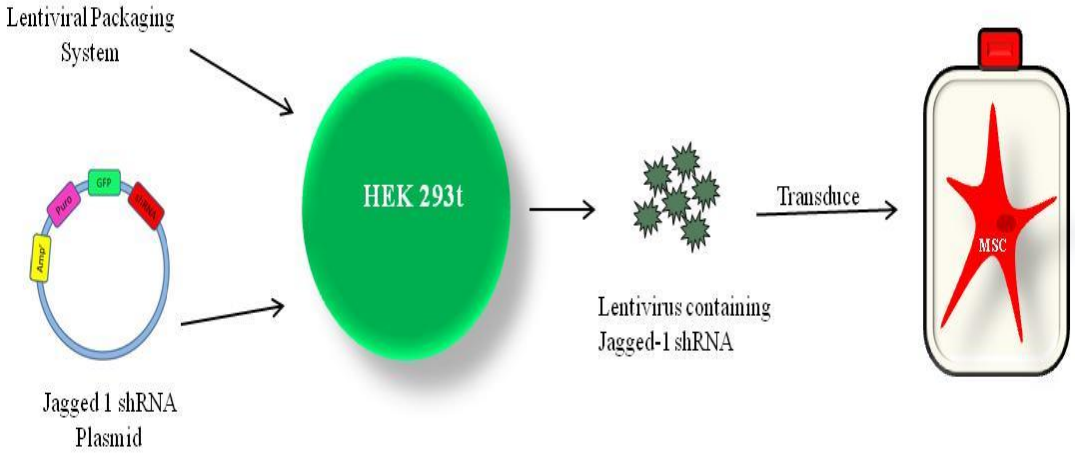

B

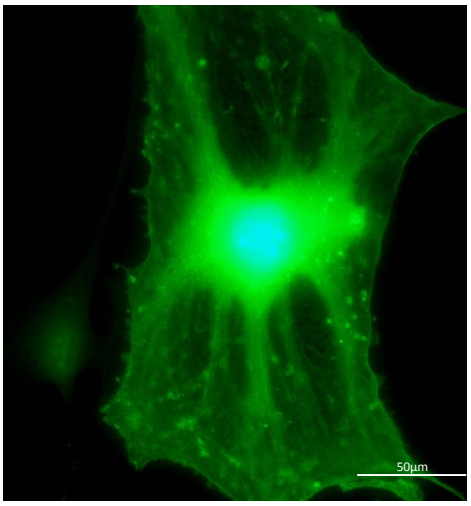

Fig. 3.15 Creation of a GFP expressing Jagged 1 knock down MSC. pGIPZ GFP plasmid constructs containing Jagged 1 shRNA were packaged into lentiviral vectors by HEK293T cells (A). The packaged virus was used to transduce MSC and positively selected for by consequential puromycin resistance. The positively selected cells containing pGIPZ fluoresced green due to the presence of the GFP gene in the vector (B); (x400).

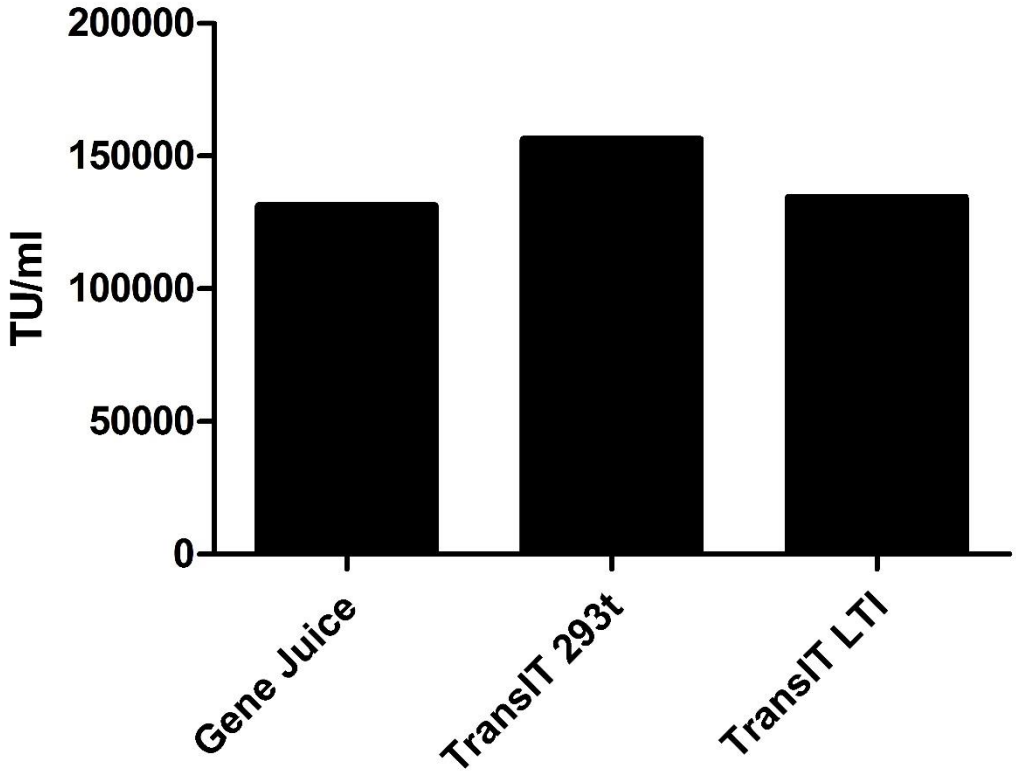

Fig. 3.16 Viral titres achieved using different transfection reagents with HEK293T cells. HEK cells were seeded at $1x10^6$ in a T75 flask overnight. Each transfection reagent was used in a 3:1 ratio with plasmid DNA. HEK cells were transfected for and viral particles collected after 48h. A serial dilution of the viral media was made and added to $4x10^5$ HEK cells plated in a 24 well plate. After 48h, the cells were examined by flow cytometry for GFP expression and the viral titer determined. All cells treated were viable 48h after transfection and capable of producing high levels of virus

3.10 Jagged 1 Knockdown MSC retain their stromal cell characteristics

In order to ensure treatment of MSC with lentiviral particles had no adverse effect on the defining characteristics of the cells. MSC were subjected to cell surface characterisation and differentiation following shRNA knockdown. The following results demonstrate that transducing the MSC with lentivirus did not alter the cell's basic characteristics. Figure 3.17 shows that Jagged 1 shMSC still expressed all the required cell surface markers while maintaining a low level of MHC Class I. This is important for any potential *in vivo* experiment for which the cells may be utilised. As with the cell surface characterisation, MSC were adherent to plastic, confirmed through successive passages and while undergoing differentiation in a 6 well plate. Figure 3.18 demonstrates that lentiviral knockdown of MSC did not affect their capacity to differentiate into bone, fat or cartilage like cells. These results are comparable to characterisation of non-transduced MSC indicating lentiviral treatment does not alter the defining characteristics of MSC.

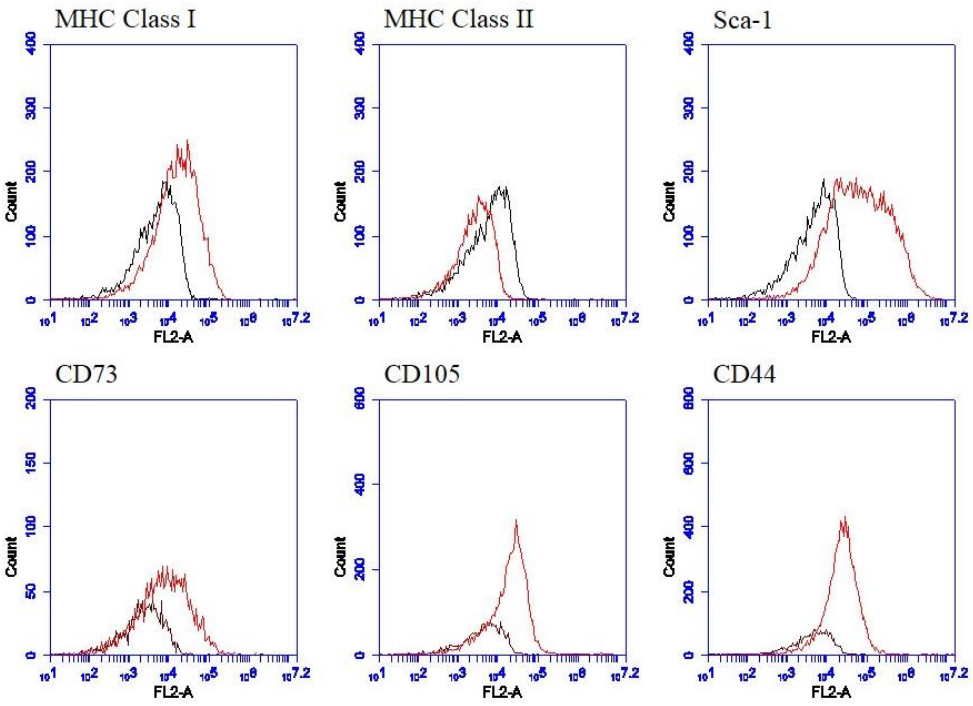

Fig. 3.17 Jagged 1 shMSC at Passage 8 continue to express appropriate MSC surface markers. BALB/c Jagged 1 shMSC were characterised by looking at the expression levels of a variety of cell surface markers (Red Line) against their corresponding isotypes (Black Line). 10,000 events were recorded for each marker. These results are representative of multiple experiments

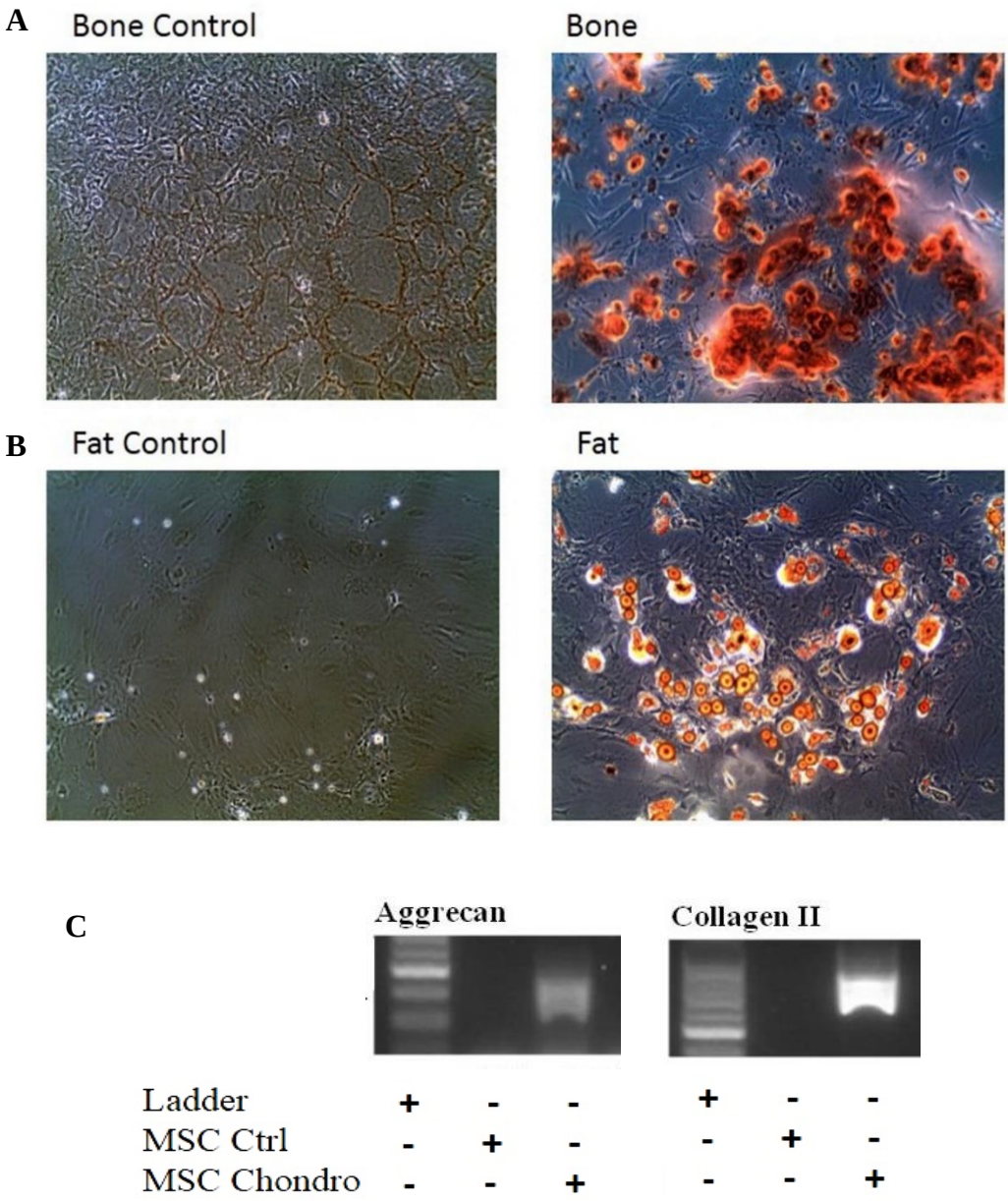

Fig. 3.18 Trilineage differentiation of Jagged 1 KD MSC. Jagged 1 KD MSC and Non-silencing control MSC ($5x10^4$) (Jag1 KD MSC shown above) were cultured for 21 days in control medium, osteogenic medium (A), or adipogenic medium (B). Cultures were stained with Alazarin Red for bone and Oil Red O for fat. $2x10^5$ MSC were centrifuged at 200xG for 8 min to form a cell pellet, control medium or chondrocyte medium was added to the tube and the cells were cultured for 21 as a 3D cell mass. After 21 days trizol was added to the cell pellet, following RNA extraction and cDNA synthesis, the mRNA was tested for the chondrocyte markers aggrecan and collagen IIa (C). The results are representative of two experiments. (Magnification x100)

3.11 Jagged 1 shRNA results in knockdown of Jagged 1 on MSC.

The GFP positive MSC that were puromycin resistant were collected and tested for Jagged 1 expression at both the protein and the mRNA level. Cells were stained with a Jagged 1-PE antibody and examined by flow cytometry, the distribution of the peak in the non-transduced MSC graph indicates that nearly all the cells express Jagged 1 on some level, though many only weakly express the ligand. However, following shRNA transduction there was a dramatic reduction in the cell surface expression of Jagged 1 (Fig 3.19 A). The cells were also tested for expression of Jagged 1 by real time PCR analysis. There was a slight increase in the expression of Jagged 1 in non-silencing control MSC compared to Jagged 1 KD MSC however expression did not return to non-transduced levels (Fig 3.19 B). The non-silencing plasmid is a control used in lentiviral work, where an empty vector is packaged into viral units and the MSC are transduced to ensure there are no unintentional side effects to the viral transduction. In the case of MSC, the non-silencing control delivered by means of a lentivirus probably stimulates the TLR3 ligand responsible for detecting viral double stranded DNA. TLR3 stimulation on MSC results in the down regulation of Jagged 1 at both the mRNA and protein level (Liotta et al., 2008), for this reason the non-silencing control cannot be used as a valid control for lentiviral transduction in this case. In an effort to overcome this, reverse transcriptase PCR was also performed on lentiviral treated MSC to establish whether knock down of Jagged 1 may interfere with expression of the other Notch ligands. Jagged 2 is not expressed by MSC but primers for Delta-like ligand 1 (Dll 1) expression was tested. Figure 3.19 C shows visible bands for Dll1 in both Jagged 1 KD MSC and non-silencing control MSC. These results confirm that treatment of MSC with Jagged 1 shRNA results in

significantly reduced expression of Jagged 1 at both an mRNA level and a protein level. Though non-silencing control cells also showed knocked down expression of Jagged 1, there was no change in the expression of other Notch ligands. Taken together these results show knockdown of Jagged 1 was achieved in MSC. However, due to the off target knockdown observed in the non-silencing control, steadfast conclusions cannot be drawn from this work alone.

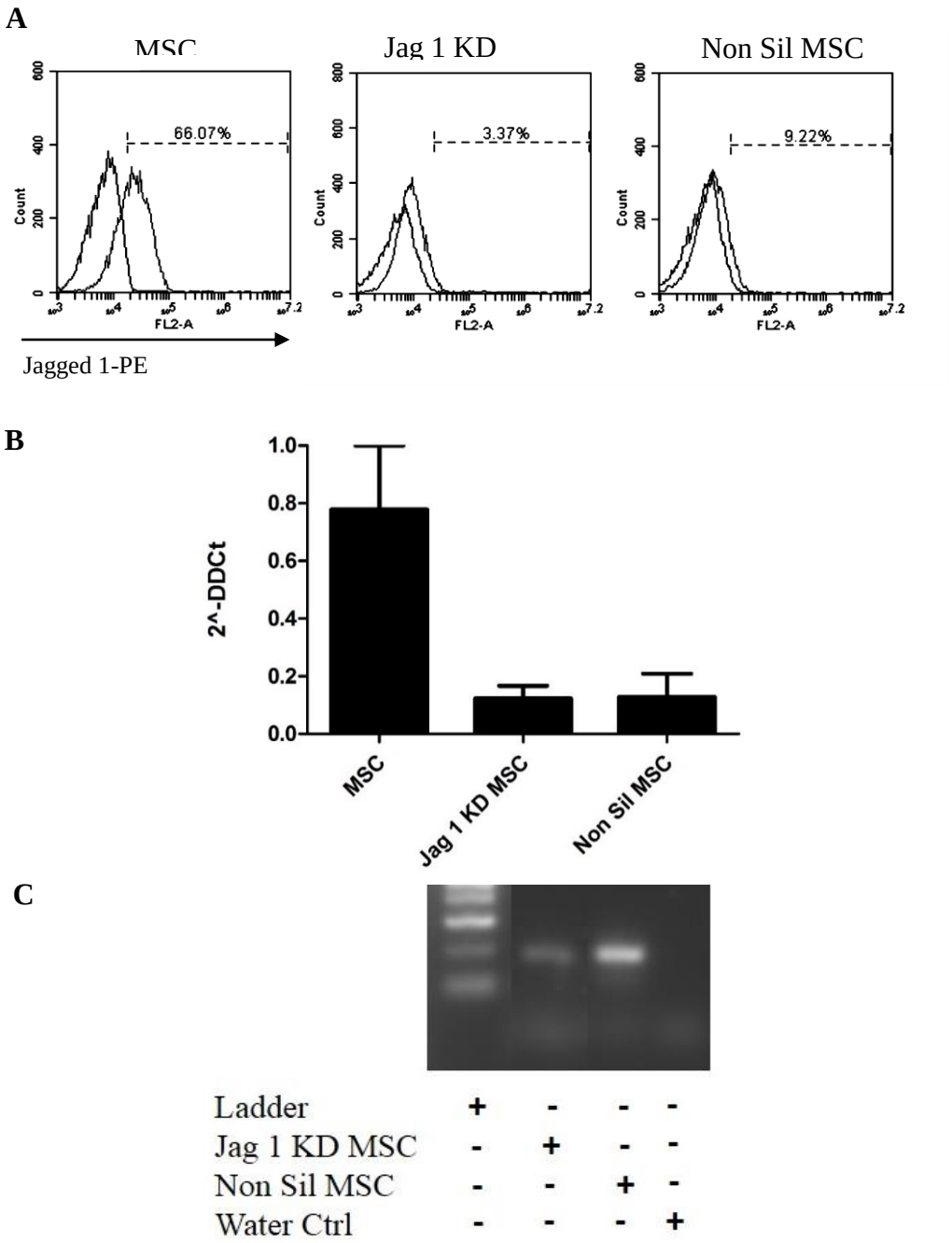

Fig. 3.19 Jagged 1 knockdown MSC no longer express Jagged 1. Jagged 1 shMSC were positively selected using puromycin and allowed to reach confluence, the cells were passaged and $5x10^6$ cells were collected using trizol for mRNA analysis. RNA was isolated and cDNA produced. The cells were examined at a protein level or Jagged 1 expression by flow cytometry (A). The cells were also tested by real time PCR for the expression of Jagged 1 (B) and reverse transcription PCR for Delta like ligand 1 (C) and the results compared with non-transduced MSC or non-silencing control MSC.

3.12 Jagged 1 knockdown MSC no longer support the expansion of regulatory T cells.

Jagged 1 knockdown MSC were used in co-culture with allogeneic $CD4^+$ T cells to determine the importance of Jagged 1 in MSC expansion of Treg. $CD4^+$ cells were separated from the spleens of FoxP3-eGFP mice and co-cultured with either knockdown MSC or non-transduced MSC for 72h. The $CD4^+$ cells had a low base level of $FoxP3^+$ cells present after 3 days, T cells cultured with non-transduced MSC showed a significant increase in expression of FoxP3 and CD25, indicating expansion. The $CD4^+$ T cells co-cultured with Jagged 1 shMSC showed levels of expression similar or lower than that of the $CD4^+$ cells cultured alone. This result indicates that the ability of MSC to expand Treg requires MSC expression of Jagged 1 (Fig. 3.20).

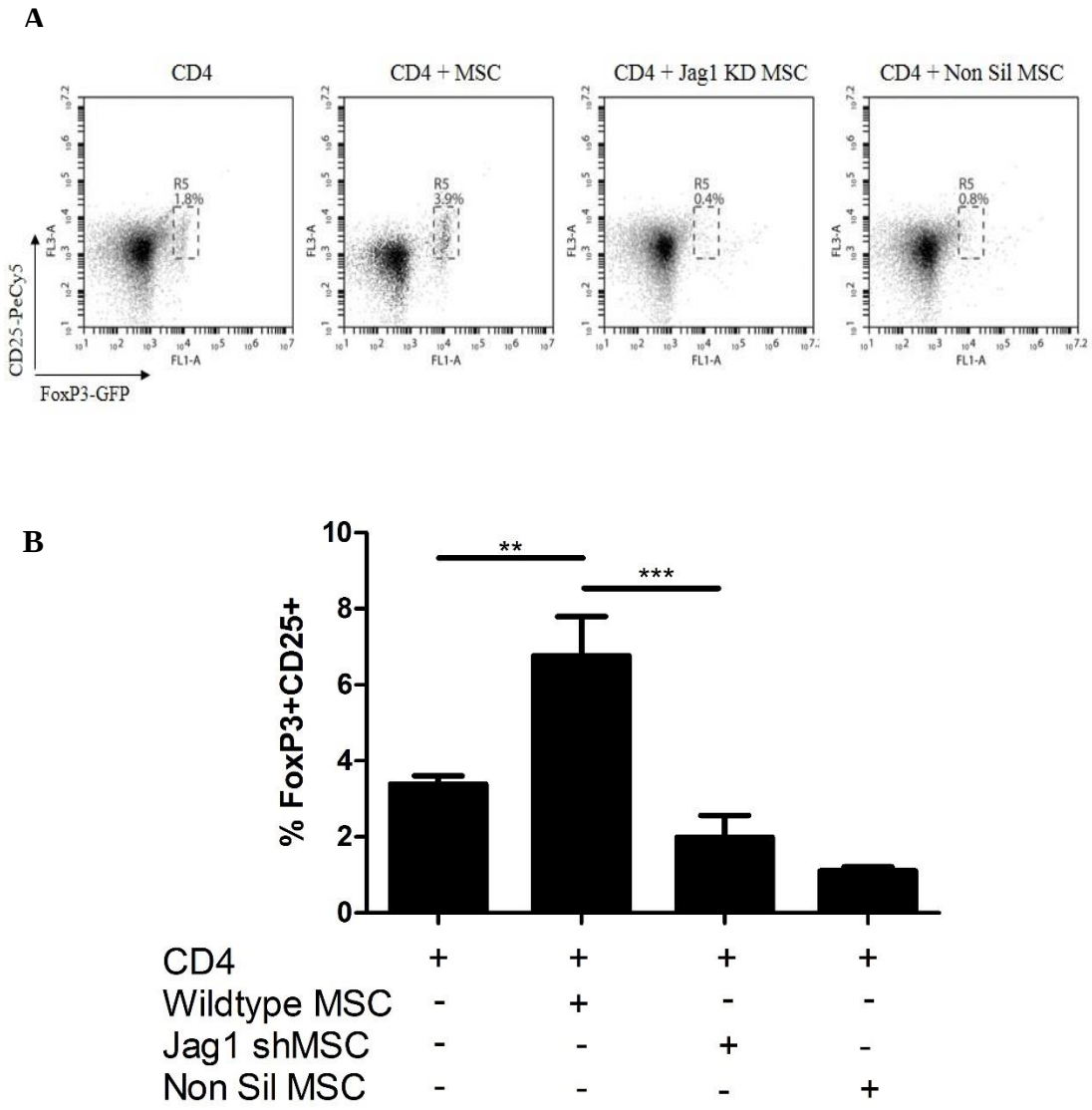

Fig. 3.20 Jagged 1 knockdown MSC are unable to expand a regulatory T cell population. $CD4^+$ T cells were separated from spleen cells isolated from a FoxP3-eGFP mouse were co-cultured with Jagged1 KD MSC or non-transduced MSC. After 72h the T cells were pulled back, washed and stained for CD4 and CD25. The CD4 cells were gated and expression of FoxP3-eGFP and CD25-PeCy5 were examined by flow cytometry. As previously shown $CD4^+$ cells cultured with non-transduced MSC expand a $FoxP3^+CD25^+$ population, however Jagged 1 KD MSC showed significantly reduced expansion, equivalent to $CD4^+$ cells cultured alone (A). This experiment was repeated several times and the average was graphed (B). Statistics achieved by ANOVA analysis, (**<0.01, ***<0.001), N=3.

3.13 Jagged 1 knockdown MSC in conjunction with anti IL-6 inhibit the maturation of DC.

Jagged 1 knockdown MSC were further used in co-culture with DC to ascertain whether Jagged 1 also plays a role in MSC modulation of DC maturation. DC were cultured with either knockdown MSC or non-transduced MSC in the presence or absence of LPS for 48h. The DC were recovered and washed before staining for the maturation markers CD86, CD40 and MHC Class II. Initial studies found that the knockdown MSC alone were not capable of fully reversing MSC inhibition of maturation, leading to the hypothesis that soluble factors may play a more important role in inhibition of DC maturation than expansion of Treg cells. This hypothesis was supported by unpublished work in the Mahon lab (English, K.E.) and previously published work showing an important role for IL-6 in the inhibition of DC maturation, while also indicating a need for cell contact (Djouad *et al.*, 2007). Further co-culture experiments were set up with the addition of an IL-6 or control neutralising antibody. The DC matured with LPS had expressed high levels of CD86 and MHC Class II and as expected these levels were reduced in the presence of MSC (Fig. 3.21). The Jagged 1 KD MSC slightly increased expression of CD86 (A) and greatly increased levels of MHC Class II (B) but when used in conjunction with anti-IL-6, the expression level of both CD86 and MHC Class II were comparable to those seen in the LPS matured DC (A&B). These results indicate an additive role for IL-6 and Jagged 1 in MSC inhibition of DC maturation. While preventing the Jagged 1 interaction with DC Notch receptors somewhat reverses MSC inhibition of DC maturation, abolition of IL-6 signalling is required to completely restore a mature phenotype.

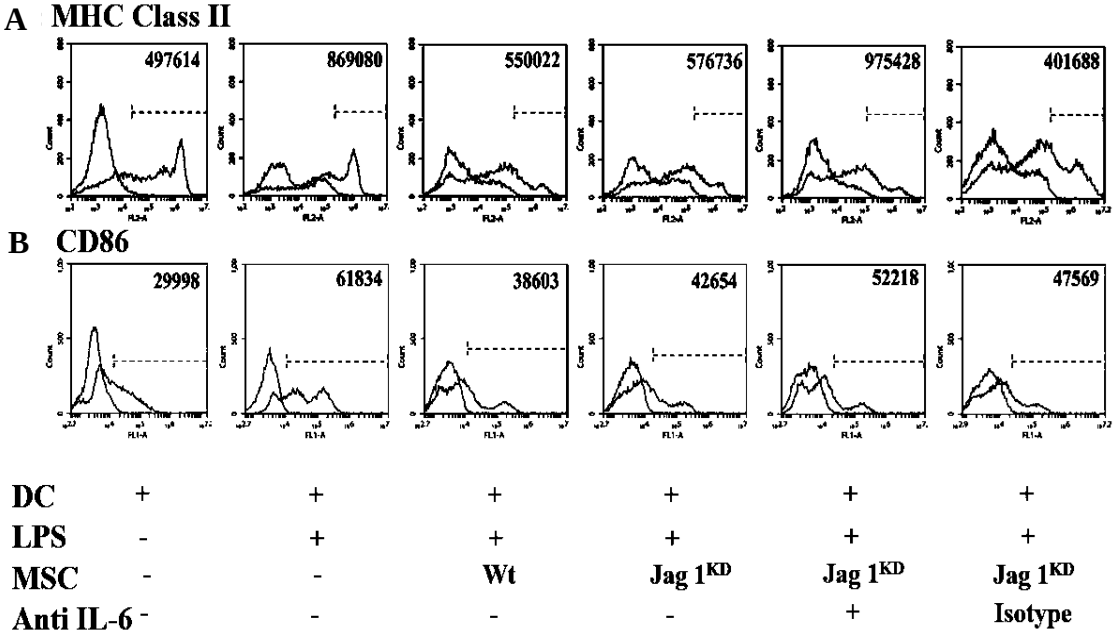

Fig. 3.21 Jagged 1 Knockdown MSC in combination with anti IL-6 reduces the expression of maturation markers on DC. DC were cultured for 48h in the presence or absence of MSC or Jag1 shMSC with or without the addition of an anti-IL-6 neutralising antibody. The DC were pulled back and examined by flow cytometry following staining for CD11c and the maturation markers MHC Class II (A) and CD86 (B). Data presented in histograms of mean fluorescence intensity (MFI) and representative of two experiments.

3.14 MSC inhibition of antigen presentation by DC is attenuated by removal of Jagged 1 signalling

Murine MSC co-cultured with DC has previously been shown to reduce the ability of DC to present a peptide/MHC class II complex on the cell surface (English et al., 2008). Unpublished work by the Mahon laboratory demonstrated addition of GSI to co-cultures reversed MSC suppression of antigen presentation (L. Tobin, unpublished data). Following on from this work, Jagged 1 knockdown MSC were co-cultured with DC in an antigen presentation assay to determine a role for Jagged 1 in this process. DC were cultured with either non-transduced MSC, or Jagged 1 knockdown MSC in the presence or absence of a peptide (52-68) from the alpha chain of I-E of the MHC Class II receptor for 24 h. The DC were recovered and washed before staining with the flurochrome labelled Y-Ae antibody, which binds to the Eα peptide bound to $I\text{-}A^b$ molecules (Honey et al., 2004). High levels of the Y-Ae antibody were detected on DC matured by LPS indicating high levels of antigen presentation. DC co-culture with non-transduced MSC led to a reduction in the level of antigen presentation, and co-culture with Jagged 1 knocked down MSC somewhat reversed this effect but not to levels seen with mature DC. This could in part be due to IL-6 signalling, which was previously shown to compensate for the lack of contact signalling in MSC inhibition of DC maturation (Fig. 3.22). Nevertheless, MSC inhibition of antigen presentation by DC is attenuated by the removal of Jagged 1 signalling.

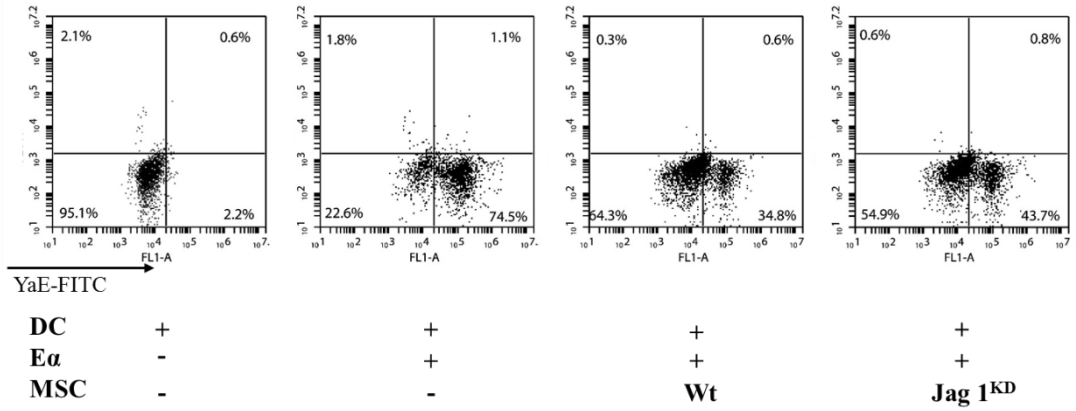

Fig. 3.22 Jagged 1 is involved in MSC suppression of DC antigen presentation. C57BL/6 DC pulsed with I-Eα peptide were co-cultured with wild-type allogeneic MSC or Jagged-1 knocked down MSC for 48h. The percentage of DC presenting I-Eα peptide was measured using a YAe biotin conjugated anti-I-A^b: Eα complex specific antibody. Percentages of cells within the marked regions are represented. Data representative of two experiments.

3.15 Summary

In Chapter 3, the aim was to demonstrate the influence of murine MSC on the immune system through examination of the induction, expansion and education of immune cells and to identify the contact dependent signal through which murine MSC modulate the immune function of T cells and DC. To this end, *in vitro* co-culture experiments were carried out between murine MSC, T cells and DC in order to address how MSC suppress immune function defining a role for Notch signalling through the ligand Jagged 1.

The immunomodulatory properties of MSC were confirmed by demonstrating their ability to expand a regulatory population of T cells and to induce tolerogenic DC. The data herein suggest that MSC can support or even initiate a cycle of suppression by inducing tolerogenic DC, these cells in turn induce regulatory T cells from a Treg negative population. MSC promote the expansion of these regulatory cells and thus suppress excessive proliferation of activated lymphocytes (Fig 3.4). The fact that MSC alone cannot induce regulatory T cells gives a level of elegance to the system, as the MSC cannot create a suppressive environment unless DC are initially activated. The importance of this is discussed in Chapter 6, Tolerogenic DC were also shown to be functional in that they had the capacity to suppress the proliferation of antigen specific T cells (Fig. 3.7).

Previous work in the Mahon laboratory indicated Notch was involved in DC maturation. Use of a gamma secretase inhibitor extended that finding, indicating that Notch was also involved in the expansion of Treg. In order to determine the precise ligand involved, many approaches were tested. Lentiviral knockdown of Jagged 1 on the MSC was the most effective means of investigating its importance in signalling.

The results from experiments with the knockdown MSC demonstrate a role for Jagged 1 in MSC expansion of Treg, a point of conjecture to this point (Liotta et al., 2008). Jagged 1 in partnership with IL-6 also plays a vital role in MSC induction of tolerogenic DC, and MSC inhibition of antigen presentation by DC.

In summary, the Notch pathway is required for the induction of a functional, tolerogenic DC population by MSC. These tolerogenic DC are in turn capable of inducing a Treg population. This work demonstrates an essential role for Jagged 1 in MSC expansion of Treg cells. MSC inhibition of DC maturation, also involves Notch as a contact signal but where IL-6 plays an additive role.

Chapter 4

Murine MSC produce trophic factors that influence tissue repair in simple models of pulmonary wound healing

4.1 Introduction

Fibrosis is characterised by the excessive production and deposition of connective tissue, leading to permanent reorganisation and loss of function in the affected organ. The most obvious example of fibrotic damage is scarring seen in the skin following injury, where native tissue is replaced by non-functional collagenous cicatrix. Wound healing is a form of damage control, a key part of which is the creation of a barrier between exposed tissue and the external environment. This process serves to prevent infection and stop blood loss, depending primarily on platelets, the coagulation cascade and fibroblasts (Robson *et al.*, 2001). Fibrosis might be viewed as an aberrant or incomplete form of wound healing but the mechanisms responsible for the switch from wound healing to fibrosis are poorly understood. In terms of phenomena, the presence of activated fibroblasts, their excessive proliferation, and apoptosis of epithelial cells are hallmarks of fibrotic pathogenesis (King *et al.*, 2011). In pulmonary fibrosis, the replacement of healthy alveolar tissue with non-functional fibrotic scaring, leads to reduced maximal oxygen consumption ($V0_2$ max), a measure of lung function (Raghu, 2012). If left unchecked, the fibrotic lesions will render the organ non-functional, with lung transplantation being the only treatment option.

In the previous chapter, murine MSC were shown to have a dramatic effect on the cells of the immune system. In this chapter the focus switches to the reparative aspects of MSC. The ability of MSC to reduce T cell proliferation and expand populations of regulatory cells, combined with potential regenerative effects make MSC attractive candidates for the treatment of pulmonary fibrosis, potentially dampening the initial inflammatory response to injury and repairing tissue damage. Thus MSC could have dual benefits therapeutically. This chapter sought to examine

the latter property, to determine the effects of murine MSC paracrine signalling on pulmonary cells, in advance of examining MSC mechanisms of action *in vivo*. This was achieved by investigating the effects of MSC on the cells directly affected in pulmonary fibrosis, namely pulmonary fibroblasts and alveolar epithelial cells. The paracrine effects of MSC were examined in relation to proliferation and migration of epithelial cells and fibroblasts. Using neutralising antibodies, inhibitors and shRNA technology, the importance of HGF and PGE2 in MSC signalling was determined.

4.2 Characterisation of primary lung fibroblasts

The first challenge to studying lung fibrosis is the isolation of appropriate cells. Primary lung fibroblasts can be isolated from murine lung and purified *in vitro* by adherence to plastic. The method of isolation and morphology of the cells is very similar to that of murine bone marrow derived MSC, however, there are distinct characteristics to each cell type.

Primary lung fibroblasts were isolated from the lungs of C57BL/6 mice according to the method described in Chapter 2.6 and were subjected to the same characterisation as MSC, in order to distinguish them from potential lung resident MSC. Flow cytometric analysis of the cells demonstrated expression of CD44, CD106, CD73, CD90, weak expression of the mesenchymal marker Sca-1, and TGFβ receptor subunit CD105, and MHC Class I. There was no expression of the haematopoietic marker CD45, lymphocyte marker CD34, or the co-stimulatory marker CD86 (Fig. 4.1).

As previously described in Chapter 3, MSC demonstrate multi lineage differentiation capabilities, specifically to osteoblasts, adipocytes, and chondrocytes. Isolated primary fibroblast cells were subjected to the same culture conditions and differentiation media. After 21 days the possible presence of bone and fat cells were examined using alazarin red or Oil Red O stain respectively, while the presence of chondrocyte marker mRNA was tested by PCR Collagen IIa, collagen III and Aggrecan. The control wells were treated with the same conditions in the absence of differentiation components. No evidence of differentiation was observed (Fig. 4.2).

A final test to distinguish fibroblasts from lung MSC involved staining both cell types for vimentin and αSMA. Vimentin is a major component of mesenchymal cell cytoskeleton, αSMA, another cytoskeletal protein is expressed by MSC and myofibroblasts, the activated form of fibroblasts. Murine MSC used in these studies expressed both proteins, in contrast isolated murine pulmonary fibroblasts expressed vimentin but not αSMA. These results not only distinguish the cells used in this study but also indicates the population of fibroblasts used for *in vitro* work hereafter are not activated myofibroblasts (Fig. 4.3).

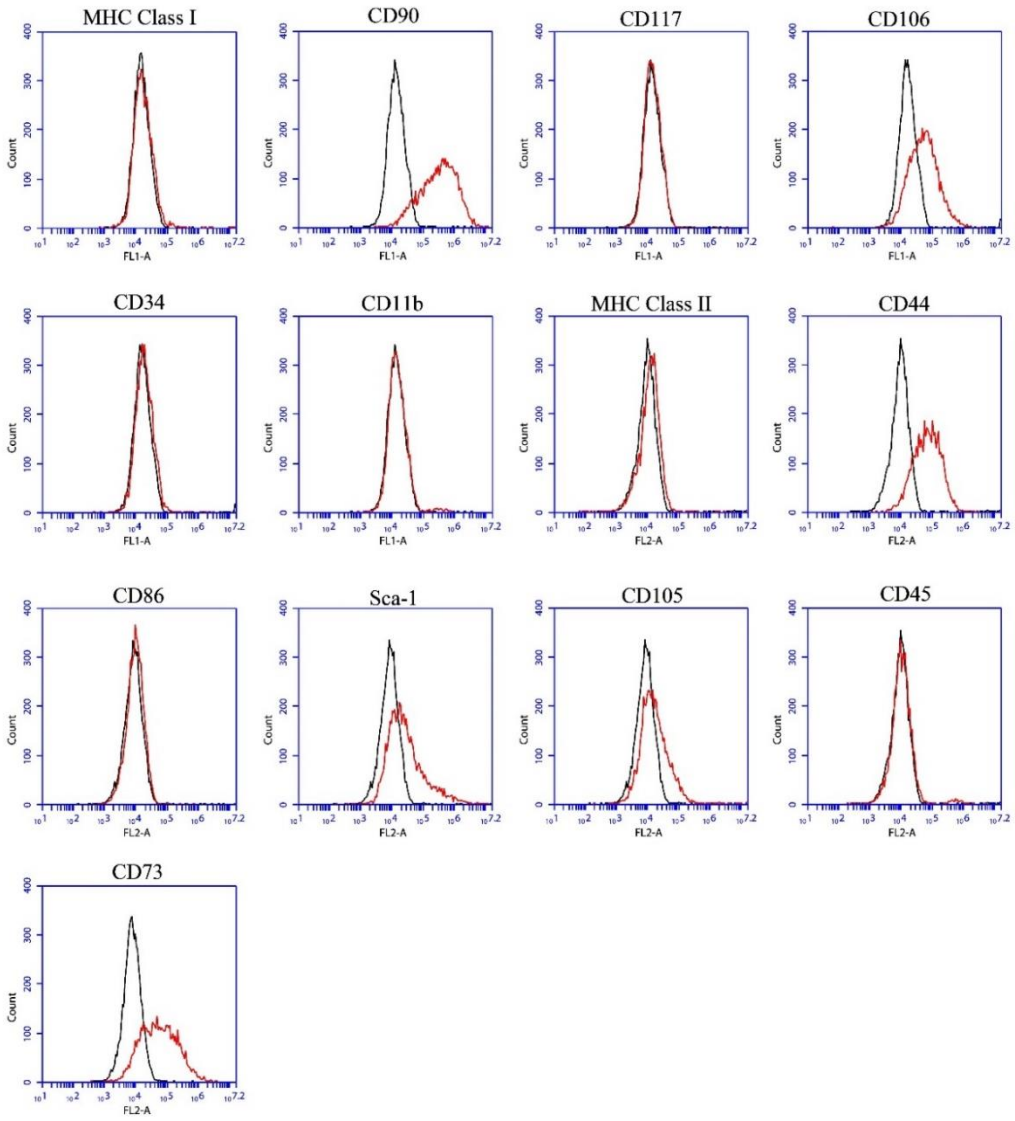

Fig. 4.1 Characterisation of Fibroblasts at Passage 3. Primary C57BL/6 lung fibroblasts were characterised by measuring the expression of a variety of cell surface markers (Red Line) against their corresponding isotypes (Black Line). 10,000 events were recorded for each marker. These results are representative of multiple experiments at passage 3, 4, and 5.

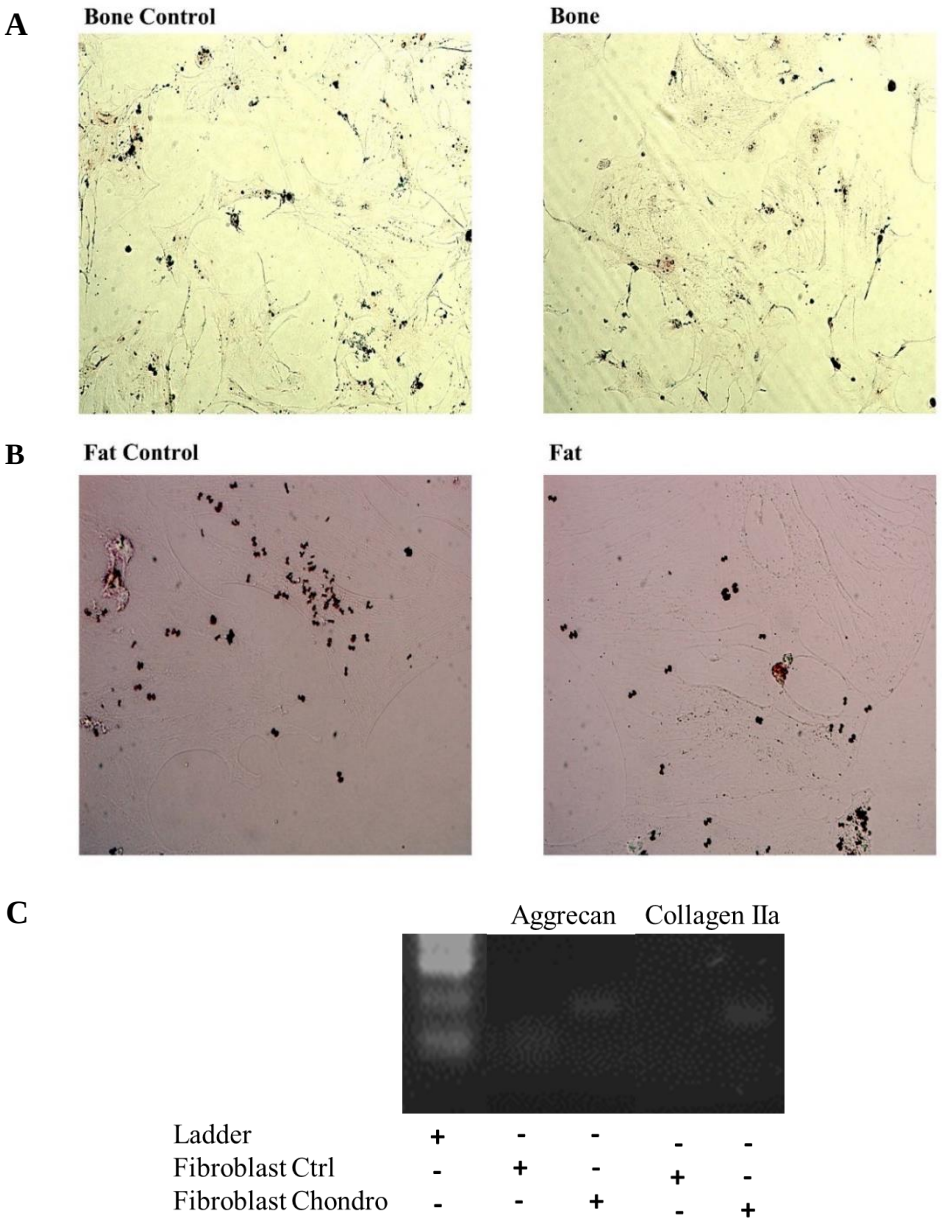

Fig. 4.2 Trilineage differentiation of Fibroblasts. Murine lung fibroblasts ($5x10^4$) were cultured for 21 days in control medium, osteogenic medium (A), or adipogenic medium (B). Cultures were stained with Alazarin Red for bone and Oil Red O for fat. $2x10^5$ MSC were centrifuged at 200xG for 8 min to form a cell pellet, control medium or chondrocyte medium was added to the tube and the cells were cultured for 21 as a 3D cell mass. After 21 days trizol was added to the cell pellet, following RNA extraction and cDNA synthesis, the mRNA was tested for the chondrocyte markers aggrecan and collagen IIa (C). The results are representative of two experiments. (A&B magnification x100).

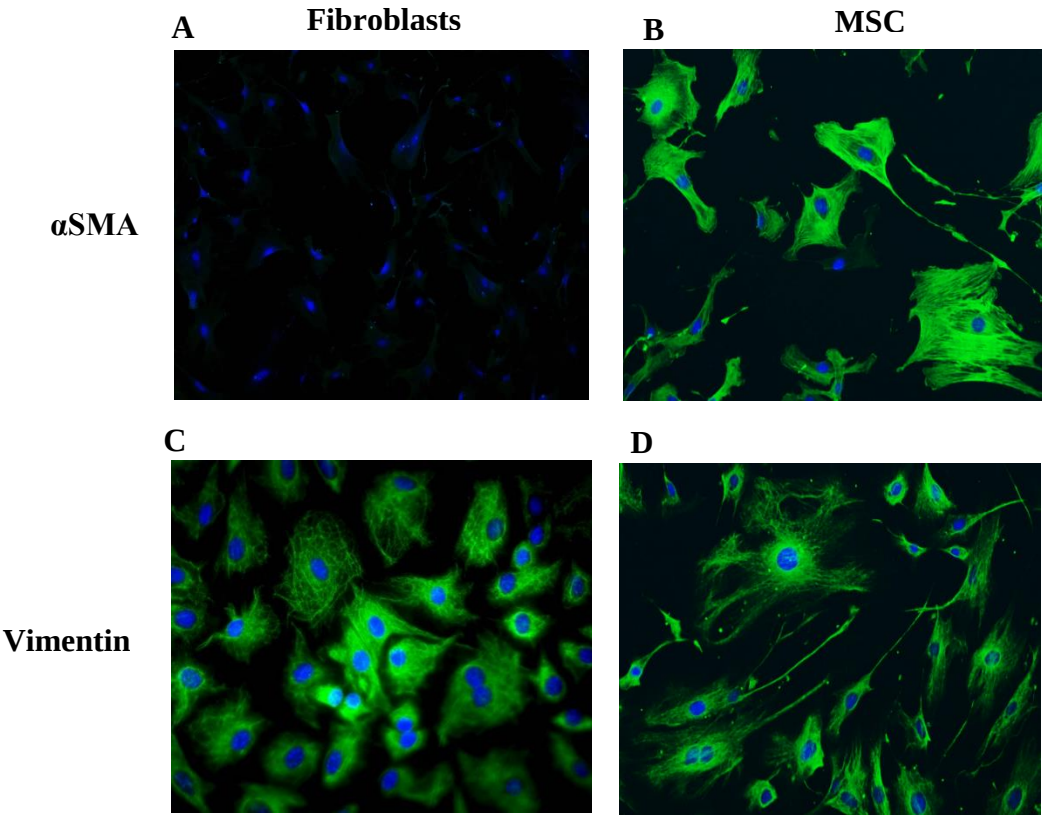

Fig. 4.3 Alpha smooth muscle actin and vimentin staining. MSC and fibroblasts ($5x10^4$) were cultured in a 6 well plate until 70-80% confluent. The cells were fixed with ice cold methanol and stained overnight with either vimentin or αSMA primary antibodies. The cells were washed and incubated with alexa-fluor 488 conjugated secondary antibody and counterstained with DAPI. The cells were examined for αSMA (A&B) or vimentin (C&D) expression using a fluorescent microscope (x100).

4.3 MSC conditioned medium promotes wound closure in a scratch model.

Studying fibrosis *in vitro* has proved challenging as wound healing is a complex system involving multiple cell types and signals. Due to the unknown trigger involved in its disregulation and the induction of fibrosis, it is difficult to replicate on the bench. In order to determine whether MSC were having an effect on this system, a simplified *in vitro* model of wound healing was used. The scratch model involves scoring the bottom of a 6 well plate with 3 horizontal lines, these act as microscope guides to align the plate in the same position for before and after photographs. A monolayer of fibroblasts or epithelial cells is cultured on these plates then disrupted by a "scratch" from a sterile pipette tip, this scratch is a mimic of damage from a physical injury. The distance between the wound edges is measured prior to and following the addition of specific treatments. The assays are inherently variable (depending on batch) so wells are closely observed and the assay stopped once the first scratch was completely closed rather than at a set time point. The extent of closure in the remaining wells was plotted as a percentage of the first, an approach which also removes the variability of scratch width.

This assay was used to examine MSC trophic effects on primary murine fibroblasts and lung alveolar epithelial cells (LA4). Medium collected from confluent MSC (24h) was concentrated using centrifugal filters for protein above a specific size and used in treatment of designated wells. Concentration of MSC conditioned medium (CM) ensured the proteins generated by MSC were applied while avoiding the detrimental effects of use of depleted medium (eg small metabolic products). When generating the MSC CM, the same number of MSC as test cells were plated in the same volume of medium and the total volume was concentrated after 24h, thus ensuring each test well received a standard amount of CM. The addition of MSC CM

to scratch cultures significantly increased percentage wound closure at day 3 in both fibroblasts (Fig. 4.4 A&B) and epithelial cells (Fig. 4.4 C&D), when compared to wells receiving only control medium. These data demonstrate soluble factors produced by MSC significantly promote wound closure by epithelial cells and fibroblasts. Traditionally the above method has been associated with investigation of cell migration (Liang et al., 2007), therefore, these results can also conclude that MSC CM supports the migration of both epithelial cells and lung fibroblasts.

A

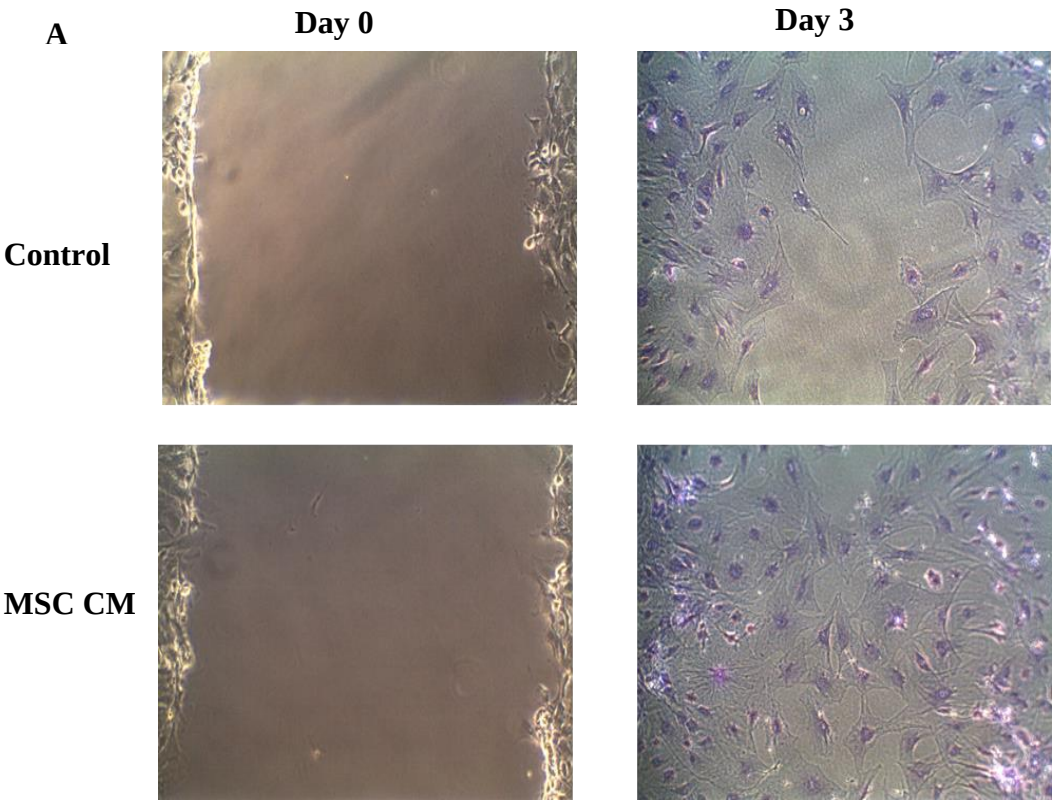

B

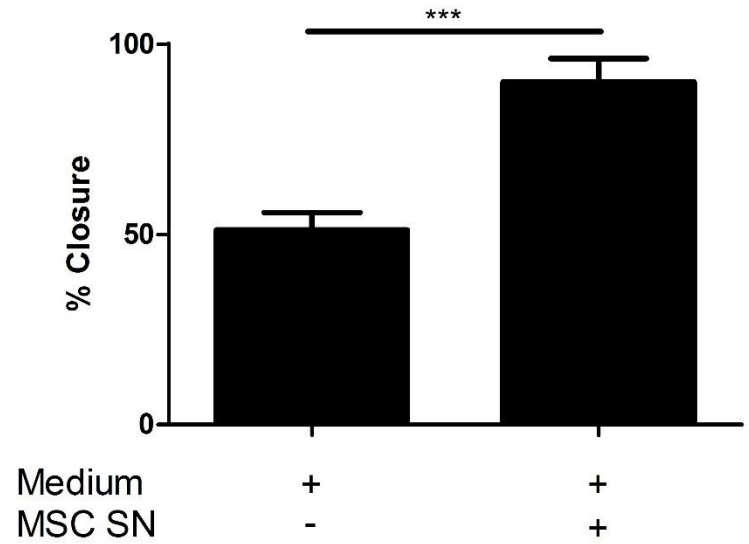

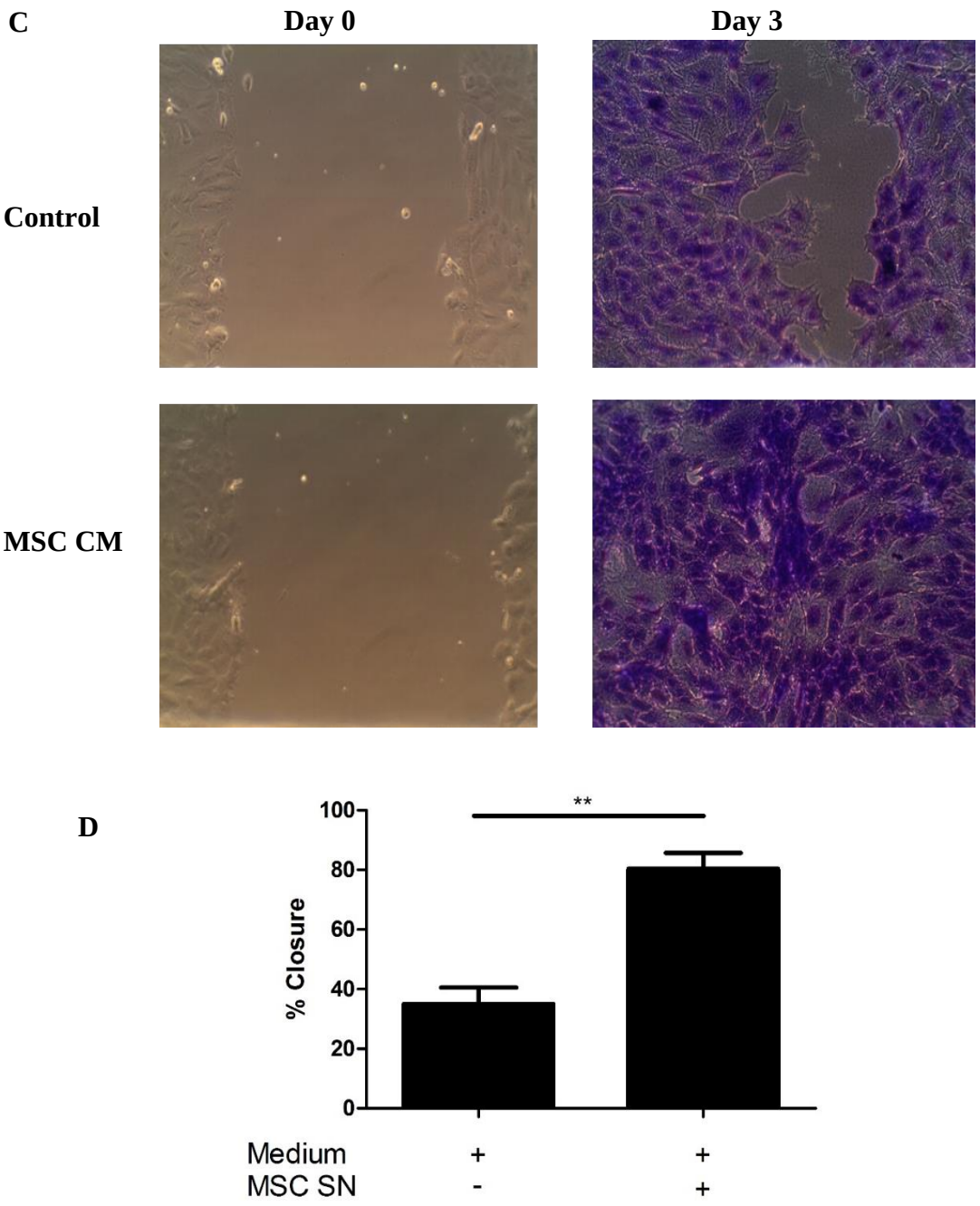

Fig. 4.4 MSC conditioned medium significantly enhances Fibroblast and Epithelial wound closure in a scratch assay. Fibroblasts and LA4 cells ($1x10^5$) were seeded in a 6 well plate and allowed to form a confluent monolayer. The wells were scratched and wound closure measured as described in section 2.19. MSC CM and control medium was concentrated, and the resulting protein fraction was added to designated wells. The width of the scratch in fibroblasts (A&B) and LA4 cells (C&D) was measured and graphed as a percentage of closure (x100). Representative of three experiments.

4.4 MSC encourage epithelial cell but inhibit fibroblast proliferation.

Excessive proliferation of fibroblasts is a hallmark of fibrosis and while fibroblasts play a vital role in wound healing, their accumulation is associated with pathogenesis. The closure of the wound area described in the previous section could be a result of cell migration into the site of damage or cell proliferation. Determining which process is affected by MSC CM has important implications for the use of MSC as a therapy in fibrosis.

In order to investigate whether MSC CM was promoting the proliferation of these cells, tritiated thymidine was added to the cultures. The scratched cells were cultured in the presence or absence of MSC CM, with the addition of tritiated thymidine at day 0. Interestingly MSC CM had opposing effects on the two cell types. When cultured with LA4 cells, MSC CM significantly increased the proliferation of the epithelial cells (Fig. 4.5 A). However, the addition of MSC CM to scratched fibroblast cultures not only prevented an increase in proliferation but reduced the proliferation to levels significantly lower than basal division, FGF was added to scratched fibroblasts as a positive control (Fig. 4.5 B). Combined, these results suggest MSC CM has the ability to encourage fibroblast migration while preventing proliferation. Conversely, MSC CM appears to promote the proliferation of murine lung epithelial cells.

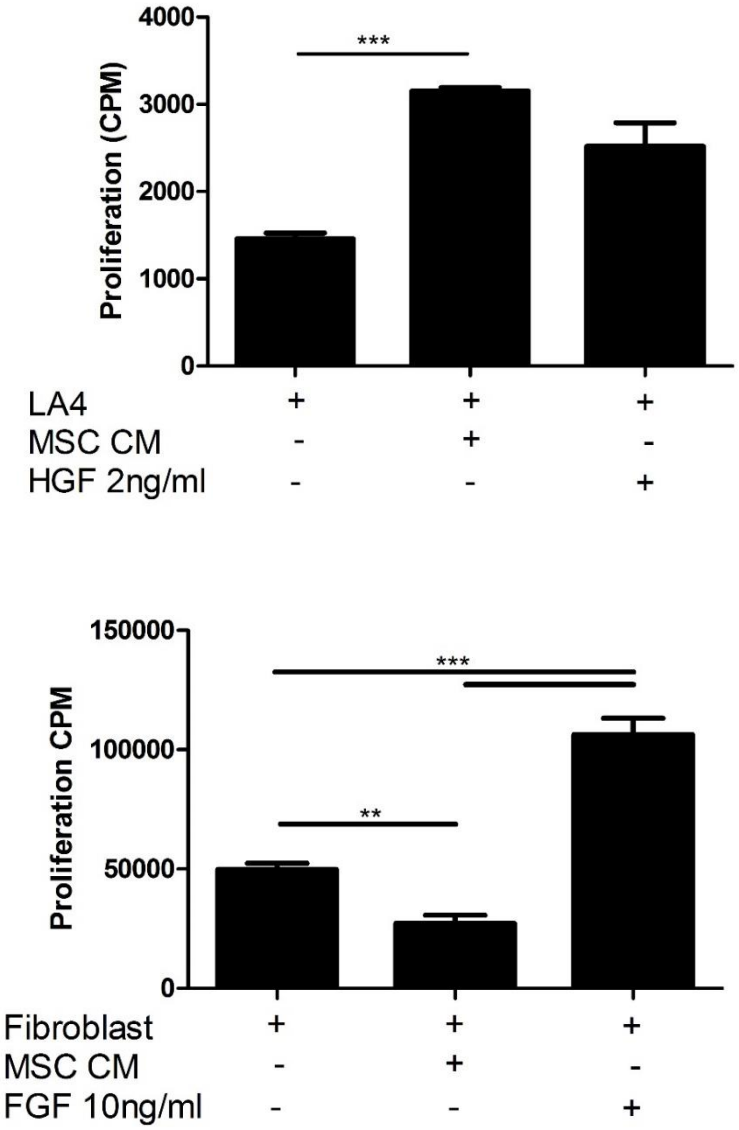

Fig. 4.5 MSC conditioned medium results in epithelial but not fibroblast proliferation. 1 x 10^5 Fibroblasts or LA4 cells were seeded in a 24 well plate and allowed to form a confluent monolayer. The cells were scratched and fresh media was added. FGF (10ng/ml) or HGF (2ng/ml) were added as positive controls. MSC CM was concentrated, and the resulting protein was added to designated wells. [^{3}H]-Thymidine was added to each well and incubated for 3 days. Cultures were harvested, washed, lysed and combined with 2 ml of β-scintillation fluid. [^{3}H]-Thymidine incorporation was quantified by a β-scintillation counter and results were expressed in counts per minute (CPM). Data representative of three experiments.

4.5 MSC reduce the TGFβ induced differentiation of fibroblasts.

The greatest damage inflicted by fibroblasts in fibrosis is mediated by their activated form, myofibroblasts. These cells are characterised by increased expression of alpha smooth muscle actin (αSMA) and increased production and deposition of collagen. As with fibroblasts, myofibroblasts are very important in wound healing especially closure, however excessive activation and proliferation is associated with fibrotic disease. Building on the work from section 4.4 it was important to examine if MSC influence the differentiation of fibroblasts to their activated form. This was achieved through examination of αSMA mRNA levels by real time PCR. In order to activate the fibroblasts *in vitro* they were stimulated with 50ng of recombinant TGFβ, this resulted in increased expression of αSMA. The addition of MSC CM to the culture medium along with TGFβ resulted in a significant decrease in αSMA expression, indicating a reduction in myofibroblasts differentiation (Fig. 4.6). These data indicate that MSC derived soluble mediators inhibit the differentiation of fibroblasts to their activated phenotype.

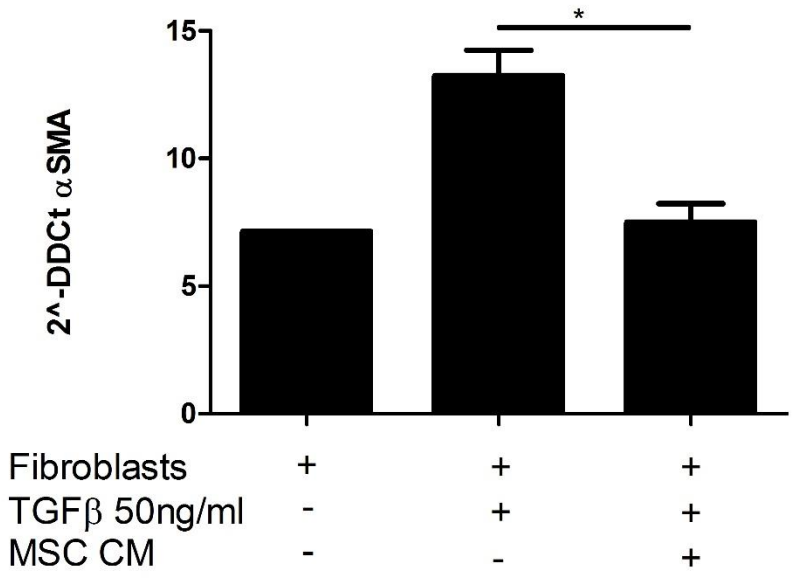

Fig. 4.6 MSC inhibit the differentiation of fibroblasts to myofibroblasts. Fibroblasts were cultured at $2x10^6$ cells/well of a 6 well plate. The cells were stimulated with 50ng/ml of TGFβ, the control well receiving no stimulant. MSC CM was added to a further well containing TGFβ, and cultured for 24 h. The cells were collected in trizol reagent, and examined for expression of αSMA by quantitative real time PCR. Statistics achieved by student t test, n=3.

4.6 PGE2 is required for MSC suppression of Fibroblast proliferation

Many studies have been carried out to determine which growth factors and cytokines are involved in wound healing and fibrosis. *In vitro* studies provide evidence that lung epithelial cells release PGE2 at levels capable of inhibiting the proliferation of fibroblasts (Moore *et al.*, 2003). Direct stimulation of fibroblasts with PGE2 has also been shown to reduce proliferation (Cilli *et al.*, 2004). The use of COX 1 and 2 knockout mice demonstrated COX 2 was important in PGE2 inhibition of fibroblast proliferation (Lama *et al.*, 2002). Previous work by the Mahon laboratory demonstrated murine MSC produce PGE2, and that levels are significantly increased following stimulation with TNFα (L. Tobin & K. English, unpublished data). The increase in PGE2 following TNFα stimulation was interesting considering the inflammatory environment associated with early wound healing. In order to test the relevance of PGE2 in MSC inhibition of fibroblast proliferation, the specific COX 2 inhibitor NS-398 was added to MSC cultures to inhibit the production of PGE2. When added to a fibroblast scratch assay containing tritiated thymidine, MSC CM from NS-398 treated cultures were no longer capable of inhibiting the proliferation of fibroblasts. Removing the inhibitory effect of PGE2 did not however lead to an increase in proliferation beyond basal levels (Fig. 4.8). These data show PGE2 plays an important role in MSC inhibition of fibroblast proliferation. Though NS-398 is commonly used as an inhibitor of PGE2 signalling, it should be noted that despite its lack of involvement in inflammatory processes, COX-1 may also result in PGE2 synthesis. Different prostaglandin subtypes also result from COX-2 actions on arachidonic acid, therefore it would be more accurate to determine MSC signal through the release of prostaglandins.

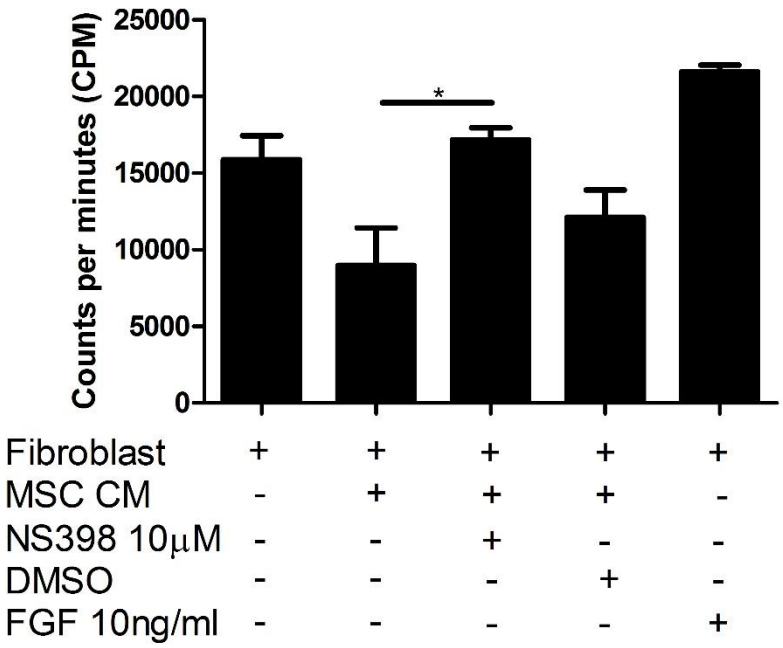

Fig. 4.7 PGE2 produced by MSC is required for suppression of fibroblast proliferation. 1 x 10^5 fibroblasts were seeded in a 24 well plate and allowed to form a confluent monolayer. The cells were scratched and fresh medium was added. FGF (10ng/ml) was added as a positive control. MSC CM from cells previously treated in the presence or absence of NS398 or DMSO control were concentrated. The resulting protein was then added to designated wells. [^{3}H]-Thymidine was added to each well and incubated for 3 days. Cultures were harvested, washed, lysed and [^{3}H]-Thymidine incorporation was quantified and results were expressed in counts per minute (CPM). Data representative of two experiments.

4.7 Investigations of role of HGF in MSC induced epithelial proliferation

As previously discussed, HGF is an important paracrine factor involved in the proliferation and migration of epithelial and endothelial cells. Given the positive influence of MSC CM on lung epithelial cell proliferation, MSC were examined for production of HGF. Supernatant from MSC was tested by ELISA for the presence of HGF, the cells were also stimulated with TNFα, a pro-inflammatory cytokine up-regulated in fibrosis. MSC were shown to constitutively produce HGF, but once stimulated with TNFα, HGF levels significantly increased (Fig. 4.8).

In order to examine a role for HGF in MSC induction of lung epithelial cell proliferation, a neutralising antibody for the HGF receptor was added to the culture system. LA4 cells were plated and scratched in the presence or absence of MSC CM, HGF receptor neutralising antibody or the isotype control added at varying concentrations to the MSC CM wells. The wells receiving the isotype control had an increased rate of closure compared to the other treatment wells. The scratch assay is concluded once the first group reaches 100% closure, as a consequence of this rapid response from the isotype control wells, the MSC alone group showed no difference to the media alone group. This approach could not therefore be used to definitively make any claim on the role of HGF in this system. However, the groups that received the HGF receptor inhibitor did not close the wound area as quickly as the MSC CM or medium alone groups. Though not significant this trend indicated that a potential role for HGF should be investigated by other approaches (Fig. 4.9).

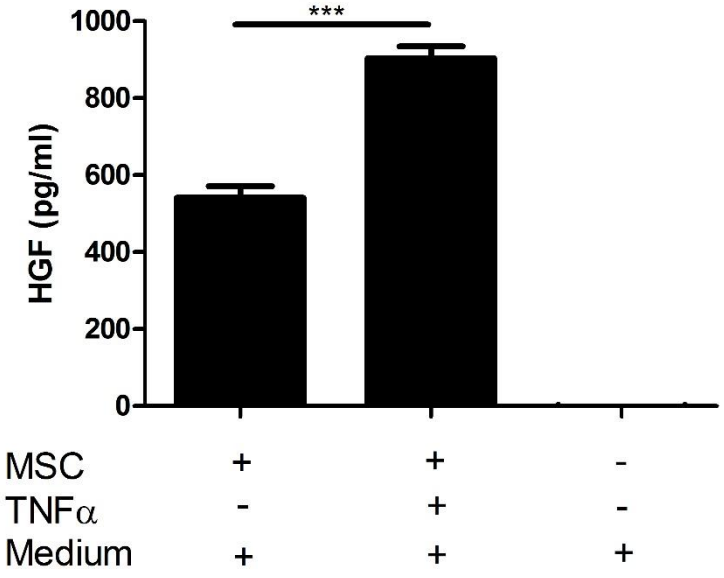

Fig. 4.8 Stimulation of MSC by inflammatory cytokines results in increased expression of HGF. MSC CM media was tested for levels of HGF by ELISA. MSC were cultured in a 6 well plate at $2x10^6$ cells/well. 50ng/ml of TNFα was added to each designated well and cultured for 24 hours. Medium alone was also examined to test for potential HGF in the serum. The supernatant was tested as described in section 2.21, and the concentration read off a standard curve in pg/ml (p***<0.001). Statistics measured using ANOVA, n=3.

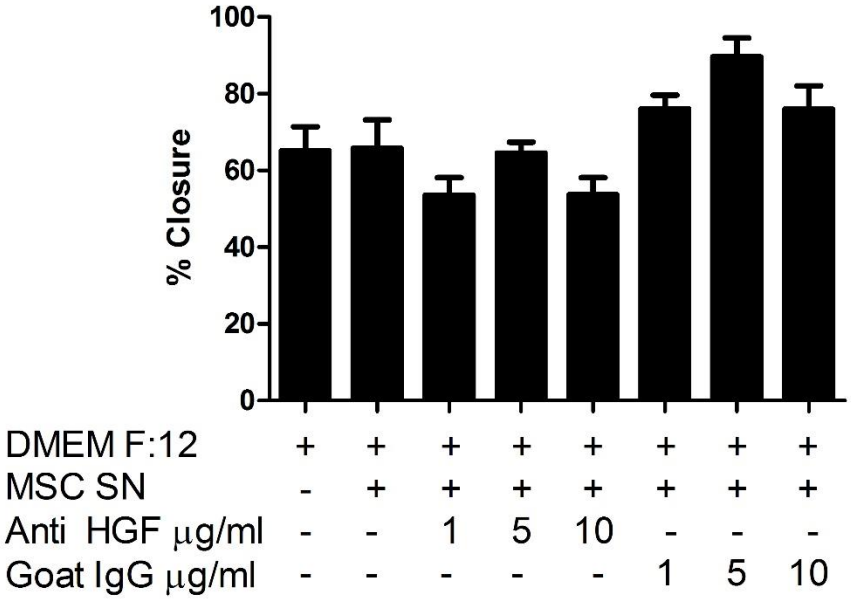

Fig. 4.9 HGF neutralising antibody titration in LA4 scratch assay. LA4 cells ($1x10^5$) were cultured in a 6 well plate and allowed to form a confluent monolayer. MSC CM was concentrated, and the resulting protein was added to designated wells. HGF receptor antagonist or isotype control was added to designated wells at increasing concentrations from 1μg/ml to 10μg/ml. The wells were cultured until the first group reached 100% closure. All wells were fixed and stained and the width of each scratch was measured and graphed as a percentage of closure as described in section 2.19. n=2.

4.8 HGF Knockdown MSC retain their stem cell characteristics

Given that the HGFR neutralising antibody failed to successfully facilitate the investigation of a role for HGF in MSC promotion of epithelial repair, alternative means to block HGF signalling in MSC were explored. Following the success of shRNA knockdown in previous experiments, constructs targeting murine HGF were designed. After much optimisation, MSC stably knocked down for HGF were generated.

Transducing the MSC with lentivirus did not alter the basic MSC characteristics. Figure 4.10 shows that HGF knocked down (KD) MSC still expressed all the required cell surface markers, similar to the profile seen in non-transduced cells. MSC demonstrated adherence to plastic and were capable of differentiating in bone, fat and cartilage (Fig. 4.11).

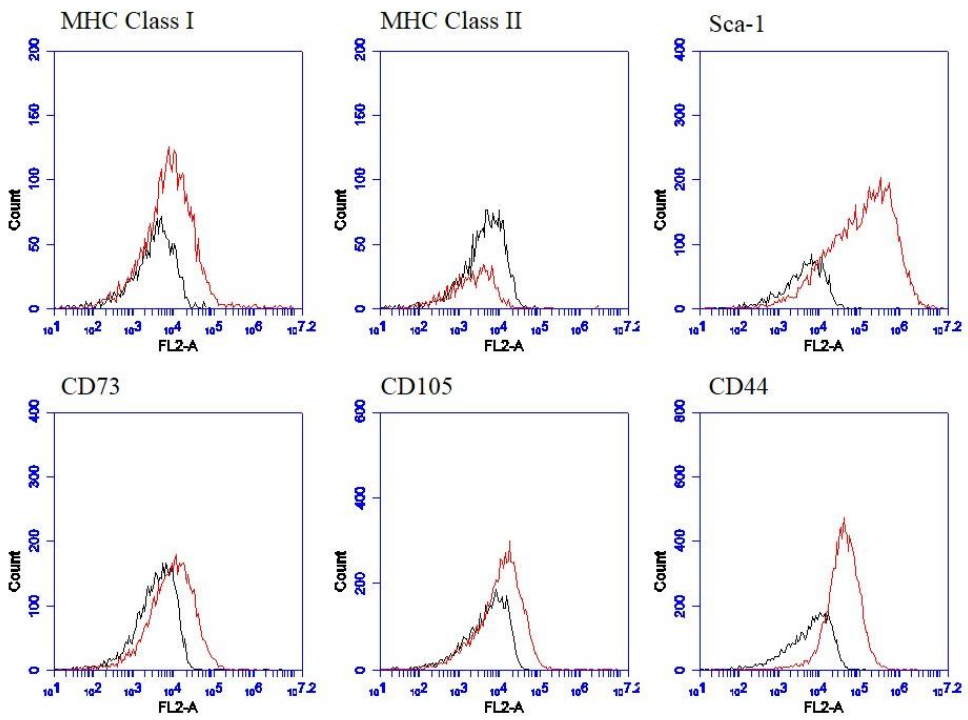

Fig. 4.10 Surface marker expression on HGF knocked down MSC. BALB/c knocked down MSC were characterised by looking at the expression levels of a variety of cell surface markers (Red Line) against their corresponding isotypes (Black Line). 10,000 events were recorded for each marker. These results are representative of at least three experiments.

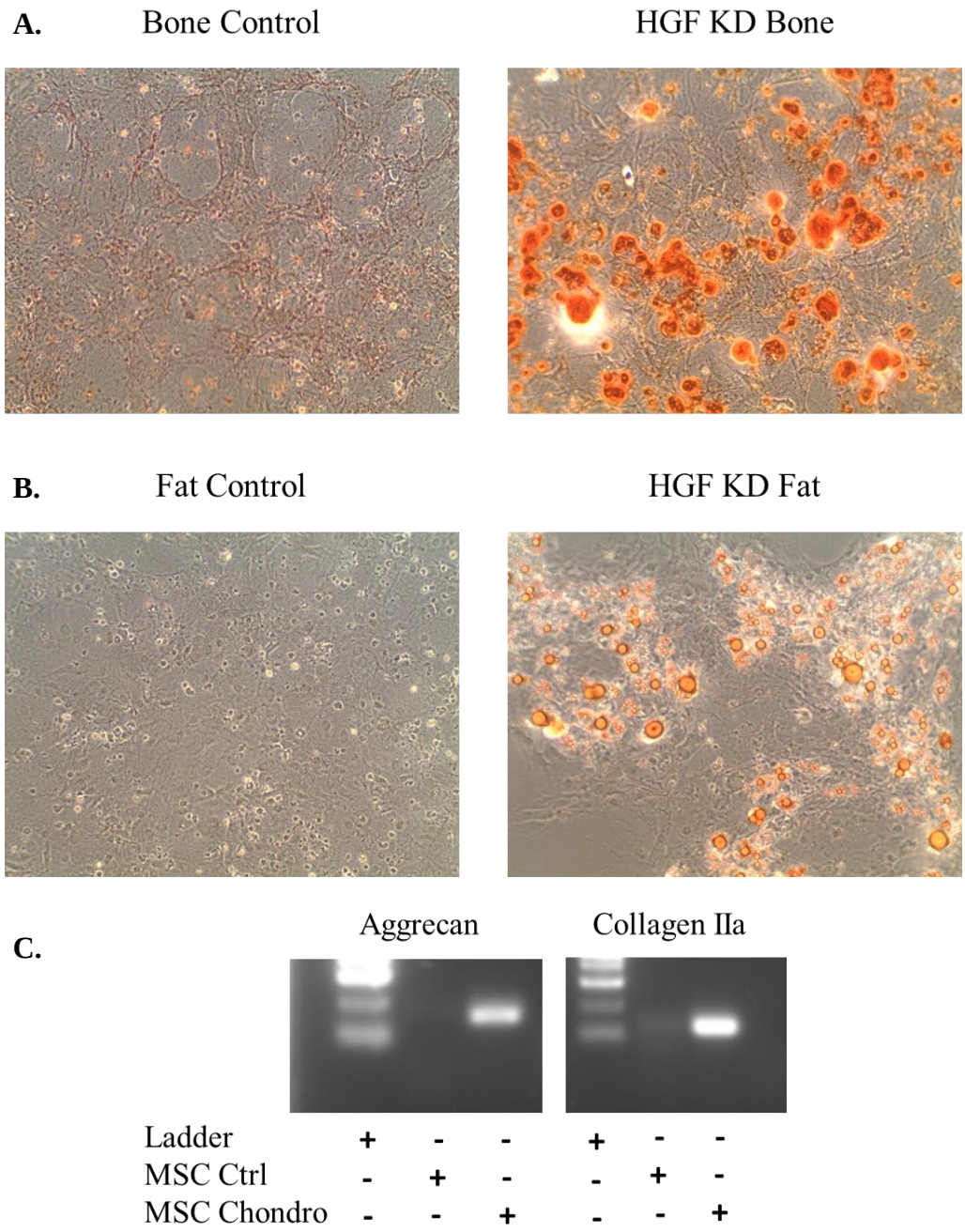

Fig. 4.11 Trilineage differentiation of HGF knock down MSC. HGF knock down MSC ($5x10^4$) were cultured for 21 days in control medium, osteogenic medium (A), or adipogenic medium (B). Cultures were stained with Alazarin Red for bone and Oil Red O for fat. $2x10^5$ MSC were centrifuged at 200xG for 8 min to form a cell pellet, control medium or chondrocyte medium was added to the tube and the cells were cultured for 21 as a 3D cell mass. After 21 days trizol was added to the cell pellet, following RNA extraction and cDNA synthesis, the mRNA was tested for the chondrocyte markers aggrecan and collagen IIa (C). The results are representative of two experiments.

4.9 Conditioned medium from HGF knocked down MSC no longer supports the proliferation of lung epithelial cells.

The GFP positive MSC that were puromycin resistant were collected and tested for HGF expression. Non-transduced MSC, HGF knock down MSC and non-silencing control MSC were plated into 6 well plates and cultured for 24 hours, supernatants were collected and examined for HGF by ELISA. (Fig. 4.12). The cells were tested at multiple passages, showing significant reduction in HGF production.

The HGF knockdown MSC CM was used in culture with LA4 cells to determine the importance of HGF in MSC induced proliferation of epithelial cells. LA4 cells were plated as a monolayer in 6 well plates, scratched and cultured with tritiated thymidine. Non-transduced MSC CM, HGF knockdown MSC CM or non-silencing control MSC CM was added to designated wells and cultured for 72h. The baseline proliferation of the LA4 cells was determined in the well containing just medium. Cultures with HGF knocked down MSC CM had significantly lower levels of proliferation compared to those containing non transduced MSC CM. Non-silencing control MSC CM resulted in higher levels of proliferation but not statistically elevated compared to the non-transduced MSC (Fig. 4.13).

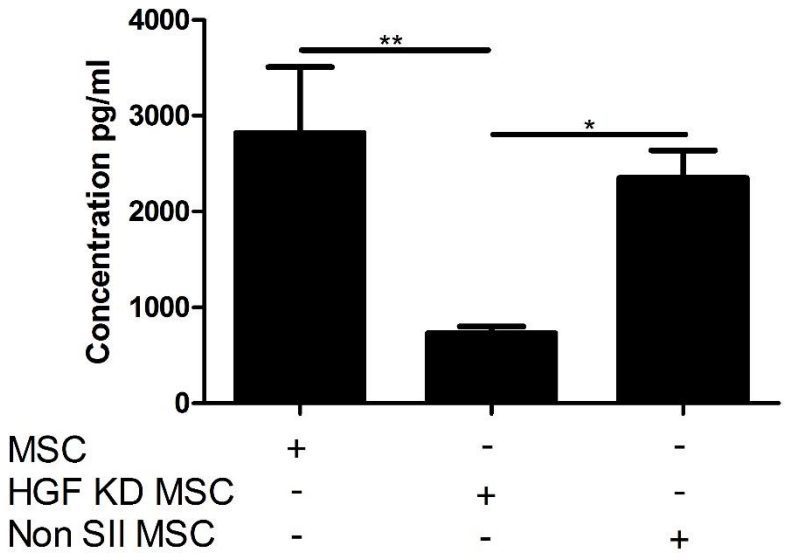

Fig. 4.12 Expression of HGF in HGF knocked down MSC HGF knock down MSC CM, non-transduced MSC CM, and non-silencing control MSC CM was tested for levels of HGF by ELISA. MSC were cultured in a 6 well plate at $2x10^6$ cells/well for 24 hours. The supernatant was tested as described in section 2.21, and the concentration read off a standard curve in pg/ml ($p^{**}<0.001$). Data representative of three experiments.

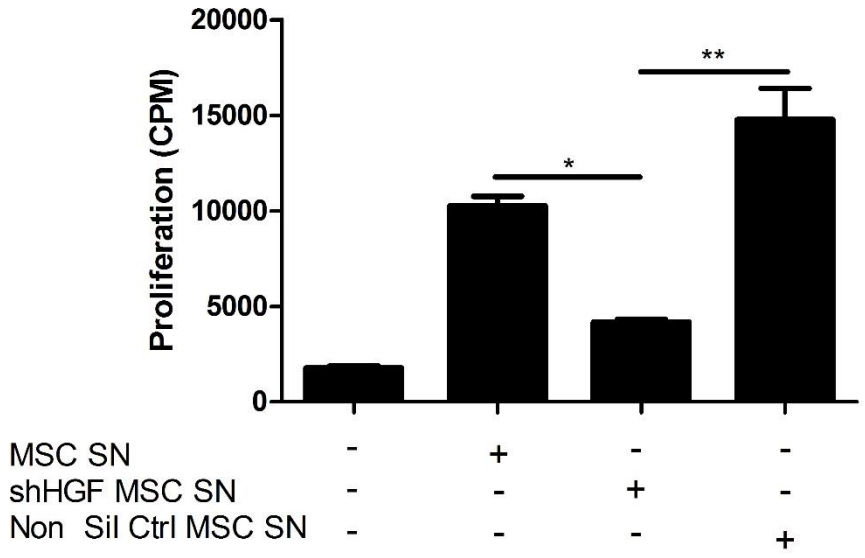

Fig. 4.13 HGF is responsible for MSC induced LA4 proliferation. 1 x 10^5 epithelial cells were plated in a 24 well plate and allowed to form a confluent monolayer. The cells were scratched and fresh medium was added. MSC, HGF KD MSC and non-silencing control MSC CM was concentrated and the resulting supernatent was then added to designated wells. [^{3}H]-Thymidine was added to each well and incubated for 3 days. Cultures were harvested, washed, lysed and combined with 2 ml of β-scintillation fluid. [^{3}H]-Thymidine incorporation was quantified by a β-scintillation counter and results were expressed in counts per minute (CPM). Data representative of two experiments.

4.10 HGF does not rescue epithelial cells from TNFα induced apoptosis.

In addition to the role of HGF in proliferation of epithelial cells, the growth factor has also been associated with a protective role against cell apoptosis. Previous studies have demonstrated HGF has the capacity to protect cardiac myocytes from oxidative stress induced apoptosis (Kitta *et al.*, 2001) and kidney epithelial cells from cyclosporine A induced apoptosis (Fornoni et al., 2001). In order to determine whether HGF was influencing apoptosis in this model, epithelial cells were subjected to TNFα induced apoptosis, mimicking the effects of TNFα in the disease state. Increasing levels of HGF were then added to culture, beginning at levels physiologically produced by MSC. Figure 4.14 shows that even at higher levels of 20ng/ml, HGF had no effect on either early (lower right quadrant) or late apoptosis (upper right quadrant). This result indicates that the influence of MSC derived HGF in this model is unlikely to be via prevention of the apoptosis of lung epithelial cells.

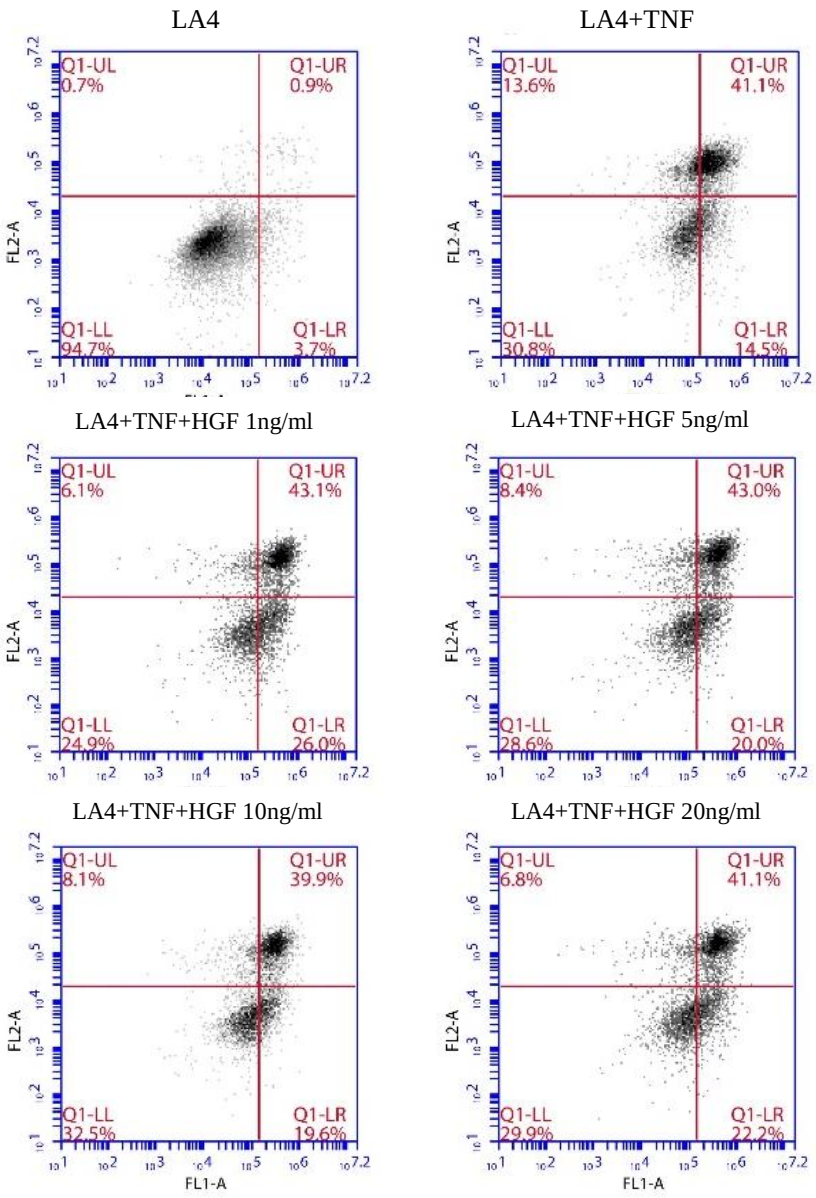

Fig. 4.14 TNFα induced apoptosis is not alleviated by HGF at concentrations produced by MSC. $1x10^5$ LA4 cells were seeded into a 24 well plate and allowed to form a confluent monolayer. 50ng/ml of TNFα was added to induce apoptosis in the cells. HGF was added to the culture medium in increments from 1ng/ml to 20ng/ml. Apoptosis was measured using annexin V and propidium iodide staining followed by flow cytometry analysis. N=3.

4.9 Summary

In this chapter primary lung fibroblasts and lung alveolar epithelial cells were treated with conditioned media form treated and untreated MSC. These data established a potential role for MSC in the proliferation of epithelial cells and inhibiting the activation and proliferation of fibroblasts.

The alternative effects of MSC on different lung cells was established using a scratch assay of wound closure. MSC CM promoted the migration of both epithelial cells and fibroblasts into the site of damage. However, MSC CM maintained control over fibroblast homeostasis, inhibiting their activation and proliferation. In the context of wound healing and fibrosis, the opposing interplay between MSC, epithelial cells and fibroblasts could be exploited for its therapeutic potential. Fibroblasts are vital in wound healing and promoting their migration into the site of injury may aid wound closure but the un-checked proliferation and activation of fibroblasts leads to disease progression, both of these latter traits are inhibited by MSC. The second crucial process in healing is remodelling, where fibrotic tissue is replaced with functional lung epithelial tissue. MSC promotion of epithelial cell proliferation could support the re-epithelialisation of tissue damaged by fibrosis in the lung.

Previous work showed the importance of MSC signalling through contact dependent methods, here MSC paracrine effects were investigated. Experiments blocking PGE2 production by MSC reversed MSC inhibition of fibroblast proliferation. Interestingly, expression of the lipid mediator by MSC is also increased in an inflammatory environment associated with early fibrosis. The same is true of the growth factor HGF, a known mitogen for epithelial cells. Using shRNA technology to knock down HGF expression in MSC, HGF was shown to be

responsible for MSC driven epithelial proliferation. These data provide a strong basis for MSC therapy in pulmonary fibrosis on two fronts. Firstly, MSC can suppress the excessive proliferation and activation of fibroblasts by PGE2, and secondly, through HGF by encouraging the growth and replenishment of functional alveolar epithelial cells.

Chapter 5

The effects of MSC treatment upon bleomycin induced lung fibrosis.

5.1 Introduction

The clinical management of lung fibrosis currently focuses on treating the symptoms but not the underlying cause, which in many cases remains unknown. As discussed in the introduction, initial treatment includes corticosteroids and immunosuppressive drugs, while cytotoxic drugs are used to improve lung function. Ultimately, lung transplantation remains the end result for many patients who don't respond to treatment. Trials to find novel targets are ongoing with pre-clinical experimental data assisting the search for potential drug candidates. In the previous chapter, the effect of murine MSC on pulmonary cells was examined with regard to potential benefits for treatment of fibrosis. In order to examine the effect of murine MSC therapy *in vivo,* the bleomycin mouse model of pulmonary fibrosis was used.

Bleomycin is a chemotherapeutic drug used to treat a variety of tumours, however in approximately 5% of cases it adversely induces pulmonary toxicity and fibrosis (Walters and Kleeberger, 2008). This side effect has been utilised in animals to create a model of pulmonary fibrosis. As discussed in the introduction, the model is used mostly in C57BL/6 mice as BALB/c mice were poor responders (Schrier et al., 1983). The model consists of a single intra-tracheal instillation that results in inflammation and increased production of collagen. Physiological changes are observed over 3-4 weeks (Izbicki et al., 2002), thereafter the model begins to resolve, and in as few as 5 weeks there is little to no evidence of fibrotic lesions. The resolution of fibrosis in the mouse model is inconsistent with the human disease. In the absence of a chronic stimulus often associated with human fibrosis, murine lungs regenerate and remove the collagen deposits. Despite the limitations of the model, bleomycin induced fibrosis still provides the best reproducible animal model of pulmonary fibrosis. Many of the drugs currently being tested in clinical trials were initially tested

in bleomycin mouse models, be they for preventative or therapeutic use (Moeller et al., 2008).

This study sought to examine the hypothesis that MSC could improve pathology in bleomycin induced fibrosis. With an aim to refine the bleomycin murine model of fibrosis resulting in a more accurate representation of therapeutic intervention, consequently using this model to determine MSC efficacy as a cellular therapy in fibrosis. This chapter also examined the importance of MSC derived HGF with regards to any positive outcome in treatment.

5.2 MSC reduce pathology in a bleomycin induced murine model of fibrosis

The standard model of bleomycin induced fibrosis involves intra-tracheal instillation (IT) of bleomycin at a concentration of 4U/kg. In this model bleomycin was administered by intranasal inhalation (IN) under anaesthetic. Previous work performed in the laboratory using crystal violet stain, demonstrated that IN administration of liquid leads to comprehensive permeation throughout the lung. An initial study aimed to ensure the model worked under these modified conditions and that the administration of allogeneic murine MSC to a control mouse had no adverse effects. The PBS treated lungs showed little sign of fibrotic damage, with no major changes to the lung architecture, and only small collagen deposits around bronchioles. These observations were consistent at day 7 (Fig. 5.1 A&B), day 14 (Fig. 5. C&D), and day 28 (Fig. 5.1 E&F). Delivery of allogeneic MSC intravenously to mice that received PBS IN resulted in a similar pathology to PBS control groups, with no statistical difference in their pathological score (Fig 5.1 G). Bleomycin treated groups displayed deposition of collagen in alveolar spaces and around bronchioles by day 7,

there was thickening of alveolar septae but the lung structure was largely preserved (Fig 5.1 A&B). At day 14 the alveolar septae had clearly thickened with larger collagen deposits radiating from the bronchioles (Fig 5.1 C&D). At day 28, fibrotic masses could be observed in over 20% of the microscopic field, and the alveolar spaces are enlarged with contiguous fibrotic thickening (Fig 5.1 E&F).

Administration of allogeneic MSC to bleomycin treated mice resulted in an improvement in pathology on day 7 and 14, there was still thickening of the alveolar septa but less collagen deposition around the bronchioles (Fig 5.1 A&B, C&D). At day 28, there was a statistically significant improvement in pathological scoring (Fig 5.1 G), with reduced fibrotic deposition in alveolar spaces and rarefied fibrotic masses. Alveolar septae displayed only localised thickening and lung structure was maintained (Fig 5.1 E&F).

Day 7

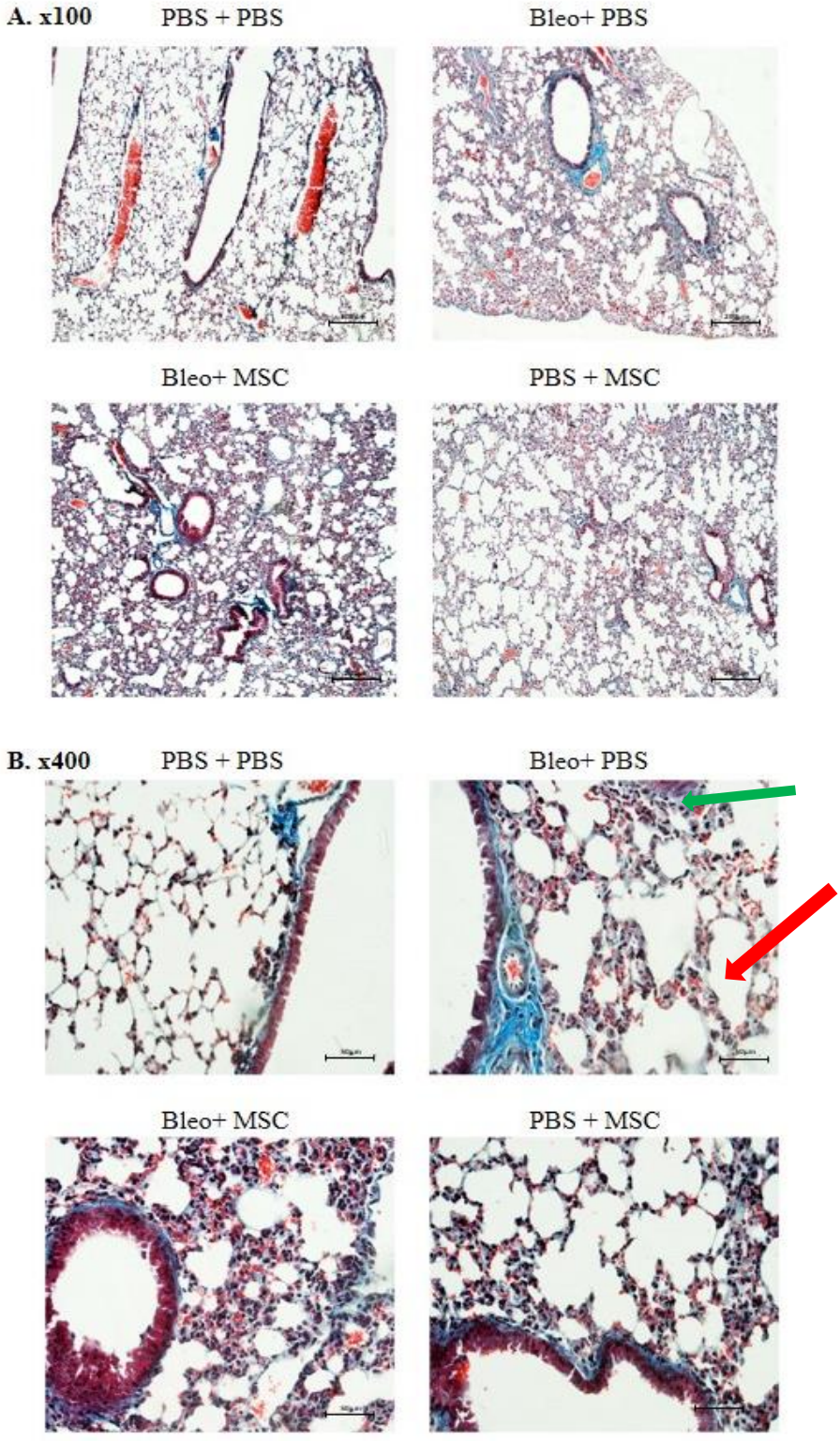
A. x100
PBS + PBS
Bleo+ PBS
Bleo+ MSC
PBS + MSC
B. x400
PBS + PBS
Bleo+ PBS
Bleo+ MSC
PBS + MSC

Day 14

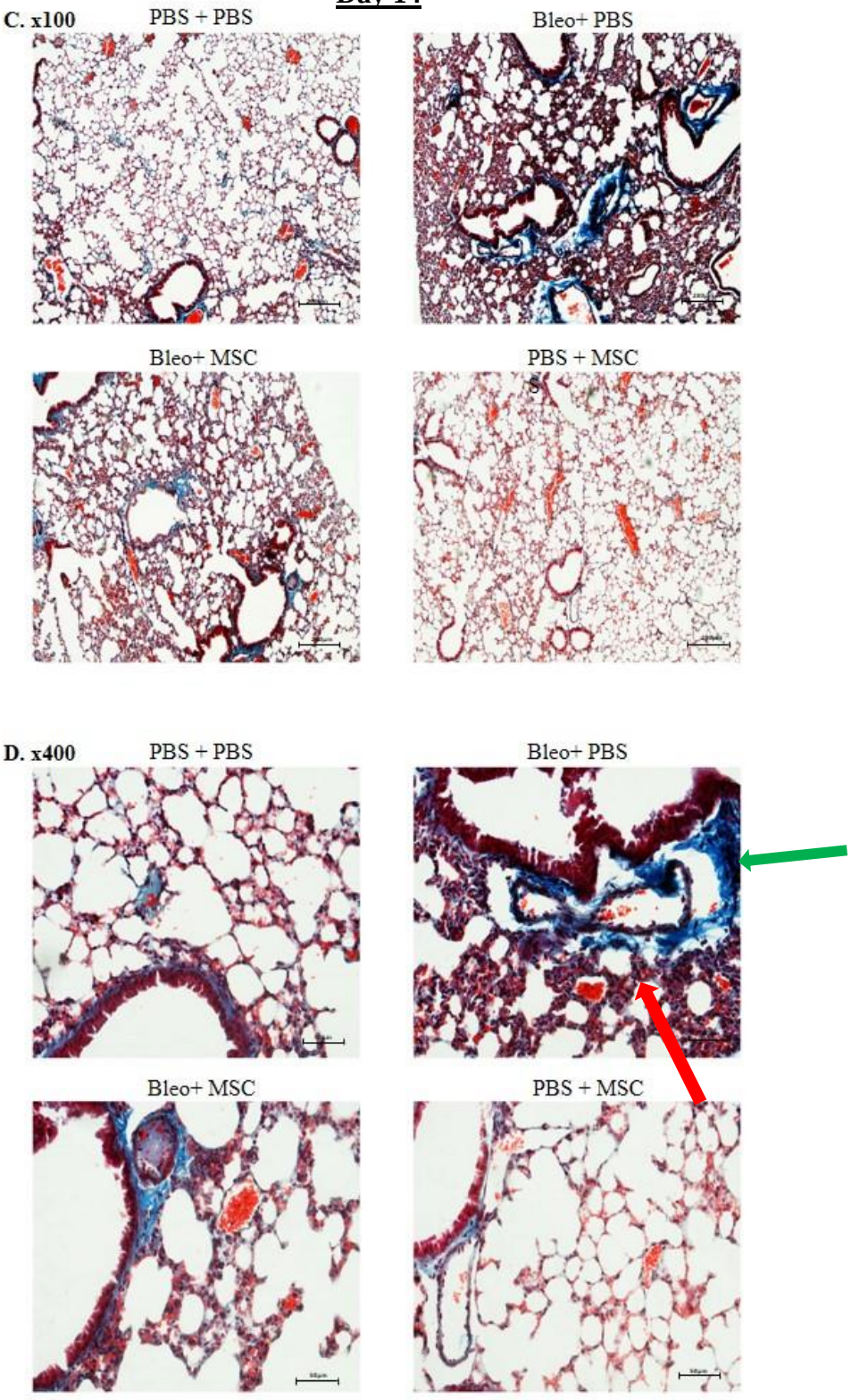
C. x100
PBS + PBS
Bleo+ PBS
Bleo+ MSC
PBS + MSC
D. x400
PBS + PBS
Bleo+ PBS
Bleo+ MSC
PBS + MSC

Day 28

E. x100

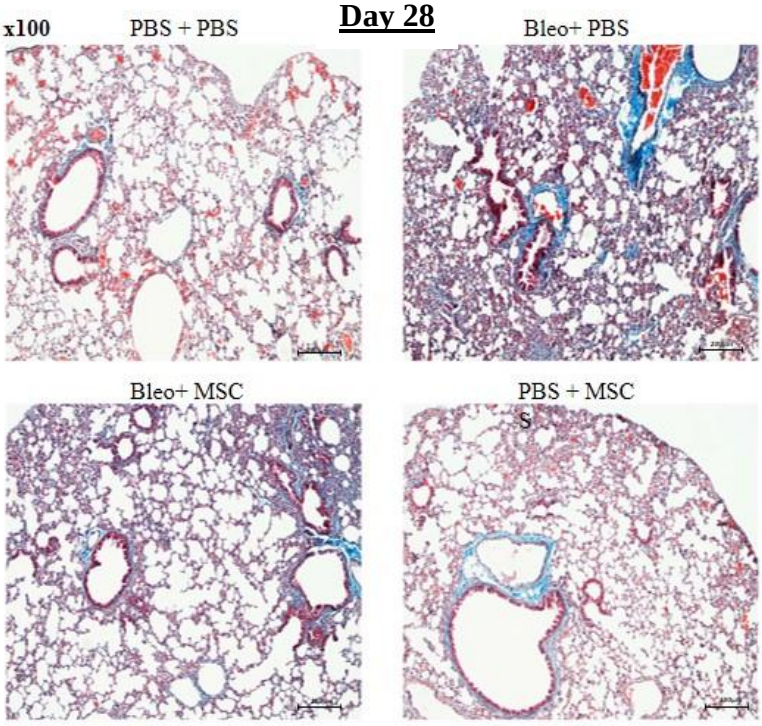

F. x400

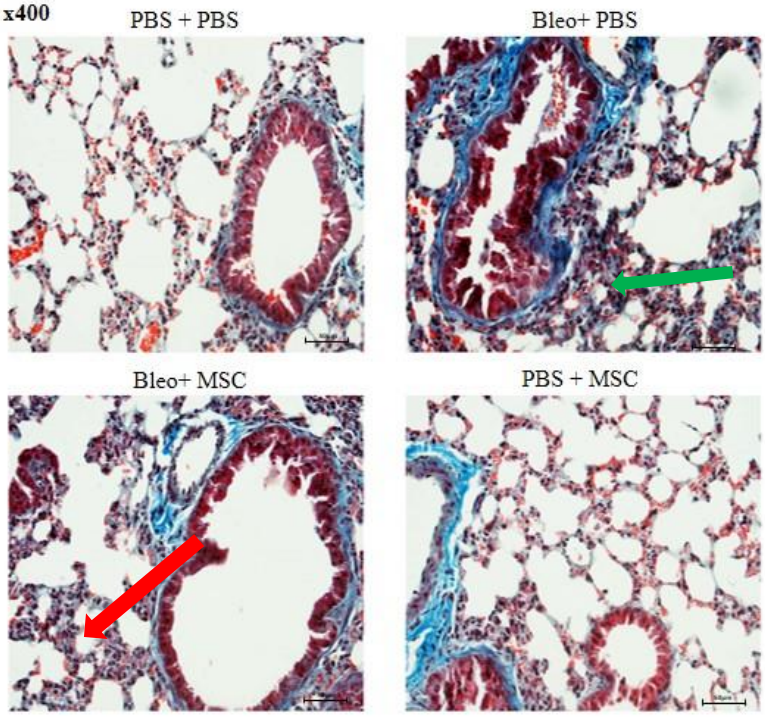

G.

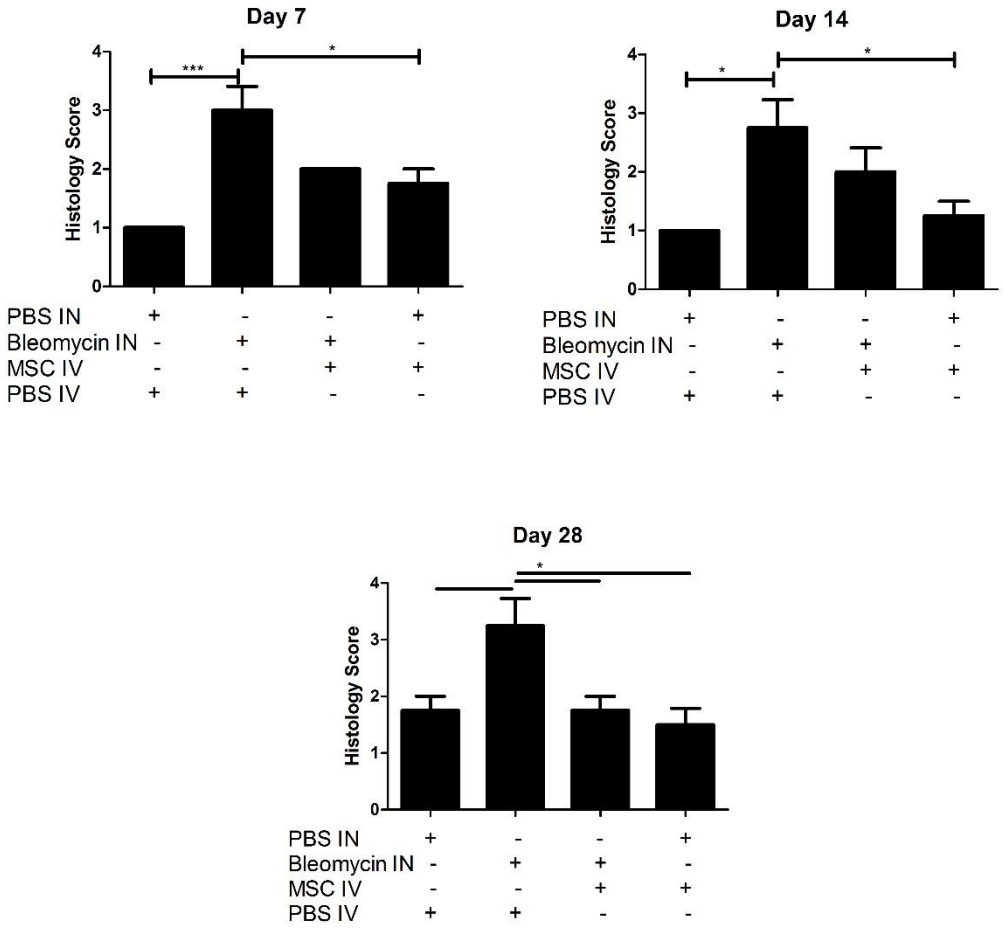

Figure 5.1 Allogeneic Murine MSC administration reduces lung pathology in a bleomycin model. Representative images of transverse lung histological sections at day 7 (A&B), day 14 (C&D), and day 28 (E&F). Airway fibrosis was detected by trichrome staining for collagen deposition as described in section 2.26. Fibrotic masses are indicated by the green arrows, thickening septae are indicated by red arrows. Histological scoring was performed by at least 2 researchers (G), n=5.

5.3 Syngeneic and allogeneic murine MSC reduce bleomycin pathology.

The bleomycin model, as mentioned above, is performed in C57BL/6 mice. In order to establish whether reduction in pathology is affected by treatment with allogeneic or syngeneic MSC, a small pilot study was performed. C57BL/6 mice were treated with bleomycin IN and injected IV with BALB/c MSC or C57BL/6 MSC 6 hours later. Lungs were collected on day 28 and examined for collagen deposition by trichrome staining. The cytokine and growth factor profile of the lungs was also examined by RT-PCR.

As with the initial pilot, the PBS control group maintained a normal lung architecture with minimal collagen deposition around the bronchioles (Fig 5.2 A&B). The bleomycin treated group had enlarged alveolar septa and heavy collagen deposition around bronchioles (Fig 5.2 A&B). Systemic administration of either C57BL/6 MSC or BALB/c MSC resulted in an improvement in pathology compared to the bleomycin treated mice. MSC treated lungs showed signs of some architectural damage but only isolated fibrotic masses, both allogeneic and syngeneic MSC treatments resulted in reduced fibrotic thickening around the bronchioles compared to bleomycin treated lungs (Fig 5.2 A&B).

Lung mRNA was tested by real time PCR for a panel of cytokines and growth factors relating to inflammation and fibrosis. At day 28 the expression of both inflammatory (Fig 5.2 C) and fibrotic (Fig 5.2 D) genes were up regulated following exposure to bleomycin when compared to the PBS control mRNA. Treatment with either BALB/c or C57BL/6 MSC reduced expression levels of the inflammatory cytokines TNFα, and IL-1β, as well as the fibrotic markers TGFβ and fibronectin in comparison to the bleomycin treated group. However, the data did not reach statistical

significance, the resolving nature of the model more than likely accounting for this. At day 28 the lungs are already beginning to recover from the single dose of bleomycin. Sampling lungs at an earlier time point was therefore tested as a means to improve the statistical relevance of MSC effect on gene expression.

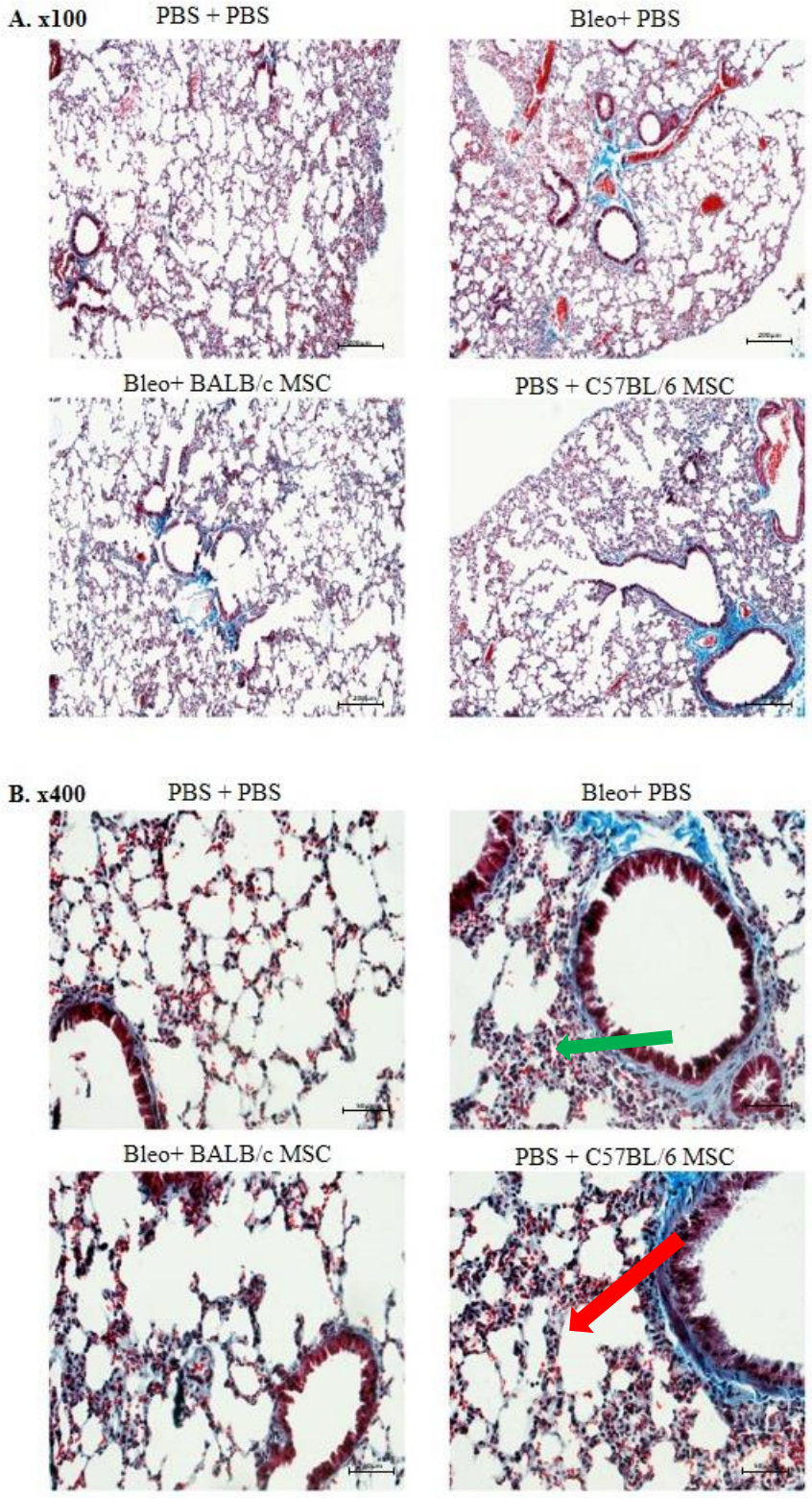
A. x100
PBS + PBS
Bleo+ PBS
Bleo+ BALB/c MSC
PBS + C57BL/6 MSC
B. x400
PBS + PBS
Bleo+ PBS
Bleo+ BALB/c MSC
PBS + C57BL/6 MSC

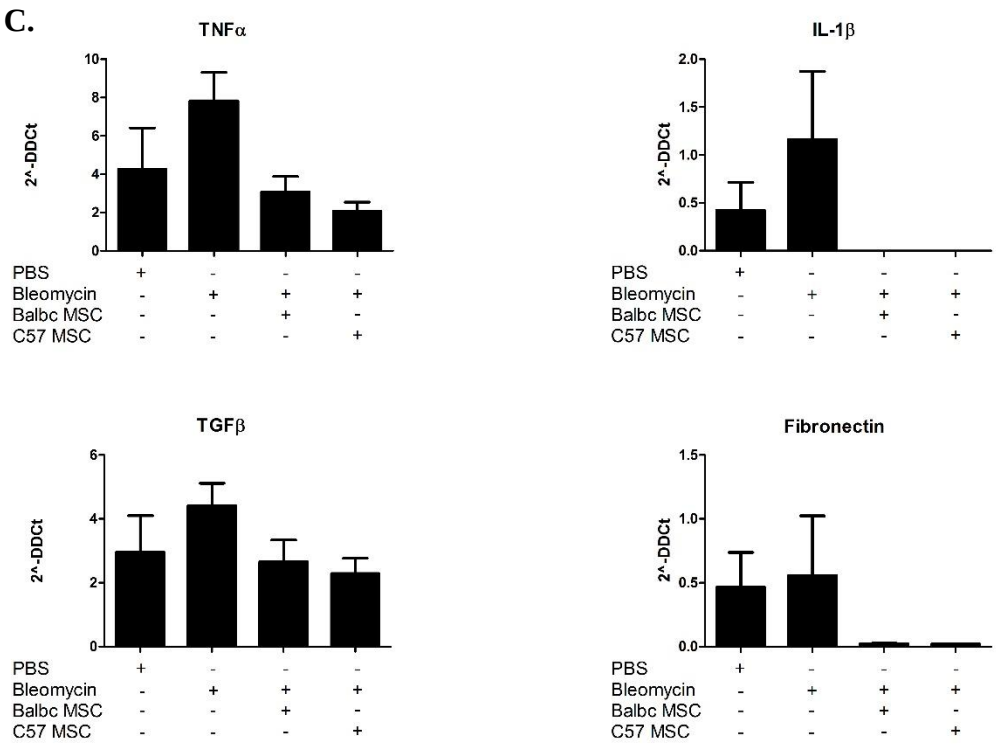

Figure 5.2 Histology and PCR results from allogeneic and syngeneic murine MSC treatment of bleomycin induced lung fibrosis. C57BL/6 mice were treated with a single IN dose of bleomycin (4U/kg). BALB/c or C57BL/6 MSC were administered 6h later by tail vein injection. Lungs were harvested at day 28. Representative images of transverse lung sections at 28 days (A&B). Airway fibrosis was detected by trichrome staining for collagen deposition. Fibrotic masses are indicated by the green arrows, thickening septae are indicated by red arrows. Real time PCR expression of inflammatory and fibrotic genes (C) from whole lung mRNA. Histology and real time data is representative of at least 2 replicates.

5.4 Time course of fibrotic development

The bleomycin model is characterised by an initial inflammatory response followed by fibrosis. The time point at which a therapy is given can determine whether or not the treatment can be considered an anti-inflammatory therapy, designed to limit the disease by combatting the side effects or whether it can be considered a treatment against established fibrosis. In order to determine the time course of the bleomycin model a pilot study was conducted, collecting samples every 3 days for 28 days. The lungs from these mice were analysed by PCR for a panel of inflammatory and fibrotic genes. By establishing the time at which fibrosis occurs, the accurate time to give MSC as a treatment can be determined, the results can also establish the optimum time point to collect samples in order to observe any potential improvement following MSC treatment.

When compared to basal levels at day 0, TNFα expression significantly increased by day 9 and peaked at day 15, after which there was a gradual decrease for the next 16 days (Fig 5.3 A). IL-1β expression was also significantly increased by day 15, however given the values either side of day 15 this may be an outlier in data collation (Fig. 5.3 B). These results indicate the inflammatory response associated with bleomycin treatment begins at approximately day 9 peaking at day 15 and reducing thereafter. The fibrosis associated growth factor TGFβ increased gradually from day 3, reaching a significant high at day 15 compared to levels observed at day 0 (Fig 5.3 C). HGF levels were examined, appearing to gradually increase over the course of the study but never reaching statistical significance (Fig 5.3 D). As demonstrated in chapter 4, HGF is a growth factor associated with epithelial growth and wound repair. A potential correlation between the positive effects of MSC on pathology and expression of HGF following MSC administration required further

examination. The above results showed the onset of fibrosis occurs at day 15, with inflammation beginning 6 days earlier allowing future studies using MSC to discriminate between anti-inflammatory responses and anti-fibrotic ones.

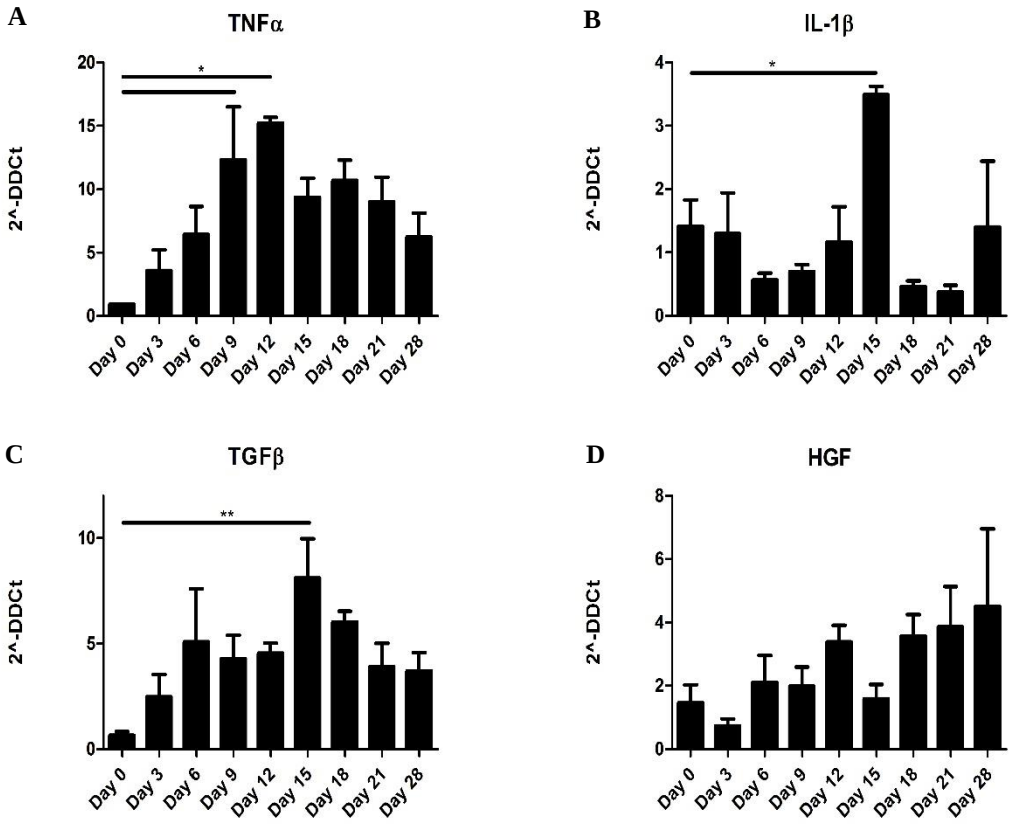

Fig 5.3 Real Time PCR on Lung samples of Bleomycin time course. C57BL/6 mice were treated with bleomycin by IN. Four mice were sacrificed every 3 days for 28 days and the lungs were processed for RNA isolation. Following cDNA synthesis, real time PCR was run for selected inflammatory (A&B) or fibrotic (C&D) markers. The results were graphed and analysed for statistical relevance (* represents $p < 0.05$)

5.5 Allogeneic murine MSC protection from bleomycin induced fibrosis is dependent on the time of administration.

In order to differentiate between MSC as an anti-inflammatory treatment and an anti-fibrotic therapeutic, the administration of MSC was delayed until the onset of fibrosis. Based on the results from the previous section MSC were given at day 0 and day 9. HGF KD MSC and non-silencing control MSC, characterised in chapter 4, were also administered at day 9. This time point was chosen in the effort to determine a role for MSC released HGF as a therapeutic target in repair of bleomycin induced fibrotic damage. Lungs were collected on day 15 and day 21, as expression levels of fibrotic genes appear to diminish after this point.

As with previous studies, PBS control mice maintained a normal lung architecture and low levels of inflammatory cytokines (Fig 5.4 & Fig 5.5). Bleomycin treated mice displayed extensive collagenous masses and enlarged alveolar spaces, as well as alveolar septum thickening at both day 15 and day 21 (Fig. 5.4 A, B&C). There was also an increase in TNFα and IL-1β levels at day 15. TNFα levels were generally reduced at day 21, however IL-1β expression was still up-regulated in the bleomycin group compared to PBS lungs (Fig. 5.5 A&B). At day 15 there was little difference in lung pathology of mice that received allogeneic MSC at day 0 compared to day 9, however, by day 21 lungs from mice treated with MSC on day 0 show a reduced pathological score, significantly reduced IL-1β levels and a significant increase in HGF expression compared to groups where MSC were given on day 9 (Fig 5.4 A&B);(Fig. 5.5). 3T3 fibroblast cells were administered at the same time points as MSC as a control, The cells, particularly those administered at day 9 increased TNFα and TGFβ levels at day 15 but this did not translate into increased pathological scoring (Fig 5.4);(Fig. 5.5). While greater statistical relevance was established when

studying gene expression at day 21, the histological scores from MSC treatment failed to reach statistical relevance suggesting extra time in needed for the physiological effects of increased fibrotic gene expression to take effect. The above results demonstrate the timing of not only therapeutic administration but also data collection is critical in bleomycin studies.

Unsurprisingly, there was no difference between untreated MSC and HGF KD MSC administered at day 9. Delayed administration of MSC appears to impair their protective effect when compared to bleomycin treated mice, therefore any detrimental effect to blocking HGF production by MSC could not be established (Fig. 5.4 C&F). These results suggest MSC may not be an ideal candidate for anti-fibrotic therapy as administration of MSC during the onset of fibrosis failed to reduce of reverse the course of the disease.

A. Day 15 x100

PBS + PBS

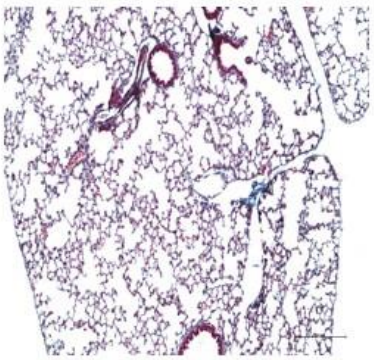

Bleo+ PBS

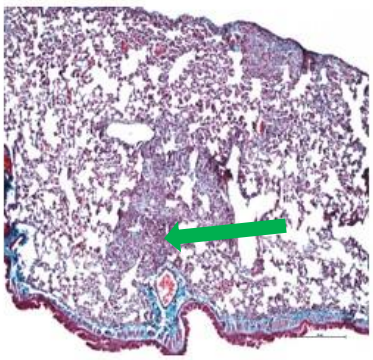

Bleo+ MSC Day 0

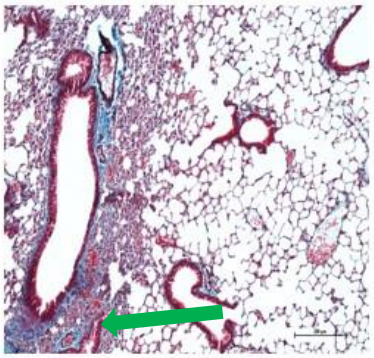

PBS + MSC Day 9

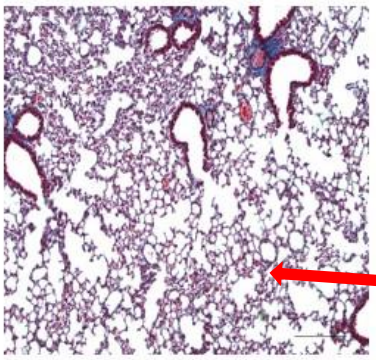

Bleo+ 3T3 Day 0

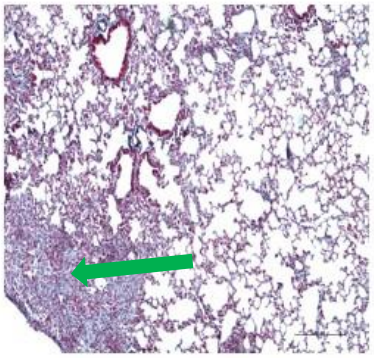

PBS + 3T3 Day 9

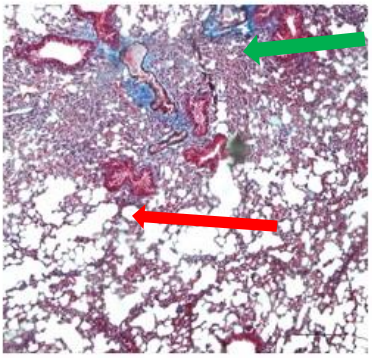

B. Day 21 x100

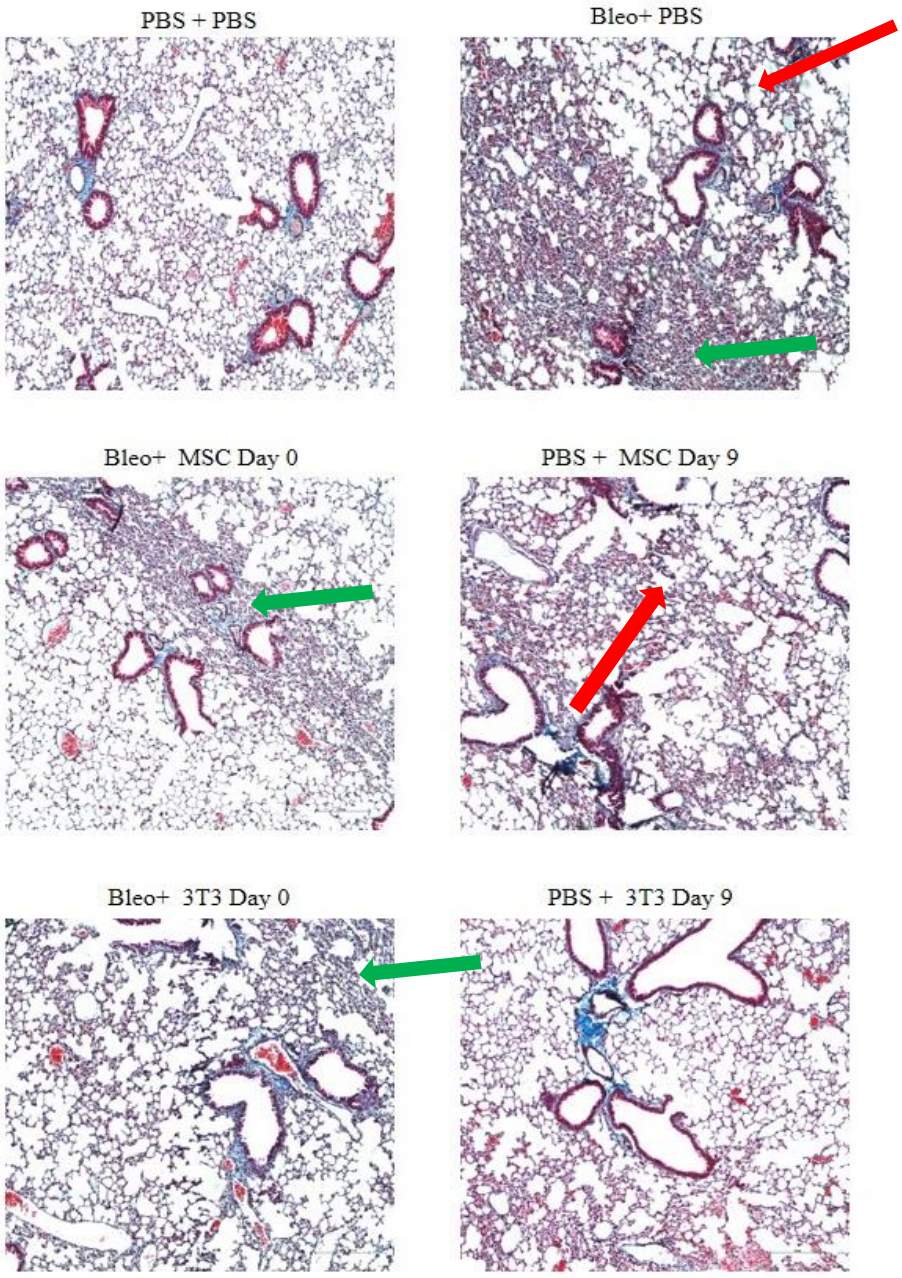
PBS + PBS
Bleo+ PBS
Bleo+ MSC Day 0
PBS + MSC Day 9
Bleo+ 3T3 Day 0
PBS + 3T3 Day 9

C. Day 21 x100

PBS + PBS

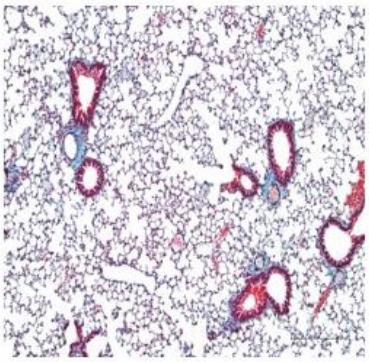

Bleo+ PBS

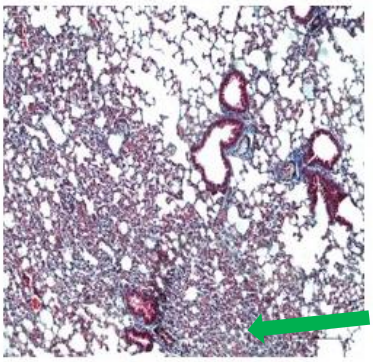

Bleo+ MSC Day 0

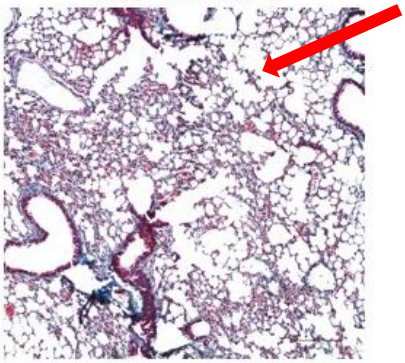

PBS + HGF KD MSC Day 9

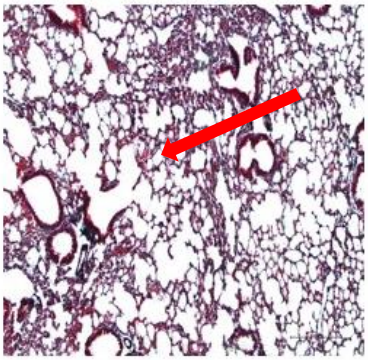

PBS + Non Sil MSC Day 9

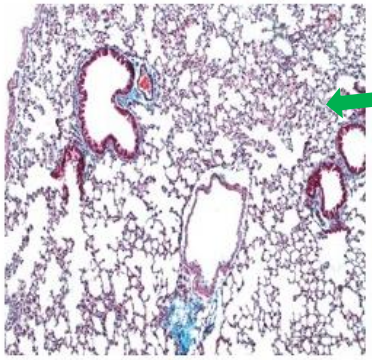

D.

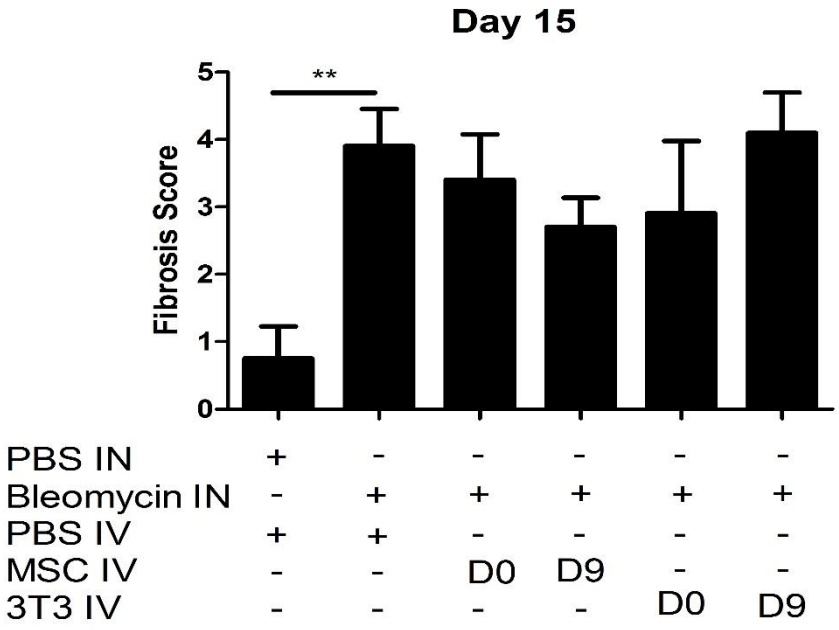
Day 15
Fibrosis Score
**
0
1
2
3
4
5
PBS IN + - - - - -
Bleomycin IN - + + + + +
PBS IV + + - - - -
MSC IV - - D0 D9 - -
3T3 IV - - - - D0 D9

E.

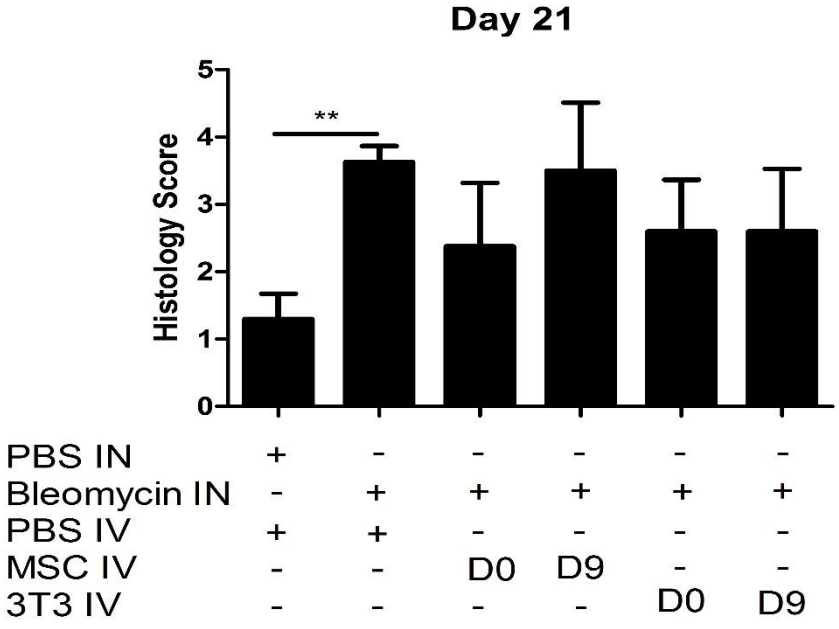
Day 21
Histology Score
**
0
1
2
3
4
5
PBS IN + - - - - -
Bleomycin IN - + + + + +
PBS IV + + - - - -
MSC IV - - D0 D9 - -
3T3 IV - - - - D0 D9

F.

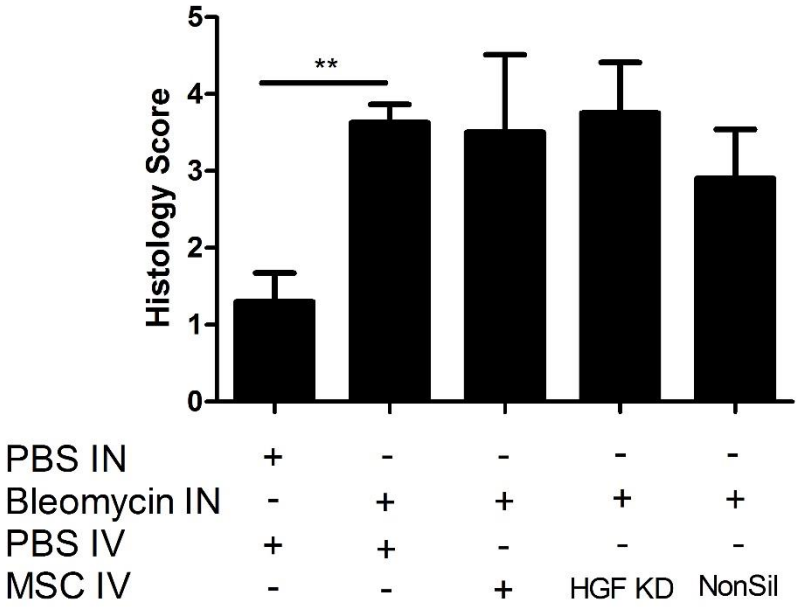

Figure 5.4 MSC administration improves lung pathology. Representative images of transverse lung pathology (magnification x100) from bleomycin treated mice at day 15 (A) and day 21 (B&C). MSC or control 3T3 cells were administered by IV either on day 0 or day 9 (A&B). HGF KD MSC and non-silencing control MSC were administered by IV on day 9 (C). Airway fibrosis was detected by trichrome staining for collagen deposition. Fibrotic masses are indicated by the green arrows, thickening septae are indicated by red arrows. Histological scoring was performed by at least 2 researchers and scores are an average of sections from 5 animals (D, E, F).

A.

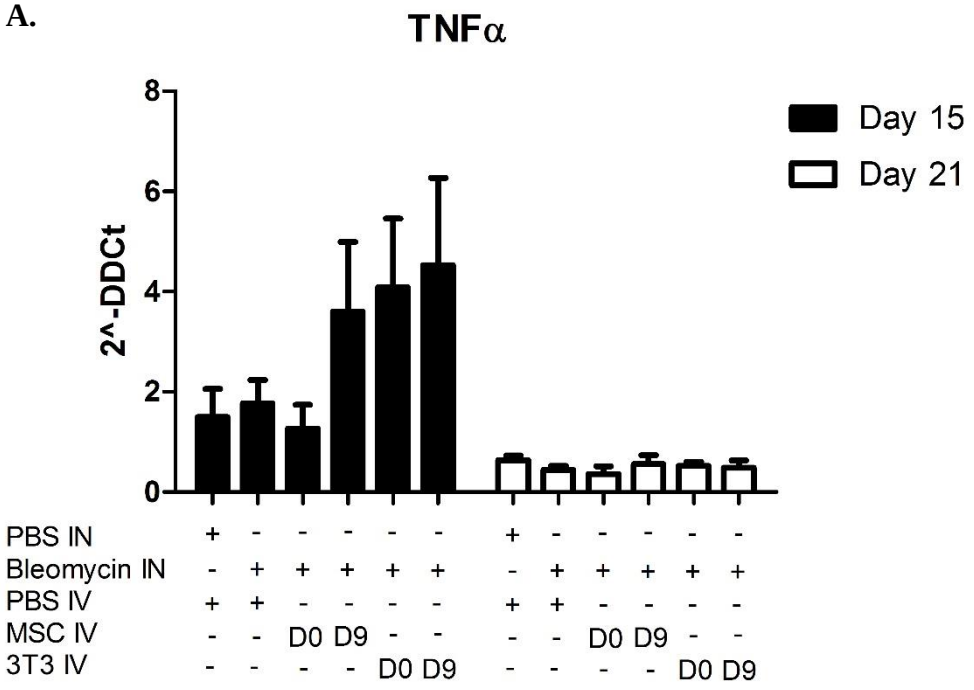
TNFα
2^-DDCt
8
6
4
2
0
Day 15
Day 21
PBS IN + - - - - - + - - - - -
Bleomycin IN - + + + + + - + + + + +
PBS IV + + - - - - + + - - - -
MSC IV - - D0 D9 - - - - D0 D9 - -
3T3 IV - - - - D0 D9 - - - - D0 D9

B.

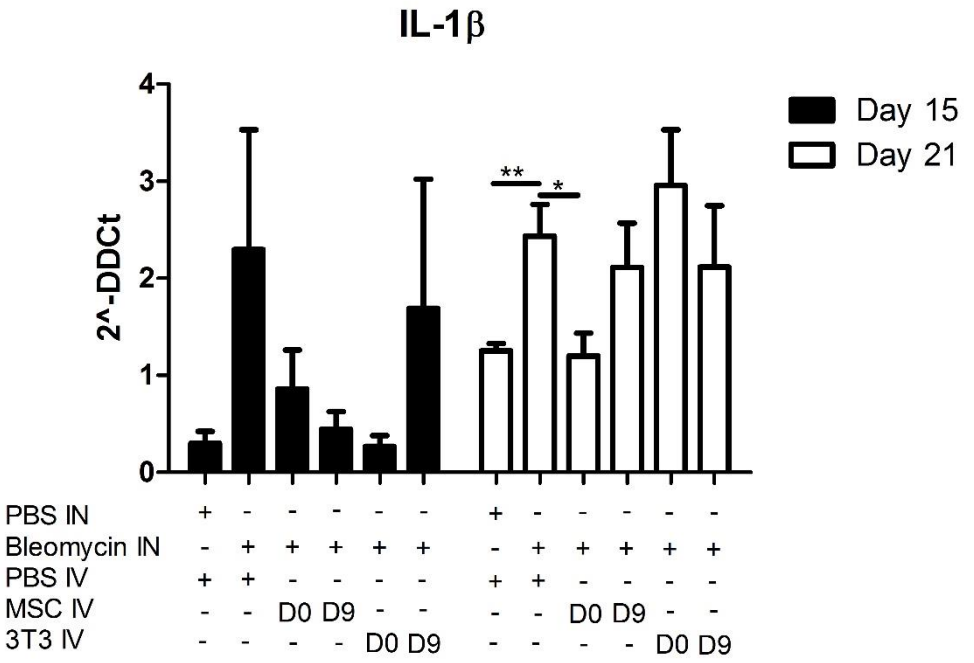
IL-1β
2^-DDCt
4
3
2
1
0
**
*
Day 15
Day 21
PBS IN + - - - - - + - - - - -
Bleomycin IN - + + + + + - + + + + +
PBS IV + + - - - - + + - - - -
MSC IV - - D0 D9 - - - - D0 D9 - -
3T3 IV - - - - D0 D9 - - - - D0 D9

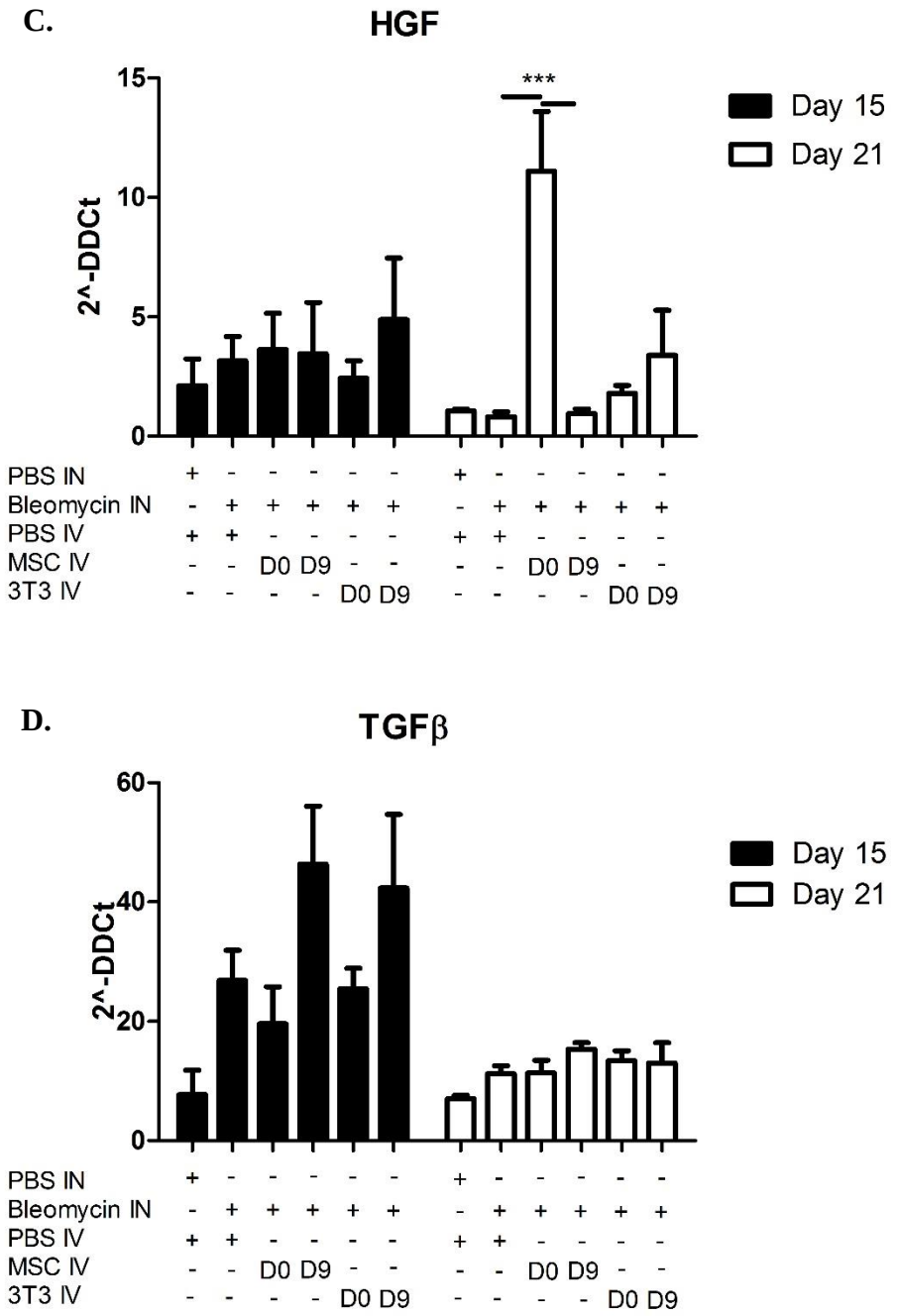

Fig 5.5 Real Time PCR on Lung samples of Bleomycin treated mice at day 15 and day 21. C57BL/6 mice were treated with bleomycin by IN. 5 mice were sacrificed on day15 and day 21 and the lungs were processed for RNA isolation. Following cDNA synthesis, real time PCR was run for selected inflammatory (A&B) or fibrotic (C&D) markers.

5.6 Summary

In this chapter allogeneic MSC were systemically administered to bleomycin treated mice on day 0 resulting in improved pathology. This was most evident in a reduction of collagenous plaque deposition, reduction in the thickness of alveolar septum and preservation of lung architecture. These observations were evident following administration of either allogeneic or syngeneic MSC. Treatment of mice with allogeneic MSC had adverse effects on healthy mice.

A time course study delineating the onset of inflammation and that of fibrosis following administration of bleomycin allowed for more accurate conclusions to be drawn about the role of MSC as a prophylactic or a therapeutic treatment. Previous work from chapter 3 showed the importance of MSC in maintaining a regulatory phenotype resulting in a reduction in inflammation. MSC were also shown to inhibit the proliferation and activation of fibroblasts while promoting re-epithelialisation. When the potential of these phenomena were examined in vivo, MSC administered at day 9, the onset of a fibrotic milieu, were shown to not be as effective as MSC administered at day 0. This interesting data provided a strong basis for MSC in treatment of early onset inflammation, however elucidation of benefits in delayed treatment will require further study.

Taken together these results achieved the aims set forth at the beginning of the study. Analysis of the bleomycin model determined the optimum time points for administration of therapeutics with a view to treatment of inflammation or fibrosis. MSC were shown to effectively reduce pathology, reduce inflammatory cytokines and increase levels of HGF but not when administration is delayed. For this reason the potential benefits of HGF produced by MSC could not be determined in knockdown

studies, as HGF KD MSC were delivered at day 9. A correlation could be made between the benefits seen with early MSC treatment and the subsequent increase in HGF levels. Despite this, and considering human patients will have pre-existing fibrosis, MSC are not likely to be a suitable candidate in anti-fibrotic therapies where fibrosis is established.

Chapter 6

Discussion

The present study sought to understand exactly how MSC mediate their positive effects in disease systems. The specific aims were to discover the contact dependent signal through which MSC modulate the responses of immune cells, namely T cells and DC. Various technologies and approaches such as neutralising antibodies, siRNA, and shRNA knockdown were employed to investigate potential key mechanisms of action in MSC. These techniques were also used to determine the effects of MSC paracrine signalling on pulmonary cells, with an aim to examine MSC mechanisms of action *in vivo.* The bleomycin model of fibrosis was investigated and refined to more accurately represent therapeutic intervention. Knowledge gained about MSC modulation of immunity and influence over pulmonary cells *in vitro* was employed to establish the efficacy of MSC as a cellular therapy in fibrosis.

A range of studies have identified the soluble factors involved in MSC suppression of immune cell functions. TGFβ and PGE2 play a role in the regulation of T cell proliferation, development and the expansion of a Treg population (English *et al.*, 2007, English *et al.*, 2009, Ge *et al.*, 2010, Nemeth *et al.*, 2010). PGE2 is also involved in MSC regulation of mast cell migration and NK cell proliferation (Brown *et al.*, 2011, Spaggiari *et al.*, 2006, Su *et al.*, 2011), while IL-6 plays an important role in suppression of DC maturation (Djouad *et al.*, 2007). Despite the obvious importance of soluble factors, some of these publications describe a role for contact signalling, with transwell and conditioned media (CM) experiments failing to reproduce the results observed in co-culture systems (English *et al.*, 2009, Spaggiari *et al.*, 2006). These seemingly conflicting findings suggest either a sequential or synergistic role for contact and soluble factors in MSC immunomodulation. However, large gaps remain in our knowledge of the contact dependent mechanisms involved in MSC signalling.

Notch signalling is involved in many cell fate decisions (Furukawa *et al.*, 2000, Hoyne *et al.*, 2000, Hellstrom *et al.*, 2007), displaying wide expression across numerous immune cells including MSC. What made Notch signalling an interesting candidate in MSC immunomodulation was its involvement in T cell regulation (Yvon *et al.*, 2003, Samon *et al.*, 2008) and DC maturation (Cheng *et al.*, 2003, Bugeon *et al.*, 2008). Global inhibition of Notch signalling *in vitro* by GSI resulted in a reduction of TGFβ induced FoxP3 expression in T cells and reduced their ability to supress allogeneic proliferation (Samon et al., 2008). *In vivo,* GSI delivery resulted in autoimmune hepatitis like symptoms associated with dysfunctional TGFβ signalling (Samon *et al.*, 2008). Over expression of Jagged 1 in EBV-lymphoblastoid B cells (LCLs) led to reduced production of IFNγ, IL-2 and IL-5 by T cells with increased expression of TGFβ, indicating a regulatory phenotype (Yvon *et al.*, 2003). These results suggested that MSC signalling through Notch ligands and receptors could have regulatory effects on T cells, with a strong indication of an important role for Jagged 1. Interestingly a similar story was observed in DC, when isolated from Notch 1 deficient mice they displayed a reduced maturation profile, indicating a role for Notch signalling in DC maturation (Cheng et al., 2003). A specific role was also demonstrated through over expression studies, resulting in accumulation in immature DC precursors (Cheng *et al.*, 2003).

The data presented in chapter 3 demonstrated that allogeneic murine bone marrow derived MSC suppress both T cells and DC through the Notch signalling pathway, specifically the Notch ligand Jagged 1. Global inhibition of Notch signalling using GSI and targeted inhibition of Jagged 1 signalling resulted in abrogation of MSC mediated suppression of DC maturation, antigen presentation and regulatory T cell expansion. While disruption of Jagged 1 signalling was sufficient to impede MSC

expansion of Treg cells, soluble factors partially compensated for the absence of a cell contact signal on DC. In addition to a successful Notch signal, MSC inhibition of DC maturation and antigen presentation required a soluble factor, IL-6, as shown using a neutralisation approach. Thus far, studies into MSC inhibition of DC function have focused on either contact signalling or soluble factors, stating a requirement for cell-cell contact but not identifying the ligand involved. The data herein is the first to identify and demonstrate the requirement of both cell contact signalling, in the form of Jagged 1 and the soluble factor IL-6. DC that encountered MSC displayed a "semi-mature" phenotype capable of inhibiting antigen specific T cell proliferation. These DC were also capable of Treg cell induction. Though the up-regulation of a Treg population is a known consequence of tolerogenic DC and T cell co-culture, this is the first time tDC have been shown to induce Treg cells from a null population.

As discussed in Chapter 3, several studies have provided evidence of MSC promoting the up-regulation of the Treg associated transcription factor FoxP3, the resulting accumulation of Treg cells were shown to be functional both *in vitro* (English *et al.*, 2009) and *in vivo* (Ge *et al.*, 2010, Kavanagh and Mahon, 2011). The present study, while also demonstrating the up regulation of FoxP3 expressing cells, addressed the as yet unresolved issue of MSC expansion over MSC induction of a Treg population. Cell sorting techniques allowed the removal of all $CD25^{+}FoxP3eGFP^{+}$ cells from a naïve $CD4^{+}$ population. Subsequent co-culture with MSC proved MSC are incapable of inducing Treg cells from a null population in this system, rather they support the expansion of a pre-existing population. This novel result has important implications for MSC use in cell therapy. The efficacy of MSC in diseases associated with depleted levels of Treg such as autoimmune hepatitis may be reduced (Vierling, 2011). A recent study by Kavanagh *et al.* elegantly

demonstrated the significance of MSC expansion of Treg in an *in vivo* model of allergic airway inflammation. MSC were shown to reduce lung pathology and cell infiltration through expansion of Treg, an effect that was abrogated when Treg populations were depleted (Kavanagh and Mahon, 2011).

MSC interactions with DC are now widely understood to produce a "tolerogenic" DC (tDC); (Beyth *et al.*, 2005, Bugeon *et al.*, 2008, Morelli and Thomson, 2007, Nauta *et al.*, 2006). This phenomenon was also investigated in Chapter 3 by examining OVA driven proliferation of DO11.10 $CD4^+$ T cells. DC that had encountered MSC (MSC educated DC) demonstrated lower expression of MHC Class II and CD86 on the cell surface and had a tolerogenic phenotype, consistent with a tDC population defined by Morelli *et al.* (Morelli and Thomson, 2007). OVA stimulated tDC co-cultured with OVA primed DO11.10 $CD4^+$ T cells, suppressed the antigen driven proliferation of T cells when compared to mature OVA presenting DC. Furthermore the cells were shown to directly induce Treg cells from a null population. It is therefore reasonable to assume that tDC inhibition of T cell proliferation is as a result of Treg induction. This hypothesis is supported by several studies where tDC were shown to up-regulate Treg cells (Ge *et al.*, 2010, Li *et al.*, 2008, Zhang *et al.*, 2009). Though Li *et al.* demonstrated tDC induction of alloantigen specific Treg cells (Li *et al.*, 2008), the finding herein is the first instance of Treg induction by MSC educated DC from a null population. Zhang *et al.* demonstrated similar tDC mediated T cell suppression, however the model used here expanded on this study by demonstrating tDC suppression of antigen specific T cells (Zhang *et al.*, 2009). The practical use of tDC has been demonstrated in an *in vivo* model of kidney transplantation, whereby the infusion of tDC improved graft tolerance, decreased donor T cell proliferation and increased the levels of $CD25^+FoxP3^+$ cells in the donor

spleen (Ge *et al.*, 2009). Taken together these observations suggest a complementary approach to MSC immunomodulation. MSC induce a regulatory tDC population, capable of suppressing T cell proliferation and inducing Treg cells *in vitro.* Additionally, MSC in turn promote the expansion of Treg cells maintaining an immunosuppressive environment.

The precise mechanisms underlying MSC modulation of T cells and DC were investigated in this study, initially employing global suppression of Notch signalling, before determining the exact ligand utilised by MSC. An essential role for cell contact in murine MSC signalling to T cells was established initially by Krampera *et al.* (Krampera *et al.*, 2003). This view was expanded by Selmani *et al.* and English *et al.*, whereby a requirement for cell contact between MSC and T cells was confirmed, while observing a non-redundant role for soluble factors. (Selmani *et al.*, 2008, English *et al.*, 2009). Selective inhibition of TGFβ and PGE2 demonstrated their role in MSC expansion of Treg cells. Transwell experiments had determined a role for cell-cell contact in this system (English *et al.*, 2009). As mentioned previously, the Notch family of receptors and ligands presented interesting candidates in MSC cell-cell signalling. They were shown here to be widely expressed by both MSC and T cells, while previous work by the Mahon lab showed they were also expressed by DC (L. Tobin, PhD Thesis NUI Maynooth). Liotta *et al.*, found that the ability of MSC to inhibit T cell proliferation was significantly reversed when Notch signalling was interrupted through the addition of a Notch signalling inhibitor (DAPT) or a Jagged-1 neutralisation antibody. In support of these findings, this study found suppression of Notch signalling by GSI resulted in a reduction of MSC driven expansion of Treg cells. More recently a study by Del Papa *et al.* identified Notch 1 on $CD4^+$ cells as the principle receptor involved in MSC recruitment of inducible Treg (iTreg). Based on

these findings, Del Papa *et al.* make a number of incorrect assumptions foremost among these were: the iTreg used there were isolated by CD25 enrichment, whereas CD25 is more commonly associated with natural Treg. Del Papa also assumed blockade of Notch signalling by GSI on the T cell resulted in iTreg recruitment. However, MSC also express Notch receptors and therefore cannot be eliminated from influencing the outcome. Although it is conceivable that MSC signal through the Notch 1 receptor, a definitive conclusion cannot be drawn from that report (Del Papa *et al.*, 2013).

Jagged 1 was chosen as the principle ligand for investigation, as previously published data using soluble Jagged 1 suggested a strong role in Treg expansion (Yvon *et al.*, 2003) and induction of tolerogenic DC (Bugeon *et al.*, 2008). Yvon *et al.* demonstrated that antigen presenting B cells overexpressing Jagged-1 were capable of reducing IFNγ, IL-5 and IL-2 secretion from naïve T cells, while up regulating the production of TGF-β, a soluble factor associated with a regulatory T cell phenotype (Yvon *et al.*, 2003). Whereas DC maturation with soluble Jagged 1 resulted in increased expression of IL-10 and IL-2, and DC promoted the proliferation of $CD4^+CD25^+$ T cells (Bugeon *et al.*, 2008). A number of approaches were tested to inhibit MSC signalling through Jagged 1. Initial failure with neutralising antibodies and the limited duration of siRNA silencing led to adoption of a lentiviral shRNA knockdown strategy. This sophisticated approach allowed for the production of lentiviral particles containing shRNA constructs against Jagged 1. Once infected with the virus, the cell's own transcription machinery would produce Jagged 1 shRNA to maintain continuous knockdown of the ligand. MSC infected with the lentivurus were examined for mRNA and protein expression of Jagged 1. They were also characterised to ensure they maintained their unique cell surface expression profile

and trilineage differentiation potential. Co-culture experiments using Jagged 1 knocked down MSC and $CD4^+$ T cells resulted in abrogation of Treg expansion by MSC. The considerable decrease in $CD25^+FoxP3eGFP^+$ strongly suggested that MSC promotion of Treg expansion occurs through Jagged 1 signalling. A caveat to interpreting these results lies in the non-silencing control which showed knockdown of Jagged 1 both at an mRNA, and a protein level. Based on these finding the remaining Notch ligands were examined for reduced expression. Jagged 2 is not expressed by MSC but Delta like ligand 1 expression remained unaffected by either Jagged 1 shRNA or non-silencing control lentiviral transduction. This aberrant reduction in Jagged 1 could be attributed to plasmid DNA contained in the lentiviral units stimulating the TLR3 receptor expressed by MSC. TLR3 signalling on MSC results in down regulation of Jagged 1 (Liotta *et al.*, 2008). Given that TLR3 stimulation did not affect the expression of other Notch ligands on MSC, these results still strongly suggest Jagged 1 is the contact signal between MSC and T cells in Treg expansion. Further evidence to support a role for Jagged 1 in MSC signalling was demonstrated using the Notch inhibitor DAPT and a Jagged 1 neutralising antibody, where inhibition of signalling resulted in abrogation of MSC suppression of T cell proliferation. Novel results described herein suggest neutralisation of Jagged 1 signalling in the previously mentioned study impeded MSC expansion of Treg leading to unsuppressed proliferation of T cells. Taken together these results indicate a definitive role for Jagged 1 in MSC expansion of Treg cells.

The relevance of Notch signalling in MSC expansion of Treg cells and the expression of Notch receptors and ligands on DC (L. Tobin, PhD thesis) suggested a further role for the pathway in MSC modulation of DC. Several studies have identified a role for Notch signalling in DC maturation (Cheng *et al.*, 2007, Cheng *et al.*, 2003,

Weijzen *et al.*, 2002). Previous work by the Mahon group used GSI to demonstrate a role for Notch in MSC inhibition of DC maturation. This study furthered this work by proving GSI mediated inhibition of Notch signalling also resulted in suppression of MSC induction of tolerogenic DC. OVA stimulated DC cultured in the presence of MSC and GSI, no longer possessed the ability to promote T cell proliferation in an antigen driven model of proliferation. This suggested that the Notch signalling pathway was involved in MSC induction of a tolerogenic DC population. These findings are consistent with a study by Li *et al.*, where DC matured in the presence of MSC and the Notch inhibitor DAPT resulted in increased T cell proliferation and IFNγ production (Li *et al.*, 2008). However, the results described here are more relevant, given the inhibition of antigen specific T cell proliferation.

Co-culture of DC with Jagged 1 knocked down MSC only partially reversed MSC induced inhibition of maturation, suggesting Jagged-1 is involved in MSC signalling to DC, but there are other contributors to this effect, such as soluble factors. In support of this hypothesis, MSC derived IL-6 was shown to play a crucial role in the inhibition of DC differentiation (Djouad *et al.*, 2007, English *et al.*, 2008). The addition of an IL-6 neutralising antibody in conjunction with Jagged-1 knock down MSC to DC co-culture experiments resulted in restoration of the maturation markers, MHC Class II and CD86 to levels equivalent to those seen in the mature DC. From these results it is reasonable to conclude for the first time that direct cell contact through Notch/Jagged-1 and the release of IL-6 were required for MSC to achieve the full modulatory effect on DC maturation. A recent study by Zhang and colleagues, further supports the importance of the Notch signalling pathway in immune regulation. Using siRNA techniques, tDC regulation of lymphocyte proliferation was demonstrated to be dependent on Jagged 2 signalling (Zhang *et al.*, 2009). Taken

together these results complete the story of Notch signalling in MSC modulation of T cells and DC. Jagged 1 expression, as well as IL-6 production by MSC induces a regulatory tDC. These cells in turn reduce lymphocyte proliferation in a Jagged 2 dependent manner, while also inducing a Treg population. MSC signalling, again through Jagged 1, promotes the expansion of said Treg cells. These observations have important ramifications for the Notch signalling family as potential therapeutic targets in MSC immunomodulation. Figure 6.1 illustrates the interplay between MSC, DC and T cells, it also depicts the role of contact and soluble factors in this system.

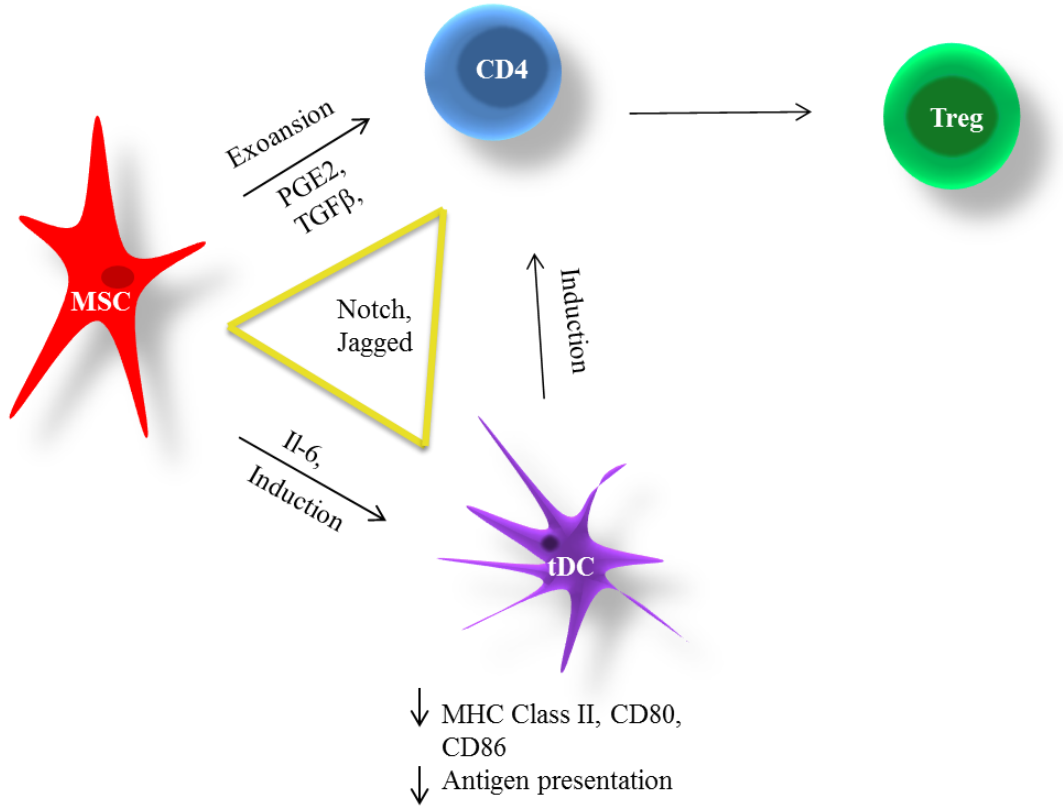

Fig. 6.1 The role of Notch signalling in MSC immunomodulation. Jagged 1 stimulation of the Notch receptor on T cells and DC by MSC leads to expansion of Treg cells, as well as inhibition of DC maturation and DC presentation of antigen. Soluble factors are involved in both processes. TGFβ and PGE2 play an important role in MSC expansion of Treg, while IL-6 release from MSC works in conjunction with Jagged 1 to achieve MSC modulation of DC. tDC suppression of lymphocyte proliferation occurs in a Jagged 2 dependent manner (Zhang *et al.*, 2009).

The immunological influence of MSC does not lie solely in immune cell suppression. In chapter 4, MSC manipulation of pulmonary cells was examined *in vitro* to explore potential benefits that might be exploited in an *in vivo* model of pulmonary fibrosis. The lung is one of the first sites MSC can be detected after IV administration in mice (Gao *et al.*, 2001). Some studies in pulmonary disease models suggest that MSC mediate their effects through engraftment in the lung and differentiation to alveolar cells, resulting in repair of damaged tissue (Ortiz *et al.*, 2003, Rojas *et al.*, 2005). Conversely, it has been proposed that MSC mediate repair through cell education and trophic manipulation of the micro-environment (Kotton *et al.*, 2005, Phinney and Prockop, 2007, Duffield and Bonventre, 2005, Caplan and Dennis, 2006). Given the heterogeneity of *in vitro* cultured MSC, the concepts of regeneration and trophic repair may not be mutually exclusive, (Phinney and Prockop, 2007, English *et al.*, 2013). Following the data generated in Chapter 3, Chapter 4 examined MSC in the context of paracrine signalling and cell manipulation. MSC conditioned medium (CM) was shown to have dynamic effects pertaining to fibrotic therapy, encouraging the migration and proliferation of alveolar epithelial cells while suppressing the activation and proliferation of pulmonary fibroblasts.

Initial data from Chapter 4 served to address scepticism with regards to distinguishing MSC from generic fibroblasts (Haniffa *et al.*, 2009). Characterisation was performed on primary lung isolated fibroblasts. While cell surface expression was the same as MSC, pulmonary fibroblasts did not differentiate into bone, fat or cartilage. In contrast, results from Haniffa *et al.*, demonstrated the trilineage differentiation potential of dermal fibroblasts. However, this may be a result of pulmonary versus dermal origin or contamination of such cultures with dermal MSC (Haniffa *et al.*, 2007). Finally, MSC and fibroblasts were examined for expression of

αSMA and vementin, both are cytoskeletal components and are expressed by MSC, however, up-regulation of αSMA is associated with the activated form of fibroblasts, myofibroblasts. The population of fibroblasts isolated in this study were not stimulated and did not express αSMA. Taken together these results distinguish MSC from pulmonary fibroblasts in this system.

Several studies have provided evidence to suggest the growth factor HGF and the arachidonic acid metabolite PGE2 play significant roles in maintaining the course of normal wound healing. Reduction in PGE2 levels in fibrotic human lung is associated with increased alveolar epithelial cell apoptosis and reduced sensitivity of fibroblasts to Fas ligand mediated apoptosis (Maher *et al.*, 2010). COX2 deficient mice also demonstrate an increased susceptibility to pulmonary fibrogenesis as a result of diminished PGE2 levels (Bonner *et al.*, 2002, Hodges *et al.*, 2004). HGF is a homeostatic mediator known to exert protective effects on epithelial cells (Matsumoto and Nakamura, 1993). Bleomycin induced lung injury in mice has been linked to an imbalance in the levels of pro-HGF and HGF (Phin *et al.*, 2010). Administration of the growth factor *in vivo* is also associated with attenuation of collagen deposition in bleomycin treated C57/BL6 mice (Dohi *et al.*, 2000). MSC have previously been shown to constitutively produce PGE2 both in human (English et al., 2009, Ryan et al., 2007) and in murine MSC (L. Tobin, unpublished data). TNFα stimulation of MSC increased release of HGF, a cytokine highly expressed in pulmonary fibrosis (Ortiz *et al.*, 1998). These observations suggested a pivotal role for HGF and PGE2 in MSC treatment of pulmonary fibrosis.

Replicating pulmonary fibrosis for *in vitro* study presents a difficult challenge for researchers. A variety of studies have examined various roles for MSC in pulmonary fibrosis *in vivo*. However, there is a void in our understanding of the basic

effects of MSC on individual cell types in this system. In order to establish a role for MSC *in vivo*, pulmonary cells were examined for beneficial effects following MSC treatment in functional *in vitro* assays Several studies have previously examined fibroblast migration using a scratch model of wound healing (Walter *et al.*, 2010, Smith *et al.*, 2010, Fronza *et al.*, 2009). Walter *et al.* used an immortalised cell line of dermal fibroblasts to demonstrate accelerated migration in response to MSC CM (Walter *et al.*, 2010). Following on from this work, data from chapter 4 demonstrated MSC CM significantly encouraged the migration of primary pulmonary fibroblasts. Alveolar epithelial cells were also assessed, with MSC CM promoting their migration into the site of damage in the *in vitro* scratch model of wound healing. In order to confirm reconstitution of the wound area was a result of migration as opposed to proliferation, both cell types were examined for tritiated thymidine uptake. While MSC CM promoted the proliferation of alveolar epithelial cells, fibroblasts proliferation was significantly inhibited. These results demonstrate MSC favour the migration and proliferation of epithelial cells and while MSC encourage the migration of fibroblast they also inhibit fibroblast proliferation. Closer examination of this system also revealed MSC CM reduced TGFβ induced activation of fibroblasts to myofibroblasts, determined by αSMA expression. Contrary to these findings, a study by Smith *et al.* showed paracrine signalling by MSC increased the migration and proliferation of dermal fibroblasts (Smith *et al.*, 2010). However, Smith and colleagues used dermal fibroblast in their study which may react differently to MSC CM, the data herein however, was obtained using primary lung fibroblasts an approach more relevant to pulmonary fibrosis studies.

Taken together these results support a role for MSC in pulmonary repair and treatment of fibrosis. Fibroblasts play a vital role in wound healing, migrating to the

site of damage where they are involved in wound contraction and closure. Here MSC were shown to actively promote fibroblast migration while also controlling the level of proliferation and activation. Pathogenesis is associated with the disproportionate activation of fibroblasts leading to excessive collagen deposition. Here MSC are shown for the first time to regulate all three major aspects of fibroblast homeostasis allowing for normal wound repair. Additionally MSC promoted both the migration and proliferation of alveolar epithelial cells, thus consolidating their potential role in tissue repair by encouraging re-epithelialisation.

Data from a number of studies into fibroblast proliferation suggested a role for PGE2 (Boyle *et al.*, 1999, Moore *et al.*, 2003, Pan *et al.*, 2001). *In vitro* studies of alveolar epithelial cells demonstrated that inhibition of fibroblast proliferation was mediated through PGE2 signalling (Moore *et al.*, 2003). Here, MSC production of PGE2 was blocked using a COX2 inhibitor (NS398), CM from NS398 treated MSC was no longer capable of inhibiting fibroblast proliferation, with proliferation reverting to basal levels observed with conventional medium. This novel data establishes MSC production of PGE2 as a potential therapeutic candidate in treatment of early fibrosis. In an effort to explore MSC potential in repair of established fibrosis, the soluble factor responsible for MSC induced epithelial expansion was determined. As previously discussed, HGF presented a likely candidate for MSC modulation of epithelial cells. Using the shRNA technologies described in Chapter 3, HGF expression was knocked down in MSC. As before, lentiviral transduction of MSC did not influence their defining characteristics, but significantly lowered secretion of HGF. CM collected from HGF knockdown MSC was cultured with epithelial cells, the results of which demonstrated an essential role for HGF in MSC induced proliferation. Similar results were observed in fetal intestinal epithelial cells where

HGF secreted by MSC, enhanced their viability and proliferation (Weil *et al.*, 2009). The aim of Chapter 4 was to identify potential therapeutic roles for MSC *in vitro* for further examination *in vivo.* This goal was achieved with the novel finding that MSC regulate the homeostasis of fibroblasts, reducing proliferation in a PGE2 dependent manner. They also promoted the migration and proliferation of epithelial cells through secretion of HGF, suggesting a role in both prevention and repair of pulmonary fibrosis. Figure 6.2 illustrates the effects of MSC CM on epithelial cells and fibroblast in the setting of pulmonary fibrosis.

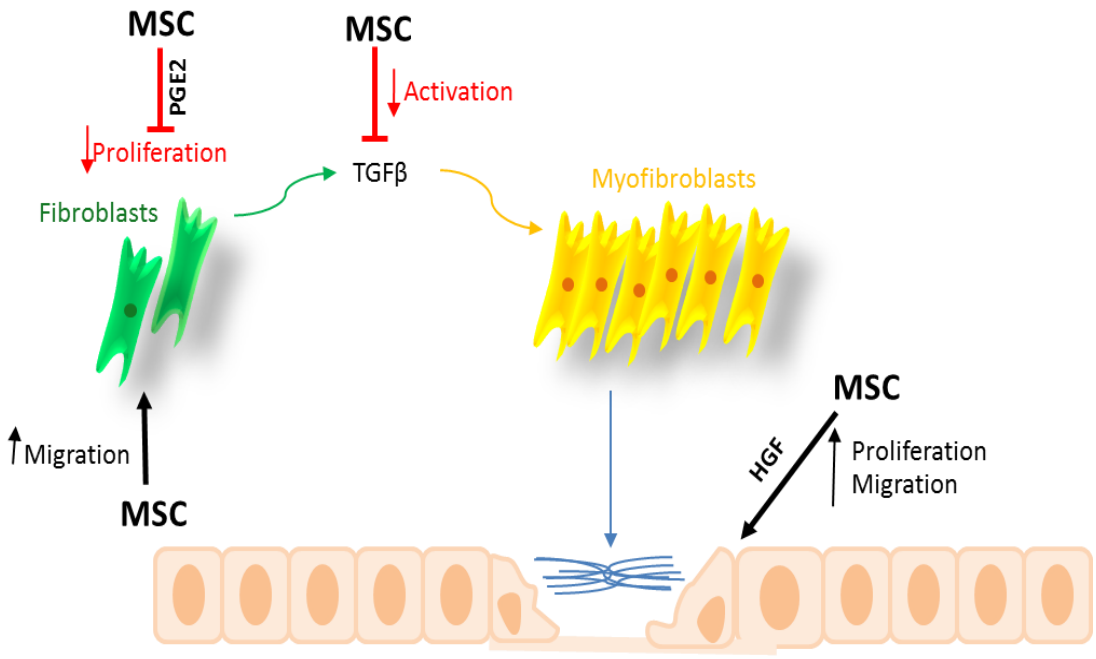

Fig. 6.2 The effect of MSC CM on pulmonary cells. MSC CM encourage the migration of alveolar epithelial cells and fibroblasts to the site of damage, but inhibit fibroblast proliferation in a PGE2 dependent manner. MSC CM also inhibit TGFβ driven activation of fibroblast to myofibroblasts. MSC CM encourages the proliferation of alveolar epithelial cells in a HGF dependent manner.

The capacity of MSC to therapeutically manipulate the immune system and pulmonary cells in order to prevent or repair fibrotic damage to the lung was examined in Chapter 5. The bleomycin model of pulmonary fibrosis is a well-established murine model of fibrotic disease, several studies involving MSC treatment have already been documented (Moodley *et al.*, 2003, Ortiz *et al.*, 2007, Ortiz *et al.*, 2003, Rojas *et al.*, 2005). Early studies looked at MSC with a view to encourage reconstitution of the lung through engraftment (Ortiz *et al.*, 2003, Rojas *et al.*, 2005), later MSC were studied for their immunomodulatory properties. Ortiz *et al.* demonstrated *in vitro* that MSC CM could inhibit the proliferation of an IL-1α dependent T cell line through production of an IL-1 receptor antagonist. MSC CM was also shown to inhibit macrophage production of TNFα through the same mechanism. Following this, MSC administration to bleomycin treated mice was shown to be more effective at reducing IL-1 and TNFα in lung mRNA and BAL fluid, than recombinant IL-1 receptor antagonist. These results suggest MSC immunomodulatory properties, demonstrated in Chapter 3, could play a beneficial role in MSC treatment of fibrosis. *In vitro* studies in Chapter 4 established a definitive role for MSC in modulation of pulmonary cells, however targeting inflammation associated with fibrosis offers a further target for MSC therapy.

A pilot study was used to confirm bleomycin induced damage and the benefits of MSC treatment, as the model was previously untested in the Mahon lab. There is variability in the route of administration in literature pertaining to bleomycin, be it intravenous (IV);(Lawson et al., 2005), intratracheal (IT)(Chaudhary et al., 2006, Iyer et al., 1999), or subcutaneous (SC) (Ortiz et al., 1998, Yaekashiwa et al., 1997). IV administration is believed to more accurately mimic chemotherapeutic administration with slower onset of fibrosis, typically 6-8 weeks. Direct administration into the lung

results in faster onset and is more efficient for studying mechanisms of pathogenesis, but can result in variable distribution of fibrotic lesions (Lawson *et al.*, 2005). Unpublished work by the Mahon lab, used crystal violet to demonstrate IN inhalation results in extensive distribution of a liquid inoculum. For the purposes of this study, IN administration was selected for delivery of bleomycin, followed by IV administration of MSC. This pilot study demonstrated systemic delivery of MSC can significantly improve airway pathology from bleomycin induced damage and collagen deposition. The effect was only significant after day 28 (Fig 5.1), an unsurprising result given the predicted peak of fibrotic pathology occurs from day 21 to day 28. Importantly, allogeneic MSC administration to PBS treated mice had no adverse effect on the architecture of the lung, with histological scoring similar to that of mice given IV PBS (Fig. 5.1). This results bears particular significance to the field of cellular therapy where adverse side effects to allogeneic MSC administration would severely diminish the attractiveness of MSC as a potential therapeutic.

A small study examining the efficacy of allogeneic and syngeneic MSC was examined at day 28 for improvement in pathology. Previous *in vivo* studies indicated both allogeneic and syngeneic MSC offer effective treatment in a multitude of disease model systems (Kavanagh and Mahon, 2011, Choi et al., 2013). No difference was detected between C57BL/6 MSC and BALB/c MSC, in all instances they reduced inflammatory cytokines to levels comparable with PBS treatment. The same was true of the fibrotic markers TGFβ and fibronectin. The failure to reach significance in this system was accounted for by the collection of lungs at day 28. Bleomycin is a resolving model of pathogenesis (Moore and Hogaboam, 2008), therefore is it conceivable that inflammatory and fibrotic mRNA levels would not be as high at day 28 compared to an earlier time point. These observations could prove limiting for the

success of further experiments. Therefore, a time course study was used to determine the onset of fibrosis and thus the optimum time for recovery of lungs. This study also offered the opportunity to establish a time frame of maximal inflammatory signalling, and onset of fibrosis. The bleomycin model of fibrosis is now known to divide into two distinct phases. An initial inflammatory phase brought about by immune cell infiltration to the site of damage, followed by a fibrotic phase resulting from fibroblast recruitment and proliferation (Moeller *et al.*, 2008). The timing of administration of potential therapeutics is essential for distinguishing between preventative anti-inflammatory therapy and anti-fibrotic therapy. Particular attention was given to TNFα, IL-1β, and TGFβ as these markers play well defined roles in fibrosis (Moodley et al., 2003, Ortiz et al., 2007, Ortiz et al., 1998, Chaudhary et al., 2006). HGF levels were also determined for the purposes of distinguishing the growth factor as a potential target in MSC therapy. Real time analysis showed a significant increase in the two principle cytokines, TNFα and IL-1β starting at day 9 and 15 respectively. TGFβ expression significantly increased by day 15, with HGF showing no significant increase or decrease during the study. These results show inflammation beginning marginally before fibrosis, as such day 9 was chosen as an appropriate time point for administration of MSC, as inflammation has been established and the effects of MSC would more accurately reflect treatment of fibrosis.

Data herein demonstrated that delayed delivery of MSC failed to protect the lung architecture from bleomycin induced damage. In comparison to MSC administered on day 0, delayed dosing resulted in significantly lower levels of HGF mRNA in lung tissue collected on day 21. The beneficial effects of HGF outlined in Chapter 4 suggest early administration could result in increased repair and faster migration to the site of damage. A critical observation here was that MSC

administered at day 0 would benefit from earlier stimulation by TNFα, with levels increasing by day 3. As discussed earlier, TNFα stimulation of MSC increases production of HGF and PGE2. Increased PGE2 could reduce the activation and proliferation of fibroblasts alleviating excessive collagen deposition. This theory is supported by reduced levels of IL-1β at day 21 in mice given MSC at day 0 compared to bleomycin treated mice, a result not achieved by MSC administered at day 9. A study by Ortiz *et al.* into the engraftment of MSC in bleomycin induced injury, showed similar results. MSC were administered at day 0 and day 7, but protective effects were only observed from MSC administered directly after bleomycin challenge. A possible explanation given for reduced engraftment was the release of cytokines and mitogens from inflammatory cells, affecting homing of MSC, which could conceivably be reduced by day 7. This hypothesis is not incompatible with the findings here.

One of the aims of Chapter 5 was to refine the bleomycin murine model of fibrosis to more accurately represent therapeutic intervention. This goal was achieved through studying the time course of the model with relation to onset of inflammation and fibrosis. Administration of therapeutics at day 0 is common practice in bleomycin animal models and reports have claimed beneficial results from MSC under these conditions (Moodley et al., 2009, Ortiz et al., 2007, Rojas et al., 2005). However, this study elegantly demonstrates the importance of timing with regards to how MSC are exerting a positive effect. Early administration of MSC improved pathology but not by ameliorating direct fibrosis. Delayed administration had no effect on reducing established fibrosis and was not as effective at reducing inflammation. These results have important implications on future therapeutic candidate studies, with the success of potential anti-fibrotic therapies being determined by their efficacy following

delayed administration in the bleomycin model. The limitations of the bleomycin model were further highlighted in an interesting study by Chaudhary *et al.* The importance of timing in administration of therapeutics was supported using an anti-inflammatory drug and an anti-fibrotic drug. Both drugs showed a reduction in TGFβ and pro-collagen 1 expression following administration at day 0. However, administration at day 10, rescinded the beneficial effects observed with use of the anti-inflammatory drug. This study by Chaudhary and colleagues into pharmacological intervention and the data here using cell therapy changes our understanding of the bleomycin model, demonstrating how the accuracy of *in vivo* testing can be skewed by inappropriate use of an animal model (Chaudhary *et al.*, 2006). A further important observation form this study was the failure to derive meaningful results from HGF KD MSC given at day 9. Evidence from Chapter 4 suggested HGF plays an important role in MSC induced tissue repair. However, the ineffectual nature of delayed dosing in MSC administration meant no meaningful conclusion could be discerned from this aspect of the study. These results reinforce the importance of diligence in animal testing, demonstrating how encouraging results observed *in vitro* do not always translate into beneficial outcomes *in vivo*.

The immunological properties of MSC appear to target inflammation associated with the initial phase of fibrotic disease. A role for MSC has been established in promoting a regulatory environment, encouraging the induction and expansion of anti-inflammatory immune cell phenotypes. Trophic interactions with pulmonary cells also promote the migration and proliferation of epithelial cells, while regulating fibroblast growth and development. *In vivo,* the protective effect of MSC may have far-reaching clinical applications but will depend on the accuracy of timing in administration. This work shows that while MSC exhibit great potential in

treatment of inflammatory based diseases, they failed to achieve the level of repair required to improve the pathology of established fibrosis. This work should influence future animal studies into anti-fibrotic candidates improving the potential for translation in human therapeutics.

Chapter 7

References

AKIRA, S. & TAKEDA, K. 2004. Toll-like receptor signalling. *Nat Rev Immunol,* 4**,** 499-511.

AKIRA, S., UEMATSU, S. & TAKEUCHI, O. 2006. Pathogen recognition and innate immunity. *Cell,* 124**,** 783-801.

AKIYAMA, K., CHEN, C., WANG, D., XU, X., QU, C., YAMAZA, T., CAI, T., CHEN, W., SUN, L. & SHI, S. 2012. Mesenchymal-stem-cell-induced immunoregulation involves FAS-ligand-/FAS-mediated T cell apoptosis. *Cell Stem Cell,* 10**,** 544-55.

ANKRUM, J. & KARP, J. M. 2010. Mesenchymal stem cell therapy: Two steps forward, one step back. *Trends in Molecular Medicine,* 16**,** 203-209.

ARRIBILLAGA, L., DOTOR, J., BASAGOITI, M., RIEZU-BOJ, J. I., BORRAS-CUESTA, F., LASARTE, J. J., SAROBE, P., CORNET, M. E. & FEIJOO, E. 2011. Therapeutic effect of a peptide inhibitor of TGF-beta on pulmonary fibrosis. *Cytokine,* 53**,** 327-33.

ARTAVANIS-TSAKONAS, S., RAND, M. D. & LAKE, R. J. 1999. Notch signaling: cell fate control and signal integration in development. *Science,* 284**,** 770-6.

ATS 2000. American Thoracic Society. Idiopathic pulmonary fibrosis: diagnosis and treatment. International consensus statement. American Thoracic Society (ATS), and the European Respiratory Society (ERS). *Am J Respir Crit Care Med,* 161**,** 646-64.

AUGELLO, A., TASSO, R., NEGRINI, S. M., AMATEIS, A., INDIVERI, F., CANCEDDA, R. & PENNESI, G. 2005. Bone marrow mesenchymal progenitor cells inhibit lymphocyte proliferation by activation of the programmed death 1 pathway. *Eur J Immunol,* 35**,** 1482-90.

BANCHEREAU, J. & STEINMAN, R. M. 1998. Dendritic cells and the control of immunity. *Nature,* 392**,** 245-52.

BATTEN, P., SARATHCHANDRA, P., ANTONIW, J. W., TAY, S. S., LOWDELL, M. W., TAYLOR, P. M. & YACOUB, M. H. 2006. Human mesenchymal stem cells induce T cell anergy and downregulate T cell allo-responses via the TH2 pathway: relevance to tissue engineering human heart valves. *Tissue Eng,* 12**,** 2263-73.

BEYTH, S., BOROVSKY, Z., MEVORACH, D., LIEBERGALL, M., GAZIT, Z., ASLAN, H., GALUN, E. & RACHMILEWITZ, J. 2005. Human mesenchymal stem cells alter antigen-presenting cell maturation and induce T-cell unresponsiveness. *Blood,* 105**,** 2214-9.

BONNER, J. C., RICE, A. B., INGRAM, J. L., MOOMAW, C. R., NYSKA, A., BRADBURY, A., SESSOMS, A. R., CHULADA, P. C., MORGAN, D. L., ZELDIN, D. C. & LANGENBACH, R. 2002. Susceptibility of cyclooxygenase-2-deficient mice to pulmonary fibrogenesis. *Am J Pathol,* 161**,** 459-70.

BOYLE, J. E., LINDROOS, P. M., RICE, A. B., ZHANG, L., ZELDIN, D. C. & BONNER, J. C. 1999. Prostaglandin-E2 counteracts interleukin-1beta-stimulated upregulation of platelet-derived growth factor alpha-receptor on rat pulmonary myofibroblasts. *Am J Respir Cell Mol Biol,* 20**,** 433-40.

BROWN, J. M., NEMETH, K., KUSHNIR-SUKHOV, N. M., METCALFE, D. D. & MEZEY, E. 2011. Bone marrow stromal cells inhibit mast cell function via a COX2-dependent mechanism. *Clinical and Experimental Allergy,* 41**,** 526-534.

BUGEON, L., GARDNER, L. M., ROSE, A., GENTLE, M. & DALLMAN, M. J. 2008. Cutting edge: Notch signaling induces a distinct cytokine profile in dendritic cells that supports T cell-mediated regulation and IL-2-dependent IL-17 production. *J Immunol,* 181**,** 8189-93.

BUHL, A. M., NEMAZEE, D., CAMBIER, J. C., RICKERT, R. & HERTZ, M. 2000. B-cell antigen receptor competence regulates B-lymphocyte selection and survival. *Immunol Rev,* 176**,** 141-53.

CANTOR, H. & WEISSMAN, I. 1976. Development and function of subpopulations of thymocytes and T lymphocytes. *Prog Allergy,* 20**,** 1-64.

CAPLAN, A. I. 1991. Mesenchymal stem cells. *J Orthop Res,* 9**,** 641-50.

CAPLAN, A. I. & DENNIS, J. E. 2006. Mesenchymal stem cells as trophic mediators. *J Cell Biochem,* 98**,** 1076-84.

CASSATELLA, M. A., MOSNA, F., MICHELETTI, A., LISI, V., TAMASSIA, N., CONT, C., CALZETTI, F., PELLETIER, M., PIZZOLO, G. & KRAMPERA, M. 2011. Toll-Like Receptor-3-Activated Human Mesenchymal Stromal Cells Significantly Prolong the Survival and Function of Neutrophils. *Stem Cells,* 29**,** 1001-1011.

CASTROMALASPINA, H., GAY, R. E., RESNICK, G., KAPOOR, N., MEYERS, P., CHIARIERI, D., MCKENZIE, S., BROXMEYER, H. E. & MOORE, M. A. S. 1980. Characterization of Human-Bone Marrow Fibroblast Colony-Forming Cells (Cfu-F) and Their Progeny. *Blood,* 56**,** 289-301.

CELLA, M., SALLUSTO, F. & LANZAVECCHIA, A. 1997. Origin, maturation and antigen presenting function of dendritic cells. *Current Opinion in Immunology,* 9**,** 10-16.

CHAUDHARY, N. I., ROTH, G. J., HILBERG, F., MULLER-QUERNHEIM, J., PRASSE, A., ZISSEL, G., SCHNAPP, A. & PARK, J. E. 2007. Inhibition of PDGF, VEGF and FGF signalling attenuates fibrosis. *Eur Respir J,* 29**,** 976-85.

CHAUDHARY, N. I., SCHNAPP, A. & PARK, J. E. 2006. Pharmacologic differentiation of inflammation and fibrosis in the rat bleomycin model. *Am J Respir Crit Care Med,* 173**,** 769-76.

CHEN, L., TREDGET, E. E., WU, P. Y. & WU, Y. 2008. Paracrine factors of mesenchymal stem cells recruit macrophages and endothelial lineage cells and enhance wound healing. *PLoS One,* 3**,** e1886.

CHENG, P., NEFEDOVA, Y., CORZO, C. A. & GABRILOVICH, D. I. 2007. Regulation of dendritic-cell differentiation by bone marrow stroma via different Notch ligands. *Blood,* 109**,** 507-15.

CHENG, P., NEFEDOVA, Y., MIELE, L., OSBORNE, B. A. & GABRILOVICH, D. 2003. Notch signaling is necessary but not sufficient for differentiation of dendritic cells. *Blood,* 102**,** 3980-8.

CHIESA, S., MORBELLI, S., MORANDO, S., MASSOLLO, M., MARINI, C., BERTONI, A., FRASSONI, F., BARTOLOME, S. T., SAMBUCETI, G., TRAGGIAI, E. & UCCELLI, A. 2011. Mesenchymal stem cells impair in vivo T-cell priming by dendritic cells. *Proc Natl Acad Sci U S A,* 108**,** 17384-9.

CHOI, E. W., SHIN, I. S., PARK, S. Y., YOON, E. J., KANG, S. K., RA, J. C. & HONG, S. H. 2013. Characteristics of mouse adipose tissue-derived stem cells and therapeutic comparison between syngeneic and allogeneic adipose tissue-derived stem cell transplantation in experimental autoimmune thyroiditis. *Cell Transplant*.

CHUNG, M. P., MONICK, M. M., HAMZEH, N. Y., BUTLER, N. S., POWERS, L. S. & HUNNINGHAKE, G. W. 2003. Role of repeated lung injury and genetic background in bleomycin-induced fibrosis. *Am J Respir Cell Mol Biol,* 29**,** 375-80.

CILLI, F., KHAN, M., FU, F. & WANG, J. H. 2004. Prostaglandin E2 affects proliferation and collagen synthesis by human patellar tendon fibroblasts. *Clin J Sport Med,* 14**,** 232-6.

COOMBS, R. R. A., FEINSTEI.A & WILSON, A. B. 1969. Immunoglobulin Determinants on Surface of Human Lymphocytes. *Lancet,* 2**,** 1157-&.

CORCIONE, A., BENVENUTO, F., FERRETTI, E., GIUNTI, D., CAPPIELLO, V., CAZZANTI, F., RISSO, M., GUALANDI, F., MANCARDI, G. L., PISTOIA, V. & UCCELLI, A. 2006. Human mesenchymal stem cells modulate B-cell functions. *Blood,* 107**,** 367-72.

DACKOR, R. T., CHENG, J., VOLTZ, J. W., CARD, J. W., FERGUSON, C. D., GARRETT, R. C., BRADBURY, J. A., DEGRAFF, L. M., LIH, F. B., TOMER, K. B., FLAKE, G. P., TRAVLOS, G. S., RAMSEY, R. W., JR., EDIN, M. L., MORGAN, D. L. & ZELDIN, D. C. 2011. Prostaglandin E(2) protects murine lungs from bleomycin-induced pulmonary fibrosis and lung dysfunction. *Am J Physiol Lung Cell Mol Physiol,* 301**,** L645-55.

DAZZI, F., RAMASAMY, R., GLENNIE, S., JONES, S. P. & ROBERTS, I. 2006. The role of mesenchymal stem cells in haemopoiesis. *Blood Rev,* 20**,** 161-71.

DEL PAPA, B., SPORTOLETTI, P., CECCHINI, D., ROSATI, E., BALUCANI, C., BALDONI, S., FETTUCCIARI, K., MARCONI, P., MARTELLI, M. F., FALZETTI, F. & DI IANNI, M. 2013. Notch1 modulates mesenchymal stem cells mediated regulatory T-cell induction. *Eur J Immunol,* 43**,** 182-7.

DEMEDTS, M., BEHR, J., BUHL, R., COSTABEL, U., DEKHUIJZEN, R., JANSEN, H. M., MACNEE, W., THOMEER, M., WALLAERT, B., LAURENT, F., NICHOLSON, A. G., VERBEKEN, E. K., VERSCHAKELEN, J., FLOWER, C. D., CAPRON, F., PETRUZZELLI, S., DE VUYST, P., VAN DEN BOSCH, J. M., RODRIGUEZ-BECERRA, E., CORVASCE, G., LANKHORST, I., SARDINA, M., MONTANARI, M. & GROUP, I. S. 2005. High-dose acetylcysteine in idiopathic pulmonary fibrosis. *N Engl J Med,* 353**,** 2229-42.

DI NICOLA, M., CARLO-STELLA, C., MAGNI, M., MILANESI, M., LONGONI, P. D., MATTEUCCI, P., GRISANTI, S. & GIANNI, A. M. 2002. Human bone marrow stromal cells suppress T-lymphocyte proliferation induced by cellular or nonspecific mitogenic stimuli. *Blood,* 99**,** 3838-43.

DJOUAD, F., CHARBONNIER, L. M., BOUFFI, C., LOUIS-PLENCE, P., BONY, C., APPARAILLY, F., CANTOS, C., JORGENSEN, C. & NOEL, D. 2007. Mesenchymal stem cells inhibit the differentiation of dendritic cells through an interleukin-6-dependent mechanism. *Stem Cells,* 25**,** 2025-32.

DOHI, M., HASEGAWA, T., YAMAMOTO, K. & MARSHALL, B. C. 2000. Hepatocyte growth factor attenuates collagen accumulation in a murine model of pulmonary fibrosis. *American Journal of Respiratory and Critical Care Medicine,* 162**,** 2302-2307.

DUFFIELD, J. S. & BONVENTRE, J. V. 2005. Kidney tubular epithelium is restored without replacement with bone marrow-derived cells during repair after ischemic injury. *Kidney Int,* 68**,** 1956-61.

DUFFY, M. M., PINDJAKOVA, J., HANLEY, S. A., MCCARTHY, C., WEIDHOFER, G. A., SWEENEY, E. M., ENGLISH, K., SHAW, G.,

MURPHY, J. M., BARRY, F. P., MAHON, B. P., BELTON, O., CEREDIG, R. & GRIFFIN, M. D. 2011. Mesenchymal stem cell inhibition of T-helper 17 cell- differentiation is triggered by cell-cell contact and mediated by prostaglandin E2 via the EP4 receptor. *Eur J Immunol,* 41**,** 2840-51.

ECKES, B., ZIGRINO, P., KESSLER, D., HOLTKOTTER, O., SHEPHARD, P., MAUCH, C. & KRIEG, T. 2000. Fibroblast-matrix interactions in wound healing and fibrosis. *Matrix Biol,* 19**,** 325-32.

ENGLISH, K., BARRY, F. P., FIELD-CORBETT, C. P. & MAHON, B. P. 2007. IFN-gamma and TNF-alpha differentially regulate immunomodulation by murine mesenchymal stem cells. *Immunol Lett,* 110**,** 91-100.

ENGLISH, K., BARRY, F. P. & MAHON, B. P. 2008. Murine mesenchymal stem cells suppress dendritic cell migration, maturation and antigen presentation. *Immunol Lett,* 115**,** 50-8.

ENGLISH, K., MAHON, B. P. & WOOD, K. J. 2013. Mesenchymal Stromal Cells; Role in Tissue Repair, Drug Discovery and Immune Modulation. *Curr Drug Deliv*.

ENGLISH, K., RYAN, J. M., TOBIN, L., MURPHY, M. J., BARRY, F. P. & MAHON, B. P. 2009. Cell contact, prostaglandin E(2) and transforming growth factor beta 1 play non-redundant roles in human mesenchymal stem cell induction of CD4+CD25(High) forkhead box P3+ regulatory T cells. *Clin Exp Immunol,* 156**,** 149-60.

FANG, X., ZHU, Y., HU, X. & LIU, Y. 2002. [Losartan in the rat model of bleomycin-induced pulmonary fibrosis and its impact on the expression of monocyte chemoattractant protein-1 and basic fibroblast growth factor]. *Zhonghua Jie He He Hu Xi Za Zhi,* 25**,** 268-72.

FORNONI, A., LI, H., FOSCHI, A., STRIKER, G. E. & STRIKER, L. J. 2001. Hepatocyte growth factor, but not insulin-like growth factor I, protects podocytes against cyclosporin A-induced apoptosis. *Am J Pathol,* 158**,** 275-80.

FRIEDENSTEIN, A. J., PIATETZKY, S., II & PETRAKOVA, K. V. 1966. Osteogenesis in transplants of bone marrow cells. *J Embryol Exp Morphol,* 16**,** 381-90.

FRONZA, M., HEINZMANN, B., HAMBURGER, M., LAUFER, S. & MERFORT, I. 2009. Determination of the wound healing effect of Calendula extracts using the scratch assay with 3T3 fibroblasts. *J Ethnopharmacol,* 126**,** 463-7.

FU, S., ZHANG, N., YOPP, A. C., CHEN, D., MAO, M., CHEN, D., ZHANG, H., DING, Y. & BROMBERG, J. S. 2004. TGF-beta induces Foxp3 + T-regulatory cells from CD4 + CD25 - precursors. *Am J Transplant,* 4**,** 1614-27.

FURUKAWA, T., MUKHERJEE, S., BAO, Z. Z., MORROW, E. M. & CEPKO, C. L. 2000. rax, Hes1, and notch1 promote the formation of Muller glia by postnatal retinal progenitor cells. *Neuron,* 26**,** 383-94.

GAO, J. Z., DENNIS, J. E., MUZIC, R. F., LUNDBERG, M. & CAPLAN, A. I. 2001. The dynamic in vivo distribution of bone marrow-derived mesenchymal stent cells after infusion. *Cells Tissues Organs,* 169**,** 12-20.

GE, W., JIANG, J., ARP, J., LIU, W., GARCIA, B. & WANG, H. 2010. Regulatory T-cell generation and kidney allograft tolerance induced by mesenchymal stem cells associated with indoleamine 2,3-dioxygenase expression. *Transplantation,* 90**,** 1312-20.

GE, W., JIANG, J., BAROJA, M. L., ARP, J., ZASSOKO, R., LIU, W., BARTHOLOMEW, A., GARCIA, B. & WANG, H. 2009. Infusion of

mesenchymal stem cells and rapamycin synergize to attenuate alloimmune responses and promote cardiac allograft tolerance. *Am J Transplant,* 9**,** 1760-72.

GERSHON, R. K., KRUGER, J., NAYSMITH, J. D. & WAKSMAN, B. H. 1971. Cellular basis for immunologic memory. *Nature,* 232**,** 639-41.

GILLARD, J. A., REED, M. W., BUTTLE, D., CROSS, S. S. & BROWN, N. J. 2004. Matrix metalloproteinase activity and immunohistochemical profile of matrix metalloproteinase-2 and -9 and tissue inhibitor of metalloproteinase-1 during human dermal wound healing. *Wound Repair Regen,* 12**,** 295-304.

GLENNIE, S., SOEIRO, I., DYSON, P. J., LAM, E. W. & DAZZI, F. 2005. Bone marrow mesenchymal stem cells induce division arrest anergy of activated T cells. *Blood,* 105**,** 2821-7.

GORDON, W. R., ARNETT, K. L. & BLACKLOW, S. C. 2008. The molecular logic of Notch signaling - a structural and biochemical perspective. *Journal of Cell Science,* 121**,** 3109-3119.

GRINNEMO, K. H., MANSSON, A., DELLGREN, G., KLINGBERG, D., WARDELL, E., DRVOTA, V., TAMMIK, C., HOLGERSSON, J., RINGDEN, O., SYLVEN, C. & LE BLANC, K. 2004. Xenoreactivity and engraftment of human mesenchymal stem cells transplanted into infarcted rat myocardium. *J Thorac Cardiovasc Surg,* 127**,** 1293-300.

GRUENLOH, W., KAMBAL, A., SONDERGAARD, C., MCGEE, J., NACEY, C., KALOMOIRIS, S., PEPPER, K., OLSON, S., FIERRO, F. & NOLTA, J. A. 2011. Characterization and in vivo testing of mesenchymal stem cells derived from human embryonic stem cells. *Tissue Eng Part A,* 17**,** 1517-25.

HANIFFA, M. A., COLLIN, M. P., BUCKLEY, C. D. & DAZZI, F. 2009. Mesenchymal stem cells: the fibroblasts' new clothes? *Haematologica,* 94**,** 258-63.

HANIFFA, M. A., WANG, X. N., HOLTICK, U., RAE, M., ISAACS, J. D., DICKINSON, A. M., HILKENS, C. M. & COLLIN, M. P. 2007. Adult human fibroblasts are potent immunoregulatory cells and functionally equivalent to mesenchymal stem cells. *J Immunol,* 179**,** 1595-604.

HARE, J. M., TRAVERSE, J. H., HENRY, T. D., DIB, N., STRUMPF, R. K., SCHULMAN, S. P., GERSTENBLITH, G., DEMARIA, A. N., DENKTAS, A. E., GAMMON, R. S., HERMILLER, J. B., REISMAN, M. A., SCHAER, G. L. & SHERMAN, W. 2009. A Randomized, Double-Blind, Placebo-Controlled, Dose-Escalation Study of Intravenous Adult Human Mesenchymal Stem Cells (Prochymal) After Acute Myocardial Infarction. *Journal of the American College of Cardiology,* 54**,** 2277-2286.

HAY, E. D. 1995. An overview of epithelio-mesenchymal transformation. *Acta Anat (Basel),* 154**,** 8-20.

HELLSTROM, M., PHNG, L. K. & GERHARDT, H. 2007. VEGF and Notch signaling: the yin and yang of angiogenic sprouting. *Cell Adh Migr,* 1**,** 133-6.

HODGES, R. J., JENKINS, R. G., WHEELER-JONES, C. P., COPEMAN, D. M., BOTTOMS, S. E., BELLINGAN, G. J., NANTHAKUMAR, C. B., LAURENT, G. J., HART, S. L., FOSTER, M. L. & MCANULTY, R. J. 2004. Severity of lung injury in cyclooxygenase-2-deficient mice is dependent on reduced prostaglandin E(2) production. *Am J Pathol,* 165**,** 1663-76.

HONEY, K., FORBUSH, K., JENSEN, P. E. & RUDENSKY, A. Y. 2004. Effect of decreasing the affinity of the class II-Associated invariant chain peptide on the

MHC class II peptide repertoire in the presence or absence of H-2M. *Journal of Immunology,* 172**,** 4142-4150.

HORWITZ, E. M., LE BLANC, K., DOMINICI, M., MUELLER, I., SLAPER-CORTENBACH, I., MARINI, F. C., DEANS, R. J., KRAUSE, D. S., KEATING, A. & INTERNATIONAL SOCIETY FOR CELLULAR, T. 2005. Clarification of the nomenclature for MSC: The International Society for Cellular Therapy position statement. *Cytotherapy,* 7**,** 393-5.

HOYNE, G. F., DALLMAN, M. J. & LAMB, J. R. 2000. T-cell regulation of peripheral tolerance and immunity: the potential role for Notch signalling. *Immunology,* 100**,** 281-8.

HU, B., WU, Z. & PHAN, S. H. 2003. Smad3 mediates transforming growth factor-beta-induced alpha-smooth muscle actin expression. *Am J Respir Cell Mol Biol,* 29**,** 397-404.

HUNT, T. K. 1988. The physiology of wound healing. *Ann Emerg Med,* 17**,** 1265-73.

IYER, S. N., GURUJEYALAKSHMI, G. & GIRI, S. N. 1999. Effects of pirfenidone on transforming growth factor-beta gene expression at the transcriptional level in bleomycin hamster model of lung fibrosis. *J Pharmacol Exp Ther,* 291**,** 367-73.

IZBICKI, G., SEGEL, M. J., CHRISTENSEN, T. G., CONNER, M. W. & BREUER, R. 2002. Time course of bleomycin-induced lung fibrosis. *Int J Exp Pathol,* 83**,** 111-9.

JIANG, X. X., ZHANG, Y., LIU, B., ZHANG, S. X., WU, Y., YU, X. D. & MAO, N. 2005. Human mesenchymal stem cells inhibit differentiation and function of monocyte-derived dendritic cells. *Blood,* 105**,** 4120-6.

KATSARA, O., MAHAIRA, L. G., ILIOPOULOU, E. G., MOUSTAKI, A., ANTSAKLIS, A., LOUTRADIS, D., STEFANIDIS, K., BAXEVANIS, C. N., PAPAMICHAIL, M. & PEREZ, S. A. 2011. Effects of Donor Age, Gender, and In Vitro Cellular Aging on the Phenotypic, Functional, and Molecular Characteristics of Mouse Bone Marrow-Derived Mesenchymal Stem Cells. *Stem Cells and Development,* 20**,** 1550-1562.

KAVANAGH, H. & MAHON, B. P. 2011. Allogeneic mesenchymal stem cells prevent allergic airway inflammation by inducing murine regulatory T cells. *Allergy,* 66**,** 523-31.

KAVANAGH, H., NOONE, C., CAHILL, E., ENGLISH, K., LOCHT, C. & MAHON, B. P. 2010. Attenuated Bordetella pertussis vaccine strain BPZE1 modulates allergen-induced immunity and prevents allergic pulmonary pathology in a murine model. *Clin Exp Allergy,* 40**,** 933-41.

KEBRIAEI, P., ISOLA, L., BAHCECI, E., HOLLAND, K., ROWLEY, S., MCGUIRK, J., DEVETTEN, M., JANSEN, J., HERZIG, R., SCHUSTER, M., MONROY, R. & UBERTI, J. 2009. Adult human mesenchymal stem cells added to corticosteroid therapy for the treatment of acute graft-versus-host disease. *Biol Blood Marrow Transplant,* 15**,** 804-11.

KIM, J. & HEMATTI, P. 2009. Mesenchymal stem cell-educated macrophages: a novel type of alternatively activated macrophages. *Exp Hematol,* 37**,** 1445-53.

KING, T. E., JR., PARDO, A. & SELMAN, M. 2011. Idiopathic pulmonary fibrosis. *Lancet,* 378**,** 1949-61.

KINNULA, V. L., FATTMAN, C. L., TAN, R. J. & OURY, T. D. 2005. Oxidative stress in pulmonary fibrosis: a possible role for redox modulatory therapy. *Am J Respir Crit Care Med,* 172**,** 417-22.

KITTA, K., DAY, R. M., IKEDA, T. & SUZUKI, Y. J. 2001. Hepatocyte growth factor protects cardiac myocytes against oxidative stress-induced apoptosis. *Free Radic Biol Med,* 31**,** 902-10.

KOLB, M., MARGETTS, P. J., GALT, T., SIME, P. J., XING, Z., SCHMIDT, M. & GAULDIE, J. 2001. Transient transgene expression of decorin in the lung reduces the fibrotic response to bleomycin. *Am J Respir Crit Care Med,* 163**,** 770-7.

KOLODSICK, J. E., PETERS-GOLDEN, M., LARIOS, J., TOEWS, G. B., THANNICKAL, V. J. & MOORE, B. B. 2003. Prostaglandin E2 inhibits fibroblast to myofibroblast transition via E. prostanoid receptor 2 signaling and cyclic adenosine monophosphate elevation. *Am J Respir Cell Mol Biol,* 29**,** 537-44.

KOTTON, D. N., FABIAN, A. J. & MULLIGAN, R. C. 2005. Failure of bone marrow to reconstitute lung epithelium. *Am J Respir Cell Mol Biol,* 33**,** 328-34.

KRAMPERA, M., COSMI, L., ANGELI, R., PASINI, A., LIOTTA, F., ANDREINI, A., SANTARLASCI, V., MAZZINGHI, B., PIZZOLO, G., VINANTE, F., ROMAGNANI, P., MAGGI, E., ROMAGNANI, S. & ANNUNZIATO, F. 2006. Role for interferon-gamma in the immunomodulatory activity of human bone marrow mesenchymal stem cells. *Stem Cells,* 24**,** 386-98.

KRAMPERA, M., GLENNIE, S., DYSON, J., SCOTT, D., LAYLOR, R., SIMPSON, E. & DAZZI, F. 2003. Bone marrow mesenchymal stem cells inhibit the response of naive and memory antigen-specific T cells to their cognate peptide. *Blood,* 101**,** 3722-9.

LAMA, V., MOORE, B. B., CHRISTENSEN, P., TOEWS, G. B. & PETERS-GOLDEN, M. 2002. Prostaglandin E2 synthesis and suppression of fibroblast

proliferation by alveolar epithelial cells is cyclooxygenase-2-dependent. *Am J Respir Cell Mol Biol,* 27**,** 752-8.

LAVOIE, M. J. & SELKOE, D. J. 2003. The Notch ligands, Jagged and Delta, are sequentially processed by alpha-secretase and presenilin/gamma-secretase and release signaling fragments. *Journal of Biological Chemistry,* 278**,** 34427-34437.

LAWSON, W. E., POLOSUKHIN, V. V., STATHOPOULOS, G. T., ZOIA, O., HAN, W., LANE, K. B., LI, B., DONNELLY, E. F., HOLBURN, G. E., LEWIS, K. G., COLLINS, R. D., HULL, W. M., GLASSER, S. W., WHITSETT, J. A. & BLACKWELL, T. S. 2005. Increased and prolonged pulmonary fibrosis in surfactant protein C-deficient mice following intratracheal bleomycin. *Am J Pathol,* 167**,** 1267-77.

LE BLANC, K., TAMMIK, L., SUNDBERG, B., HAYNESWORTH, S. E. & RINGDEN, O. 2003. Mesenchymal stem cells inhibit and stimulate mixed lymphocyte cultures and mitogenic responses independently of the major histocompatibility complex. *Scandinavian Journal of Immunology,* 57**,** 11-20.

LEBLANC, K., FRASSONI, F., BALL, L., LOCATELLI, F., ROELOFS, H., LEWIS, I., LANINO, E., SUNDBERG, B., BERNARDO, M. E., REMBERGER, M., DINI, G., EGELER, R. M., BACIGALUPO, A., FIBBE, W., RINGDEN, O. & M, D. C. E. G. B. 2008. Mesenchymal stem cells for treatment of steroid-resistant, severe, acute graft-versus-host disease: a phase II study. *Lancet,* 371**,** 1579-1586.

LEE, R. H., PULIN, A. A., SEO, M. J., KOTA, D. J., YLOSTALO, J., LARSON, B. L., SEMPRUN-PRIETO, L., DELAFONTAINE, P. & PROCKOP, D. J. 2009. Intravenous hMSCs Improve Myocardial Infarction in Mice because Cells

Embolized in Lung Are Activated to Secrete the Anti-inflammatory Protein TSG-6. *Cell Stem Cell,* 5**,** 54-63.

LEE, R. H., SEO, M. J., REGER, R. L., SPEES, J. L., PULIN, A. A., OLSON, S. D. & PROCKOP, D. J. 2006. Multipotent stromal cells from human marrow home to and promote repair of pancreatic islets and renal glomeruli in diabetic NOD/scid mice. *Proceedings of the National Academy of Sciences of the United States of America,* 103**,** 17438-17443.

LI, Y. P., PACZESNY, S., LAURET, E., POIRAULT, S., BORDIGONI, P., MEKHLOUFI, F., HEQUET, O., BERTRAND, Y., OU-YANG, J. P., STOLTZ, J. F., MIOSSEC, P. & ELJAAFARI, A. 2008. Human mesenchymal stem cells license adult CD34+ hemopoietic progenitor cells to differentiate into regulatory dendritic cells through activation of the Notch pathway. *J Immunol,* 180**,** 1598-608.

LIAN, Q. Z., ZHANG, Y. L., ZHANG, J. Q., ZHANG, H. K., WU, X. G., ZHANG, Y., LAM, F. F. Y., KANG, S., XIA, J. C., LAI, W. H., AU, K. W., CHOW, Y. Y., SIU, C. W., LEE, C. N. & TSE, H. F. 2010. Functional Mesenchymal Stem Cells Derived From Human Induced Pluripotent Stem Cells Attenuate Limb Ischemia in Mice. *Circulation,* 121**,** 1113-U91.

LIANG, C. C., PARK, A. Y. & GUAN, J. L. 2007. In vitro scratch assay: a convenient and inexpensive method for analysis of cell migration in vitro. *Nat Protoc,* 2**,** 329-33.

LIN, W., HARIBHAI, D., RELLAND, L. M., TRUONG, N., CARLSON, M. R., WILLIAMS, C. B. & CHATILA, T. A. 2007. Regulatory T cell development in the absence of functional Foxp3. *Nat Immunol,* 8**,** 359-68.

LIOTTA, F., ANGELI, R., COSMI, L., FILI, L., MANUELLI, C., FROSALI, F., MAZZINGHI, B., MAGGI, L., PASINI, A., LISI, V., SANTARLASCI, V., CONSOLONI, L., ANGELOTTI, M. L., ROMAGNANI, P., PARRONCHI, P., KRAMPERA, M., MAGGI, E., ROMAGNANI, S. & ANNUNZIATO, F. 2008. Toll-like receptors 3 and 4 are expressed by human bone marrow-derived mesenchymal stem cells and can inhibit their T-cell modulatory activity by impairing Notch signaling. *Stem Cells,* 26**,** 279-89.

LOWN, J. W. & SIM, S. K. 1977. The mechanism of the bleomycin-induced cleavage of DNA. *Biochem Biophys Res Commun,* 77**,** 1150-7.

LU, X., LIU, T., GU, L., HUANG, C., ZHU, H., MENG, W., XI, Y., LI, S. & LIU, Y. 2009. Immunomodulatory effects of mesenchymal stem cells involved in favoring type 2 T cell subsets. *Transpl Immunol,* 22**,** 55-61.

MAGGINI, J., MIRKIN, G., BOGNANNI, I., HOLMBERG, J., PIAZZON, I. M., NEPOMNASCHY, I., COSTA, H., CANONES, C., RAIDEN, S., VERMEULEN, M. & GEFFNER, J. R. 2010. Mouse Bone Marrow-Derived Mesenchymal Stromal Cells Turn Activated Macrophages into a Regulatory-Like Profile. *Plos One,* 5.

MAHER, T. M., EVANS, I. C., BOTTOMS, S. E., MERCER, P. F., THORLEY, A. J., NICHOLSON, A. G., LAURENT, G. J., TETLEY, T. D., CHAMBERS, R. C. & MCANULTY, R. J. 2010. Diminished prostaglandin E2 contributes to the apoptosis paradox in idiopathic pulmonary fibrosis. *Am J Respir Crit Care Med,* 182**,** 73-82.

MAHER, T. M., WELLS, A. U. & LAURENT, G. J. 2007. Idiopathic pulmonary fibrosis: multiple causes and multiple mechanisms? *European Respiratory Journal,* 30**,** 835-839.

MARSHALL, R. P., GOHLKE, P., CHAMBERS, R. C., HOWELL, D. C., BOTTOMS, S. E., UNGER, T., MCANULTY, R. J. & LAURENT, G. J. 2004. Angiotensin II and the fibroproliferative response to acute lung injury. *Am J Physiol Lung Cell Mol Physiol,* 286**,** L156-64.

MATSUMOTO, K. & NAKAMURA, T. 1993. Roles of HGF as a pleiotropic factor in organ regeneration. *EXS,* 65**,** 225-49.

MILLS, C. R. 2009. Osiris Therapeutics Reports Interim Data for COPD Stem Cell Study.

MIZUNO, S., MATSUMOTO, K., LI, M. Y. & NAKAMURA, T. 2005. HGF reduces advancing lung fibrosis in mice: a potential role for MMP-dependent myofibroblast apoptosis. *FASEB J,* 19**,** 580-2.

MOELLER, A., ASK, K., WARBURTON, D., GAULDIE, J. & KOLB, M. 2008. The bleomycin animal model: a useful tool to investigate treatment options for idiopathic pulmonary fibrosis? *Int J Biochem Cell Biol,* 40**,** 362-82.

MOLINA-MOLINA, M., SERRANO-MOLLAR, A., BULBENA, O., FERNANDEZ-ZABALEGUI, L., CLOSA, D., MARIN-ARGUEDAS, A., TORREGO, A., MULLOL, J., PICADO, C. & XAUBET, A. 2006. Losartan attenuates bleomycin induced lung fibrosis by increasing prostaglandin E2 synthesis. *Thorax,* 61**,** 604-10.

MOODLEY, Y., ATIENZA, D., MANUELPILLAI, U., SAMUEL, C. S., TCHONGUE, J., ILANCHERAN, S., BOYD, R. & TROUNSON, A. 2009. Human umbilical cord mesenchymal stem cells reduce fibrosis of bleomycin-induced lung injury. *Am J Pathol,* 175**,** 303-13.

MOODLEY, Y. P., MISSO, N. L., SCAFFIDI, A. K., FOGEL-PETROVIC, M., MCANULTY, R. J., LAURENT, G. J., THOMPSON, P. J. & KNIGHT, D. A.

2003. Inverse effects of interleukin-6 on apoptosis of fibroblasts from pulmonary fibrosis and normal lungs. *Am J Respir Cell Mol Biol,* 29**,** 490-8.

MOORE, B. B. & HOGABOAM, C. M. 2008. Murine models of pulmonary fibrosis. *Am J Physiol Lung Cell Mol Physiol,* 294**,** L152-60.

MOORE, B. B., PETERS-GOLDEN, M., CHRISTENSEN, P. J., LAMA, V., KUZIEL, W. A., PAINE, R., 3RD & TOEWS, G. B. 2003. Alveolar epithelial cell inhibition of fibroblast proliferation is regulated by MCP-1/CCR2 and mediated by PGE2. *Am J Physiol Lung Cell Mol Physiol,* 284**,** L342-9.

MORELLI, A. E. & THOMSON, A. W. 2007. Tolerogenic dendritic cells and the quest for transplant tolerance. *Nat Rev Immunol,* 7**,** 610-21.

MURPHY, K. M., HEIMBERGER, A. B. & LOH, D. Y. 1990. Induction by Antigen of Intrathymic Apoptosis of Cd4+Cd8+Tcrlo Thymocytes Invivo. *Science,* 250**,** 1720-1723.

NAKAO, A., FUJII, M., MATSUMURA, R., KUMANO, K., SAITO, Y., MIYAZONO, K. & IWAMOTO, I. 1999. Transient gene transfer and expression of Smad7 prevents bleomycin-induced lung fibrosis in mice. *J Clin Invest,* 104**,** 5-11.

NAKAZATO, H., OKU, H., YAMANE, S., TSURUTA, Y. & SUZUKI, R. 2002. A novel anti-fibrotic agent pirfenidone suppresses tumor necrosis factor-alpha at the translational level. *Eur J Pharmacol,* 446**,** 177-85.

NALYSNYK, L., CID-RUZAFA, J., ROTELLA, P. & ESSER, D. 2012. Incidence and prevalence of idiopathic pulmonary fibrosis: review of the literature. *Eur Respir Rev,* 21**,** 355-61.

NAUTA, A. J., KRUISSELBRINK, A. B., LURVINK, E., WILLEMZE, R. & FIBBE, W. E. 2006. Mesenchymal stem cells inhibit generation and function of both

CD34+-derived and monocyte-derived dendritic cells. *J Immunol,* 177**,** 2080-7.

NEMETH, K., KEANE-MYERS, A., BROWN, J. M., METCALFE, D. D., GORHAM, J. D., BUNDOC, V. G., HODGES, M. G., JELINEK, I., MADALA, S., KARPATI, S. & MEZEY, E. 2010. Bone marrow stromal cells use TGF-beta to suppress allergic responses in a mouse model of ragweed-induced asthma. *Proc Natl Acad Sci U S A,* 107**,** 5652-7.

NEMETH, K., LEELAHAVANICHKUL, A., YUEN, P. S., MAYER, B., PARMELEE, A., DOI, K., ROBEY, P. G., LEELAHAVANICHKUL, K., KOLLER, B. H., BROWN, J. M., HU, X., JELINEK, I., STAR, R. A. & MEZEY, E. 2009. Bone marrow stromal cells attenuate sepsis via prostaglandin E(2)-dependent reprogramming of host macrophages to increase their interleukin-10 production. *Nat Med,* 15**,** 42-9.

NIESSEN, K. & KARSAN, A. 2008. Notch signaling in cardiac development. *Circ Res,* 102**,** 1169-81.

NOBLE, P. W., ALBERA, C., BRADFORD, W. Z., COSTABEL, U., GLASSBERG, M. K., KARDATZKE, D., KING, T. E., JR., LANCASTER, L., SAHN, S. A., SZWARCBERG, J., VALEYRE, D., DU BOIS, R. M. & GROUP, C. S. 2011. Pirfenidone in patients with idiopathic pulmonary fibrosis (CAPACITY): two randomised trials. *Lancet,* 377**,** 1760-9.

NOONE, C., KIHM, A., ENGLISH, K., O'DEA, S. & MAHON, B. P. 2013. IFN-gamma stimulated human umbilical-tissue derived cells potently suppress NK activation and resist NK mediated cytotoxicity in vitro. *Stem Cells Dev*.

OFFICE, C. C. S. 2010. Deaths from diseases of the circulatory system (I00-I99) in 2010 classified by underlying cause of death and sex. *Report on Vital Statistics***,** 79-85.

OKUMA, T., TERASAKI, Y., KAIKITA, K., KOBAYASHI, H., KUZIEL, W. A., KAWASUJI, M. & TAKEYA, M. 2004. C-C chemokine receptor 2 (CCR2) deficiency improves bleomycin-induced pulmonary fibrosis by attenuation of both macrophage infiltration and production of macrophage-derived matrix metalloproteinases. *J Pathol,* 204**,** 594-604.

OMATSU, Y., SUGIYAMA, T., KOHARA, H., KONDOH, G., FUJII, N., KOHNO, K. & NAGASAWA, T. 2010. The Essential Functions of Adipo-osteogenic Progenitors as the Hematopoietic Stem and Progenitor Cell Niche. *Immunity,* 33**,** 387-399.

ORTIZ, L. A., DUTREIL, M., FATTMAN, C., PANDEY, A. C., TORRES, G., GO, K. & PHINNEY, D. G. 2007. Interleukin 1 receptor antagonist mediates the antiinflammatory and antifibrotic effect of mesenchymal stem cells during lung injury. *Proc Natl Acad Sci U S A,* 104**,** 11002-7.

ORTIZ, L. A., GAMBELLI, F., MCBRIDE, C., GAUPP, D., BADDOO, M., KAMINSKI, N. & PHINNEY, D. G. 2003. Mesenchymal stem cell engraftment in lung is enhanced in response to bleomycin exposure and ameliorates its fibrotic effects. *Proc Natl Acad Sci U S A,* 100**,** 8407-11.

ORTIZ, L. A., LASKY, J., HAMILTON, R. F., JR., HOLIAN, A., HOYLE, G. W., BANKS, W., PESCHON, J. J., BRODY, A. R., LUNGARELLA, G. & FRIEDMAN, M. 1998. Expression of TNF and the necessity of TNF receptors in bleomycin-induced lung injury in mice. *Exp Lung Res,* 24**,** 721-43.

PADDISON, P. J., CAUDY, A. A., BERNSTEIN, E., HANNON, G. J. & CONKLIN, D. S. 2002. Short hairpin RNAs (shRNAs) induce sequence-specific silencing in mammalian cells. *Genes Dev,* 16**,** 948-58.

PAN, T., MASON, R. J., WESTCOTT, J. Y. & SHANNON, J. M. 2001. Rat alveolar type II cells inhibit lung fibroblast proliferation in vitro. *Am J Respir Cell Mol Biol,* 25**,** 353-61.

PHIN, S., MARCHAND-ADAM, S., FABRE, A., MARCHAL-SOMME, J., BANTSIMBA-MALANDA, C., KATAOKA, H., SOLER, P. & CRESTANI, B. 2010. Imbalance in the pro-hepatocyte growth factor activation system in bleomycin-induced lung fibrosis in mice. *Am J Respir Cell Mol Biol,* 42**,** 286-93.

PHINNEY, D. G. & PROCKOP, D. J. 2007. Concise review: mesenchymal stem/multipotent stromal cells: the state of transdifferentiation and modes of tissue repair--current views. *Stem Cells,* 25**,** 2896-902.

PIGUET, P. F., GRAU, G. E., COLLART, M. A., VASSALLI, P. & KAPANCI, Y. 1989. Pneumopathies of the graft-versus-host reaction. Alveolitis associated with an increased level of tumor necrosis factor mRNA and chronic interstitial pneumonitis. *Lab Invest,* 61**,** 37-45.

PIGUET, P. F. & VESIN, C. 1994. Treatment by Human Recombinant Soluble Tnf Receptor of Pulmonary Fibrosis Induced by Bleomycin or Silica in Mice. *European Respiratory Journal,* 7**,** 515-518.

PITTENGER, M. F., MACKAY, A. M., BECK, S. C., JAISWAL, R. K., DOUGLAS, R., MOSCA, J. D., MOORMAN, M. A., SIMONETTI, D. W., CRAIG, S. & MARSHAK, D. R. 1999. Multilineage potential of adult human mesenchymal stem cells. *Science,* 284**,** 143-7.

RAFFAGHELLO, L., BIANCHI, G., BERTOLOTTO, M., MONTECUCCO, F., BUSCA, A., DALLEGRI, F., OTTONELLO, L. & PISTOIA, V. 2008. Human mesenchymal stem cells inhibit neutrophil apoptosis: A model for neutrophil preservation in the bone marrow niche. *Stem Cells,* 26**,** 151-162.

RAFII, R., JUAREZ, M. M., ALBERTSON, T. E. & CHAN, A. L. 2013. A review of current and novel therapies for idiopathic pulmonary fibrosis. *J Thorac Dis,* 5**,** 48-73.

RAGHU, G. 2012. Idiopathic pulmonary fibrosis: new evidence and an improved standard of care in 2012. *Lancet,* 380**,** 699-701.

RAGHU, G., ANSTROM, K. J., KING, T. E., LASKY, J. A., MARTINEZ, F. J. & CLINICAL, I. P. F. 2012a. Prednisone, Azathioprine, and N-Acetylcysteine for Pulmonary Fibrosis. *New England Journal of Medicine,* 366**,** 1968-1977.

RAGHU, G., COLLARD, H. R., ANSTROM, K. J., FLAHERTY, K. R., FLEMING, T. R., KING, T. E., JR., MARTINEZ, F. J. & BROWN, K. K. 2012b. Idiopathic pulmonary fibrosis: clinically meaningful primary endpoints in phase 3 clinical trials. *Am J Respir Crit Care Med,* 185**,** 1044-8.

RAGHU, G., COLLARD, H. R., EGAN, J. J., MARTINEZ, F. J., BEHR, J., BROWN, K. K., COLBY, T. V., CORDIER, J. F., FLAHERTY, K. R., LASKY, J. A., LYNCH, D. A., RYU, J. H., SWIGRIS, J. J., WELLS, A. U., ANCOCHEA, J., BOUROS, D., CARVALHO, C., COSTABEL, U., EBINA, M., HANSELL, D. M., JOHKOH, T., KIM, D. S., KING, T. E., JR., KONDOH, Y., MYERS, J., MULLER, N. L., NICHOLSON, A. G., RICHELDI, L., SELMAN, M., DUDDEN, R. F., GRISS, B. S., PROTZKO, S. L., SCHUNEMANN, H. J. & FIBROSIS, A. E. J. A. C. O. I. P. 2011. An official ATS/ERS/JRS/ALAT statement: idiopathic pulmonary fibrosis: evidence-

based guidelines for diagnosis and management. *Am J Respir Crit Care Med,* 183**,** 788-824.

RAGHU, G., WEYCKER, D., EDELSBERG, J., BRADFORD, W. Z. & OSTER, G. 2006. Incidence and prevalence of idiopathic pulmonary fibrosis. *American Journal of Respiratory and Critical Care Medicine,* 174**,** 810-816.

RAMASASTRY, S. S. 2005. Acute wounds. *Clin Plast Surg,* 32**,** 195-208.

REN, G., ZHANG, L., ZHAO, X., XU, G., ZHANG, Y., ROBERTS, A. I., ZHAO, R. C. & SHI, Y. 2008. Mesenchymal stem cell-mediated immunosuppression occurs via concerted action of chemokines and nitric oxide. *Cell Stem Cell,* 2**,** 141-50.

ROBSON, M. C., STEED, D. L. & FRANZ, M. G. 2001. Wound healing: Biologic features and approaches to maximize healing trajectories. *Current Problems in Surgery,* 38**,** 72-140.

ROJAS, M., XU, J., WOODS, C. R., MORA, A. L., SPEARS, W., ROMAN, J. & BRIGHAM, K. L. 2005. Bone marrow-derived mesenchymal stem cells in repair of the injured lung. *Am J Respir Cell Mol Biol,* 33**,** 145-52.

RYAN, J. M., BARRY, F., MURPHY, J. M. & MAHON, B. P. 2007. Interferon-gamma does not break, but promotes the immunosuppressive capacity of adult human mesenchymal stem cells. *Clin Exp Immunol,* 149**,** 353-63.

SAMON, J. B., CHAMPHEKAR, A., MINTER, L. M., TELFER, J. C., MIELE, L., FAUQ, A., DAS, P., GOLDE, T. E. & OSBORNE, B. A. 2008. Notch1 and TGFbeta1 cooperatively regulate Foxp3 expression and the maintenance of peripheral regulatory T cells. *Blood,* 112**,** 1813-21.

SATO, K., OZAKI, K., OH, I., MEGURO, A., HATANAKA, K., NAGAI, T., MUROI, K. & OZAWA, K. 2007. Nitric oxide plays a critical role in

suppression of T-cell proliferation by mesenchymal stem cells. *Blood,* 109**,** 228-34.

SCHENA, F., GAMBINI, C., GREGORIO, A., MOSCONI, M., REVERBERI, D., GATTORNO, M., CASAZZA, S., UCCELLI, A., MORETTA, L., MARTINI, A. & TRAGGIAI, E. 2010. Interferon-gamma-dependent inhibition of B cell activation by bone marrow-derived mesenchymal stem cells in a murine model of systemic lupus erythematosus. *Arthritis Rheum,* 62**,** 2776-86.

SCHEULE, R. K., PERKINS, R. C., HAMILTON, R. & HOLIAN, A. 1992. Bleomycin stimulation of cytokine secretion by the human alveolar macrophage. *Am J Physiol,* 262**,** L386-91.

SCHRIER, D. J., KUNKEL, R. G. & PHAN, S. H. 1983. The role of strain variation in murine bleomycin-induced pulmonary fibrosis. *Am Rev Respir Dis,* 127**,** 63-6.

SCOLLAY, R., JACOBS, S., JERABEK, L., BUTCHER, E. & WEISSMAN, I. 1980. T cell maturation: thymocyte and thymus migrant subpopulations defined with monoclonal antibodies to MHC region antigens. *J Immunol,* 124**,** 2845-53.

SELMAN, M., PARDO, A., BARRERA, L., ESTRADA, A., WATSON, S. R., WILSON, K., AZIZ, N., KAMINSKI, N. & ZLOTNIK, A. 2006. Gene expression profiles distinguish idiopathic pulmonary fibrosis from hypersensitivity pneumonitis. *American Journal of Respiratory and Critical Care Medicine,* 173**,** 188-198.

SELMANI, Z., NAJI, A., ZIDI, I., FAVIER, B., GAIFFE, E., OBERT, L., BORG, C., SAAS, P., TIBERGHIEN, P., ROUAS-FREISS, N., CAROSELLA, E. D. & DESCHASEAUX, F. 2008. Human leukocyte antigen-G5 secretion by human mesenchymal stem cells is required to suppress T lymphocyte and natural

killer function and to induce CD4+CD25highFOXP3+ regulatory T cells. *Stem Cells,* 26**,** 212-22.

SICA, A. & MANTOVANI, A. 2012. Macrophage plasticity and polarization: in vivo veritas. *J Clin Invest,* 122**,** 787-95.

SMITH, A. N., WILLIS, E., CHAN, V. T., MUFFLEY, L. A., ISIK, F. F., GIBRAN, N. S. & HOCKING, A. M. 2010. Mesenchymal stem cells induce dermal fibroblast responses to injury. *Exp Cell Res,* 316**,** 48-54.

SMITH, R. E., STRIETER, R. M., PHAN, S. H., LUKACS, N. W., HUFFNAGLE, G. B., WILKE, C. A., BURDICK, M. D., LINCOLN, P., EVANOFF, H. & KUNKEL, S. L. 1994. Production and function of murine macrophage inflammatory protein-1 alpha in bleomycin-induced lung injury. *J Immunol,* 153**,** 4704-12.

SOUSA, C. R. E., HIENY, S., SCHARTONKERSTEN, T., JANKOVIC, D., CHAREST, H., GERMAIN, R. N. & SHER, A. 1997. In vivo microbial stimulation induces rapid CD40 ligand-independent production of interleukin 12 by dendritic cells and their redistribution to T cell areas. *Journal of Experimental Medicine,* 186**,** 1819-1829.

SPAGGIARI, G. M., CAPOBIANCO, A., ABDELRAZIK, H., BECCHETTI, F., MINGARI, M. C. & MORETTA, L. 2008. Mesenchymal stem cells inhibit natural killer-cell proliferation, cytotoxicity, and cytokine production: role of indoleamine 2,3-dioxygenase and prostaglandin E2. *Blood,* 111**,** 1327-33.

SPAGGIARI, G. M., CAPOBIANCO, A., BECCHETTI, S., MINGARI, M. C. & MORETTA, L. 2006. Mesenchymal stem cell-natural killer cell interactions: evidence that activated NK cells are capable of killing MSCs, whereas MSCs can inhibit IL-2-induced NK-cell proliferation. *Blood,* 107**,** 1484-90.

STEINMAN, R. M. & COHN, Z. A. 1973. Identification of a novel cell type in peripheral lymphoid organs of mice. I. Morphology, quantitation, tissue distribution. *J Exp Med,* 137**,** 1142-62.

SU, W. R., ZHANG, Q. Z., SHI, S. H., NGUYEN, A. L. & LE, A. D. 2011. Human Gingiva-Derived Mesenchymal Stromal Cells Attenuate Contact Hypersensitivity via Prostaglandin E-2-Dependent Mechanisms. *Stem Cells,* 29**,** 1849-1860.

SYED, B. A. & EVANS, J. B. 2013. From the Analyst's Couch Stem Cell Therapy Market. *Nature Reviews Drug Discovery,* 12**,** 185-186.

TAKAHASHI, K., TANABE, K., OHNUKI, M., NARITA, M., ICHISAKA, T., TOMODA, K. & YAMANAKA, S. 2007. Induction of pluripotent stem cells from adult human fibroblasts by defined factors. *Cell,* 131**,** 861-872.

TRAGGIAI, E., VOLPI, S., SCHENA, F., GATTORNO, M., FERLITO, F., MORETTA, L. & MARTINI, A. 2008. Bone marrow-derived mesenchymal stem cells induce both polyclonal expansion and differentiation of B cells isolated from healthy donors and systemic lupus erythematosus patients. *Stem Cells,* 26**,** 562-9.

TROPEL, P., NOEL, D., PLATET, N., LEGRAND, P., BENABID, A. L. & BERGER, F. 2004. Isolation and characterisation of mesenchymal stem cells from adult mouse bone marrow. *Exp Cell Res,* 295**,** 395-406.

VIERLING, J. M. 2011. Autoimmune Hepatitis and Antigen-Specific T Regulatory Cells: When Can We Send in the Regulators? *Hepatology,* 53**,** 385-388.

WALTER, M. N., WRIGHT, K. T., FULLER, H. R., MACNEIL, S. & JOHNSON, W. E. 2010. Mesenchymal stem cell-conditioned medium accelerates skin

wound healing: an in vitro study of fibroblast and keratinocyte scratch assays. *Exp Cell Res,* 316**,** 1271-81.

WALTERS, D. M. & KLEEBERGER, S. R. 2008. Mouse models of bleomycin-induced pulmonary fibrosis. *Curr Protoc Pharmacol,* Chapter 5**,** Unit 5 46.

WANG, R., ZAGARIYA, A., IBARRA-SUNGA, O., GIDEA, C., ANG, E., DESHMUKH, S., CHAUDHARY, G., BARABOUTIS, J., FILIPPATOS, G. & UHAL, B. D. 1999. Angiotensin II induces apoptosis in human and rat alveolar epithelial cells. *Am J Physiol,* 276**,** L885-9.

WATERMAN, R. S., TOMCHUCK, S. L., HENKLE, S. L. & BETANCOURT, A. M. 2010. A new mesenchymal stem cell (MSC) paradigm: polarization into a pro-inflammatory MSC1 or an Immunosuppressive MSC2 phenotype. *PLoS One,* 5**,** e10088.

WEIJZEN, S., VELDERS, M. P., ELMISHAD, A. G., BACON, P. E., PANELLA, J. R., NICKOLOFF, B. J., MIELE, L. & KAST, W. M. 2002. The Notch ligand Jagged-1 is able to induce maturation of monocyte-derived human dendritic cells. *J Immunol,* 169**,** 4273-8.

WEIL, B. R., MARKEL, T. A., HERRMANN, J. L., ABARBANELL, A. M. & MELDRUM, D. R. 2009. Mesenchymal stem cells enhance the viability and proliferation of human fetal intestinal epithelial cells following hypoxic injury via paracrine mechanisms. *Surgery,* 146**,** 190-7.

WICK, G., GRUNDTMAN, C., MAYERL, C., WIMPISSINGER, T. F., FEICHTINGER, J., ZELGER, B., SGONC, R. & WOLFRAM, D. 2013. The immunology of fibrosis. *Annu Rev Immunol,* 31**,** 107-35.

WILLIS, B. C., LIEBLER, J. M., LUBY-PHELPS, K., NICHOLSON, A. G., CRANDALL, E. D., DU BOIS, R. M. & BOROK, Z. 2005. Induction of

epithelial-mesenchymal transition in alveolar epithelial cells by transforming growth factor-beta1: potential role in idiopathic pulmonary fibrosis. *Am J Pathol,* 166**,** 1321-32.

WILSON, M. S. & WYNN, T. A. 2009. Pulmonary fibrosis: pathogenesis, etiology and regulation. *Mucosal Immunology,* 2**,** 103-121.

YAEKASHIWA, M., NAKAYAMA, S., OHNUMA, K., SAKAI, T., ABE, T., SATOH, K., MATSUMOTO, K., NAKAMURA, T., TAKAHASHI, T. & NUKIWA, T. 1997. Simultaneous or delayed administration of hepatocyte growth factor equally represses the fibrotic changes in murine lung injury induced by bleomycin. A morphologic study. *Am J Respir Crit Care Med,* 156**,** 1937-44.

YAO, H. W., ZHU, J. P., ZHAO, M. H. & LU, Y. 2006. Losartan attenuates bleomycin-induced pulmonary fibrosis in rats. *Respiration,* 73**,** 236-42.

YVON, E. S., VIGOUROUX, S., ROUSSEAU, R. F., BIAGI, E., AMROLIA, P., DOTTI, G., WAGNER, H. J. & BRENNER, M. K. 2003. Overexpression of the Notch ligand, Jagged-1, induces alloantigen-specific human regulatory T cells. *Blood,* 102**,** 3815-21.

ZAPPIA, E., CASAZZA, S., PEDEMONTE, E., BENVENUTO, F., BONANNI, I., GERDONI, E., GIUNTI, D., CERAVOLO, A., CAZZANTI, F., FRASSONI, F., MANCARDI, G. & UCCELLI, A. 2005. Mesenchymal stem cells ameliorate experimental autoimmune encephalomyelitis inducing T-cell anergy. *Blood,* 106**,** 1755-61.

ZHANG, B., LIU, R., SHI, D., LIU, X., CHEN, Y., DOU, X., ZHU, X., LU, C., LIANG, W., LIAO, L., ZENKE, M. & ZHAO, R. C. 2009. Mesenchymal stem

cells induce mature dendritic cells into a novel Jagged-2-dependent regulatory dendritic cell population. *Blood,* 113**,** 46-57.

ZHANG, K., GHARAEE-KERMANI, M., JONES, M. L., WARREN, J. S. & PHAN, S. H. 1994. Lung monocyte chemoattractant protein-1 gene expression in bleomycin-induced pulmonary fibrosis. *J Immunol,* 153**,** 4733-41.